Computer-Assisted Musculoskeletal Surgery

Thinking and Executing in 3D

Lucas E. Ritacco
Federico E. Milano
Edmund Chao
Editors

Springer

Computer-Assisted Musculoskeletal Surgery

Lucas E. Ritacco • Federico E. Milano
Edmund Chao
Editors

Computer-Assisted Musculoskeletal Surgery

Thinking and Executing in 3D

Springer

Editors
Lucas E. Ritacco
Computer-Assisted Surgery Unit
Hospital Italiano de Buenos Aires
Buenos Aires
Argentina

Edmund Chao
Johns Hopkins University
Baltimore, MD
USA

Federico E. Milano
Bioengineering
Instituto Tecnologico de Buenos Aires
Buenos Aires
Argentina

ISBN 978-3-319-12942-6 ISBN 978-3-319-12943-3 (eBook)
DOI 10.1007/978-3-319-12943-3

Library of Congress Control Number: 2015953344

Springer Cham Heidelberg New York Dordrecht London

Printed on acid-free paper

Springer International Publishing AG Switzerland is part of Springer Science+Business Media (www.springer.com)

Preface

It is an honor and pleasure to have been asked to write the Preface of a book I regard as "intimate" since it deals with the topic, that has occupied much of my career for more than four decades! Instead of dwelling only on the subject material in each chapter, I choose a different approach to reflect my personal view of the general topic using a commentary style, and with brief historical reviews. As computer-assisted surgery is subjected to both enthusiastic acceptance and cautious scrutiny, it is fare for me to express my thoughts by assessing its current status and future outlook. To end, I offered a provocative thought for us all to contemplate that may impact on medical technology now and years to come.

Computer-assisted surgery (CAS) by definition is a process in which a surgical procedure is planned and executed using computer simulation and navigation technology. From the engineering point of view, simulation was a relatively old innovation started in the late 1950s and early 1960s using the analog computer in the aerospace and automobile industry. The digital computer was then in its infancy with limited memory, inadequate processing speed, and the lack of numerical methods to solve differential equations. The basic practice of spatial navigation was already in existence in tracking aircraft and vehicular movements in high speed using triangular photogrammetry. It was interesting that applications of engineering principles to medicine and surgery were beginning to emerge at about the same time. This early development of simulation had a major drawback in that the models were primarily analytical and scaled prototypes, thus making analysis of results difficult to visualize and the optimal design process time-consuming and costly.

The explosion of digital computer technology with large core memory and processing speed in the 1970s stimulated the development of numerical methods, which had replaced the use of analog computer in data processing and the solution of the analytical models. With the advances in imaging technology, 3D graphics provided the unique capability of generating solid and surface models in the late 1980s. This advancement also enhanced the navigation technology by coordinating the virtual model with the real system monitored using different stereometric methods with sensors and markers, thus making computer-assisted surgery (CAS) possible. Subsequently, the development of surgical robot gave rise to the "Robodoc" in hip

replacement surgery, which set the pace and laid down the standards for future CAS development.

Before commenting on the contents of this book, several historical developments should be mentioned to explain the evolutional passage of CAS technology. Computer-aided preoperative planning based on biomechanical analysis using 2D radiographic images for osteotomy of the knee and hip joints using the discrete element analysis (the Rigid Body Spring Modeling technique) was well established for clinical trial and eventually received reimbursement for the preoperative planning service for nearly a decade between the 1980s and the 1990s. The execution of these difficult procedures was less precise, however; but the need to expand this innovative concept to 3D laid down the impetus and foundation to build today's CAS. For bone fracture reduction, adjustment and fixation, under unilateral external fixator, were extensively investigated in the late 1990s using kinematic theories and virtual models of the bone-fixator complex for application planning and visualization. This developmental effort was short lived due to the overwhelming favor towards internal fixation devices at the turn of the Millennium. Fortunately, such trend may have effectually reversed by the improvement in external fixator design and their application software, which will be discussed in detail in this book. The combination of virtual interactive anatomical model and biomechanical analysis was successfully developed in the latter part of 1990s owing to the remarkable advancement in computer graphics stimulated by the movie, video, gaming and advertisement industry! These progressive passages made CAS what it is today!

This book is logically structured into six well-coordinated and balanced sections. Their contents cover a broad spectrum of the current R&D status of CAS in musculoskeletal surgery and related fields. Brief comments on each section may help in guiding the readership in surgery, bioengineering and the related clinical fields.

Preoperative Planning: Using computer-aided segmental allograft transplantation in osteotomy and limb salvage surgery, the model-building process for the grafts available in bone banks and the recipient host skeletal structure are presented as a lead chapter to describe the preoperative planning process for CAS. Although precision may be less desirable due to the inevitable system and image data errors, human musculoskeletal structure is capable to adjust for the motion and load-bearing requirements. The computerized tools for allograft selection, size-matching, fixation device selection, registration, and reconstruction have made the concept of "Digital Bone Bank and Computer-aided Graft Transplantation" first conceived in the 1990s, now a clinical reality! Virtual testing under static and cyclic loading became a new concept more than a decade ago which allowed both time and cost saving. However, real models on a testing machine or a wear simulator are necessary to verify the results. To minimize long-term side effects caused by wear particles, ex vivo and in situ animal models must be utilized. Finally, clinical trial studies of sufficient follow-up length remain the gold standard to assure safety and efficacy when new material or implant designs were first introduced.

Surgical Navigation: The contributors of this section have done a remarkable job of reviewing and introducing the field of surgical navigation in orthopaedics.

Their comprehensive and clear deliberations on the potential pitfalls of this technology are worthy for the surgical robot industry to note and rectify their claims. To justify its medical application, this technology should be evaluated based on its efficacy, safety, cost, and reliability. It should be noted that surgery is still regarded as an art by many. The ability to visualize the operative field in 3D while able to feel and manipulate vital anatomical parts by the surgeons' hands during surgery cannot be duplicated by the robot. Therefore, surgical navigation and robot technology is intended to aid the experienced surgeons, not to replace them.

Local Ablation of Bone Tumor – Using heat or extreme cold to ablate local tumorous tissues en bloc leaving the devitalized bony structure as a scaffold to facilitate biological reconstruction has been in clinical trial for decades. However, the optimal dosages of these physical energies, their practical and effective implementation technique for different tumor types and extent to minimize local recurrence of the malignant process have not been worked out satisfactorily and thus prevented a wide utilization. In difficult anatomical locations, where en bloc resection of cancer-afflicted region is impossible, local ablation using diffusible energy source to allow the therapeutic effect reaching beyond the anticipated resection volume while able to protect the adjacent vital organ function would be a monumental advance in orthopaedic oncology! The use of CAS technology can accomplish these goals through biomechanical and heat-transfer analyses to optimize the thermal energy delivery in the pretreatment planning and execution strategy. Ultimately, when such technology becomes successful and reliable in orthopaedic application, it can easily be transferred to other oncologic fields.

Custom Implants: In revision surgery after failed joint replacement prosthesis with massive bone loss and after bone tumor resection, the use of custom implant is an important service to save the patient's limb. The argument for patient-specific implant design and surgical guidance cannot be over emphasized due to the bone and soft tissue deficiency heavy loading demands which may lead to implant failure and poor joint function. Although orthopaedic device companies have always regarded such service as an act of charity, disputes sometimes ensued due the high cost involved if the anticipated results and durability of the implant were less desirable. Occasionally, the issue of inadequate implant fit in difficult bone tumor cases due to intraoperative change of resection margin would lead to unacceptable reconstruction. Hence, it would be hard to expect that the technology of CAS will be able to resolve these difficulties. It is time to explore biological reconstruction using patient's own bone stock as scaffold after local en bloc tumor ablation.

Validation in Computer-assisted Surgical Workflow: Virtual model formation, the operative planning strategy, and surgical guidance of implant placement used in CAS must all be carefully evaluated for their accuracy and adequacy. In addition, the efficacy of the proposed technology should be supported by the results of evidence-based clinical studies. In musculoskeletal reconstructive surgery, it is important that the planning strategy will be based on biomechanical analysis to assure the functional requirements in terms of safety and durability with no long-term side effects. In the justification of any new technology, cost factors must also enter into the overall assessment process.

Emerging Trends and Applications: The 3D projection-based navigation using that consist in overlapping skeletal and soft tissue images with implant and pathology data is an attractive and powerful tool for operative guidance. This may even be more useful in a teaching or training scenario combined with tactile and sensory feedbacks. The inclusion of CMS (cranio-maxillofacial surgery) in this section is commendable due to its large patient population while the same technology and biomechanical analysis can be readily shared to save cost. The use of a pure-axial quasi-static tractive force to assess spinal flexibility in scoliotic patients is an interesting concept which may be helpful to the recent development of the remote-controlled spinal curvature correction rod in adolescent idiopathic scoliosis (AIS) patients with severe deformity. However, there are other important factors and problems in treating scoliosis patients both in the adolescent and adult population that need be addressed. In nonoperative management of AIS patients with mild to moderate deformity, adjustable braces that are designed and applied based on computer-assisted analysis and corrective strategy can be an exciting and beneficial trend for CAS. Furthermore, some of the high-return and low-risk clinical applications of CAS in orthopaedics not mentioned in this book deserve brief introduction as follows.

1. *Fracture Reduction and Deformity Correction using External Robot*: In the 1970s and 1980s, the use of external fixator (EF) of various designs and clinical applications became wide spread in trauma and orthopaedic fields. Computer-aided fracture reduction, adjustments, stimulation and callus distraction planning and execution treating the fixator as an external robot were introduced in the early 1990s. Unfortunately, owing to the strong development and marketing effort of the internal fixation devices, the EF field faced a dramatic decline. The revival of EF method in orthopaedics and traumatology is evidenced in the chapters presented in this section. Three-dimensional joint osteotomy has become a reality as presented here. With a single closed or open wedge through a gradual callus distraction (EF devices) or an one-step correction procedure performed open using a computer-aided quick prototyping custom wedge-cutting instrument block are now well in their clinical trial. This indeed is a remarkable landmark achievement in orthopaedics! Although, consecutive hinge joints in a fixator can achieve the needed single angular correction with respect to the screw axis, the extra space requirement makes it bulky and not convenient for clinical usage. Similar corrections can also be achieved using redundant linear displacement actuators, such as the Taylor Frame®. The application of the "virtual hinge" concept or an instrumented ball-and-socket joint can achieve the same angular correction and bone length adjustment while able to make the external robot slim, easy to adjust, and improve the patient's daily activities. These advances are expected to bring the EF technology back to orthopaedics, thanks to the concept of computer-assisted surgery.

2. *Minimal Invasive Tissue Engineering* – Based on the science and technology of bone fracture tendon to bone junction healing augmentation using biophysical stimulation, it would be quite possible that these connective tissues' properties and composition can be manipulated to facilitate the highly sought for tissue engineering process. If the biomechanical and morphological properties of bone, tendon, cartilage, vessels, and even the nerve could be monitored noninvasively during distraction, compression or angular deformation under external immobilization, minimally invasive tissue, or structure regeneration will become a reality. All these could be worked using the fixator as a robot. The energy field of proper intensity and pulse frequency produced either by ultrasound or electromagnetic power may also carry a pain control effect making this difficult and painful procedure more acceptable to the patients. This innovative application can greatly enhance bioengineering's contribution to health care.
3. *Computer-Assisted Rehabilitation* – Although it may seem that such application would be out of the scope of this book, it is a well-recognized fact that the success of any major orthopaedic procedure would depend on safe and effective postoperative care through rehabilitation. The same modeling, analysis, and execution technology used in CAS can easily be adapted here making it a new field. In addition, the emphasis on conservative management and injury prevention will be the spin-off benefits for patients suffering pain and dysfunction due to skeletal and joint trauma, deformity, and degeneration.

To conclude this commentary essay in support of CAS in musculoskeletal surgery, it is pertinent to briefly address some of the nonmedical issues related to these technical innovations. The concept of CAS and its technology were largely stimulated and complemented by the game and entertainment industry, although each carries an entirely different motivation and ethics. When medical technology is transformed from bench top to bedside and for general dispersion, the manufacturing firms cannot avoid being contaminated by bias and commercialism. Though such accusation may seem unfair and even altruistic, unproven and ill-justified application with unsubstantiated claims have caused unpleasant and even serious consequences leading to legal and economic dispute, which had eroded their noble intent of do no harm to humankind. Bioengineering effort of the past, present, and future may also fall into this trap without recognizing its inherent limitations and primary obligations to medicine professionals! A special value concept based on the balance of efficacy, safety, durability, education, and cost should be worked out and adhered to beyond the government enforced regulatory guidelines for any medical technology! Hence, it is of vital importance that CAS or any other technology-driven innovations be extremely cautious and take a rather conservative attitude in promoting their clinical claims. Therefore, a self-induced jurisprudence is necessary for the bioengineers, their collaborating physicians, and industry. Finally, I wish to leave three questions to the readership and the contributors of this book that

are derived from the true history of the two Mayo Clinic clinical scientists, Philip Hench and Edward Kendall, the winners of the 1950 Nobel Prize in Medicine for the discovery of corticosteroids who willingly relinquished the patent right of cortisone process to the US government for $1!

Should medical discoveries be allowed to be patented?

Should advertisement and marketing of any medical advances be outlawed?

Should the practice of medicine and surgery be awarded according to the outcome?

It will be interesting to speculate what medical advancement and the quality of care would be like if the answers of these questions were all positive!

Corona, CA, USA Edmund Y.S. Chao, PhD
April 15, 2015

Contents

Part I Preoperative Planning

1 Virtual Preoperative Planning 3
Lucas E. Ritacco

2 Computerized Tools: Allograft Selection 9
Habib Bousleiman

3 Computer Guided Navigation and Pre-operative Planning for Arthroscopic Hip Surgery 17
Simon Lee, Asheesh Bedi, Shane J. Nho, and Alejandro A. Espinoza Orías

4 Virtual Cranio-Maxillofacial Surgery Planning with Stereo Graphics and Haptics 29
Ingela Nyström, Pontus Olsson, Johan Nysjö, Fredrik Nysjö, Filip Malmberg, Stefan Seipel, Jan-Michaél Hirsch, and Ingrid B. Carlbom

5 Computational Image-Guided Technologies in Cranio-Maxillofacial Soft Tissue Planning and Simulation 43
Mauricio Reyes, Kamal Shahim, and Philipp Jürgens

Part II Surgical Navigation

6 Introduction to Surgical Navigation 59
Kwok-Chuen Wong

7 Bone Tumor Navigation in the Pelvis 71
Lee Jeys and Philippa L. May

8 Bone Tumor Navigation in Limbs 89
German L. Farfalli and Luis A. Aponte-Tinao

9 Direct Navigation of Surgical Instrumentation 99
O. Andres Barrera and H. Haider

10 Navigation in Spinal Surgery 115
Joseph H. Schwab

11 Knee Prosthesis Navigation 129
Andrea Ensini, Michele d'Amato, Paolo Barbadoro, Claudio Belvedere, Andrea Illuminati, and Alberto Leardini

12 Local Tumor Ablation Using Computer-Assisted Planning and Execution 151
Jasper G. Gerbers, E.D. Dierselhuis, and P.C. Jutte

Part III Custom Implants

13 Patient-Specific Instruments in Orthopedics 163
Paul Laurent

14 Custom Implants 181
Paul S. Unwin and Abtin Eshraghi

15 Patient's Specific Template for Spine Surgery 199
Paolo D. Parchi, Gisberto Evangelisti, Valentina Cervi, Lorenzo Andreani, Marina Carbone, Sara Condino, Vincenzo Ferrari, and Michele Lisanti

Part IV Robotics

16 The Use of ROBODOC in Total Hip and Knee Arthroplasty 219
Nathan A. Netravali, Martin Börner, and William L. Bargar

17 A Comparative Study for Touchless Telerobotic Surgery 235
Tian Zhou, Maria E. Cabrera, and Juan P. Wachs

Part V Validation in Computer-Assisted Surgical Workflows

18 Accuracy and Precision in Computer-Assisted Methods for Orthopaedic Surgery 259
Federico E. Milano and Olivier Cartiaux

Part VI Emerging Trends

19 Computer Simulation Surgery for Deformity Correction of the Upper Extremity 271
Tsuyoshi Murase

20 Spinal Loading System: A Novel Technique for Assessing Spinal Flexibility in Adolescent Idiopathic Scoliosis 293
Marcelo Elias de Oliveira, Daniel Brandenberger, Daniel Studer, Jacques Schneider, Carol-Claudius Hasler, and Philippe Büchler

21 3D Projection-Based Navigation 303
Kate A. Gavaghan and Matteo Fusaglia

Afterword 315

Index 319

Contributors

Lorenzo Andreani, MSc, PhD 1st Orthpedic and Traumatology Division – Department of Traslational Research and New Technology in Medicine and Surgery, University of Pisa, Pisa, Italy

Luis A. Aponte-Tinao, MD Orthopaedics and Traumatology, Hospital Italiano de Buenos Aires, Buenos Aires, Argentina

William L. Bargar, MMAE Department of Orthopaedics, Sutter Joint Replacement Center, University of California at Davis School of Medicine, Sutter General Hospital, Sacremento, CA, USA

Andres Barrera, PhD (Med S), MSc (CompS), BioEng Orthopaedic Surgery and Rehabilitation, University of Nebraska Medical Center, Omaha, NE, USA

Asheesh Bedi, MD Department of Orthopaedic Surgery, University of Michigan, Ann Arbour, MI, USA

Martin Börner, MD Chairman of the Board, Dr. Erler Clinics, Nuremberg, Germany

Retired, Berufsgenossenschaftliche Unfallclinic (BGU) Frankfurt, Frankfurt am Main, Germany

Habib Bousleiman, PhD Institute for Surgical Technology and Biomechanics, University of Bern, Bern, Switzerland

Daniel Brandenberger Department of Orthopaedics, University Children's Hospital Basel, Basel, Switzerland

Philippe Büchler Computational Bioengineering Group, Institute for Surgical Technology and Biomechanics, University of Bern, Bern, Switzerland

Maria E. Cabrera School of Industrial Engineering, West Lafayette, IN, USA

Marina Carbone, MSc, PhD EndoCAS – Department of Translational Research and of New Surgical and Medical Technologies, University of Pisa, Pisa, Italy

Ingrid B. Carlbom Department of Information Technology, Centre for Image Analysis, Uppsala University, Uppsala, Sweden

Olivier Cartiaux, Ir, PhD Computer Assisted and Robotic Surgery, Institut de Recherche Expérimentale et Clinique, Université Catholique de Louvain, Brussels, Belgium

Valentina Cervi, MSc 1st Orthpedic and Traumatology Division – Department of Traslational Research and New Technology in Medicine and Surgery, University of Pisa, Pisa, Italy

Edmund Chao, PhD John Hopkins University, Baltimore, MD, USA

Sara Condino, MSc, PhD EndoCAS – Department of Translational Research and of New Surgical and Medical Technologies, University of Pisa, Pisa, Italy

E.D. Dierselhuis Department of Orthopedics, University Medical Center Groningen, Groningen, The Netherlands

Marcelo Elias de Oliveira, BSc, MSc, PhD Institute of Microengineering, Laboratory of Robotics System, Swiss Federal Institute of Technology Lausanne, EPFL STI IMT LSRO, Lausanne, Switzerland

Graduate School for Cellular and Biomedical Sciences, University of Bern, Bern, Switzerland

Abtin Eshraghi, MEng Stanmore Implants Worldwide Ltd, Elstree, UK

Alejandro A. Espinoza Orías, PhD Spine Biomechanics Laboratory, Department of Orthopedic Surgery, Rush University Medical Center, Chicago, IL, USA

Hip Preservation Center, Division of Sports Medicine, Department of Orthopedic Surgery, Rush University Medical Center, Rush Medical College of Rush University, Chicago, IL, USA

Gisberto Evangelisti, MSc 1st Orthpedic and Traumatology Division – Department of Traslational Research and New Technology in Medicine and Surgery, University of Pisa, Pisa, Italy

German L. Farfalli, MD Orthopaedics and Traumatology, Hospital Italiano de Buenos Aires, Buenos Aires, Argentina

Vincenzo Ferrari, MSc, PhD EndoCAS – Department of Translational Research and of New Surgical and Medical Technologies, University of Pisa, Pisa, Italy

Matteo Fusaglia, MSc, BEng Image Guided Therapy, ARTORG Center for Biomedical Engineering Research, University of Bern, Bern, Switzerland

Kate A. Gavaghan, PhD, BSc, Beng Image Guided Therapy, ARTORG Center for Biomedical Engineering Research, University of Bern, Bern, Switzerland

Jasper G. Gerbers Department of Orthopedics, University Medical Center Groningen, Groningen, The Netherlands

H. Haider, PhD Orthopaedics Biomechanics & Advanced Surgical Technologies Laboratory, Department of Orthopaedic Surgery and Rehabilitation, University of Nebraska Medical Center, Omaha, NE, USA

Carol-Claudius Hasler Department of Orthopaedics, University Children's Hospital Basel, Basel, Switzerland

Jan-Michaél Hirsch Department of Surgical Sciences, Oral and Maxillofacial Surgery, Uppsala University, Uppsala, Sweden

Lee Jeys, MB, ChB, MSc (Ortho. Eng), FRCS Royal Orthopaedic Hospital, Birmingham, UK

Philipp Jürgens Department of Cranio-Maxillofacial Surgery, University Hospital Basel, Basel, Switzerland

P.C. Jutte Department of Orthopedics, University Medical Center Groningen, Groningen, The Netherlands

Paul Laurent, PhD, Ir 3-D-Side, Louvain-La-Neuve, Belgium

Simon Lee, MPH, MD Department of Orthopaedic Surgery, University of Michigan, Ann Arbor, MI, USA

Michele Lisanti, MSc 1st Orthpedic and Traumatology Division – Department of Traslational Research and New Technology in Medicine and Surgery, University of Pisa, Pisa, Italy

Filip Malmberg Department of Information Technology, Centre for Image Analysis, Uppsala University, Uppsala, Sweden

Phillippa L. May, BMedSci (Clin Sci), MBChB College of Medical and Dental Sciences, University of Birmingham, Edgbaston, UK

Federico E. Milano Department of Bioengineering, Instituto Tecnologico de Buenos Aires, Buenos Aires, Argentina

Tsuyoshi Murase, MD, PhD Department of Orthopaedic Surgery, Osaka University, Graduate School of Medicine, Suita, Osaka, Japan

Nathan A. Netravali, PhD Think Surgical, Inc., Fremont, CA, USA

Shane J. Nho, MD, MS Hip Preservation Center, Division of Sports Medicine, Department of Orthopedic Surgery, Rush University Medical Center, Chicago, IL, USA

Frederik Nysjö Department of Information Technology, Centre for Image Analysis, Uppsala University, Uppsala, Sweden

Johan Nysjö Department of Information Technology, Centre for Image Analysis, Uppsala University, Uppsala, Sweden

Ingela Nyström, PhD, Docent Department of Information Technology, Centre for Image Analysis, Uppsala University, Uppsala, Sweden

Pontus Olsson Department of Information Technology, Centre for Image Analysis, Uppsala University, Uppsala, Sweden

Paolo D. Parchi, MSc, Phd 1st Orthpedic and Traumatology Division – Department of Traslational Research and New Technology in Medicine and Surgery, University of Pisa, Pisa, Italy

Mauricio Reyes Institute for Surgical Technology and Biomechanics, University of Bern, Bern, Switzlerland

Lucas E. Ritacco, MD, PhD Computer-Assisted Surgery Unit, Hospital Italiano de Buenos Aires, Buenos Aires, Argentina

Jacques Schneider Department of Orthopaedics, University Children's Hospital Basel, Basel, Switzerland

Department of Paediatric Radiology, Children's Hospital Basel, Basel, Switzerland

Joseph H. Schwab, MD, MS Department of Orthopaedics, Massachusetts General Hospital, Boston, MA, USA

Stefan Seipel Department of Information Technology, Centre for Image Analysis, Uppsala University, Uppsala, Sweden

Kamal Shahim Institute for Surgical Technology and Biomechanics, University of Bern, Bern, Switzlerland

Daniel Studer Department of Orthopaedics, University Children's Hospital Basel, Basel, Switzerland

Paul S. Unwin, BSc (Hons), MSc, PhD Stanmore Implants Worldwide Ltd, Elstree, UK

Juan P. Wachs, BEdTech, MSc, PhD School of Industrial Engineering, West Lafayette, IN, USA

Kwok-Chuen Wong, FRCSEd (Ortho) Department of Orthopaedics and Traumatology, Prince of Wales Hospital, Hong Kong, China

Andrea Ensini 1st Clinic Orthopaedic and Traumatology, Istituto Ortopedico Rizzoli, Bologna, Italy

Michele d'Amato Division of Orthopaedic Surgery, Rizzoli Orthopaedic Institute, Bologna, Italy

Paolo Barbadoro Division of Orthopaedic Surgery, Rizzoli Orthopaedic Institute, Bologna, Italy

Claudio Belvedere Movement Analysis Laboratory, Rizzoli Orthopaedic Institute, Bologna, Italy

Andrea Illuminati Movement Analysis Laboratory, Rizzoli Orthopaedic Institute, Bologna, Italy

Alberto Leardini Movement Analysis Laboratory, Rizzoli Orthopaedic Institute, Bologna, Italy

D. Luis Muscolo, MD, PhD, Honorary Chairman, Department of Orthopaedics, Italian Hospital of Buenos Aires, Buenos Aires, Argentina

Miguel A. Ayerza, MD, PhD, Chairman Orthopaedic Oncology Section, Department of Orthopaedics, Italian Hospital of Buenos Aires, Buenos Aires, Argentina

Part I
Preoperative Planning

Chapter 1
Virtual Preoperative Planning

Lucas E. Ritacco

Abstract Virtual Preoperative Planning (VPP) involves a group of virtual tools that help surgeons to determine structures in a virtual scenario. Furthermore it allows to define distances and oncology margins in 2D and locate this measurements in the 3D space. In this way, it is possible to interact with medical images and create virtual osteotomies.

Although we believe that this tool is powerful, the key to that is to integrate VPP with weekly meetings in order to improve the analysis of the cases before surgery.

In this manner a group of professionals could discuss technical aspects.

Indirectly we save time in the operating room and lead to a more predictable procedure.

Keywords Preoperative planning • Computer aid surgery • Virtual scenario • Navigation surgery • Bone tumor navigation

The concept of Virtual Preoperative Planning (VPP) is a digital platform to visualize and interact with medical images [1–3]. Magnetic resonance imaging (MRI), 2D tomography and 3D tomography, are integrated in the same simulation scenario. Thus, it is possible to overlap MRI with CT or 3D-CT; this functionality is called image fusion [4, 5]. Through this method the surgeon is able to visualize the tumour behaviour and the compromised structures at three-dimensional rendering. At the same time, VPP allows comparing the similarities between 2D images and 3D anatomical models. Moreover, it is possible to merge angio tomography and the vascular tree together. In this way, the surgeon can visualize a 3D bone model, together with the tumour, arteries and veins. Although VPP is a novel application for physicians, they still have the option to compare, both 3D anatomical modes with 2D image slices (which they are more familiarised with) in the same scenario.

Furthermore, the surgeon can interact with the 3D scenario not only to indentify structures but also to execute virtual osteotomies on the bone tissue in order to gather accurate information about the surgical site (Fig. 1.1).

L.E. Ritacco, MD, PhD
Computer-Assisted Surgery Unit, Hospital Italiano de Buenos Aires,
Potosi 4247, Buenos Aires C1199ACK, Argentina
e-mail: ritacco.lucas@gmail.com; Lucas.ritacco@hiba.org.ar

L.E. Ritacco et al. (eds.), *Computer-Assisted Musculoskeletal Surgery: Thinking and Executing in 3D*, DOI 10.1007/978-3-319-12943-3_1

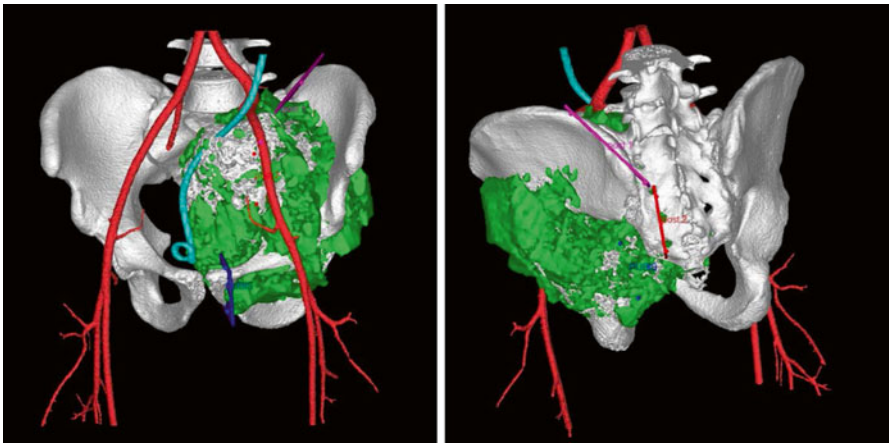

Fig. 1.1 Preoperative virtual planning. Pelvis tumor planned with 3 planes

Advantages

- Obtain real anatomic three-dimensional information.
- Compare conventional 2D images with 3D models.
- Interact with 3D models.
- Plan an oncological margin in a three-dimensional environment.
- Plan an osteotomy, surgical approach or place an implant.

Drawbacks

This study cannot be done optimally with images acquired for diagnosis. 3D reconstructive resolution is subjected to the way in which the image has been acquired in tomography and MRI. To reach an adequate resolution in 3D we need to adjust acquisition for tomography images and MRI protocol within 1 mm or smaller cuts and modify some other specific parameters of reconstructing three-dimensional relevant regions.

Moreover, some VPP limitations are due to the tomography or MRI, such as oncology margin determination. This is going to be limited on what we call suspicious image in nuclear magnetic resonance (MRI). Tumour images in MRI is an indirect acquisition, that is, we can only see a shadow left by the tumour in healthy tissue and we cannot see tumour activity site in the image directly. Although positron emission tomography (PET Scan) allows to see cellular activity, the image is not accurate enough for millimetre oncology margin measurement. Suspicious images can also be generated due to MRI signal changes by peri-tumoral liquid, post chemotherapy changes or radiotherapy. In this case, specialists are to define definitive oncology margin limits in MRI.

Fig. 1.2 (**a**) Preoperative planning meeting defining margins and planar conformation. (**b**) Surgeon in OR, executing the osteotomy previously planned

Instructions

First VPP instruction is on tumour injuries either to state the length in big injuries or anatomic three-dimensional situation in smaller injuries [6].

Visualizing tumour location before surgery in anatomic space is useful to take decisions about surgical techniques.

Head and neck cases in need of VPP are usually tumours located in complex anatomic sites, generally demands several medical specialists teams.

Holding meetings involving different specialists turns VPP into a tool for exchanging knowledge between several fields and help diagramming surgical logistic (Fig. 1.2).

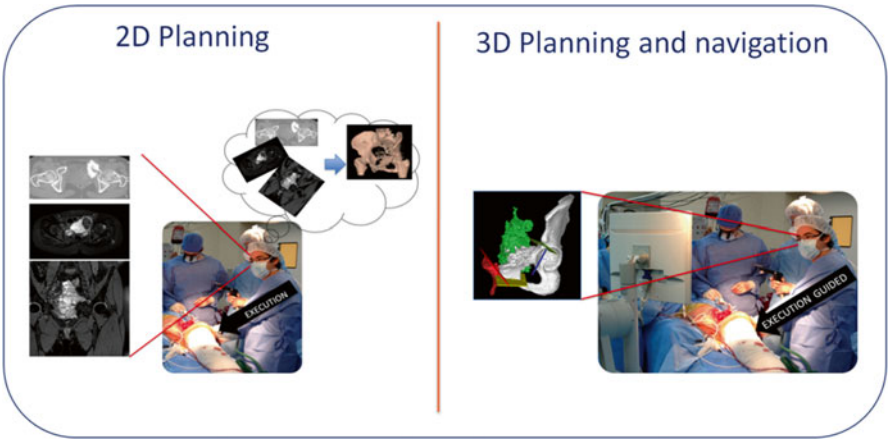

Fig. 1.3 Two dimensional planning implies an extra mental effort. However virtual navigation allows to surgeons to apply 3D Planning previously planned

At these meetings issues about patient positioning, boarding and types of instruments are discussed. This kind of information helps to diagram and organize surgical methodology at complex interventions. In other words, we are indirectly saving time in the operating room and leading to a more predictable procedure (Fig. 1.3). This techniques affect directly on the quality of the intervention.

What Is Virtual Preoperative Planning?

In order to obtain a VPP it is necessary to recreate anatomic structures in 3D.

This technique includes three steps:

1. *Image acquisition step*:
   Every patient suffering from bone sarcoma is evaluated with tomography and nuclear magnetic resonance. Toshiba Aquilion (Japan) tomograph has been used according to the following acquisition plan: 512×512 pixels matrix, pixel length average: 0.5 mm, cuts of 0.5 mm thick every 0.5 mm, magnified focus on bone tumour. Resonance 1.5 T, Magnetom Avanto, Siemens (Germany) was used acquiring images in time T1 and T2 with 265×265 pixels matrix, pixel length average: 0.7 mm and cuts of 0.1 mm thick every 0.1 mm, magnified focus on bone tumour. Images were stored in DICOM digital format.
2. *Image segmentation step:*
   Once the image files are acquired, these are imported into a medical image processing software. In the tomography images the objective is to remove elements that may appear to be bones but they are not. This can be obtained establishing a colour metric value. The colour distinction aims to dismiss other elements such as muscle, fat, skin, etc. The procedure is called image segmentation and it is done

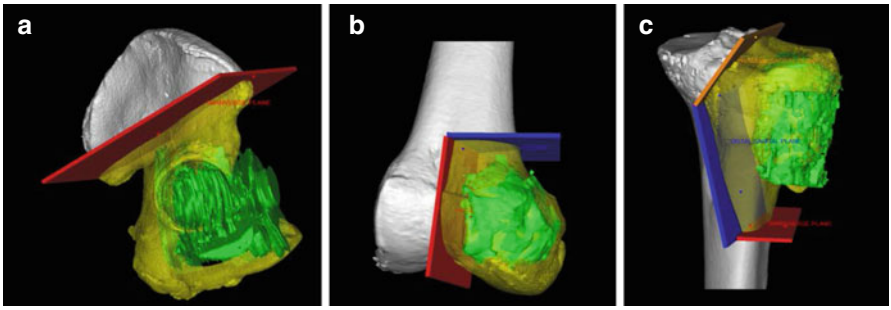

Fig. 1.4 Planar conformation for bone tumor resection. (**a**) Uniplanar. (**b**) Biplanar. (**c**) Multiplanar

manually. By eliminating structures that could alter the bone tissue shape the process determines the final bone reconstruction. That is how bone surface area will be reconstructed colouring each segment from tomography images. However, tumour volume will be segmented since magnetic resonance.

3. *Tomography and resonance fusion step:* due to the difference between the tomography coordinate system and the resonance system, at this step we have to produce the fusion of both segmented images volumes. It is also done manually, verifying that sagittal, axial and coronal slices correspond accurately in both images. After fusion process, the next step is three-dimensional reconstruction of bone and bone tumour.
4. *3D Preoperative Planning step:* Once the images from tomography and resonance are together, a team of orthopaedic oncology experts planned each step for determining the saw path (cutting planes) in three-dimensions. The thickness of the saw (2 mm) has been considered in the virtual planning. According to the length of the tumour the types of osteotomy virtually planned have been divided into uniplanar, biplanar and multiplanar (Fig. 1.4).

   Oncology margin has been calculated in bi-dimensional images from tomoresonance fusion. It expresses the existing distance between: nearest spot of the tumour to cutting plane, which is created by the side of the saw facing the tumour. We call this distance minimum margin.

   Minimum margin will be calculated for each osteotomy plan in millimetres. That is to say, there will be only one minimum margin in uniplanar osteotomies, therefore there will be four minimum margins in cuadriplanar osteotomies.

Conclusions

Planning a tumor resection days before surgery in a virtual scenario involves a mental exercise that helps the surgeon to have more information before surgery, avoiding purely technical contingencies and surgical errors.

This visual exercise of planning must be added to the guidance by intraoperative navigation. This procedure potentially shortens surgical times since it allows the

surgeon to invest time in planning and then be guided in executing a clean geometric osteotomy while preserving optimum margins in the tumor resection.

References

1. Chao EY. Graphic-based musculoskeletal model for biomechanical analyses and animation [Research Support, Non-U.S. Gov't Research Support, U.S. Gov't, Non-P.H.S.]. Med Eng Phys. 2003;25(3):201–12.
2. Chao EY, Armiger RS, Yoshida H, Lim J, Haraguchi N. Virtual Interactive Musculoskeletal System (VIMS) in orthopaedic research, education and clinical patient care. J Orthop Surg Res. 2007;2:2. doi:10.1186/1749-799X-2-2.
3. Chao EY, Barrance P, Genda E, Iwasaki N, Kato S, Faust A. Virtual reality (VR) techniques in orthopaedic research and practice. Stud Health Technol Inform. 1997;39:107–14.
4. Wong K, Kumta S, Tse L, Ng E, Lee K. Image fusion for computer-assisted tumor surgery (CATS). Image Fusion. 2011: 373–90.
5. Wong KC, Kumta SM, Antonio GE, Tse LF. Image fusion for computer-assisted bone tumor surgery. [Evaluation studies]. Clin Orthop Relat Res. 2008;466(10):2533–41. doi:10.1007/s11999-008-0374-5.
6. Ferrari V, Carbone M, Cappelli C, Boni L, Melfi F, Ferrari M, Mosca F, Pietrabissa A. Value of multidetector computed tomography image segmentation for preoperative planning in general surgery. Surg Endosc. 2012;26(3):616–26. doi: 10.1007/s00464-011-1920-x.

Chapter 2
Computerized Tools: Allograft Selection

Habib Bousleiman

Abstract Various techniques for defect reconstruction after oncologic orthopaedics surgery exist, and the use of each technique vary depending on the complexity of the case. Biological reconstruction in great defects is a huge challenge for orthopaedics due to the high complication rate. However, bone allografts are highly recommended for major defects especially in younger patients. Clinical reports propose that this technique preserves the durability of bone stock and limb functionality plus a responsible handling of bone banks decreases loss of the usually scarce cadaver bone stock. Access to allografts has been improved owing to centralised bone banks, which develop threedimensional copies for storage and use them for the selection process. Virtual modelling has been recently demonstrated to be a potential predictor to select adequate allograft in preoperative virtual planning. Moreover, shape matching is the foremost method for proper allograft selection.

Manual selection based on key measurements has been for years the industry standard. Computerized manual selection has developed so as to step forward in the allograft selection process. Donors stock can be compared with the patient's anatomy and make the selection more accurate than before. This chapter will depict the optimistic results of using automatic allograft selection method based on surface registration.

Keywords Defect reconstruction • Biological reconstruction • Centralised bone banks • Three dimensional allografts • Shape matching • Computerised manual selection

Introduction

Bone resection and consecutive reconstruction is an accepted surgical procedure in a wide number of patients suffering from malignant bone tumours or traumatic defects. Various reconstruction methods exist, and the applicability of each of the methods is a strictly case-dependent decision [1].

H. Bousleiman, PhD
Institute for Surgical Technology and Biomechanics, University of Bern,
Stauffacherstrasse 78, Bern 3014, Switzerland
e-mail: bousleiman.habib@gmail.com

L.E. Ritacco et al. (eds.), *Computer-Assisted Musculoskeletal Surgery: Thinking and Executing in 3D*, DOI 10.1007/978-3-319-12943-3_2

Biological reconstructions in great defects following tumour resection is a major challenge of oncologic orthopaedics. Despite their high complication rate and their relative slow incorporation into the host bed, massive bone allografts are recommended for great defect cases. Clinical reports suggest that this approach preserves the long-term bone stock and limb functionality [1–5]. Furthermore, long-term follow-up studies support and promote the use of allografts instead of prosthetic implants especially in younger patients [2, 5–7]. A good allograft also facilitates and enhances the fitting procedure of the fixation plate(s). Furthermore, optimal handling of the bone bank ensures minimal loss of the usually scarce cadaver bone stock.

A poor anatomical matching between the host and the donor can alter the joint kinematics and load distribution, leading to articular fractures or joint degeneration [3, 8]. Therefore, size and shape determination is critical to obtain an appropriate allograft [9].

Access to bone allografts was facilitated with the development of centralised bone banks where bones are collected from cadavers, fresh-frozen for storage, and distributed to medical centres [10]. The bank systems sometime digitally store three-dimensional copies of the bones and use them for the selection process. However, the task of selecting a suitable allograft remains a major challenge [11].

Recent studies demonstrated that a virtual model is a potential predictor to select the adequate allograft in a preoperative planning environment [12, 13]. Furthermore, shape matching is the chief method to be considered when a proper allograft is to be selected [11, 13–15].

This chapter is a compiled description of recent developments in the area of computerised selection of allografts and related surgical planning (Ritacco [9], [13, 15–17]). The methods take advantage of modern computer hardware and software in order to carry out computationally demanding processes in reasonable amounts of time. More importantly, the methods aimed to assist in the decision-making and improve the prognosis of the interventions.

Preoperative Preparation

When faced with a bone resection case, surgeons must first decide for which reconstruction method they would opt. Cadaveric implants is a recommended option for several cases, especially for younger patients. Bone banks operate as suppliers of biological bone implants. They collect bone or bone parts from cadavers of organ donors and store them adequately. Upon the request of the operating surgeons, they browse through the bone stock and deliver the part deemed most suitable for the patient.

The bottleneck in this model stands in the selection process. Simple manual selection based on key measurements supplied by the surgeon or radiologist has been for a long time the industry standard. Bone banks are occasionally supplied with radiographs to have additional information about the target shape of the implant.

One step ahead of manual measurement is the computerised manual selection (Ritacco et al. [9]). In this approach, the donor stock is digitised and stored in the form of three-dimensional computer models. Various morphometric dimensions

could be extracted in a virtual environment. More importantly, donor bones could be compared side-by-side to the model of the patient's anatomy. This boosts the flexibility of the process and allows for a higher throughput and more accurate selection. Nevertheless, the bulk part of the work is to browse through all available donor bones and rate them for suitability for the specific case. The visual inspection is often augmented by virtual measurement to increase accuracy.

Paul et al. [15] presented a template-based method in which a two-dimensional outline of the target anatomy is printed on transparent paper. The outline is then placed on two-dimensional projections of the available donor bones. The adequate allograft is selected based on a visual judgement of matching quality. In this method the projections limit the perspective to one or few viewports, hence missing morphological aspects that might be of crucial importance for the success of the intervention. Moreover, the method was illustrated by the selection of a whole hemi-pelvis, a rather non-realistic scenario.

In a more recent attempt Paul et al. [13] used image-to-image volume registration approach. In this method a binary mask of the target implant is rigidly registered in the image or voxel space to all bones in the database. Measurements quantifying the quality of the matching are subsequently recorded and used to rank the donors. The method shares the same pitfall of the template-based selection as it was also presented for the whole hemipelvis. However, the reported results were superior in terms of speed, quality, and reliability, to those obtained using the template method.

In the following section, a novel allograft selection method based on 3D surface registration will be described. An elaborate evaluation and comparison to the methods presented above is also presented.

Technique with Pearls and Pitfalls

This section introduces a surface-based registration method for the selection of cadaveric allografts from a digital bone bank. The method was first described in Bou Sleiman et al., 2011 and aimed to speed-up and improve the results of the selection of the allograft that best matches the patient-specific anatomy. It was designed and evaluated for the cases of transepiphyseal tumor resection around the knee, i.e., in the distal femur and proximal tibia, a site that presents high incidence of bone malignancies (Bielack et al. [18]; Paulussen et al. [19, [2]).

Unlike selection methods described elsewhere [13, 15], this method mimics clinically realistic scenarios. It was initially presented for intercalary implants around the knee and did not assume that the target anatomy is known beforehand. The target anatomy is usually deformed due to trauma or the presence of a tumor. The selection approach extracts the target anatomy from the contralateral limb of the patient. It was later extended to be applied on intercalary implants of the pelvis and compared to other manual and automatic methods in a separate study (Bousleiman et al. [16]).

The method takes advantage of the concept of contralateral limb symmetry (Ritacco et al. [9]; Schmidt et al. [20]; Seiler et al. [21]) to reconstruct the original

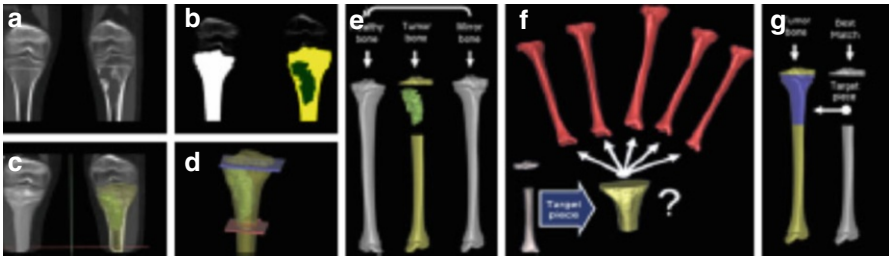

Fig. 2.1 Processing pipeline. (**a**) Original CT image. (**b**) Segmentation mask. (**c**) 3D reconstruction of the tibiae and the tumour. (**d**) Cutting out the tumour in a virtual environment. (**e**) Illustration of the similarity between the diseased bone and the mirrored version of the contralateral tibia. (**f**) Illustration of how the template matching algorithm searches through the virtual bone database. (**g**) Illustration of the good fit of a part cut out from the best matching tibia and placed at the location of the resected section (With kind permission from Springer Science and Business Media)

shape of a diseased portion of the bone. A template corresponding to the location of the tumour is extracted from the patient's healthy contralateral bone. An iterative three-dimensional template matching process is then applied through the virtual cadaver bone databank to locate bone portions that resemble the template in terms of both morphology and scale.

System testing and validation was carried out by simulating clinical cases from the available data. The method presented herein was developed, tested, and validated using a set of 50 patient CT images of the lower limbs (varying image parameters and scanners). The bones were semi-automatically segmented using Amira® (Visage Imaging, Inc., San Diego, CA, USA), and stored in the form of surface point models and surface meshes (vertices per sample – tibiae: 42,004; femora: 58,837). This data is regarded as a digitally stored cadaver bone databank, in analogy to the one presented in Ritacco et al. [9]. From this point onward, we will be referring to those bones as cadaver bones.

The overall application of this method can be briefly described as follows: having a diseased bone, one can use the hereby presented tool in order to find amongst a set of healthy ipsilateral cadaver bones, the allograft that best matches the anatomy of the part to be resected. Knowledge about the original shape of that section is obtained from the contralateral bone of the same patient. This is achieved by first pre-registering the healthy contralateral bone to the diseased bone and manually cutting the part that corresponds to the location of the tumour. The processing pipeline therefore consists of the following steps, which are graphically illustrated in Fig. 2.1 (Bousleiman et al. [17]):

1. Acquisition of the CT images and segmentation of the patient's bones and tumour (Fig. 2.1a–c)
2. Virtually cutting out a part of the healthy contralateral bone that corresponds to the location of the tumour (Fig. 2.1d)
3. Automatic registration of the template with all bones in the databank and storing measured distance metrics (Fig. 2.1f)

4. Automatic selection of the closest (or few closest) match(es) from the databank (Fig. 2.1f)
5. Using the boundaries of the registered template to outline the physical cutting planes on the selected bone and extract the allograft

As mentioned earlier, the original anatomy of the diseased bone is extracted from the patient's healthy contralateral limb and used as a template to guide the search within the databank of cadaver bones. The search is illustrated in the form of a pseudo-code in the algorithm (Please refer to algorithm in the figure below). For each cadaver bone in the databank (line 2), the algorithm applies an iterative closest point- (ICP) based registration on the point clouds of the template and the bone itself to find the transformation that minimises the difference between the two surfaces (lines 4–7). This is done in an iterative fashion and only stops when a certain convergence criterion (cc = 0:001 mm, line 8) is met, or when the number of iterations exceeds a preset value (maxIt = 200, line 8). Surface distance metrics are measured and stored for further processing (line 7). The rigid transformation is then applied to the template to place it in the best fitting location and orientation. This process is repeated until all bones in the databank are examined.

At this stage, each bone in the databank is represented by the minimum surface distance metric between the bone itself and the best fit of the template. Since the goal is to find the closest global match, one or more closely matching donors can be selected (lines 16, 17), thus giving the surgeon one-to-few possibilities to choose from.

In:	Search template s and all bones in the databank $DB = \{b_1, ..., b_{\|DB\|}\}$
Out:	Index of the closest matching bone in the databank and the corresponding transformation parameters

```
1:  Initialise j ← 0; maxIt; cc
2:  for each b_i in DB
3:    loop
4:      find corresponding points
5:      T_j ← estimate updated parameters
6:      s_T ← T_j ∘ s
7:      d_j ← MSD(s_T, b_i)
8:      if (d_j − d_{j−1}) < cc ‖ j > maxIt then
9:        D_i = min{d_k|k = 1...j}
10:       TR_i = T_{argmin{d_k|k=1...j}}
11:       break loop
12:     end if
13:     j ← j + 1
14:   end loop
15: end for
16: bestMatch ← argmin{D_i|i = 1... ‖ DB ‖}
17: bestTransf ← TR_{bestMatch}
```

Following the initial presentation of the method, a thorough evaluation was carried out where all three methods, namely, the manual selection, the volume-based selection, and the surface-based automatic selection were compared (Bousleiman et al. [16]). All three methods were applied on the exact same data set of the hemipelvis where realistic clinical scenarios of intercalary implants were mimicked.

Results

The automatic allograft selection method based on surface registration showed promising results in its initial presentation. However, its advantages were highlighted when it was compared to other gold standard methods.

Overall, the allografts selected by the surface-based registration method were superior to those selected by other approaches in terms of surface-to-surface fit with the target shape. More importantly, the junctions between the host bone and the intercalary allografts were reported to be significantly better. Additionally processing time was several orders of magnitude lower that those recorded for the manual and the volume registration methods.

Conclusion

Computer-assisted or computer-aided surgery and surgical systems are key components of many modern clinical interventions. Better surgical outcome, shorter surgical time, and improved decision making are typical benefits of using such systems. Development of surgical software and associated tools is a rather popular field among research scientists and industrial manufacturers alike. The field itself has a wide coverage as well. It could include the pre-operative planning, the intra-operative assistance, and the computationally-based design of instruments and tools.

Bone grafting is a common procedure, and several reports supported the use of grafts extracted from cadavers. The selection and planning process is a tedious and time-consuming manual task. In this chapter, a fully automatic method was presented that indicates which cadaveric bone is suitable for a certain patient, and defines how the donor and recipient bones are to be cut. The presented method was thoroughly evaluated and compared to state-of-the-art methods through an active multi-national collaboration with developers of other approaches for the same application. The methodology presented in this chapter outperformed its competing counterparts. The assessment of the method yielded conclusive results that it is at a ripe stage where it can be transferred to a clinical setup for evaluation and long-term patient follow-up.

A particular focus in the evaluation of the method was set on the contact areas between the host and the graft. The quality of surface overlap at the junctions

between the donor and recipient is a major aspect that dictates the outcome of the surgery and the difficulty of the transplantation procedure. Furthermore, a smoother transition between the bones facilitates the placement of reconstruction plates and might have positive impact on the incorporation of the allograft into the host bed, thus might decrease the non-union rate.

The applicability of the method is not limited to the selection of allografts from a bone bank. With minor adaptation, the method can be applied to almost any bone of any scale and complexity. The developed algorithms can be used for the selection of autografts for bone augmentation and reconstruction. For instance, dentistry and delicate orthopaedic interventions are typical applications, where bone augmentation is common and the choice of the harvesting site is usually a difficult task. The method can also be used to generate a harvest guide for autotransplantation. It can help minimise the invasiveness of the procedure, optimise the usage of the bone stock, reduce the trauma at the donor site, speed-up the surgical time, and provide accurately shaped implants.

A further modification of the core method could also be proposed. Instead of relying on symmetry to learn the original morphology of the bone, one can use shape and surface prediction methods to recover the shape of the damaged bone. A statistical shape model can be generated and used to predict missing parts of a certain bone. This could overcome the problems of asymmetric patients, unilateral images, and cases where both sides are diseased or traumatised. Furthermore, the inaccuracies due to the manual or automatic definition of the contralateral template and the time could be substantially reduced.

References

1. Ozger H, Bulbul M, Eralp L. Complications of limb salvage surgery in childhood tumors and recommended solutions. Strategies Trauma Limb Reconstr. 2010;5:11–5.
2. Matejovsky Z, Kofranek I. Massive allografts in tumour surgery. Int Orthop. 2006; 30:478–83.
3. Muscolo DL, Ayerza MA, Aponte-Tinao L, Ranalletta M. Partial epiphyseal preservation and intercalary allograft reconstruction in osteosarcoma of the knee. J Bone Joint Surg. 2004; 86:2686–93.
4. Muscolo DL, Ayerza MA, Aponte-Tinao L, Farfalli G. Allograft reconstruction after sarcoma resection in children younger than 10 years old. Clin Orthop Relat Res. 2008;466:1856–62.
5. Ramseier LE, Malinin TI, Temple HT, Mnaymneh WA, Exner GU. Allograft reconstruction for bone sarcoma of the tibia in the growing child. J Bone Joint Surg Br. 2006;88:95–9.
6. Donati D, Di Bella C, Frisoni T, Cevolani L, DeGroot H. Alloprosthetic composite is a suitable reconstruction after periacetabular tumor resection. Clin Orthop Relat Res. 2011;469:1450–8.
7. Malhotra R, Kumar V. Acetabular revision using a total acetabular allograft. Indian J Orthop. 2009;43:218–21.
8. Mankin HJ, Gebhardt MC, Jennings L, Springfield DS, Tomford WW. Long-term results of allograft replacement in the management of bone tumors. Clin Orthop Relat Res. 1996;324:86–97.
9. Ritacco LE, Espinoza Orias AA, Aponte-Tinao L, Muscolo DL, de Quirós FGB, Nozomu I. Three-dimensional morphometric analysis of the distal femur: a validity method for allograft selection using a virtual bone bank. Studies Health Technol Inform. 2010;160:1287–90.

10. Mankin H, Gebhardt M, Tomford W. The use of frozen cadaveric allografts in the management of patients with bone tumors of the extremities. Orthop Clin North Am. 1987;18:275–89.
11. Delloye C, Banse X, Birchard B, Docquier PL, Cornu O. Pelvic reconstruction with a structural pelvic allograft after resection of a malignant bone tumor. J Bone Joint Surg Am. 2007;89:579–87.
12. Juergens P, Krol Z, Zeilhofer HF, Beinemann J, Schicho K, Ewers R, Klug C. Computer simulation and rapid prototyping for the reconstruction of the mandible. J Oral Maxillofac Surg. 2009;67:2167–70.
13. Paul L, Docquier PL, Cartiaux O, Cornu O, Delloye C, Banse X. Selection of massive bone allografts using shape-matching 3-dimensional registration. Acta Orthop. 2010;81:252–7.
14. Delloye C, Cornu O, Druez V, Barbier O. Bone allografts: what they can offer and what they cannot. J Bone Joint Surg. 2007;89:574–9.
15. Paul L, Docquier PL, Cartiaux O, Cornu O, Delloye C, Banse X. Inaccuracy in selection of massive bone allograft using template comparison method. Cell Tissue Bank. 2008;9:83–90.
16. Bousleiman H, Paul L, Nolte L-P, Reyes M. Comparative evaluation of pelvic allograft selection methods. Ann Biomed Eng. 2013;41(5):931–8.
17. Bou Sleiman H, Ritacco LE, Aponte-Tinao L, Muscolo DL, Nolte L-P, Reyes M. Allograft selection for transepiphyseal tumor resection around the knee using 3-dimensional surface registration. Ann Biomed Eng. 2011;39(6):1720–27.
18. Bielack S, Kempf-Bielack B, Schwenzer D, Birkfellner T, Delling G, Ewerbeck V, et al. Neoadjuvant therapy for localized osteosarcoma of extremities. Results from the cooperative osteosarcoma study group COSS of 925 patients. Klin Padiatr. 1999;211(4):260–70.
19. Paulussen M, Ahrens S, Dunst J, Winkelmann W, Exner GU, Kotz R, et al. Localized Ewing tumor of bone: final results of the cooperative Ewing's Sarcoma Study CESS 86. J Clin Oncol. 2001;19(6):1818–29.
20. Seiler C, Weber S, Schmidt W, Fischer F, Reimers N, Reyes M. Automatic landmark propagation for left and right symmetry assessment of tibia and femur: a computational anatomy based approach. In: Proceedings of 9th Ann Meeting of CAOS International. 2009:195–8.
21. Schmidt W, Reyes M, Fischer F, Geesink R, Nolte LP, Racanelli J, et al. Quantifying human knee anthropometric differences between ethnic groups and gender using shape analysis. In: Proceedings of Ann Meeting American Society of Biomechanics. 2009:26–9.

Chapter 3
Computer Guided Navigation and Pre-operative Planning for Arthroscopic Hip Surgery

Simon Lee, Asheesh Bedi, Shane J. Nho, and Alejandro A. Espinoza Orías

Abstract Femoroacetabular impingement (FAI) has only relatively recently been recognized as an orthopaedic pathology, but growing awareness and the development of innovative management techniques are contributing an increasing rate of diagnosis. Hip arthroscopy of FAI to address these morphologic deformities and their subsequent pathologic sequela is becoming a common, effective, and safe method of treating hip pain. However, hip arthroscopy remains technically difficult and presents a steep learning curve for surgeons. The challenges of preoperative characterization of the mechanical deformities combined with the difficulties of reliable intraoperative exposure and correction of impingement lesions leads to natural interest in computer assisted pre-operative planning and intra-operative navigation systems. The purpose of these emerging technologies is to benefit the surgeon's reproducibility, efficiency and long-term clinical outcomes, while reducing the incomplete correction of the osseous deformities and subsequent symptoms. While the long-term clinical outcomes of hip arthroscopy are rooted in many aspects, consistent reproducibility and accuracy during intraoperative osseous FAI correction may represent the factor most manageable by the surgeon to maximize the likelihood of success. We discuss the

S. Lee, MPH, MD • A. Bedi, MD
Department of Orthopaedic Surgery, University of Michigan,
24 Frank Lloyd Wright Drive, Ann Arbor, MI 48106, USA
e-mail: simon.x.lee@gmail.com; abedi@med.umich.edu

S.J. Nho, MD, MS
Hip Preservation Center, Division of Sports Medicine,
Department of Orthopedic Surgery, Rush University Medical Center,
1611 W Harrison, Suite 300, Chicago, IL 60612, USA

A.A. Espinoza Orías, PhD (✉)
Spine Biomechanics Laboratory, Department of Orthopedic Surgery, Rush University Medical Center, 1611 W Harrison, Suite 201, Chicago, IL 60612, USA
e-mail: Alejandro_Espinoza@rush.edu

L.E. Ritacco et al. (eds.), *Computer-Assisted Musculoskeletal Surgery: Thinking and Executing in 3D*, DOI 10.1007/978-3-319-12943-3_3

current and future state of computer-assisted hip arthroscopy, as well as several examples of available pre-operative and navigation systems.

Keywords Surgical planning • Femoroacetabular Impingement • Surgical navigation • Three-dimensional models • Hip arthroscopy

Introduction

Femoroacetabular impingement (FAI) has only relatively recently been recognized as an orthopaedic pathology, but growing awareness and the development of innovative management techniques are contributing an increasing rate of diagnosis. Ganz et al. have characterized the complex morphology of the hip joint and have studied various biomechanical pathways in which abnormal morphology of the region may produce symptomatic pathology [1–3]. FAI is possibly the most common cause of these symptoms and typically leads the patient to seek medical attention for labral tears, hip pain, and even early osteoarthritis [4–10]. The most common anatomical lesions found associated with FAI are abnormalities in the head-neck offset in the proximal femur (cam lesion) and over-coverage of the acetabular rim (pincer lesion) [11]. Dynamic hip motion in the setting of these osseous deformities leads to bony impingement and consequently applies abnormally high loading forces onto the surrounding soft tissue. This may result in chondral delamination, labral injury, and altered mechanics leading to other non-specific intra-articular damage [12–15].

The diagnosis and treatment of symptomatic FAI in the United States has grown rapidly in recent years [16–22]. Hip arthroscopy of FAI to address these morphologic deformities and their subsequent pathologic sequelae is becoming a common, effective, and safe method of treating hip pain [16–23]. However, hip arthroscopy remains technically difficult and presents a steep learning curve for surgeons. The challenges of preoperative characterization of the mechanical deformities combined with the difficulties of reliable intraoperative exposure and correction of impingement lesions leads to natural interest in computer assisted pre-operative planning and intra-operative navigation systems. The potential for improved modeling of pathological FAI lesions, enhancing visualization of cam and pincer osseous structures, may prove effective in providing superior accuracy in their anatomical reduction intraoperatively. The purpose of these emerging technologies is to benefit the surgeon's reproducibility, efficiency and long-term clinical outcomes, while reducing the incomplete correction of the osseous deformities and subsequent symptoms. Although the long-term clinical outcomes of hip arthroscopy are rooted in many aspects, consistent reproducibility and accuracy during intraoperative osseous FAI correction may represent the factor most manageable by the surgeon to maximize the likelihood of success.

Computer-Aided Surgery in Femoroacetabular Impingement

The advent of computer-aided navigation and pre-operative planning in hip arthroscopy was developed to address the technical difficulties and limitations present in the treatment of FAI. The procedure has a "steep" learning curve, incomplete exposure and incomplete correction of the osseous deformities may even be a cause for arthroscopic surgical failure [24, 25]. The femoroacetabular hip joint is surrounded by numerous layers of muscles, ligaments, and critical neurovascular structures, making accessibility difficult. In addition, a limited working space is created by its constrained osseous geometry and enveloping capsule, causing limited visualization and mobility within the joint [26]. These anatomic factors may prevent the surgeon from fully appreciating the size, location, and shape of cam or pincer deformities. This results in incomplete information and may lead to either an inadequate resection or overzealous resection, precipitating an increased risk of complications such as of femoral neck fracture [27, 28]. The theoretical goals of computer-assisted navigation include improved objective kinematics and clinical outcomes through resection of the entire impingement zone in an accurate, reproducible, and efficient way that is less dependent upon surgical experience. In addition, it should provide greater advantages in identification and protection of neurovascular structures at risk. While further exploration into this technology is required to improve the integration of computer navigation with current surgical management, it is an emerging concept that holds many potential benefits in the treatment of pre-arthritic hip disease and FAI.

While several systems currently exist in an attempt to accomplish these goals, each one begins at a common point: adequate pre-operative computed tomography (CT) or magnetic resonance imaging (MRI) scans. These scans may be integrated into navigation and pre-operative planning software, subsequently creating 3D models of the patient's hip joint. High fidelity scans are necessary to allow clear definition of the FAI osseous deformities and their resulting areas of impingement, therefore providing high quality information to be used to each system. This results in the software's ability to accurately "template" the amount and location of osteoplasty preoperatively and compare the intraoperative fluoroscopic images to the template, ideal correction, giving the surgeon a visual advantage while performing surgery. The previously obtained CT or MRI imaging data may also be linked to the patient's position through identification of anatomic landmarks that allow computer-guided navigation systems to accurately track of the location of acetabulum and femur in real time.

The mechanical axis of the femur, as defined by the center of the femoral head and the midpoint between the femoral condyles, in addition to the anatomic axis of the femur is defined. The position of the pelvis is also entered based on specific landmarks. The areas of pathologic bone can be highlighted and complete removal ensured through the use of navigation software. By registration of the tools as well, their position in real time can be tracked relative to the femur and pelvis to help guide the surgeon to resect the impingement lesions in the anatomically correct regions.

Examples of Current Computer-Navigated and Pre-operative Planning Systems

HipMotion

There have been multiple studies that have described specific computer-aided systems for the arthroscopic treatment of FAI [29–32]. Tannast et al. developed and validated a software program called HipMotion prior to testing in a clinical pilot study [32]. This system was a noninvasive, three-dimensional CT-based method to evaluate the accuracy and reliability of a computer-assisted system in the assessment and treatment of FAI. HipMotion renders a 3D model of the femoroacetabular joint based on preoperative CT imaging of the pelvis and utilizes various landmarks such as the anterior superior iliac spines and the pubic tubercles to define the so-called anterior pelvic plane (APP). The program also develops reference points for the femur which, setting the mechanical axis with center of the femoral head and knee, and setting the coronal femoral reference with the plane of the posterior aspect of the femoral condyles (Fig. 3.1). The authors then performed a validation study of the system using cadaveric hips and sawbones involving 150 normal hips in the control group, and 31 hips with clinical and radiographic signs of FAI in the study group. The performed a side-by-side comparison of the biomechanics and kinetics of the HipMotion predicted movements with real hip motion. The FAI hips had significantly decreased flexion, decreased internal rotation at 90° of flexion, and decreased abduction ($P < 0.001$). A trend toward decreased flexion in hips with pincer-type impingement was also demonstrated when compared to those with cam-type impingement, although it was not statistically significant ($P = 0.08$). They determined that the HipMotion software provides reliable kinematic analysis of hip range of motion for the evaluation of hip impingement, both preoperatively and after femoral and acetabular reshaping procedures (Fig. 3.1).

Kubiak-Langer et al. further validated this model by surgically simulating femoroacetabular osteoplasty within the system [31]. They demonstrated predictable decreases in flexion, internal rotation at 90° of flexion, and abduction in those with FAI and subsequently significant improvements in these parameters after virtual resection of the osseous lesions. Limitations within these models do exist, however. The system currently incorporates only osseous structures and foes not take into account the hip joint's surrounding musculature and ligaments and their effect on hip motion. This system also depends on concentric joint geometry, which allows a reliable determination of the femoral head center of rotation. Dysplastic and osteoarthritic hips presents challenges to this requirement as their inconsistent and nonconcentric morphology make predictive rotational and translational motion difficult. Although HipMotion was not directly linked to a surgical navigation system, it nevertheless represents a useful tool for the development of future computer-navigated technologies in hip arthroscopy.

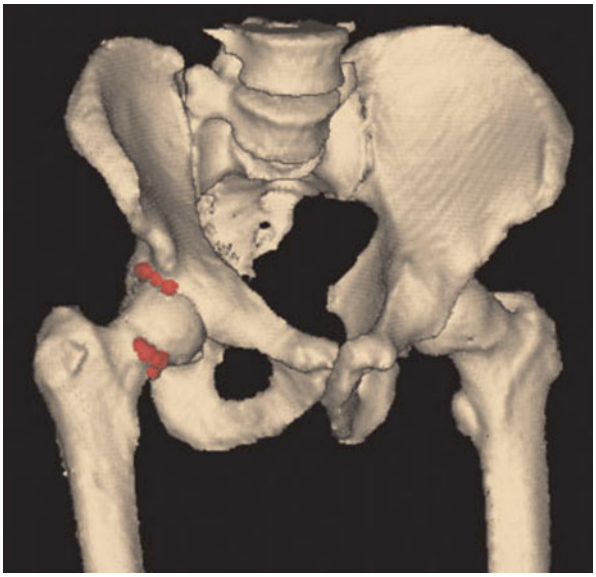

Fig. 3.1 The software HipMotion predicts the acetabular and femoral sources of impingement. Reproduced from Tannast et al. [32] with permission from John Wiley & Sons, Inc.

Brainlab Hip CT

Brunner et al. developed Brainlab Hip CT (modified version of Brainlab Hip CT, Brainlab AG, Feldkirchen, Germany), a computer-navigated system utilizing CT imaging to assess head-neck offset correction after resection of cam-type FAI lesions [30]. This navigation system generated a 3D image of the hip based on preoperative CT scans, allowing the surgeon to cross-reference with intraoperative fluoroscopy. Real-time visualization of instrument position in relation to the head-neck junction and cam lesion during the procedure was therefore made possible (Fig. 3.2). The authors prospectively evaluated and treated 50 study patients with cam FAI randomly assigned to differing experimental cohorts, 25 patients assigned to a navigated treatment group and 25 to non-navigated treatment. Preoperative CT scans of the pelvis and postoperative MRI imaging were compared to determine if there was a significant reduction in the alpha angle after hip arthroscopy. The treatment was considered successful if a post-operative alpha angle less than 50° or an absolute reduction in the alpha angle greater than 20° was observed. The mean alpha angle was reduced from 76.6° to 54.2° after hip arthroscopy with Brainlab Hip CT, however, six patients in each cohort failed to demonstrate adequate femoral head-neck restoration of offset (12/50 = 24 %). Stemming from these results, Brunner et al. determined that the magnitude of alpha angle correction was not reliably improved with a computer-based navigation system as compared to controls. Of note, however, there were no significant differences in clinical outcomes among patients with adequate alpha angle reduction and as compared to patients who

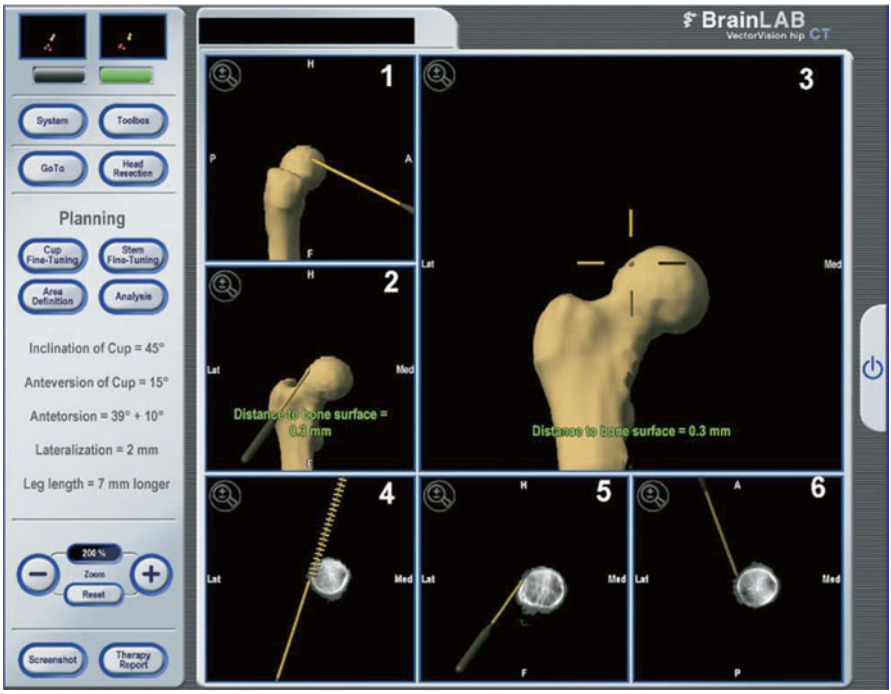

Fig. 3.2 The screen shows the position of the surgical instrument in relation to the femoral neck (frame *1*, lateral 3-dimensional view; frames *2* and *3*, anteroposterior 3-dimensional views; frame *4*, anteroposterior 2-dimensional view; frame *5*, lateral 2-dimensional view; and frame *6*, transversal 2-dimensional view). The scripture at the right part of the screen represents a residuum of the original Hip-CT program and is not used in navigated hip arthroscopy. Reproduced from Brunner et al. [30] with permission from Elsevier.

did at a mean follow-up of 26.5 months. This raises the question of whether postoperative alpha angle is an adequate predictor of clinical success. The limitations of this study include the relatively short-term follow-up as well as the utilization of preoperative CT for 3D modeling and alpha angle measurement while subsequent alpha angle postoperative comparisons were made on 2D MRI studies.

Computer-Aided Navigation Using Encoder Linkages for Position Tracking

Monahan and Shimada developed and tested a computer system that utilizes a set of linkage encoders that are attached to the surgical instrumentation and to an anatomical reference base pin, providing increased visual feedback to the surgeon in real time (Fig. 3.3) [29, 33]. This computer-aided navigation system uses the encoder linkage to determine arthroscopic tool position in relation to the patient's anatomic structures [33]. The base pin is implanted in the patients' pelvis and acts as the connector between the linkage system and the patient. 3D reconstructions of preoperative CT or MRI imaging

Fig. 3.3 Computer-Aided arthroscopic hip surgery system from Gunay et al. [34]. (a) Setup of complete computer-aided system. (b) Encoder linkage tracks an arthroscopic camera applied to a hip joint model. (c) Snapshot of computer display which shows the surgical tools and patient anatomy from multiple angles. Reproduced from Monahan et al. [33] with permission from IOS Press.

data are utilized to render a model of the patient's anatomy, including critical neurovascular structures. This allows the surgeon to visualize and appreciate soft tissue entities that must be protected during hip arthroscopy. The authors created a physical hip model which included simulated plastic skin and a cotton filling to mimic soft tissue resistance, ten participants were then subsequently instructed to visualize two targets on the femur utilizing an arthroscope linked to the encoder system. Recorded measures included time for task completion and tool path distance based on the 3D coordinates of the arthroscope throughout each simulation. After completing the simulation both with and without the computer-aided navigation encoder linkage system, there was an average 38 % reduction in the time to task completion and an average 71.8 % decrease in tool path length with the navigation system. While there are clear benefits to decreasing tool motion during a hip arthroscopy procedure, such as a decreased risk of damage to soft tissues and neurovascular structures, the authors acknowledge there is much room for improvement in computer-aided hip navigation, including better visual display of the tool position alongside the camera display, and obtaining input and feedback regarding the system from experienced, adept hip arthroscopists.

The Equidistant Method

Puls et al. developed a novel in-vitro hip joint simulation algorithm termed "the equidistant method" to detect the location and size of FAI lesions [29]. This system calculates a dynamic hip center of rotation instead of a predefined, fixed center of

rotation as used in the other algorithms. To validate this method, the authors utilized artificial but anatomically correct pelvis and femur models (Sawbones, Pacific Research Laboratories, Vashon, WA), simulating the pathological cam and pincer lesions and subsequently their dynamic impingement point by creating modifications to the head-neck junction of the proximal femur and to the rim of the acetabulum. Based on these physical models, computer simulated 3D renderings were created. The physical pelvis model was rigidly fixed in space and a 3D coordinate system was subsequently created utilizing specific anatomic landmarks (i.e., anterior superior iliac spine, anterior inferior iliac spine, etc.) to register the plastic bones with their respective digital computer models. These models were then taken through various paths of motions and were subsequently recorded through a computer navigation system. Areas of impingement were identified, and four simulation algorithms (equidistant, simple, constrained, and translated) were applied to the motion paths and 3D modeling data to detect impingement (Fig. 3.4). The results demonstrated that the author's equidistant method was the most accurate hip joint

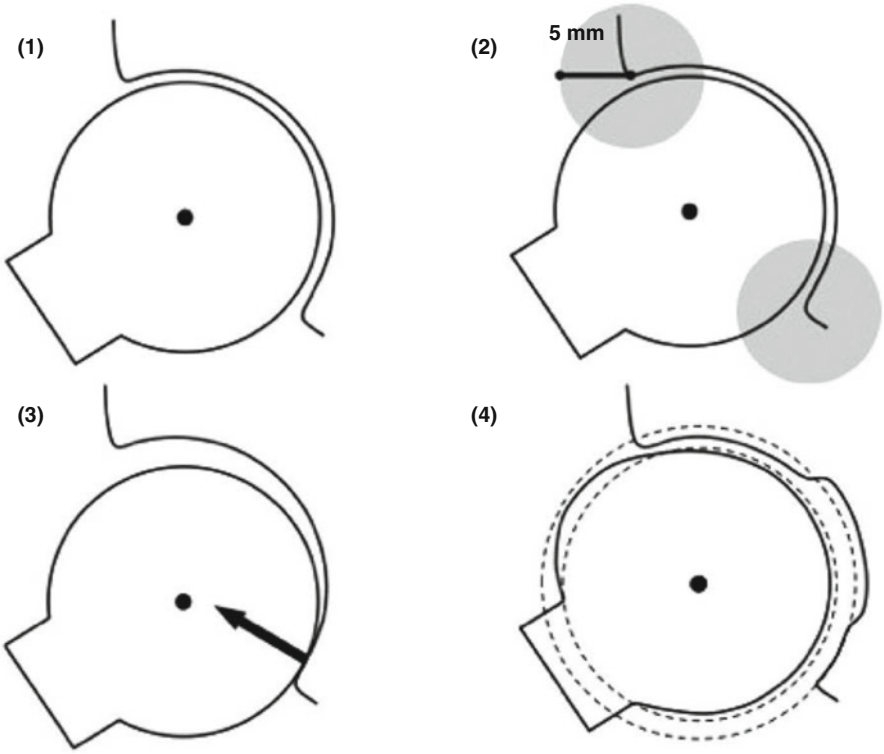

Fig. 3.4 This schematic drawing of the femur and acetabulum explains the different hip joint simulation methods: (1) The Simple Method with a fixed, determined center of rotation, detecting any kind of impingement; (2) The Constrained Method with a 5-mm detection perimeter for impingement at the acetabular rim; (3) The Translated Method with an additional translation vector perpendicular to any detected intra-articular impingement area; and (4) The Equidistant Method with a computed acetabular and femoral sphere, maintaining a dynamic center of rotation and equidistant joint space. Reproduced from Puls et al. [29] with permission from Taylor & Francis, Inc.

simulation algorithm tested in the study ($P<0.05$) and that the size of the impingement zone with the equidistant method was smaller when compared to the other methods. Nevertheless, there were several limitations the authors noted in the study. These included the use of man-made bone replicas as opposed to human cadaveric models, as well as the omission of load-bearing and dynamic muscular contribution kinematic effects in the analysis. Following this concept, the algorithm also only models areas of osseous impingement and does not account from biomechanical alterations from both static (i.e., labrum, capsule) and dynamic (i.e., muscle, tendon) factors. Further investigation is required to determine the clinical utility of this model and its ability to achieve efficient and reproducible resection of impingement pathology.

A2 Surgical

This system is the only one currently available for clinical use with software that includes the complex anatomical parameters on both the femoral and acetabular morphology and dynamically determines all potential sources of mechanical impingement. The system is unique in that it provides assistance in surgical decision making of whether an arthroscopic, open, or combined approach is necessary to address the present pathology. This software also allows the surgeon to predict the specific location of impingement with dynamic maneuvers of the hip. Lastly, the system provides insight on the amount of resection required to eliminate impingement and achieve a target improvement in hip kinematics and motion.

High-resolution CT imaging is incorporated into the system and the software subsequently calculates and determines the center of the femoral head. A 3D model of the femur is generated and the neck-shaft angle and anteversion is determined along with a 3D map of the head-neck junction [35]. A 3D model of the pelvis and acetabulum is also generated. Virtual digital fluoroscopic images are also generated allowing the surgeon to match with the preoperative radiographs with intraoperative fluoroscopic image to correct for pelvic tilt or rotation. The 3D model will correspondingly adjust with the fluoroscopic image to reflect these changes in tilt and obliquity. The target alpha angle for the cam osteochondroplasty is then template to restore desired femoral head sphericity. The software then determines the region of asphericity and generates a topographic map of the cam lesion. The peak zone of loss of offset is also defined along the clockface of the head-neck junction and is of significant utility in defining the optimal intraoperative fluoroscopic position necessary to identify and resect bone at the location of maximum deformity. The volume of the necessary resection is also defined. The desired correction on the acetabular rim can also be template. The system has the ability to generate a predictive virtual fluoroscopic image that demonstrates changes that occur post-correction of the femur and acetabulum. This feature is of great utility intraoperatively in

correlating the template resection with anticipated changes in radiographic landmarks.

The kinematics of this model can also be simulated to provide a dynamic analysis of the hip joint, allowing determination of the specific locations of mechanical impingement. Dynamics-based algorithms can simulate standard physical examination maneuvers, but may also include sport-specific motions that are specific athletic complaints secondary to the hip impingement. This allows the system to assist the surgeon in creating individualized treatment options that is unique to the patient's specific demands and expectations.

The Future of Computer Guided Navigation and Pre-operative Planning

Computer-navigation has many potential applications in the diagnosis and treatment of FAI. An ideal system would allow for an accurate dynamic, preoperative assessment of hip impingement based on CT imaging studies and subsequently link this data to the intraoperative anatomy to facilitate an accurate and complete osseous resection. The demand for these systems from both experienced hip arthroscopists as well as novices to the procedure is high, but there remain roadblocks to their widespread implementation. The challenges are numerous, including the financial burden of software development and maintenance, as well as the learning curve associated with these advanced technologies.

While the examples described here demonstrate successful innovation and progress for FAI computer-assisted surgery, the predominant focus on computer-assisted techniques for large implant surgeries. This is due to the high volume of these procedures and superior market size. However, as the recognition of FAI and the exponential growth of hip arthroscopy continues trend upward, the financial considerations will lean in favor of further development of these systems for arthroscopic surgery. Additionally, no current studies are available to show improved clinical outcomes as a result of computer-assistance in hip arthroscopy. Nevertheless, preliminary work has been encouraging, with the development of software applications that have improved safety and accuracy of tool motion paths and orientation for surgeons relatively new to the practice of hip arthroscopy.

As our understanding of the kinematics and biomechanics of FAI continues to mature, we are gaining a deeper appreciation of the complexities of managing this intricate pathology. A highly complex amalgamation of factors causing hip pain has supplemented the simple definitions of a cam, pincer, or combined lesions, factors which are unique to each patient. As our knowledge of this pathology grows, our appreciation of the need to individualize treatment plans for each patient is also developing. In addition, this greater understanding also elevates the complexity and skill required in surgeons to successfully perform

arthroscopic surgery of the hip. The continued development of computer-assisted navigation and pre-operative planning will not only assist surgeons in comprehensively diagnose FAI with greater accuracy, but also increase our ability to treat these deformities more precisely, efficiently, and safely.

References

1. Ganz R, Leunig M, Leunig-Ganz K, Harris WH. The etiology of osteoarthritis of the hip. Clin Orthop Relat Res. 2008;466(2):264–72. doi:10.1007/s11999-007-0060-z.
2. Ganz R, Gill TJ, Gautier E, Ganz K, Krügel N, Berlemann U. Surgical dislocation of the adult hip: a technique with full access to the femoral head and acetabulum without the risk of avascular necrosis. J Bone Joint Surg Br. 2001;83-B(8):1119–24. doi:10.1302/0301-620X.83B8.11964.
3. Ganz R, Parvizi J, Beck M, Leunig M, Nötzli H, Siebenrock KA. Femoroacetabular impingement: a cause for osteoarthritis of the hip. Clin Orthop Relat Res. 2003;417:112–20. doi:10.1097/01.blo.0000096804.78689.c2.
4. Tanzer M, Noiseux N. Osseous abnormalities and early osteoarthritis: the role of hip impingement. Clin Orthop Relat Res. 2004;429:170–7.
5. Peters CL, Erickson JA, Anderson L, Anderson AA, Weiss J. Hip-preserving surgery: understanding complex pathomorphology. J Bone Joint Surg Am. 2009;91 Suppl 6:42–58. doi:10.2106/JBJS.I.00612.
6. Peters CL, Erickson JA. Treatment of femoro-acetabular impingement with surgical dislocation and débridement in young adults. J Bone Joint Surg Am. 2006;88(8):1735–41. doi:10.2106/JBJS.E.00514.
7. Bedi A, Dolan M, Leunig M, Kelly BT. Static and dynamic mechanical causes of hip pain. Arthroscopy. 2011;27(2):235–51. doi:10.1016/j.arthro.2010.07.022.
8. Clohisy JC, John LCS, Schutz AL. Surgical treatment of femoroacetabular impingement: a systematic review of the literature. Clin Orthop Relat Res. 2010;468(2):555–64. doi:10.1007/s11999-009-1138-6.
9. Beck M, Kalhor M, Leunig M, Ganz R. Hip morphology influences the pattern of damage to the acetabular cartilage: femoroacetabular impingement as a cause of early osteoarthritis of the hip. J Bone Joint Surg Br. 2005;87-B(7):1012–8. doi:10.1302/0301-620X.87B7.15203.
10. Beaulé PE, Allen DJ, Clohisy JC, Schoenecker PL, Leunig M. The young adult with hip impingement: deciding on the optimal intervention. Instr Course Lect. 2009;58:213–22.
11. Van Thiel GS, Harris JD, et al. Age-related differences in radiographic parameters for femoroacetabular impingement in hip arthroplasty patients. Arthroscopy. 2013;29(7):1182–7. doi:10.1016/j.arthro.2013.04.013.
12. Anderson LA, Peters CL, Park BB, Stoddard GJ, Erickson JA, Crim JR. Acetabular cartilage delamination in femoroacetabular impingement. Risk factors and magnetic resonance imaging diagnosis. J Bone Joint Surg Am. 2009;91(2):305–13. doi:10.2106/JBJS.G.01198.
13. Khanduja V, Villar RN. Arthroscopic surgery of the hip: current concepts and recent advances. J Bone Joint Surg Br. 2006;88-B(12):1557–66. doi:10.1302/0301-620X.88B12.18584.
14. Crawford JR, Villar RN. Current concepts in the management of femoroacetabular impingement. J Bone Joint Surg Br. 2005;87-B(11):1459–62. doi:10.1302/0301-620X.87B11.16821.
15. Allen D, Beaulé PE, Ramadan O, Doucette S. Prevalence of associated deformities and hip pain in patients with cam-type femoroacetabular impingement. J Bone Joint Surg Br. 2009;91-B(5):589–94. doi:10.1302/0301-620X.91B5.22028.
16. Byrd JWT, Jones KS. Hip arthroscopy for labral pathology: prospective analysis with 10-year follow-up. Arthroscopy. 2009;25(4):365–8.
17. Espinosa N, Beck M, Rothenfluh DA, Ganz R, Leunig M. Treatment of femoro-acetabular impingement: preliminary results of labral refixation. Surgical technique. J Bone Joint Surg Am. 2007;89 Suppl 2 Pt.1:36–53.

18. Farjo LA, Glick JM, Sampson TG. Hip arthroscopy for acetabular labral tears. Arthroscopy. 1999;15(2):132–7.
19. Fitzgerald Jr RH. Acetabular labrum tears. Diagnosis and treatment. Clin Orthop Relat Res. 1995;311:60–8.
20. Larson CM, Giveans MR, Stone RM. Arthroscopic debridement versus refixation of the acetabular labrum associated with femoroacetabular impingement: mean 3.5-year follow-up. Am J Sports Med. 2012;40(5):1015–21.
21. O'leary JA, Berend K, Vail TP. The relationship between diagnosis and outcome in arthroscopy of the hip. Arthroscopy. 2001;17(2):181–8.
22. Philippon MJ, Yen Y-M, Briggs KK, Kuppersmith DA, Maxwell RB. Early outcomes after hip arthroscopy for femoroacetabular impingement in the athletic adolescent patient: a preliminary report. J Pediatr Orthop. 2008;28(7):705–10.
23. Domb BG, Stake CE, Botser IB, Jackson TJ. Surgical dislocation of the hip versus arthroscopic treatment of femoroacetabular impingement: a prospective matched-pair study with average 2-year follow-up. Arthroscopy. 2013;29(9):1506–13. doi:10.1016/j.arthro.2013.06.010.
24. Philippon MJ, Schenker ML, Briggs KK, Kuppersmith DA, Maxwell RB, Stubbs AJ. Revision hip arthroscopy. Am J Sports Med. 2007;35(11):1918–21. doi:10.1177/0363546507305097.
25. Heyworth BE, Shindle MK, Voos JE, Rudzki JR, Kelly BT. Radiologic and intraoperative findings in revision hip arthroscopy. Arthroscopy. 2007;23(12):1295–302. doi:10.1016/j.arthro.2007.09.015.
26. Monahan E, Shimada K. Computer-aided navigation for arthroscopic hip surgery using encoder linkages for position tracking. Int J Med Robot. 2006;2(3):271–8. doi:10.1002/rcs.100.
27. McCarthy JC, Lee J. Hip arthroscopy: indications and technical pearls. Clin Orthop Relat Res. 2005;441:180–7.
28. Stähelin L, Stähelin T, Jolles BM, Herzog RF. Arthroscopic offset restoration in femoroacetabular cam impingement: accuracy and early clinical outcome. Arthroscopy. 2008;24(1):51–7. e1. doi:10.1016/j.arthro.2007.08.010.
29. Puls M, Ecker TM, Tannast M, Steppacher SD, Siebenrock KA, Kowal JH. The Equidistant Method – a novel hip joint simulation algorithm for detection of femoroacetabular impingement. Comput Aided Surg. 2010;15(4–6):75–82. doi:10.3109/10929088.2010.530076.
30. Brunner A, Horisberger M, Herzog RF. Evaluation of a computed tomography-based navigation system prototype for hip arthroscopy in the treatment of femoroacetabular cam impingement. Arthroscopy. 2009;25(4):382–91. doi:10.1016/j.arthro.2008.11.012.
31. Kubiak-Langer M, Tannast M, Murphy SB, Siebenrock KA, Langlotz F. Range of motion in anterior femoroacetabular impingement. Clin Orthop Relat Res. 2007;458:117–24. doi:10.1097/BLO.0b013e318031c595.
32. Tannast M, Kubiak-Langer M, Langlotz F, Puls M, Murphy SB, Siebenrock KA. Noninvasive three-dimensional assessment of femoroacetabular impingement. J Orthop Res. 2007;25(1):122–31. doi:10.1002/jor.20309.
33. Monahan E, Shimada K. Verifying the effectiveness of a computer-aided navigation system for arthroscopic hip surgery. Stud Health Technol Inform. 2008;132:302–7.
34. Gunay M. Three-dimensional bone geometry reconstruction from x-ray images using hierarchical free-form deformation and non-linear optimization [Dissertation]. Pittsburgh, PA: Carnegie-Mellon University, 2003.
35. Knesek M, Skendzel JG, Bedi A. Computer-Navigation in Hip Arthroscopy. in J.W.T. Byrd (Ed.) Operative Hip Arthroscopy. Springer Science+Business Media, New York, NY. 2013. doi:10.1007/978-1-4419-7925-4_19.

Chapter 4
Virtual Cranio-Maxillofacial Surgery Planning with Stereo Graphics and Haptics

Ingela Nyström, Pontus Olsson, Johan Nysjö, Fredrik Nysjö, Filip Malmberg, Stefan Seipel, Jan-Michaél Hirsch, and Ingrid B. Carlbom

Abstract Cranio-maxillofacial surgery to restore normal skeletal anatomy in patients with serious facial conditions is both complex and time consuming. There is, however, ample evidence that careful pre-operative planning leads to a better outcome with a higher degree of function and reduced morbidity and at the same time reduced time in the operating room. We are building a cranio-maxillofacial surgery planning system that, based on patient specific three-dimensional CT data, allows the surgeon to plan the surgical procedure without the help of a technician. Using a combination of stereo visualization with six degrees-of-freedom, high-fidelity haptic feedback, the system allows the surgeon to test alternative surgical solutions, move bone fragments, and design patient-specific implants and plates. Our goal is a system where the surgeon, after minimal training, can plan a complex procedure in less than an hour. Preliminary tests indicate that this goal is achievable.

Keywords Cranio-Maxillofacial Surgery • Virtual Surgery Planning • Haptics • 3D Visualization • Image Segmentation

Introduction

Patients with severe injuries, cancer, and birth defects to the head and neck require cranio-maxillofacial (CMF) surgery. Yearly, approximately 560,000 cases of head and neck cancer are diagnosed worldwide, and 300,000 patients die annually from

I. Nyström, PhD, Docent (✉) • P. Olsson • J. Nysjö • F. Nysjö
F. Malmberg • S. Seipel • I.B. Carlbom
Department of Information Technology, Centre for Image Analysis,
Uppsala University, Uppsala, Sweden
e-mail: ingela.nystrom@it.uu.se

J.-M. Hirsch
Department of Surgical Sciences, Oral and Maxillofacial Surgery,
Uppsala University, Uppsala, Sweden
e-mail: jan.michael.hirsch@akademiska.se

L.E. Ritacco et al. (eds.), *Computer-Assisted Musculoskeletal Surgery: Thinking and Executing in 3D*, DOI 10.1007/978-3-319-12943-3_4

these conditions [1]. Traffic accidents, that are expected to rank third in the world-wide health-care burden by the year 2020 [2], are a major cause of severe injuries with trauma to the face and head for 50–75 % of the accident survivors [3]. Of 10,000 live births, four to five infants are born with severe deformities and another one or two with jaw anomalies requiring surgery [4]. The outcome of the surgery affects both function and aesthetics and has a profound impact on the patient's quality of life.

CMF surgery to restore normal skeletal anatomy in patients with serious facial conditions from, for example, gunshot wounds, work related injuries, natural disasters, and traffic accidents, is both complex and time consuming. Studies show that careful pre-operative planning leads to a better outcome with a higher degree of function and reduced morbidity and at the same time leads to reduced time in the operating room [5, 6]. In addition, customized scaffolds functioning as delivery systems for biological molecules or carrier of bone or bone substitutes hold the promise for further improvements.

Three-dimensional (3D) imaging techniques such as computed tomography (CT) are capable of generating high-resolution volumetric images of the human body, and thus allow the surgeon to inspect the anatomy of the individual patient prior to surgery, and to virtually plan the surgical procedure. However, today's commercial surgery planning systems, such as those from Brainlab[1] and Materialise,[2] rely on the user's ability to plan complex tasks with a two-dimensional (2D) graphical interface. In research, haptics-assisted CMF surgery planning systems are beginning to emerge [7].

In clinical practice, plate and implant design and manufacturing are often outsourced, relying on skilled technicians to carry out complex designs. The process requires several iterations with the surgeon, and the resulting design often need modification even after production, causing a lead time to surgery of days or even weeks. Time and cost would be reduced significantly, if the surgeon him/herself could design implants without the help of a technician, and the required implants and plates could be produced in-house.

We are building a CMF surgery planning system that lets the surgeon test alternative surgical solutions, move bone fragments, and design patient-specific implants and plates. Our goal is that the surgeon, after minimal training, should be able to plan a complex procedure in 1 h, leading to a reduction of time in the operating room by several hours for complex cases. In-house production of the system-designed, patient-specific devices will lead to considerable additional cost savings, and allow surgery on trauma patients within hours, rather than days that out-sourced planning and production require today. Custom-made solutions with optimal load-bearing properties that contain bone or bone substitutes and with surfaces that can function as delivery systems to promote bone regeneration will yield surgical results superior to what is currently achievable.

[1] https://www.brainlab.com/, accessed July 1, 2014.

[2] http://biomedical.materialise.com/mimics, accessed July 1, 2014.

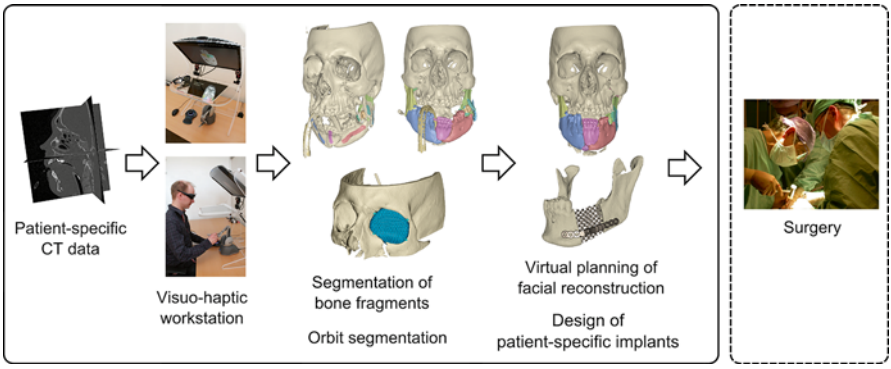

Fig. 4.1 Illustration of the components of our system for virtual surgery planning

Here, we present a system combining stereo visualization with six degrees-of-freedom (DOF), high-fidelity haptic feedback that allows a surgeon, with minimal training, to plan complex surgical procedures in about 1 h, including the design of plates and implants that can be produced with additive manufacturing. The planning includes semi-automatic segmentation of patient-specific CT head data, and then the use of this segmented CT data for analysis, planning, and testing of alternative solutions for restoring bone fragments of complex fractures into their proper positions and the design of plates and scaffold implants as needed in complex cases. The process is illustrated in Fig. 4.1.

Stereoscopic Visualization and Motion Parallax

Stereoscopy, from Greek: *stereos* (solid) and *skopein* (watching), is the study of techniques and methods to render and display 3D objects to be perceived through binocular vision. Studies show that in surgical treatment planning and training stereoscopic visualization aids surgeons to accurately orient in spatially complex anatomical regions and helps improving their visuo-spatial positioning [8]. Thus, it is not surprising that 3D stereoscopic visualization was adopted very early in CMF surgery, since it requires highly accurate spatial precision [9]. A variety of techniques have been invented to provide the user's left and right eye with stereo images, among which auto-stereoscopic displays are a recent technology that does not require the use of headgear. Another class of stereoscopic displays utilizes glasses to provide the correct stereo views, of which shutter-glasses are the most mature technology yielding brilliant colors and high resolutions at a fairly low cost.

Due to the tremendous development of 3D visualization technology, stereo display systems have received much attention, but it is clear from numerous studies that stereoscopic visualization does not in general improve user performance when compared with traditional monoscopic visualization [10]. However, what has been

identified to be a highly effective cue for spatial understanding, in particular when combined with stereo is motion parallax [11, 12]. Motion parallax is the apparent dynamic displacement of objects in the view of the observer due to observer motion and requires accurate and robust tracking of the observer's viewing position when used in 3D visualization.

There are very few studies of working environments combining stereo, motion parallax and haptics [13]. We have opted to create a system that gives surgeons the visualization cues that they use in real surgery: binocular vision, parallax from self motion, and parallax from object motion, and that at the same time co-locates the visual and haptic workspace.

Haptics

Haptics, from Greek: *haptesthai* (to contact, to touch), encompasses both hardware devices and rendering algorithms that mediate the human sense of touch. In medicine, haptics has been used primarily in simulators for procedures such as palpation, laparoscopic surgery, and needle insertion. Haptics increases the realism and immersion in such simulators, as medical professionals rely on their sense of touch in these procedures. Coles et al. [14] provide a broad survey of the use of haptics in surgery training simulators. Pre-operative planning systems based on anatomical models from patient-specific CT and/or MRI data may also benefit from haptics. The addition of haptic interaction to a planning system lets the user not only view the relevant patient-specific anatomy, but also touch and manipulate virtual representations of, for example, bone structures.

A common type of haptic device is an input/output interface with which a user interacts by grasping and manipulating a handle, or *end-effector*, attached to a mechanical linkage. The device contains sensors that continuously track motion and/or forces applied to the handle, as well as actuators to generate force and/or torque feedback to the user. Haptic devices thus provide a bi-directional channel between the user and a virtual environment.

Haptic devices vary greatly in workspace size, number of degrees-of-freedom (DOF) and degrees-of-force-feedback (DOFF), maximum force and torque, and price. The target application determines the requirements for a haptic device, which often become a trade-off between force, fidelity, DOF, and cost. For example, if a high maximum force is important, strong mechanical linkages and actuators are required, which typically increase the inertia of the interface. An example of a commercially available haptic device is the Phantom Omni from Geomagic[3] (Fig. 4.2), which tracks the handle position and orientation in six DOF and provides three DOFF. It offers a good compromise in terms of force, fidelity, and cost, for our application.

[3] http://geomagic.com/, accessed July 1, 2014.

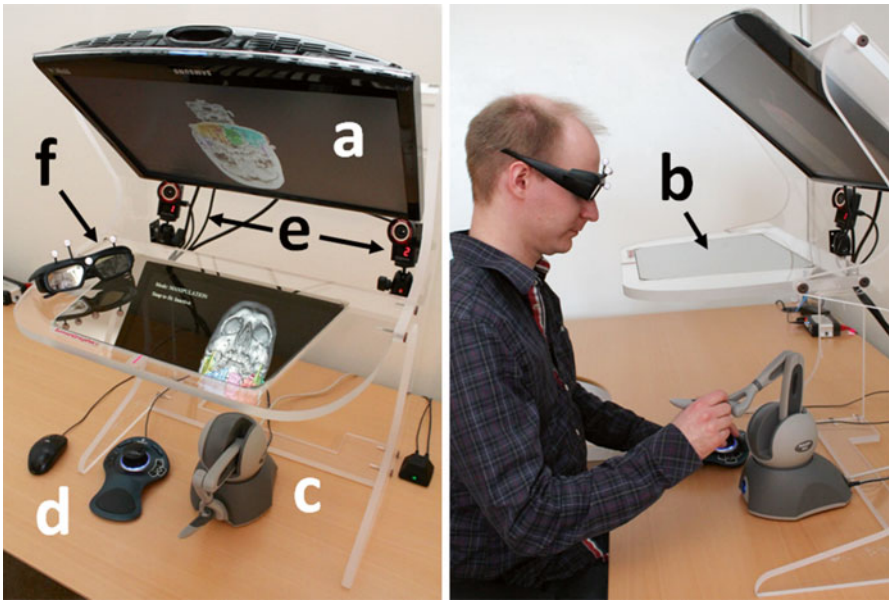

Fig. 4.2 The planning system hardware as seen from above (*left*) and from the side (*right*). The graphical objects are displayed by the monitor (**a**) and reflected on the half-transparent mirror (**b**). The user manipulates the 3D graphical objects with the haptic device (**c**) under the half-transparent mirror. The push-buttons on the 3D-Connexion controller (**d**) activate the grouping tool and the tool Snap-to-fit. The two infra-red cameras (**e**) track the marker rig on the shutter glasses (**f**) for user look-around

Haptic rendering algorithms compute context-dependent, real-time, force-feedback to the user when interacting with a virtual environment. The force-feedback could for example consist of contact forces when the user is in contact with a virtual object, that is the haptic device then generates forces stopping the users hand, or guiding forces that assist the user in performing specific tasks. Realistic force feedback requires a high update rate, as much as 1 kHz, which can be compared to 30–60 frames per second required for smooth graphical update. This poses great demands on haptic rendering software that requires a combination of highly optimized algorithms, carefully designed data structures, and pre-computation, in addition to large computational power.

System Overview

Our system for CMF surgery planning, which combines stereoscopic 3D visualization with six DOF haptic rendering, is shown in Fig. 4.2. The system executes on an HP Z400 Workstation with an Nvidia Quadro 4000 Graphics Processing Unit (GPU) driving a Samsung 120 Hz time-multiplexed stereo monitor. The

monitor with stereo glasses gives the user a stereoscopic view of the patient CT data, and the Geomagic Omni haptic device, positioned under the mirror, allows interaction. The monitor is mounted on a half-transparent mirror rig, a Display 300 from Sense-Graphics,[4] which makes it possible to co-locate the stereo graphics and the haptic device workspace. This way, the user can see and interact with objects in the same physical space. A head tracker, based on a NaturalPoint Optitrack system,[5] continually tracks optical markers mounted on the stereo glasses. This enables look-around, that is the ability to view objects from different angles, by using head motion.

System Components

In this section, we describe the components in our system. To make a restoration plan, the surgeon follows the workflow chart in Fig. 4.1, which illustrates the order in which the components are used.

Bone Segmentation

The first step in our CMF surgery planning pipeline is to segment bones and bone fragments in the skull. A collective bone segmentation can be obtained by thresholding the gray-scale CT volume at a Hounsfield value corresponding to bone tissue. However, to plan the reconstruction of complex bone fractures, we also need to separate individual bone fragments from each other. Due to noise and partial volume effects, adjacent bones in the CT volume might become connected to each other after the thresholding and cannot be separated by simple connected component analysis.

To separate the bones, we have developed an interactive bone separation method based on the random walks algorithm [15]. Similarly to [16], we construct a weighted graph from a binary bone segmentation and then use random walks and user-defined seeds to separate the individual bone fragments. For each foreground voxel, we compute the probability that a random walker starting from that voxel will encounter a particular seed label before any other seed label. The vertices in the graph represent the foreground voxels and the edges represent the connections between adjacent foreground voxels in a 6-connected neighborhood. Each edge is assigned a weight based on the absolute difference between the intensities of the image elements corresponding to the vertices spanned by the edge.

[4] http://www.sensegraphics.com/, accessed July 1, 2014.

[5] https://www.naturalpoint.com/, accessed July 1, 2014.

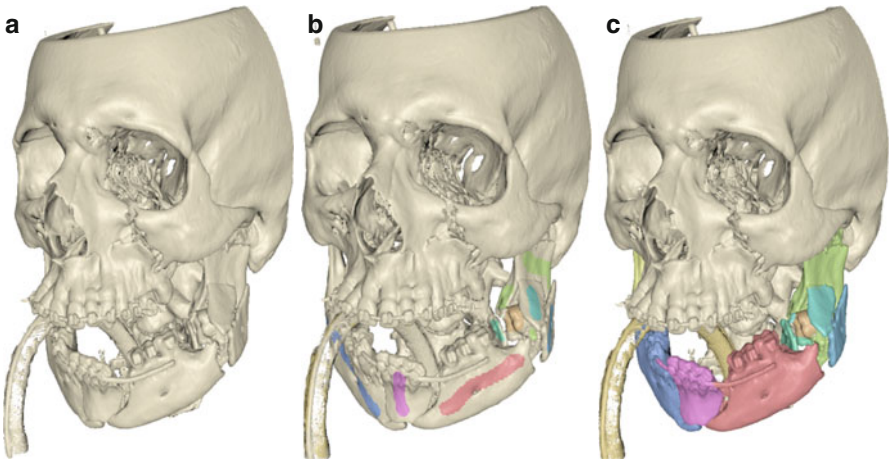

Fig. 4.3 Random walks bone separation. (**a**) Initial bone segmentation obtained by thresholding. (**b**) User-defined seeds painted directly on the bone surfaces. (**c**) Bone separation result obtained with random walks

To simplify marking of individual bone fragments, we provide a brush tool that allows the user to paint seeds directly on the bone surfaces. The bones are rendered using GPU-accelerated ray-casting [17]. We represent the random walks segmentation problem as a sparse linear system [15] and use an algebraic multigrid solver [18] to solve the system. Figure 4.3 illustrates the segmentation process.

Using this method, segmentation results comparable with manual segmentations can typically be obtained in a few minutes. Minor leaks or artifacts in the segmentation result can be corrected by manual slice-by-slice editing. The segmented bone fragments can then be loaded into the virtual planning system.

Bone-Puzzle

One fundamental task in CMF surgery is to restore the skeletal anatomy in patients with extensive fractures of the facial skeleton and jaws, a task that in complex cases resembles solving a 3D puzzle. The accuracy requirements are high; small errors in the positioning of each fragment may accumulate and result in inadequate reconstruction.

Our system supports planning of the restoration of skeletal anatomy using a virtual model, segmented from volumetric CT data as described in the previous section, in which independent bone fragments are labeled and visualized in a unique color for clear identification [19]. See Fig. 4.4. The user may touch, move, and rotate the individual bone fragments with the haptic device, or move and rotate the entire working volume to view it from different angles. During fragment manipulation, force and torque from contacts with other fragments are rendered haptically,

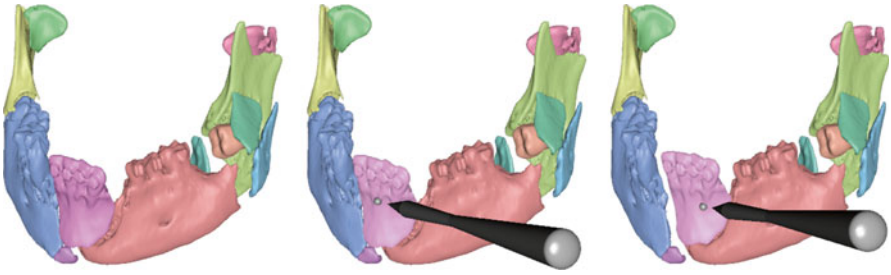

Fig. 4.4 Virtual reconstruction of a mandible. Each individual bone fragment is given a unique color (*left*). When the haptic cursor is held close to a bone fragment, it is highlighted (*middle*) and the user can then grasp and manipulate it with the six DOF haptic handle (*right*)

giving the user an impression similar to that of manipulating a real, physical object among other objects. As penetration between fragments may be difficult to discern visually, contact forces help the user to avoid impossible placement of fragments during the planning. When two or more fragments have been positioned relative to one another, the user may group them and manipulate them as one unit. Additional fragments may subsequently be attached to extend the group and they may also be detached from the group.

Precise alignment of the bone fragments is important since even small rotational and translational errors between fragments may accumulate as a result of the reconstruction of a series of fragments, for example, of a mandible with multiple fractures. But due to occlusion, it may be difficult to visually discern the ideal fit between two bone fragments. Just as we use our human haptic ability in the real world to assemble a broken object, contact forces may provide haptic guidance to find an optimal fit between two fragments. However, limited force fidelity in most commercial haptic devices of today makes it difficult to feel when the optimal fit is found as clearly as can be done with real, physical objects. To improve the precision of the alignment, we have developed a semi-automatic alignment tool we call *Snap-to-fit*. The tool complements haptic contact forces in search for a good fit between two bone fragments. For a detailed description of Snap-to-fit, we refer the reader to [20]. In summary, the user begins by moving a bone fragment close to a matching fracture surface on another bone fragment. From this approximate initial position of the two fragments, the user activates Snap-to-fit that engages attraction forces computed from the fracture surfaces. The forces pull the manipulated objects toward the closest local stable fit, that is, it snaps the fragments into place. Snap-to-fit works best when the fracture surfaces of both fragments are well preserved by the segmentation and the fragments are not too thin or too small. For some types of fractures, such as compression fractures, the fracture surface may be damaged with portions of the bone missing. In these cases, Snap-to-fit may not find a good match between the fracture surfaces and the user has to use his/her expertise to manually find a suitable placement of the bone fragments.

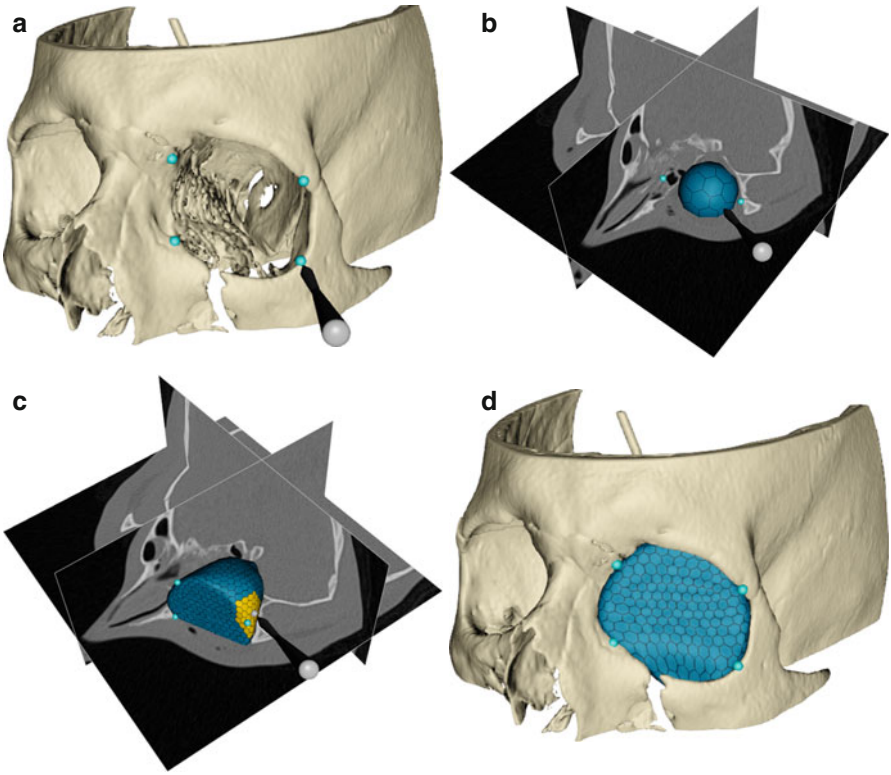

Fig. 4.5 Overview of the semi-automatic orbit segmentation method. (**a**) The user defines a bounding plane at the orbital opening by placing four landmarks (*blue dots*) on the perimeter of the orbital opening. Haptic feedback facilitates the landmark positioning. (**b**) The user initializes a deformable simplex mesh (*blue*) as a coarse sphere inside the orbit. (**c**) The simplex mesh is deformed, using information from the underlying CT data, to fit the orbit. If necessary, the user guides the deformation process interactively, using the haptic stylus. (**d**) Resulting orbit segmentation

Orbit Segmentation

In CMF surgery planning, it is often of interest to measure the shape and volume of the bony orbit (eye-socket). We have developed a haptic-aided semi-automatic technique for segmenting the orbit in CT volume images [21]. The method consists of the following main steps, illustrated in Fig. 4.5:

1. Segment the bone structures in the skull and the orbit.
2. Calculate, based on user-defined anatomical landmarks, a bounding plane that defines the extent of the orbital opening.
3. Fit a deformable model to the orbit, using the data obtained in the previous steps.

In the first step, a binary segmentation of the bone structures around the orbit is extracted. Since the intensity range of bone is well-defined in CT images, the bone

structures can be segmented using hysteresis thresholding [22] with fixed upper and lower threshold values. By using hysteresis thresholding, we aim to extract as much as possible of the thin and, due to partial volume effects, diffuse orbital bone structures without including noise and soft tissue. Bilateral filtering [23] may also be used to reduce noise in the images, prior to segmenting the bones.

Inside the skull, the orbit is surrounded by bone structures that prevent the deformable model from extending too far. At the orbital opening, however, there are no bone structures preventing the deformable model from growing indefinitely. Thus, in the second step, we explicitly define the extent of the orbital opening. The user selects four landmarks on the perimeter of the orbital opening. These landmarks are used to define a bounding plane, beyond which the deformable model is not allowed to grow.

In the third step, the user positions a coarse sphere-shaped deformable simplex mesh inside the orbit. This mesh is deformed and refined in real-time to accurately fit the orbit. The deformation is driven by a distance potential force computed from the segmented bones and the bounding plane. More specifically, we seek a surface that (1) minimizes the distance from each vertex of the mesh to the bone surface and the barrier and (2) has some degree of smoothness. During the deformation process, the user can select mesh faces with the haptic stylus and pull or push these faces into their correct position. This is useful for correcting eventual segmentation leaks that might occur at the diffuse boundaries of the orbit.

Implant Design

We have also developed a semi-automatic method for reconstructing missing bone that allows patient-specific scaffold implants for the mandible to be designed [24]. Our method consists of the following steps: After the user has loaded the mandible into the system and prepared the defect site with good load bearing contact surfaces, by using a virtual resection tool, the user places a bounding surface around the defect (Fig. 4.6a). The bounding surface can be obtained from, for example, the mirrored healthy contra-lateral side, or an approximately matching mandible from a database of healthy mandibles. The defect contact surfaces and the bounding surface will form a mold for the implant. The implant shape is generated by growing a deformable model inside the mold (see Fig. 4.6b), using the deformable model representation and force model described above. Interactive forces allow the user to refine the implant shape while the model is deforming.

When the implant shape has been generated, haptic feedback allows the user to assess the fit of the implant by moving the implant inside the defect. When he/she is satisfied with the result, the system generates the scaffold structures (see Fig. 4.6c). Haptic feedback also helps the user to place control points on the mandible for generating fixation plates.

The design in Fig. 4.6 took less than half an hour to complete; this included loading of pre-segmented patient data, model deformation, fit testing, manual adjustment,

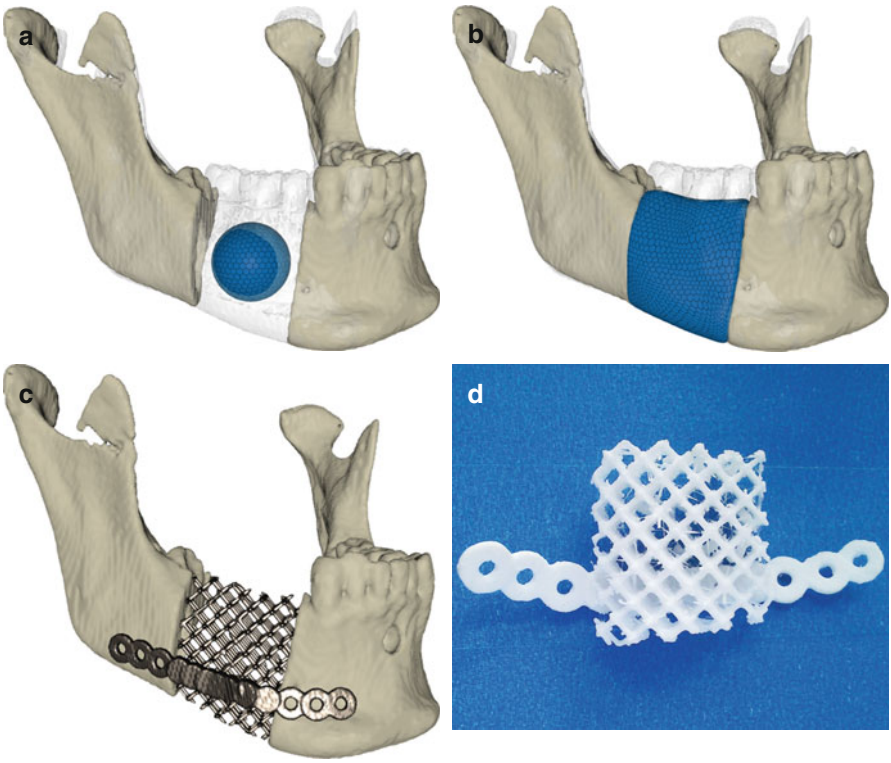

Fig. 4.6 Implant design steps and results. (**a**) Placement of bounding surface (*transparent light gray*) and initialization of deformable model (*blue*) — its growth is constrained by the bounding surface and the defect surfaces. (**b**) Deformation and fine-tuning. (**c**) Scaffold generation and addition of fixation plates with screw holes. (**d**) Prototype implant printed in PLA

and plate placement. To test the manufacturability of the design, we printed the implant in polylactide (PLA) on an Ultimaker [6] 3D printer, with the result shown in Fig. 4.6d.

Evaluation

We invited an experienced CMF surgeon, who did not have any prior experience with our system, to plan the reconstruction of the facial skeleton in two trauma cases. He first received 45 min of training, which consisted of planning the reconstruction of a practice case, while we supported the planning process with oral instructions of how to use the system features. After the training, we asked him to

[6] http://www.ultimaker.com/, accessed July 1, 2014.

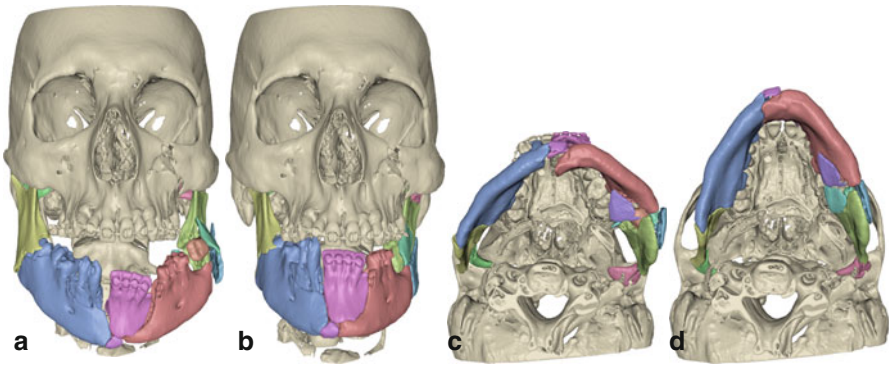

Fig. 4.7 Evaluation case before (**a**, **c**) and after (**b**, **d**) virtual restoration with our system. All mandibular fractures are adequately reduced, even though the occlusion is not optimal due to interference from dislocated teeth

complete, on his own, a plan of the case shown in Fig. 4.7; a patient with complex fractures of the skull, mid-face and mandible after falling from a sky lift.

The surgeon completed the mandibular reconstruction in Fig. 4.7 in 22 min. He noted that he could perceive haptically when a bone fragment under manipulation did not fit due to misplacement or due to inadequate reconstruction of previously positioned fragments. The fractures in the mandible are adequately reduced. However, it was not possible to obtain perfect occlusion, due to interference from dislocated teeth; we have subsequently developed a virtual resection tool to remove unwanted parts [24]. The surgeon made extensive use of the grouping tool to build groups of fragments once he found a good fit. He also used the head-tracking feature more and more throughout the session to look around objects, instead of relying on rotation to get good visibility. He also commented that the system is useful for understanding the complexity of the specific case and that he during the planning process gained insights on preferred order of fragment placement; assembling the fragments in a certain order may provide valuable clues towards the best global reconstruction.

Conclusions and Future Work

We have described the prototype of a system for CMF surgery planning. The system allows the pre-operative development of a patient-specific plan for restoring the skeletal anatomy of the face and neck region to correct congenital and acquired conditions. In less than 1 h, a CMF surgeon can develop a surgery plan that includes the segmentation of the patient CT data, repositioning of displaced skeletal bone fragments, and the design of personalized fixation plates and implant scaffolds that may carry bone replacement. A detailed surgery plan may shorten surgery time by as much as 25 %, and increase the function and reduce morbidity for the patient. The shortened surgery time will lead to considerable cost savings, and in-house

production of patient specific cutting guides and fixation plates would lead to additional savings. The initial promising results of the system can be attributed to the combination of stereo graphics, parallax from both self and object motion, and haptic feedback that guide the surgical planning.

Our current system only addresses bone reconstruction. The next step is to add soft tissue reconstruction to the planning system. Currently, we are developing a method to plan the use of a fibula free-flap, for free tissue transfer with the use of a fibula free-flap, e.g., skin, fat, muscle, bone, and donor blood vessels, to the facial region with reattachment of the artery and veins to separate recipient artery and veins. This includes segmentation of the donor vessels adjacent to the fibula and recipient vessels in the neck region, the determination of the osteotomy angles and positions, and the modeling of the connection of the donor vessels to the recipient vessels. It will also include the size, position, and orientation of the skin flap and in particular the optimal position for the perforator, that is whether it should be lingual or buccal. Further soft tissue modeling will include modeling of muscle tissue, vessels, and nerves in the head and neck region, and the virtual testing of function, including mandibular occlusion and movement.

Another important aspect of a CMF surgery planning system is to bring the resulting plan into the operating room. As part of the plan the surgeon prepares optimal load-bearing contact surfaces in the defect region, which can be translated into models of a saw guides for printing with additive manufacturing techniques. Similarly, the system can produce saw guides for the fibula osteotomies to be used during surgery. Other ways to bring the plan into the operating room is to transfer it to a surgical navigator or a surgical robot. And yet other techniques involve augmented reality, that is mixing real and synthetic imagery to guide the surgeon during the real procedure.

The techniques used in our CMF surgery planning system are not limited to the head and neck area, but are applicable to general orthopedic surgery and neurosurgery, and has the potential not only as a planning tool, but also as a teaching tool in these disciplines.

References

1. Boyle P, Levin B, editors. World cancer report 2008. Lyon: IARC Press; 2008.
2. Murray CJL, Lopez AD. Alternative projections of mortality and disability by cause 1990–2020: global burden of disease study. Lancet. 1997;349(9064):1498–504.
3. Peden M, et al. World report on road traffic injury prevention. Geneva: World Health Organization; 2004.
4. Ridgway EB, Weiner HL. Skull deformities. Pediatr Clin North Am. 2004;51(2):359–87.
5. Roser SM, et al. The accuracy of virtual surgical planning in free fibula mandibular reconstruction: comparison of planned and final results. J Oral Maxillofac Surg. 2010;68(11):2824–32.
6. Antony AK, et al. Use of virtual surgery and stereolithography-guided osteotomy for mandibular reconstruction with the free fibula. Plast Reconstr Surg. 2011;128(5):1080–4.
7. Schvartzman S, et al. A computer-aided trauma simulation system with haptic feedback is easy and fast for oral-maxillofacial surgeons to learn and use. J Oral Maxillofac Surg. 2014; 72(10):1984–93.

8. Held RT, Hui TT. A guide to stereoscopic 3D displays in medicine. Acad Radiol. 2011; 18(8):1035–48.
9. Zachow S, et al. 3D osteotomy planning in cranio-maxillofacial surgery: experiences and results of surgery planning and volumetric finite-element soft tissue prediction in three clinical cases. In Computer Assisted Radiology and Surgery (CARS). Springer; 2002. p. 983–7.
10. McIntire JP, Havig PR, Geiselman EE. Stereoscopic 3D displays and human performance: a comprehensive review. Displays. 2014;35(1):18–26.
11. van Schooten BW, et al. The effect of stereoscopy and motion cues on 3D interpretation task performance. In Proceedings of the International Conference on Advanced Visual Interfaces. ACM; 2010. p. 167–70.
12. Ware C, Mitchell P. Visualizing graphs in three dimensions. ACM Trans Appl Percept (TAP). 2008;5(1):2.
13. Olsson P, Nysjö F, Seipel S, Carlbom IB. Physically co-located haptic interaction with 3D displays. In Haptics Symposium (HAPTICS). IEEE; 2012. p. 267–72.
14. Coles TR, Meglan D, John N. The role of haptics in medical training simulators: a survey of the state of the art. IEEE Trans Haptic. 2011;4(1):51–66.
15. Grady L. Random walks for image segmentation. IEEE Trans Pattern Anal Mach Intell. 2006; 28(11):1768–83.
16. Liu L, et al. Interactive separation of segmented bones in CT volumes using graph cut. In Medical Image Computing and Computer-Assisted Intervention, MICCAI, LNCS 5241. Springer; 2008. p. 296–304.
17. Kruger J, Westermann R. Acceleration techniques for GPU-based volume rendering. In Proceedings of the IEEE Visualization (VIS'03); 2003. p. 38.
18. Bell WN, Olson LN, Schroder J. PyAMG: algebraic multigrid solvers in Python; 2008. Version 1.1.
19. Olsson P, Nysjö F, Hirsch J-M, Carlbom IB. A haptics-assisted cranio-maxillofacial surgery planning system for restoring skeletal anatomy in complex trauma cases. Int J Comput Assist Radiol Surg. 2013;8(6):887–94.
20. Olsson P, Nysjö F, Hirsch J-M, Carlbom IB. Snap-to-fit, a haptic 6 DOF alignment tool for virtual assembly. In World Haptics Conference. IEEE; 2013. p. 205–10.
21. Nyström I, Nysjö J, Malmberg F. Visualization and haptics for interactive medical image analysis: image segmentation in cranio-maxillofacial surgery planning. In Proceedings of International Visual Informatics Conference, LNCS 7066. Springer; 2011. p. 1–12.
22. Canny J. A computational approach to edge detection. IEEE Trans Pattern Anal Mach Intell. 1986;8(6):679–98.
23. Tomasi C, Manduchi R. Bilateral filtering for gray and color images. In Proceedings of the Sixth International Conference on Computer Vision (ICCV 1998). IEEE Computer Society; 1998. p. 839–46.
24. Nysjö F, Olsson P, Hirsch J-M, Carlbom IB. Custom mandibular implant design with deformable models and haptics. In Proceedings of Computer Assisted Radiology and Surgery (CARS), 20th Computed Maxillofacial Imaging Congress; 2014. p. 246.

Chapter 5
Computational Image-Guided Technologies in Cranio-Maxillofacial Soft Tissue Planning and Simulation

Mauricio Reyes, Kamal Shahim, and Philipp Jürgens

Abstract Due to the complexity and unpredictability of cranio-maxillofacial (CMF) surgery, computer simulations have been proposed to assist the surgeon in the decision-making process of surgical planning. Current planning solutions require the use of different and unconnected tools to account for the necessary balance and interplay between functional and aesthetic aspects of CMF surgery, which ultimately makes an effective combination and analysis of the information difficult. In this article we present current approaches and new trends suggested to alleviate these issues and to promote the development of clinically relevant and seamless, yet effective, computational solutions for CMF surgical planning.

Keywords Neurosurgical procedures • Computer assisted systems • Preoperative planning • Intraoperative navigation • Charge coupled device • Dynamic reference frame

Introduction

Cranio-Maxilofacial Surgery

Cranio-maxillofacial (CMF) surgery is a surgical specialty that deals with the treatment of inborn or acquired facial disfigurements. These conditions can be such as cleft lip- and palate, craniofacial malformations, aftermath of facial trauma or of ablative tumor surgery. Surgical interventions in the CMF area and even their planning make high demands on the spatial sense of the surgeons.

M. Reyes (✉) • K. Shahim
Institute for Surgical Technology and Biomechanics, University of Bern, Staufacherstrasse 78, Bern 3014, Switzerland
e-mail: mauricio.reyes@istb.unibe.ch

P. Jürgens
Department of Cranio-Maxillofacial Surgery, University Hospital Basel, Basel, Switzerland

L.E. Ritacco et al. (eds.), *Computer-Assisted Musculoskeletal Surgery: Thinking and Executing in 3D*, DOI 10.1007/978-3-319-12943-3_5

This is on one the hand due to the close proximity of highly vulnerable anatomical structures and on the other hand due to the complex morphology of the region. Modern image-guided techniques are the basis for diagnostics, therapy and documentation. These technologies enable us to produce patient-specific models of the clinical situation. They give us the possibility to perform accurate planning and transfer the planning to the operation theatre. These technologies have made their way into the clinical routine of highly advanced treatment centers [1–5]. One of the most evident indications for the use of virtual planning tools in CMF Surgery is the planning of surgical intervention for patients suffering of malocclusion. Malocclusion can either be caused by a malposition of teeth in the level of the alveolar crest or by an incorrect positioning of the upper and lower jaw relative to each other. For the former, an orthodontic treatment will deliver satisfactory results. For the latter, only a surgical procedure will provide a causal therapy. These interventions are called orthognathic surgeries and their aim is to change the position of the maxillary and mandibular bone, relative to each other and to the skull base. As these interventions are highly elective, an accurate and extensive preoperative planning has to be conducted.

To update the planning procedure several systems for virtual three-dimensional visualization and procedure planning based on volume datasets have been recently introduced in some clinical centers, routinely substituting the conventional two-dimensional cephalogram based planning-approach, and especially improving the prediction of soft tissue deformations [6]. In order to ensure an optimal pre-operative skeletal planning of the patient with his postoperative facial appearance, a highly reliable and accurate prediction system is required. In order to realize the pre-operative surgical plan in the operation theatre, the planning and prediction software should be linked to a navigation system for the intra-operative control of the relocation of the upper and lower jaw.

Image-Guided in CMF Soft-Tissue Surgical Planning

Over the last 20 years computer-assisted surgical simulation and intervention planning has made its way into clinical routine in CMF surgery. Due to the close proximity of highly vulnerable structures in the viscero-cranium region, virtual planning has been used to create highly accurate three-dimensional (3D) models of the patient's anatomy and clinical scenario (virtual osteotomies, cephalometric analysis, etc.). Furthermore, in CMF surgery the complexity of the surgical scenario is enhanced by the difficulties to predict soft-tissue variations from bone relocations due to the low correlation between hard-, and soft-tissue variations [7–10]. This makes the surgical plan very challenging and highly dependent on the surgeon's experience. This has led to the development of computer simulations, which provide a unique tool to predict the surgical outcome. With these tools, surgeons are able to pre-operatively assess the implications of various surgical scenarios (bone relocations). However, several deficiencies presumably stemming from the lack of

interdisciplinary work between scientists and medical practitioners still exist. The following summarizes the main technical challenges in CMF soft tissue simulation.

The basic components for CMF soft-tissue simulation are:

- *Geometrical modeling of hard and soft tissues from Computed Tomography (CT) medical images.*
- *Physical models employed to realistically link the internal stress and deformation of tissues.*
- *Realistic modeling of external forces and constraints to establish a connection between internal deformation and applied forces.*
- *Fast and reliable solver for the resulting differential equations.*

The generation of patient-specific models involves the task of semi- or fully-automatic segmentation of hard and soft tissues. Research in automatic segmentation of the facial soft tissues is, however, still in its infancy. The segmentation of facial soft tissues from diagnostic Computed Tomography (CT) or Magnetic Resonance Images (MRI) is thus still an active research area [11–14]. There are several aspects that make the segmentation a complex task. First, the facial region is one of the most complex anatomical regions of the human body. Second, most of the facial muscles are paper-thin and often even smaller than the voxel resolution of the imaging device, which leads to partial volume effects. Lastly, the complexity of the segmentation task is further increased by imaging noise and poor contrast (in particular in cone beam computed tomography – CBCT); by the presence of high-density artifacts (*e.g.* from dental fillings or implants), and muscles that are overlapping or in contact one with another.

As stated above, segmenting the facial soft tissues is in the mathematical sense an ill-posed problem and still a very active field of research. In [15] Rezaeitabar et al. proposed a specifically tailored region growing approach to segment two facial muscles *i.e.* the masseter and the temporalis. Ng et al. published a series of papers [16–18] where they described segmentation approaches for different facial muscles. Their methods are based on a Gradient Vector Flow (GVF) snake based approach. Kale et al. proposed in [19] a Bayesian and Level-set framework to segment facial soft-tissue from CT and MRI data sets. Through modeling of the partial volume effect they also tried to segment the very thin facial muscles. Drawback of the method is that they require a co-registered CT and MRI data set of the patient. Whereas CT is commonly available, MRI is generally not used and would only add to the costs of the intervention.

Once the segmentation is completed, a computer simulation can be executed to predict the deformation behavior of facial tissues following an orthognathic procedure. Computer-assisted facial soft-tissue simulation was originally introduced by Terzopoulos et al. [20] and Lee et al. [21] where a simple mass-spring modeling (MSM), consisting of a multi-layered facial tissue was applied for soft tissue simulation in CMF. Keeve et al. [22] presented a MSM-based approach with prismatic elements, and compared the result with FEM simulations (Finite-Element Model) in terms of accuracy and computational cost. Zachow et al. [23] suggested a fast tetrahedral volumetric FEM, which can be used in clinical practice.

Due to the high computational and modeling demands of advanced FEM methods, none of the proposed approaches have reached clinical routine and have only been used with clinical data through a dedicated setup where an specialist conducts the modeling and simulations, which are then presented and discussed back with the surgeon [24–28]. **For clinical use, it is important to provide the surgeon with the ability to seamlessly test different surgical approaches without incurring into long computational times or overly complex modeling processes**. From discussions with opinion leaders and own experience, we believe that the surgeon needs to be in control of the surgical plan (as opposed to rely on back-and-forth interactions with an engineer) and should have appropriate tools (i.e. speed, usability and accuracy compatible with the clinical workflow) to plan the surgical procedure.

Cotin et al. [29] proposed a hybrid method using MTM (Mass-Tensor Modeling) for enhanced local deformations in simulation of liver surgery. Mass Tensor Modeling was later extended by Picinbono et al. [30] to consider non-linear, anisotropic elasticity. Chabanas et al. [31] proposed a mesh-morphing algorithm to minimize the laborious efforts in preparing finite-element meshes. Based on the seminal work of Cotin et al. [29], Mollemans et al. [32] first applied MTM to CMF soft-tissue simulation, and evaluated the method qualitatively and quantitatively on ten clinical cases. From the simulation point of view, MTM has been widely accepted for CMF soft-tissue simulation due to its efficiency, accuracy and low computational time. Similarly, GPU-based simulation models have been proposed to deliver fast mechanical simulations [33–37]. Nonetheless, the integration of these methodologies to clinical routine is hindered by the lack of a complete solution that considers the clinical workflow and moreover provides an acceptable accuracy in the error sensitive regions of the face [38–42]. Furthermore, available commercial packages for CMF soft tissue simulation lack appropriate segmentation routines and rely on extensive manual corrections.

Developing clinically relevant solutions that counter accuracy limitations by bringing additional non-imageable anatomical and clinical information into the simulation workflow has shown to leverage the development of new technologies in CMF soft tissue simulation [43–49]. These implementations have resulted in an average simulation error of 1 mm, which is sufficient for surgical planning. In this way, the simulation is capable of providing the surgeon with a post-operative scenario, from which adaptations or changes to the surgical plan can be performed in order to prepare the patient for the changes in his/her appearance. In these approaches, however, the surgeon follows a trial-and-error scheme to determine the final surgical plan that yields a satisfactory soft tissue outcome.

Functional Aspects in CMF Planning

In cranio-maxillofacial surgery the determination of a proper surgical plan that yields a desired aesthetic facial profile while considering functional aspects of the post-operative scenario is very important for a successful treatment outcome. As described above, current solutions do not provide surgeons with tools to effectively

consider the complex interplay between aesthetic and functional aspects, which in light of the complexity of the surgical scenario makes the planning of CMF surgeries very difficult, and ultimately highly dependent on the surgeon's experience. The functional aspects independently investigated in the literature are described below.

Functional aspects to be considered for the surgical plan include reestablishment of the dental occlusion through occlusion analysis [50]. This analysis requires the identification and geometrical assessment of the upper and lower dental arches. The common clinical approach is to use dental casts to define pre-operatively the desired occlusion, which is then transferred intra-operatively using a manufactured splinter. These approaches present some limitations, such as reduced spatial information with respect to the rest of the anatomy, as only a partial observation of the surgical scenario is represented. Furthermore they do not allow for a comprehensive analysis of the effects of the planned occlusion on surrounding hard and soft tissues [51].

Computerized models haven been proposed to perform a virtual assessment of the occlusion. The accuracy of these models has been analyzed with respect to the different imaging parameters and processing steps [52–54], and improvements to deal with metal artifacts and low image resolution have been proposed by combining information from CT imaging and laser scanned dental casts [55–57].

Virtual assessment of occlusion has been proposed by applying semi-, and automatic approaches using registration techniques incorporating collision constraints [58–60]. These approaches enable a precise alignment of the dental arches in a virtual scenario. However, they decouple the occlusion analysis from the other functional and aesthetic aspects of the surgical plan.

Another aspect of the surgical plan to be considered is the evaluation of the airways after orthognathic surgery. Several studies have analyzed the impact of different surgical plans (e.g. mandibular setback, advancement, bimaxillary, etc.) on the geometrical and volumetric changes of the upper and lower airways [61–69]. Similarly, these approaches do not consider the joint analysis of functional and aesthetics aspects of the surgical plan.

To obtain a clinically relevant solution including airway analysis, it is important to develop automatic or nearly automatic segmentation approaches that can be seamlessly integrated into a unique platform.

Airway segmentation is an active area of research since many years. Of particular interest are the segmentation techniques using CT images, see for example [70]. The main application has been the analysis of airways for geometric measurements or navigated interventions. With the availability of CBCT the need for semi- or even fully automatic airway segmentation has become essential for surgical plans incorporating this functional aspect. As CBCT mainly finds its application in the cranio-maxillofacial surgical field, a heuristic approach was proposed in [71] for the analysis of the upper airway. In [72] a more elaborated snake-based method has been described to automatically segment the upper airway.

Due to the low radiation dose of CBCT, its use has recently attracted attention for CMF soft-tissue prediction. In [38] an evaluation of a commercial system for CMF soft-tissue prediction was conducted using CBCT data of patients undergoing orthognathic surgery. The study highlighted the marked simulation errors around the error-sensitive regions of the lips, as well as the importance of evaluating the

accuracy of the soft-tissue predictions on the different regions of the face, as opposed to an overall global evaluation over the entire face [73]. Nonetheless, the common agreement is that CBCT presents great opportunities for CMF soft-tissue prediction and surgical planning, and thus it should be further investigated [39].

Fast Patient-Specific Modeling

Generating patient-specific models has been a bottleneck in the CMF surgical planning pipeline. Current commercially available software tools typically rely on basic image thresholding techniques followed by cumbersome manual corrections. Moreover, the situation is worse when such approaches are used on CBCT images, as their low contrast hinders the task of image segmentation. It is therefore crucial to develop appropriate approaches for fast and accurate bone and soft tissue segmentation. One such approach employed for CMF planning has been the use of statistical shape modeling techniques, which learn from data the anatomical variability of the studies population [74]. When combining these approaches with domain-knowledge, where the user assists the automated approach by placing anatomically or surgically important landmarks, it is possible to realize a fast patient-specific modeling [75]. Furthermore, the topology-preserving feature of this approach enables incorporation of other type of valuable information used for modeling and simulation.

Dealing with Metal Artefacts: Spatially-Varying Gaussian Process Modeling

To deal with image artefacts in CBCT imaging, new modeling schemes are being proposed. One of them is the so-called spatially-varying Gaussian Process Modeling [76]. In this framework, a-priori information on the localization of the metal artefacts can be encoded on the reference model and used during model morphing (see Fig. 5.1). In this way, noisy information stemming from the metal artefacts can be neglected and exchanged with the statistical information built in the statistical shape model driving the model morphing process. The framework, also available through the open source library Statismo [75], enables definition of different morphing models, allowing in turn definition of different transformation properties and features (Fig. 5.2).

Seamless Surgical Planning: The Direct and Inverse Surgical Planning

Despite of the complexity of the surgical scenario, the available technologies must ultimately serve as a vehicle for the surgeon to plan the surgical plan in a seamless manner. It is thus crucial to develop technologies that leverage the work of the

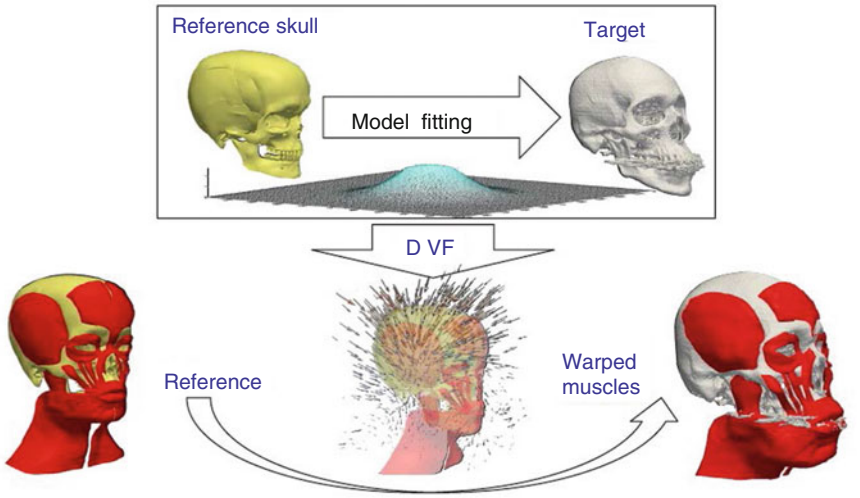

Fig. 5.1 Fast patient-specific modeling using statistical shape modeling techniques. A Reference skull is morphed to match the patient's anatomy, as imaged via CT or CBCT, following population-level statistics and anatomical landmarks. A displacement vector field (*DVF*) is then obtained allowing propagation of other type of information. As exemplified in the lower part of the figure, facial muscle information can then be effectively estimated

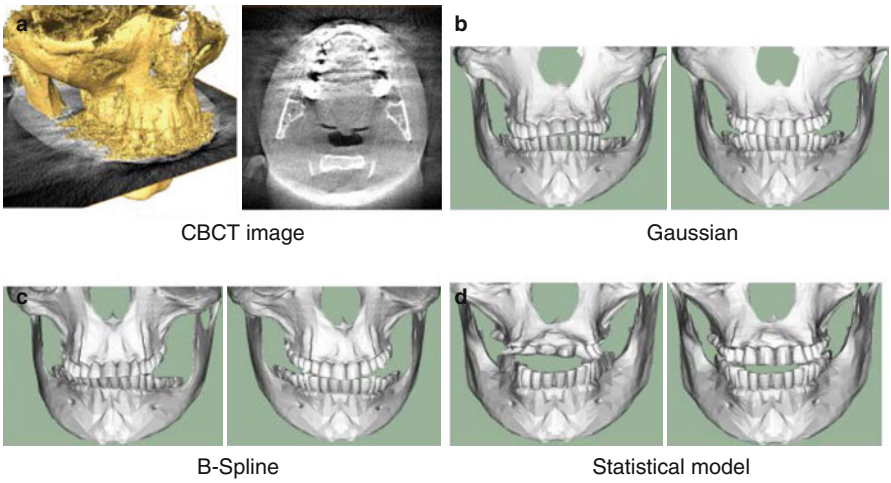

Fig. 5.2 Registration of skulls from CBCT data: (**a**) shows a slice through the image and a reconstruction of the surface obtained using threshold segmentation. (**b**–**d**) show registration results obtained using different deformation models. The left images show a normal registration, while in the right images a spatially-varying registration has been used, showing the ability of the method to deal with metal artefacts

surgeon, allowing him to test different options and interact with the bone and soft tissue components of the surgical plan.

Recently, a shift paradigm was presented whereby the necessary planning is computed from the desired post-operative outcome [75]. This paradigm shift, coined *"Inverse Planning"*, enables the surgeon to look at the surgical plan from a different perspective, allowing him to directly define the desired outcome, without the need of the commonly used trial-and-error scheme available in current solutions.

Inverse Soft Tissue Modeling

The proposed approach employs a fast biomechanical model to derive from the desired facial outlook the necessary surgical plan. Based on the desired facial outlook the deformation of internal soft tissues is calculated, followed by constrained surface registration between bone segments and internal soft tissues. The proposed registration component considers collision and occlusion constraints, and its formulation allows us to derive in a straightforward manner different levels of interplay between quality of occlusion and compliance to the desired outlook (i.e. constraints relaxation). Furthermore, and in regards to a biomechanical simulation that would model the entire ensemble of bone and soft tissues, the proposed approach avoids known issues of layer detachment and convergence related to the high elasticity transition present at the interface of bone and soft tissue materials. We remark that this approach differs from the classical inverse modeling proposed in computational mechanics and used in implant shape design in [28], as our method deals with the ill-posedness of the problem by considering occlusion and geometrical constraints through a registration component that effectively penalizes the set of numerical solutions.

By combining the direct (i.e. soft tissue simulation from bone displacements) and the inverse soft tissue modeling (i.e. specification of bone displacement to yield a desired outcome) it is possible to yield an effective system that, in a transparent way, enables the surgeon to work on the surgical plan.

Due to airways and tongue volume constraints in complex CMF cases, large rotational and translational planning are rarely operated in one single step and surgeons typically divide it into a series of surgeries, which in turns translates into small deformations in engineering mechanics. Nonetheless, to cover these rare cases for large deformation problems, we will consider modifying the classical FEM inverse approach [77] in which the inverse modelling is transferred to a direct problem by super-imposing boundary conditions and transferring the unknown set of displacements to the other side of the continuity equation [78].

Preliminary results, shown on Fig. 5.3, on a set of clinical cases showed in five out of six CT cases a high level of agreement to the actual surgical plan. In one case the proposed approach was confirmed to improve the actual executed plan. As an additional evaluation, simulated soft-tissue outcomes were compared using the predicted and real clinical plan, resulting in a close agreement between the facial simulation results using the predicted and actual planed approach (Fig. 5.4.).

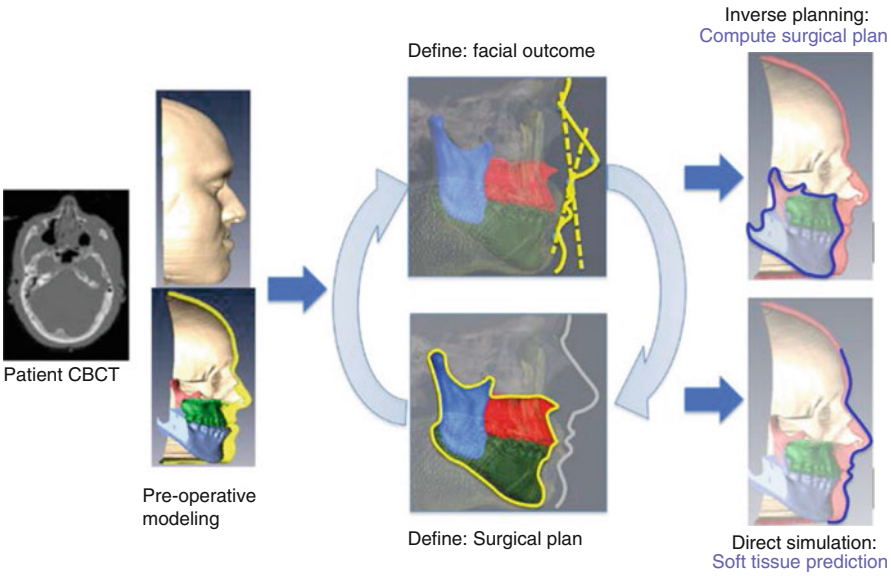

Fig. 5.3 Direct-inverse planning approach. From the pre-operative CBCT scan, a detailed patient-specific model will be created. The surgeon then has the option to interact with the bone segments and perform a direct simulation for soft tissue prediction (*lower part of the figure*), or define the desired facial outcome and obtain the required surgical plan, subject to functional considerations (*upper part of figure*), and assisted by cephalometric guides (illustrated with *dashed lines*). A fast simulation enables the surgeon to seamlessly interact in one mode or the other

Discussion and Conclusions

The human face is a fundamental part of our identity. It centralizes the senses of vision, hearing, taste and smelling, and provides us with channels to participate and integrate in society. The complexity of the clinical scenario is complex, as it requires high understanding of the balance amongst aesthetic, functional, psychological and sociological implications of the surgical outcome. Furthermore, the degree of unpredictability on the surgical outcome makes the decision-making process, on a patient-basis, highly complex. This has called for the development of computational means to assist the surgeon on the task of planning the surgical approach. We believe, however, that more research efforts are essential and needed in order to bring these tools to a level where they can effectively and jointly consider aesthetic and functional aspects for the planning of CMF surgeries.

Based on the observations from the state of the art it can be concluded that functional aspects are of importance and need to be considered in CMF planning. However, there is need to foster the interdisciplinary research with the development of novel approaches that concurrently make use of functional and aesthetic information, and are developed in light of the clinical requirements and workflow. In this regard, it is necessary to enhance these enabling-technologies by developing advanced segmentation

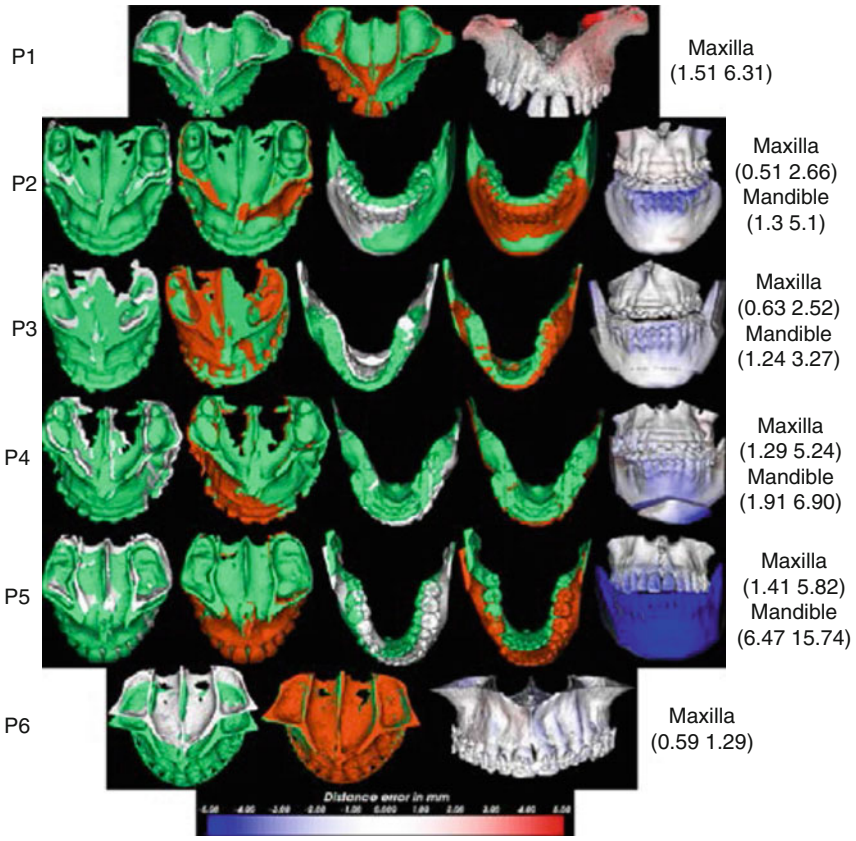

Fig. 5.4 Predicted (*orange color*), actual post-operative (*green color*), and pre-operative segments (*white color*) for the respective patients. The distance errors from the post-operative segments are shown as color-coded images on the predicted model on the rightmost column with the (median maximum) error values in mm indicated for the respective segments. The *blue color* means the proposed approach falls posteriorly than the real post-operative segment (Adapted from Luthi et al. [74])

algorithms for CBCT imaging as well as algorithms allowing the surgeon to seamlessly interact with the surgical plan or the desired soft tissue outcome, all while jointly considering the functional and aesthetics aspects mentioned above.

References

1. Juergens P, Ratia J, Beinemann J, Krol Z, Schicho K, Kunz C, Zeilhofer H-F, Zimmerer S. Enabling an unimpeded surgical approach to the skull base in patients with cranial hyperostosis, exemplarily demonstrated for craniometaphyseal dysplasia. J Neurosurg. 2011;115(3):528–35.
2. Juergens P, Beinemann J, Zandbergen M, Raith S, Kunz C, Zeilhofer H-F. A computer-assisted diagnostic and treatment concept to increase accuracy and safety in the extracranial correction of cranial vault asymmetries. J Oral Maxillofac Surg. 2012;70(3):677–84.

3. Juergens P, Klug C, Krol Z, Beinemann J, Kim H, Reyes M, Guevara-Rojas G, Zeilhofer H-F, Ewers R, Schicho K. Navigation-guided harvesting of autologous iliac crest graft for mandibular reconstruction. J Oral Maxillofac Surg. 2011;69(11):2915–23.
4. Juergens P, Krol Z, Zeilhofer H-F, Beinemann J, Schicho K, Ewers R, Klug C. Computer simulation and rapid prototyping for the reconstruction of the mandible. J Oral Maxillofac Surg. 2009;67(10):2167–70.
5. Wittwer G, Adeyemo WL, Beinemann J, Juergens P. Evaluation of risk of injury to the inferior alveolar nerve with classical sagittal split osteotomy technique and proposed alternative surgical techniques using computer-assisted surgery. Int J Oral Maxillofac Surg. 2012;41(1):79–86.
6. Gateno J, Xia JJ, Teichgraeber JF. New 3-dimensional cephalometric analysis for orthognathic surgery. J Oral Maxillofac Surg. 2011;69(3):606–22.
7. Kim B-R, Oh K-M, Cevidanes LHS, Park J-E, Sim H-S, Seo S-K, Reyes M, Kim Y-J, Park Y-H. Analysis of 3D soft tissue changes after 1- and 2-jaw orthognathic surgery in mandibular prognathism patients. J Oral Maxillofac Surg. 2013;71(1):151–61.
8. Ryckman MS, Harrison S, Oliver D, Sander C, Boryor AA, Hohmann AA, Kilic F, Kim KB. Soft-tissue changes after maxillomandibular advancement surgery assessed with cone-beam computed tomography. Am J Orthod Dentofacial Orthop. 2010;137(4 Suppl): S86–93.
9. Altman JI, Oeltjen JC. Nasal deformities associated with orthognathic surgery: analysis, prevention, and correction. J Craniofac Surg. 2007;18(4):734–9.
10. Stella JP, Streater MR, Epker BN, Sinn DP. Predictability of upper lip soft tissue changes with maxillary advancement. J Oral Maxillofac Surg. 1989;47(7):697–703.
11. Majeed T, Fundana K, Lüthi M, Beinemann J, Cattin P. A shape prior-based MRF model for 3D masseter muscle segmentation. In: SPIE image processing. San Diego: SPIE Digital Library; 2012. p. 83140O–83140O-7.
12. Majeed T, Fundana K, Luthi M, Kiriyanthan S, Beinemann J, Cattin PC. Using a flexibility constrained 3D statistical shape model for robust MRF-based segmentation. In: Mathematical methods in biomedical image analysis (MMBIA), 2012 IEEE workshop on, Breckenridge. 2012. p. 57–64.
13. Majeed T, Fundana K, Kiriyanthan S, Beinemann J, Cattin P. Graph cut segmentation using a constrained statistical model with non-linear and sparse shape optimization. In: Medical computer vision. Recognition techniques and applications in medical imaging. Berlin/Heidelberg: Springer; 2013. p. 48–58.
14. Boykov YY. Jolly M-P. Interactive graph cuts for optimal boundary & region segmentation of objects in ND images. In: Computer vision, 2001. ICCV 2001. Proceedings. Eighth IEEE international conference on. 2001, vol. 1. p. 105–12.
15. Rezaeitabar Y, Ulusoy I. Automatic 3D segmentation of individual facial muscles using unlabeled prior information. Int J Comput Assist Radiol Surg. 2012;7(1):35–41.
16. Ng HP, Ong SH, Hu Q, Foong KWC, Goh PS, Nowinski WL. Muscles of mastication model-based MR image segmentation. Int J Comput Assist Radiol Surg. 2006;1(3):137–48.
17. Ng HP, Ong SH, Huang S, Liu J, Foong KWC, Goh PS, Nowinski WL. Salient features useful for the accurate segmentation of masticatory muscles from minimum slices subsets of magnetic resonance images. Mach Vis Appl. 2010;21(4):449–67.
18. Ng HP, Ong SH, Liu J, Huang S, Foong KWC, Goh PS, Nowinski WL. 3D segmentation and quantification of a masticatory muscle from MR data using patient-specific models and matching distributions. J Digit Imaging. 2009;22(5):449–62.
19. Kale EH, Mumcuoglu EU, Hamcan S. Automatic segmentation of human facial tissue by MRI-CT fusion: a feasibility study. Comput Methods Programs Biomed. 2012;108(3):1106–20.
20. Terzopoulos D, Waters K. Physically-based facial modelling, analysis, and animation. J Vis Comput Animat. 1990;1(2):73–80.
21. Lee Y, Terzopoulos D, Waters K. Realistic modeling for facial animation. In: Proceedings of the 22nd annual conference on computer graphics and interactive techniques. New York; 1995. p. 55–62.

22. Keeve E, Girod S, Kikinis R, Girod B. Deformable modeling of facial tissue for craniofacial surgery simulation. Comput Aided Surg. 1998;3(5):228–38.
23. Zachow S, Gladiline E, Hege H, Deuflhard P. Finite-element simulation of soft tissue deformation. Proc CARS. 2000;28:23–8.
24. Koch RM, Gross MH, Carls FR, von Büren DF, Fankhauser G, Parish YIH. Simulating facial surgery using finite element models. In: Proceedings of the 23rd annual conference on computer graphics and interactive techniques, New Orleans. 1996. p. 421–8.
25. Zachow S, Hege H-C, Deuflhard P. Computer assisted planning in cranio-maxillofacial surgery. J Comput Inf Technol. 2006;14(1):53–64.
26. Gladilin E, Ivanov A, Roginsky V. Generic approach for biomechanical simulation of typical boundary value problems in cranio-maxillofacial surgery planning. Med Image Comput Comput Interv 2004. 2004;147(2):380–8.
27. Wang S, Yang J. Simulating cranio-maxillofacial surgery based on mixed-element biomechanical modelling. Comput Methods Biomech Biomed Engin. 2010;13(3):419–29.
28. Gladilin E, Ivanov A. Computational modelling and optimisation of soft tissue outcome in cranio-maxillofacial surgery planning. Comput Methods Biomech Biomed Engin. 2009;12(3):305–18.
29. Cotin S, Delingette H, Ayache N. A hybrid elastic model for real-time cutting, deformations, and force feedback for surgery training. Vis Comput. 2000;16:437–52.
30. Picinbono G. Non-linear anisotropic elasticity for real-time surgery simulation. Graph Models. 2003;65(5):305–21.
31. Chabanas M, Luboz V, Payan Y. Patient specific finite element model of the face soft tissues for computer-assisted maxillofacial surgery. Med Image Anal. 2003;7(2):131–51.
32. Mollemans W, Schutyser F, Nadjmi N, Maes F, Suetens P. Predicting soft tissue deformations for a maxillofacial surgery planning system: from computational strategies to a complete clinical validation. Med Image Anal. 2007;11(3):282–301.
33. Courtecuisse H, Allard J, Kerfriden P, Bordas SPA, Cotin S, Duriez C. Real-time simulation of contact and cutting of heterogeneous soft-tissues. Med Image Anal. 2014;18(2):394–410.
34. Faure F, Duriez C, Delingette H, Allard J, Gilles B, Marchesseau S, Talbot H, Courtecuisse H, Bousquet G, Peterlik I, Cotin S. SOFA: a multi-model framework for interactive physical simulation. In: Payan Y, editor. Soft tissue biomechanical modeling for computer assisted surgery SE – 125, vol. 11. Berlin/Heidelberg: Springer; 2012. p. 283–321.
35. Taylor ZA, Cheng M, Ourselin S. High-speed nonlinear finite element analysis for surgical simulation using graphics processing units. IEEE Trans Med Imaging. 2008;27(5):650–63.
36. Faure X, Zara F, Jaillet F, Moreau J-M, et al. Implicit tensor-mass solver on the GPU. In: Proccedings of eurographics/ACM SIGGRAPH symposium on computer animation, Lausanne. 2012.
37. Nesme M, Payan Y, Faure F, et al. Efficient, physically plausible finite elements. In: Eurographics, Dublin. 2005.
38. Shafi MI, Ayoub A, Ju X, Khambay B. The accuracy of three-dimensional prediction planning for the surgical correction of facial deformities using Maxilim. Int J Oral Maxillofac Surg. 2013;42:801–6.
39. Kolokitha O-E, Chatzistavrou E. Factors influencing the accuracy of cephalometric prediction of soft tissue profile changes following orthognathic surgery. J Maxillofac Oral Surg. 2012;11(1):82–90.
40. Aboul-Hosn Centenero S, Hernández-Alfaro F. 3D planning in orthognathic surgery: CAD/CAM surgical splints and prediction of the soft and hard tissues results – our experience in 16 cases. J Craniomaxillofac Surg. 2012;40(2):162–8.
41. Scolozzi P, Momjian A, Courvoisier D. Dentofacial deformities treated according to a dentoskeletal analysis based on the divine proportion: are the resulting faces de facto 'divinely' proportioned? J Craniofac Surg. 2011;22(1):147–50.
42. Terzic A, Combescure C, Scolozzi P. Accuracy of computational soft tissue predictions in orthognathic surgery from three-dimensional photographs 6 months after completion of surgery: a preliminary study of 13 patients. Aesthetic Plast Surg. 2014;38(1):184–91.

43. Kim H, Jürgens P, Cattin P, Weber S, Nolte L-P, Reyes M. Fast soft-tissue simulation method for cranio-maxillofacial surgery using facial muscle template models. In: 14th annual conference of the international society for computer aided surgery, Geneva, June 2010.
44. Kim H, Jurgens P, Nolte L-P, Weber S, Zeilhofer H-F, Reyes M. Anatomically considered, fast soft-tissue simulation for cranio-maxillofacial surgery. In: In proceedings of computer aided surgery around the Head, Paris; 2009.
45. Kim H, Jurgens P, Cattin P, Weber S, Nolte L-P, Reyes M. Patient-specific, fast soft-tissue simulation for cranio-maxillofacial surgery. In: 17th congress of the European society of biomechanics, Edinburgh, U.K. – Accepted for podium presentation; 2010.
46. Kim H, Jürgens P, Nolte L-P, Reyes M. Anatomically-driven soft-tissue simulation strategy for cranio-maxillofacial surgery using facial muscle template model. Med Image Comput Comput Interv. 2010;13(Pt 1):61–8.
47. Kim H, Jürgens P, Weber S, Nolte L-P, Reyes M. A new soft-tissue simulation strategy for cranio-maxillofacial surgery using facial muscle template model. Prog Biophys Mol Biol. 2010;103(2–3):284–91.
48. Kim H, Jürgens P, Reyes M. Soft-tissue simulation for cranio-maxillofacial surgery: clinical needs and technical aspects. In: Patient-specific modeling in tomorrow's …, no. October 2011, 2012. p. 413–40.
49. Kim H, Jürgens P, Weber S, Nolte L, Reyes M. A new soft-tissue simulation strategy for cranio-maxillofacial surgery using facial muscle template model. Prog Biophys Mol Biol Spec Issue Soft Tissue Model. 2010;103(2–3):284–91.
50. Botticelli S, Verna C, Cattaneo PM, Heidmann J, Melsen B. Two- versus three-dimensional imaging in subjects with unerupted maxillary canines. Eur J Orthod. 2011;33(4):344–9.
51. Franco AL, de Andrade MF, Segalla JCM, Gonçalves DA, Camparis CM. New approaches to dental occlusion: a literature update. Cranio. 2012;30(2):136–43.
52. Hassan B, Couto Souza P, Jacobs R, de Azambuja Berti S, van der Stelt P. Influence of scanning and reconstruction parameters on quality of three-dimensional surface models of the dental arches from cone beam computed tomography. Clin Oral Investig. 2010;14(3):303–10.
53. Varga E, Hammer B, Hardy BM, Kamer L. The accuracy of three-dimensional model generation. What makes it accurate to be used for surgical planning? Int J Oral Maxillofac Surg. 2013;42:1159–66.
54. Cevidanes LHC, Tucker S, Styner M, Kim H, Chapuis J, Reyes M, Proffit W, Turvey T, Jaskolka M. Three-dimensional surgical simulation. Am J Orthod Dentofacial Orthop. 2010;138(3):361–71.
55. Swennen GRJ, Barth E-L, Eulzer C, Schutyser F. The use of a new 3D splint and double CT scan procedure to obtain an accurate anatomic virtual augmented model of the skull. Int J Oral Maxillofac Surg. 2007;36(2):146–52.
56. Swennen GRJ, Mommaerts MY, Abeloos J, De Clercq C, Lamoral P, Neyt N, Casselman J, Schutyser F. A cone-beam CT based technique to augment the 3D virtual skull model with a detailed dental surface. Int J Oral Maxillofac Surg. 2009;38(1):48–57. Churchill Livingstone.
57. Dai J, Hu G, Wang X, Tang M, Dong Y, Yuan H, Xin P, Yang T, Shen SG. CBCT combining with plaster models: application in virtual three-dimensional subapical segmental osteotomy to obtain more precise occlusal splint. J Craniofac Surg. 2012;23(6):1759–62.
58. Chang Y-B, Xia JJ, Gateno J, Xiong Z, Teichgraeber JF, Lasky RE, Zhou X. In vitro evaluation of new approach to digital dental model articulation. J Oral Maxillofac Surg. 2012;70(4):952–62.
59. Chang Y-B, Xia JJ, Gateno J, Xiong Z, Zhou X, Wong STC. An automatic and robust algorithm of reestablishment of digital dental occlusion. IEEE Trans Med Imaging. 2010;29(9):1652–63.
60. Nadjmi N, Mollemans W, Daelemans A, Van Hemelen G, Schutyser F, Bergé S. Virtual occlusion in planning orthognathic surgical procedures. Int J Oral Maxillofac Surg. 2010;39(5):457–62.
61. Lee J-Y, Kim Y-I, Hwang D-S, Park S-B. Effect of maxillary setback movement on upper airway in patients with class III skeletal deformities: cone beam computed tomographic evaluation. J Craniofac Surg. 2013;24(2):387–91.

62. Sahoo NK, Jayan B, Ramakrishna N, Chopra SS, Kochar G. Evaluation of upper airway dimensional changes and hyoid position following mandibular advancement in patients with skeletal class II malocclusion. J Craniofac Surg. 2012;23(6):e623–7.
63. Kim M-A, Kim B-R, Choi J-Y, Youn J-K, Kim Y-JR, Park Y-H. Three-dimensional changes of the hyoid bone and airway volumes related to its relationship with horizontal anatomic planes after bimaxillary surgery in skeletal class III patients. Angle Orthod. 2013;83:623–9.
64. Kochel J, Meyer-Marcotty P, Sickel F, Lindorf H, Stellzig-Eisenhauer A. Short-term pharyngeal airway changes after mandibular advancement surgery in adult class II-patients-a three-dimensional retrospective study. J Orofac Orthop. 2013;74(2):137–52.
65. de Souza Carvalho ACG, Magro Filho O, Garcia IR, Araujo PM, Nogueira RLM. Cephalometric and three-dimensional assessment of superior posterior airway space after maxillomandibular advancement. Int J Oral Maxillofac Surg. 2012;41(9):1102–11.
66. Lee Y, Chun Y-S, Kang N, Kim M. Volumetric changes in the upper airway after bimaxillary surgery for skeletal class III malocclusions: a case series study using 3-dimensional cone-beam computed tomography. J Oral Maxillofac Surg. 2012;70(12):2867–75.
67. Abramson Z, Susarla S, August M, Troulis M, Kaban L. Three-dimensional computed tomographic analysis of airway anatomy in patients with obstructive sleep apnea. J Oral Maxillofac Surg. 2010;68(2):354–62.
68. Pereira-Filho VA, Castro-Silva LM, de Moraes M, Gabrielli MFR, Campos JADB, Juergens P. Cephalometric evaluation of pharyngeal airway space changes in class III patients undergoing orthognathic surgery. J Oral Maxillofac Surg. 2011;69(11):e409–15.
69. Zinser MJ, Zachow S, Sailer HF. Bimaxillary 'rotation advancement' procedures in patients with obstructive sleep apnea: a 3-dimensional airway analysis of morphological changes. Int J Oral Maxillofac Surg. 2013;42(5):569–78.
70. Aykac D, Hoggman EA, McLennan G, Reinhardt JM. Segmentation and analysis of the human airway tree from three-dimensional X-ray CT images. IEEE Trans Med Imaging. 2003;22(8):940–50.
71. Shi H, Scarfe W, Farman A. Upper airway segmentation and dimensions estimation from cone-beam CT image datasets. Int J Comput Assist Radiol Surg. 2006;1(3):177–86.
72. Cheng I, Nilufar S, Flores-Mir C, Basu A. Airway segmentation and measurement in CT images. Conf Proc IEEE Eng Med Biol Soc. 2007;2007:795–9.
73. Bianchi A, Muyldermans L, Di Martino M, Lancellotti L, Amadori S, Sarti A, Marchetti C. Facial soft tissue esthetic predictions: validation in craniomaxillofacial surgery with cone beam computed tomography data. J Oral Maxillofac Surg. 2010;68(7):1471–9.
74. Luthi M, Blanc R, Albrecht T, Gass T, Goksel O, Buchler P, Kistler M, Bousleiman H, Reyes M, Cattin PC, et al. Statismo-a framework for PCA based statistical models. Insight J. 2012;1:1–18.
75. Shahim K, Jürgens P, Cattin PC, Nolte L-P, Reyes M. Prediction of cranio-maxillofacial surgical planning using an inverse soft tissue modelling approach. Med Image Comput Comput Assist Interv. 2013;16(Pt 1):18–25.
76. Gerig T, Shahim K, Reyes M, Vetter T, Lüthi M. Spatially -varying registration using gaussian processes. In: Medical image computing and computer-assisted intervention-MICCAI 2014. Springer International Publishing Switzerland; 2014. p. 413–20.
77. Tanaka M, Dulikravich GS. Inverse problems in engineering mechanics. Amsterdam/Oxford: Elsevier; 1998.
78. Dennis BH, Dulikravich GS. A finite element formulation for the detection of boundary conditions in elasticity and heat conduction. In: Inverse problems in engineering mechanics. Amsterdam: Elsevier; 1998. p. 61.

Part II
Surgical Navigation

Chapter 6
Introduction to Surgical Navigation

Kwok-Chuen Wong

Abstract Surgical navigation was first adopted by neurosurgeons to increase surgical accuracy in neurosurgical procedures, ranging from biopsies to intracranial tumor resections. As bony anatomies remain unchanged between the time of image acquisition and surgical procedures, computer navigation is ideal for assisting orthopaedic interventions. Studies have demonstrated that computer navigation technology can improve the accuracy of various orthopedic surgical procedures, such as spinal pedicle screw insertion, joint arthroplasty, trauma surgery, anterior cruciate ligament reconstruction and recently bone tumor surgery. However, the evidence of improving long-term clinical outcome as a result of improved surgical accuracy with the computer technology is still lacking. Knowledge of computer navigation and its potential advantages and limitations in various orthopaedic procedures are essential to the successful applications of the computer technology to orthopaedic care. This chapter is to introduce the basic principles of surgical navigation and give an overview on the evidence of its use in orthopaedic applications.

Keywords Computed assisted surgery • Surgical navigation • Registration and navigation errors

Introduction

Surgical navigation was first adopted by neurosurgeons to increase surgical accuracy in neurosurgical procedures, ranging from biopsies to intracranial tumor resections. As bony anatomies remain unchanged between the time of image acquisition and surgical procedures, computer navigation is ideal for assisting orthopaedic interventions. Studies have demonstrated that computer navigation technology can improve the accuracy of various orthopedic surgical procedures, such as spinal pedicle screw insertion, joint arthroplasty, and trauma surgery. This chapter is to

K.-C. Wong, FRCSEd (Ortho)
Department of Orthopaedics and Traumatology, Prince of Wales Hospital, Hong Kong, China
e-mail: skcwong3@gmail.com

L.E. Ritacco et al. (eds.), *Computer-Assisted Musculoskeletal Surgery: Thinking and Executing in 3D*, DOI 10.1007/978-3-319-12943-3_6

introduce the basic principles of surgical navigation and give an overview on the evidence of its use in orthopaedic applications.

Computer-assisted systems are categorized into three systems: active robotic system, semi-active robotic system and passive system [1]. Surgical navigation is a passive system that does not actively carry out surgical tasks on patients. It provides information and guidance to surgeons who perform operation with conventional instruments. It allows linking between the patient's imaging information and anatomy through the use of tracking and registration of the preoperative and/or intraoperative acquired images.

Navigation Setup

Navigation machine use charged coupled device (CCD) cameras as optical sensors to obtain positional information of the target bones and surgical tools (Fig. 6.1). A dynamic reference frame (DRF) with infrared light-emitting diodes or reflective markers is attached to the target bones and surgical tools. The optical sensors detect the infrared light from the DRF and measure the position of the tracking objects at the operative site. This optical tracking is accurate with the positional error of <0.1 mm. The real-time positions are then visualized on the acquired medical images in the navigation display. However, one disadvantage of the setup is that the line of sight cannot be interrupted between the tracking objects and CCD cameras. The newer technology like magnetic sensors does not have this disadvantage and are not affected by obstacles between cameras and tracking objects.

Navigation involves three essential steps: data acquisition, registration and tracking.

Data Acquisition

Data can be acquired preoperatively and intraoperatively. All medical images are stored in the form of Digital Imaging and Communications in Medicine (DICOM). The preoperative medical images (CT / MR) in the format of DICOM are transferred to the navigation system where image analysis and surgical planning can be performed before the actual operation. The 2D and even 3D fluoroscopic images can be obtained intraoperatively for navigation surgery. Imageless based navigation does not rely on medical images but uses Bone Morphing technique that is a process of recovering the 3D shape of a patient's anatomy from a few available digitized landmarks and surface points. After surgeons defined specific anatomical bony landmarks using a navigation pointer, a bone model that is derived from the large number of stored CT datasets and fit to the defined bony surface points is generated. These data are then used for registration and tracking.

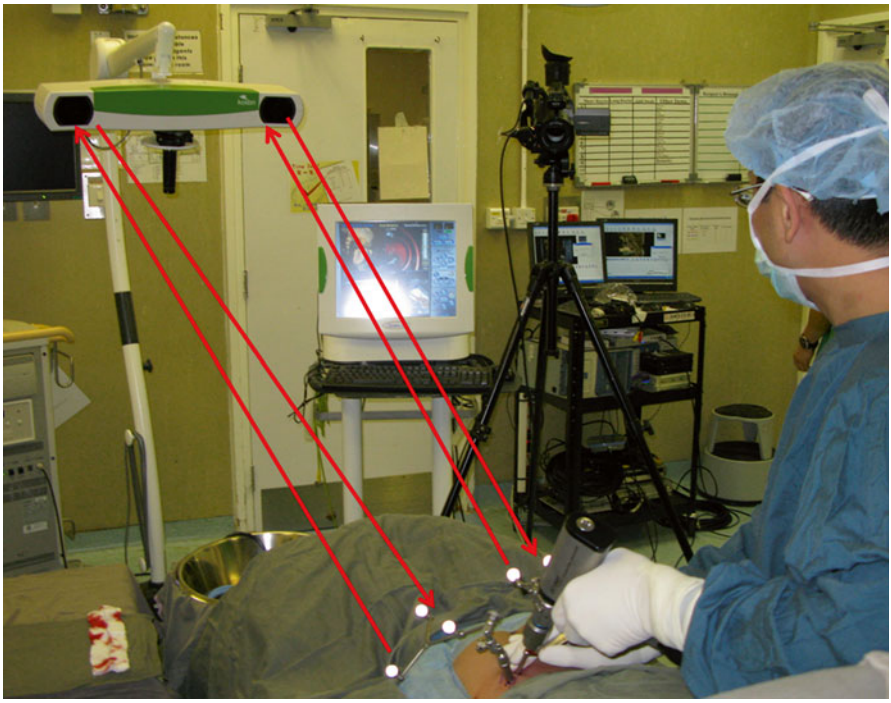

Fig. 6.1 Shows the intraoperative setup of surgical navigation that includes a stereotactic cameras, a computer station with a monitor showing navigation images and dynamic reference trackers (passive trackers with reflective spheres in this procedure) firmly attached to the patient's bone and the surgical tool

Registration

Image-to-patient registration is a process in which surgeons tell the computer where the bone is in the space by identifying the anatomical landmarks for the computer. Therefore, it links up the medical images (Xray, CT, MRI or patient's 3D bone model) with the patient's anatomy at the operative site. The first method of registration is by placement of tracker pins or fiducial markers at the target bones during 2D/3D image acquisition. Registration is completed after images are acquired or the fiducial markers are identified at the surgery. The second method of registration is surface-matching technique (Fig. 6.2). To start the initial registration, paired-points matching is used to start the initial registration. Four to five predefined points on the preoperative images are matched with the corresponding points on the patient's anatomy during surgery. To further improve the registration accuracy, more surface points are collected from the target bone that are then matched to the shape of the bone surface model generated from preoperative CT images. The third method is 2D-3D registration (Fig. 6.3). Two fluoroscopic images obtained intraoperatively are matched automatically with preoperative CT images after manual image adjustment.

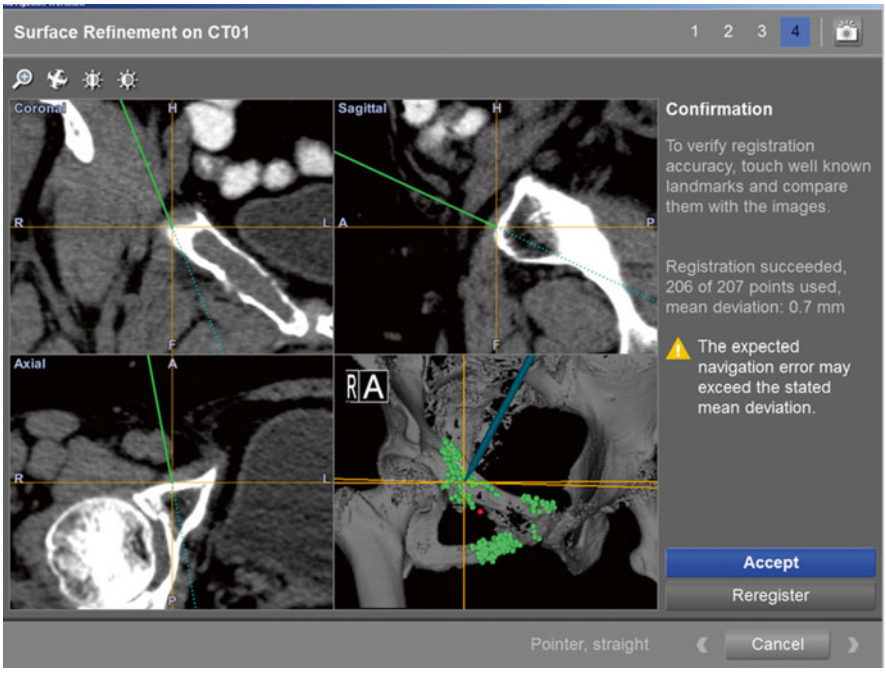

Fig. 6.2 Shows the navigation display after paired-points and surface registration during a CT-based navigated resection in a patient with right pubic malignant tumor. The registration error generated from the navigation machine was 0.7 mm. By placing the navigation probe on the bone surface, the tip of the navigation probe was exactly matching to the preoperative images, thereby verifying the registration accuracy before we can rely on the preoperative images to execute the surgical planning

Tracking

The target bones and the relative position of surgical tools to the target bone are tracked by 3D optical or magnetic sensors during surgery. Trackers are placed at the target bones while surgical tools are connected with another trackers (Fig. 6.4a, b). The information can be used for identifying the distorted anatomy, visualizing the bone or implant alignment and determining the orientation or level of bone osteotomy.

Based on the method of referencing information, computer-assisted navigation systems are subdivided into computer tomography (CT) based, fluoroscopic based and imageless. CT-based navigation is the most accurate but it requires additional preoperative CT scanning. It adds extra time for planning and radiation exposure. Fluoroscopic-based navigation is convenient and registered images can be acquired intraoperatively after the placement of patient's tracker. It is good for trauma fracture fixation and spine surgery in particular with minimally invasive techniques. Imageless-based navigation does not require images. As it does not take into account the unique bony anatomy of each individual, error may arise when surgeons perform the registration by just pointing at bony landmarks.

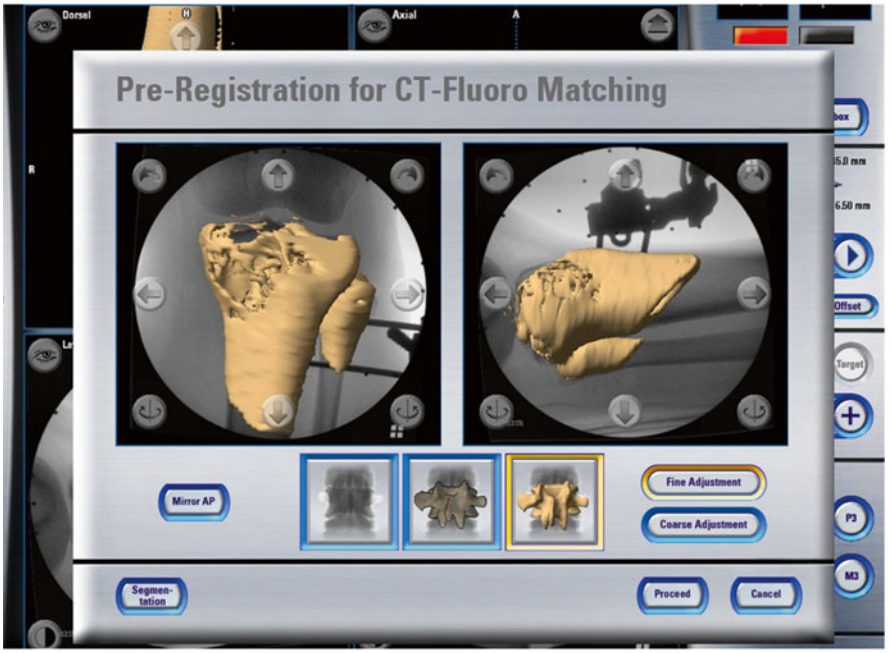

Fig. 6.3 Shows the navigation display after 2D to 3D registration (CT-fluoro matching) during a CT-based navigated procedure in a patient with proximal tibia tumor. A dynamic reference tracker was first attached to the patient's tibia. Two fluoroscopic images with different views were then acquired by a navigation-phantom-mounted Xray machine. The two registered images were automatically matched with the 3D bone model generated from the preoperative CT images. This registration method allows registration of preoperative CT images without an open surgical procedure and thus facilitates minimally invasive surgery

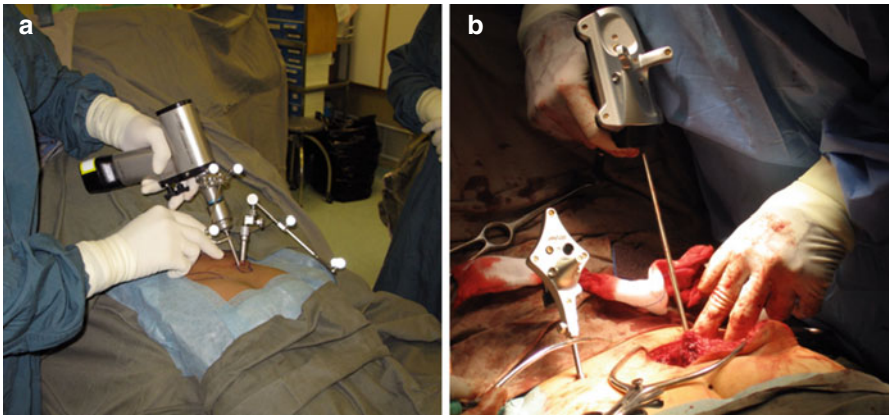

Fig. 6.4 shows passive trackers with reflective spheres (**a**) and active trackers with infrared light-emitting diodes (**b**) attaching to the patients' bones and surgical tools. A stereotactic cameras tracks the target bones and the relative position of surgical tools to the target bones by 3D optical sensors during surgery

Clinical Applications and Results

Surgical navigation has been investigated as an adjunct in assisting orthopaedic procedures, particularly in (1) spine surgery; (2) joint arthroplasty; (3) fracture fixation; (4) anterior cruciate ligament reconstruction; (5) bone tumor surgery. In general, use of surgical navigation aims to improve the accuracy of surgical procedures by achieving better position of implants, restoring correct alignment of articular joints or decreasing contaminated tumor resection margin. It is believed that improving surgical accuracy can lead to a better clinical outcome with regards to limbs function, surgical revision rate or tumor recurrence rate. Also, as surgical navigation improves accuracy of surgical instrumentation, it not only may reduce the intraoperative radiation exposure but also allow minimally invasive surgery to be performed.

Spine Surgery

Malpositioning of screws may damage nearby neural and vascular structures in spine surgery, which requires instrumentation. Image guided navigation helps improve the accuracy of screw placement and the surgical safety. It evolves from 2D and then 3D fluoroscopic navigation during surgery. The current intraoperative CT scanner, O arm (Medtronic, Inc., Louisville, CO, USA) allows imaging of the screws intraoperatively.

In a meta analysis of 30 studies with 1973 patients in whom 9310 pedicle screws were inserted, a significantly better accuracy of pedicle screw placement in the cervical, thoracic, and lumbosacral spine was achieved with intraoperative 3D fluoroscopic navigation (95.5 % accuracy) than with 2D fluoroscopic navigation (83.4 % accuracy). Also, both 2D and 3D navigation achieved a better accuracy of pedicle screw insertion than that with traditional fluoroscopy techniques (68.1 % accuracy) [13].

A comparative meta-analysis was carried out by Bourgeois et al. [3]. 3D fluoroscopic-navigated, percutaneous placement of 2132 lumbar pedicle screws were reviewed and compared with 2D fluoroscopic-navigated placement of 4248 screws. The breach rate of screw placement was 0.33 and 13.1 % in 3D and 2D navigated group respectively. 3D fluoroscopic navigation offers markedly improved accuracy of percutaneous lumbar pedicle screw placement in minimally invasive spine surgery.

The surgical navigation may be most beneficial in scoliosis or dysplastic with significant spinal deformity for safe and accuracy instrumentation [8, 23] and in thoracic or cervical spines where the accuracy is critical for narrow bone corridor in screw placement [10].

Joint Replacement Surgery

Surgical navigation was used to increase the accuracy of implant positioning during total knee and total hip arthroplasty as malposition of implant components may compromise implant function and its survival.

Cheng et al. [6] reported a meta-analysis of 41 randomized controlled trials (RCTs) about navigated total knee arthroplasty (TKA). The results suggested that navigation technique improved the accuracy of mechanical leg axis and component orientation. Bauwens et al. [2] did a meta-analysis by reviewing 33 studies (11 RCTs) about navigated TKA with varying methodological quality involving 3423 patients. The alignment of mechanical axes did not differ between navigated and conventional surgery group. However, patients managed with navigated surgery had a lower risk of malalignment at critical thresholds of >3°. Its clinical benefits are unclear as no conclusive inferences could be drawn on functional outcomes or complication rates. Currently, most studies reported that the technique can reduce the outliers of leg alignment and implant malpositioning when compared with conventional technique. There is still no convincing evidence that the marginal benefits can improve the long-term clinical outcome of patient with navigated TKA.

There are few controlled studies examining the role of surgical navigation in total hip arthroplasty (THA). Parratte et al. [18] reported a RCT of 60 individuals undergoing THA with and without imageless computer navigation. There were no significant differences between the two groups in terms of cup anteversion and abduction angles, but with the lowest variations in the navigation group. The authors concluded that the use of imageless navigation can improve cup positioning in THA by reducing the percentage of outliers. Iwana D et al. [11] reported a study of 117 hips undergoing CT-based navigated THA, showing the absolute spatial error of cup position was ≤2 mm for each axis, and the angle error was ≤2° for the cup inclination and anteversion. Current clinical studies suggest that navigation system can help surgeons perform accurate cup placement. CT-based Navigated THA also enabled intraoperative assessment of hip range of motion and limb length [15, 16, 21]. Accurate cup placement was shown to have a better clinical outcome in patients with CT-based navigated THA [22]. In a study with a minimum of 10 years' follow-up, 46 patients (60 hips) and 97 patients (120 hips) receiving cementless THA with or without CT-based navigation, respectively, were retrospectively reviewed. The navigation group has reduced rates of dislocation and impingement-related mechanical complications leading to revision.

Fracture Fixation

Image-guided navigation has been reported as an adjunct for fixation in pelvic, acetabular fracture as these fractures not only are located at complex anatomical sites but also frequently requires percutaneous screw fixation. The correct entry point and the small target corridor may be difficult to visualize using only an image intensifier.

In a meta analysis of 51 studies including 2353 percutaneous iliosacral screw implantations following pelvic fractures in 1731 patients [27], CT navigation had the lowest rate of screw malposition (0.1 % for 262 screws), but it could not be used for all type of fractures where surgical procedures (reduction maneuvers, additional osteosynthetic procedures) are necessary. The 2D and 3D fluoroscopic navigation and reconstruction techniques provide encouraging results with slightly lower rate of complications 1.3 % (total 445 screws) compared with the conventional technique

2.6 % (total 1832 screws). Rate of screws revision was similar among the three techniques. The study concludes that image-guided navigation is an additional tool to enhance the precision of screw placement and may decrease the rate of revision.

Matityahu A et al. [14] reported a multicenter randomized study of percutaneous sacroiliac screws for pelvic fracture fixation. For 72 patients from the navigated group and 58 patients from the conventional fluoroscopic group, the misplaced screws in navigated and conventional groups are 0 % and 40 % respectively. The authors recommend the use of 3D navigation, where available, for insertion of sacroiliac screws in patients with pelvic fracture.

Ochs BG et al. [17] did a cadaveric study and investigated the role of 3D fluoroscopic navigation in percutaneous periacetabular screw insertion for minimally displaced acetabular fracture. 210 screws were inserted into 30 pelvic models and 30 cadaveric hemipelvis with either conventional 2D fluoroscopy or 3D fluoroscopic navigation. Especially for posterior column screws, due to a lower perforation rate and a higher accuracy in periacetabular screw placement, 3D fluoroscopic navigation procedure appears to be the method of choice for image guidance in acetabular surgery. It remains to be seen whether the favourable results of the navigation technique can be shown in future clinical studies.

Other indication such as intramedullary nailing of long bone fractures has been recently reported by Hawi N et al. [9]. 24 patients who received navigation-assisted treatments and 48 patients who received unassisted treatments, were matched for age, sex, and femur fracture type. Femoral nailing was performed. The results did not support the routine use of navigation in femoral nailing as no improvement in postoperative results or reduction in radiation exposure could be demonstrated when compared with unassisted group. Computer navigation may provide advantages for complicated or sophisticated cases, such as complex 3D deformity corrections.

Anterior Cruciate Ligament Reconstruction

Inaccurate bone tunnel placement is an important cause of failure or poor results in anterior cruciate ligament (ACL) reconstruction. Use of surgical navigation in addressing this problem remains controversial. Cheng T et al. [4] have carried out a systematic review of five RCTs/quasi-RCTs comparing conventional versus computer-navigated ACL reconstruction. It showed that both navigated and conventional ACL reconstructions have similar radiographic results as both groups placed the tibial tunnel in acceptable positions. However, the risk of notch impingement was less in the navigated group than the conventional group. The same groups of authors went on to assess the early clinical outcomes after navigated ACL reconstruction in another meta-analysis of the existing RCTs [5]. The use of computer-assisted navigation systems led to additional operative time (8–17 min).

No significant differences between navigated and conventional groups were found in terms of knee stability and functional assessment during short-term follow-up. High-quality studies with long-term follow-up are still needed to prove the clinical significance of the navigation assistance in ACL reconstruction.

Bone Tumor Surgery

Clear resection margin is important for oncological outcomes in surgical management of primary bone sarcoma. Inadequate resection margin may result in increase rate of local recurrence and compromise patients' survival. Therefore, computer navigation approach has been developed to improve surgical accuracy with the goal of achieving clear resection margins and better oncologic results.

Currently, there are no RCTs as it is still in the early development phase of computer assisted tumor surgery (CATS) in orthopaedic oncology. Few short-term clinical studies in various centers reported that CATS technique can aid and reproduce surgical planning with good accuracy and help in safe tumor resection. It may lead to better oncological and functional outcomes [7, 19, 24]. One study confirmed the finding in a series of 31 patients with pelvic or sacral malignant bone tumors undergoing resection with CATS technique that reduced intralesional resection from 29 to 8.7 % [12].

Given the complexity of CATS planning and additional time for intraoperative setup, CATS technique is in general restricted to tumor resection at complex anatomical sites in pelvis and sacrum or more technically demanding procedures such as multiplanar tumor resections [26].

Conclusion

When compared with conventional techniques, extra operative time, cost of navigation facilities, initial learning curve and complications related to tracker pins placement are some of the concerns when using surgical navigation for orthopaedic intervention. Surgeons should understand and know about the potential errors during the whole navigated procedures as any misinterpretation of the virtual navigational information may result in inaccuracy and potentially adverse clinical results (Table 6.1). Though the majority of the referenced studies showed that computer navigation can assist surgeons in performing more consistent and accurate orthopaedic procedures, the evidence of significantly improved clinical outcomes comparing with conventional procedures is still lacking. Therefore, long-term studies are needed to prove its clinical efficacy.

Table 6.1 Potential errors and the ways to minimize the errors during Computer Navigation Orthopaedic Surgery [20, 25]

System error (inherent hardware and software error from the position measuring of surgical navigation system)
Check correct placement and function of the tracking elements on surgical tool and dynamic reference frame (DRF)
Check batteries for navigation system using active trackers
Keep 15–30 min for warm-up of the stereotactic camera
Calibrate each probe and navigated tools with care
Check correct positioning range of the tracking elements on surgical tool and the DRF related to the stereotactic camera
Preoperative stage
Imaging error (error of the imaging modality in geometrically correct depiction of the anatomic structures)
Use Multi-slice CT machine with small isotropic voxels and high-resolution bone kernels
Only scan the region of interest to maximize the resolution of target region
Use CT slice thickness of 0.625 mm and MR slice thickness of at least 2 mm for better quality of images and planning
Images should be acquired as close to the date of the operation as possible, so to minimize the discrepancy between imaging information and patients' pathology
Error in CT-based navigation planning (accuracy and quality of planning is limited by the quality of the original preoperative images)
Always choose >4 registration points that are easily identified by surgeons on both preoperative images and on the patient's anatomy
Registration markers should be broadly selected around the region of operative interest and not be on the same 3D coordinate plane
If using different image modality datasets, always visually check that image coregistration is accurate before proceeding to intraoperative execution
Intraoperative stage
Check the correct placement and stable fixation of DRF on the patient's bone that the navigated procedure will be performed
Image-to-patient Registration error (*CT-based navigation*)
Paired-point registration
Within your surgical exposure, select anatomical identifiable bony locations that allow accurate definition of paired-points both on the image data and on the patient
Recollect and re-perform the registration again for those points with high errors
Surface matching registration
Select points from the surface of the exposed bones with contoured and complex shape
The calculated registration errors from the navigation system cannot be trusted completely as they only represent the mismatch between the planned and chosen points
Always verify the registration accuracy by touching anatomical points or tracing along the bone surface
Accept the registration only if the calculated position on the navigation display is comparable with the real position on the patient
Application error
Avoid displacement of the DRF
Avoid operators' errors including hand tremors and visual misinterpretation of navigation information during surgical procedure

References

1. Bae DK, Song SJ. Computer assisted navigation in knee arthroplasty. Clin Orthop Surg. 2011;3(4):259–67. doi:10.4055/cios.2011.3.4.259. Epub 2011 Dec 1. Review.
2. Bauwens K, Matthes G, Wich M, Gebhard F, Hanson B, Ekkernkamp A, Stengel D. Navigated total knee replacement. A meta-analysis. J Bone Joint Surg Am. 2007;89(2):261–9 (TKR).
3. Bourgeois AC, Faulkner AR, Bradley YC, Pasciak A, Barlow PB, Gash JR, Reid WS Jr. Improved accuracy of minimally invasive transpedicular screw placement in the lumbar spine with three-dimensional stereotactic image guidance: a comparative meta-analysis. J Spinal Disord Tech. 2014 Aug 1. [Epub ahead of print].
4. Cheng T, Liu T, Zhang G, Zhang X. Computer-navigated surgery in anterior cruciate ligament reconstruction: are radiographic outcomes better than conventional surgery? Arthroscopy. 2011;27(1):97–100. doi:10.1016/j.arthro.2010.05.012. Epub 2010 Oct 15. Review.
5. Cheng T, Zhang GY, Zhang XL. Does computer navigation system really improve early clinical outcomes after anterior cruciate ligament reconstruction? A meta-analysis and systematic review of randomized controlled trials. Knee. 2012;19(2):73–7. doi:10.1016/j.knee.2011.02.011. Epub 2011 Apr 1. Review.
6. Cheng T, Zhao S, Peng X, Zhang X. Does computer-assisted surgery improve postoperative leg alignment and implant positioning following total knee arthroplasty? A meta-analysis of randomized controlled trials? Knee Surg Sports Traumatol Arthrosc. 2012;20(7):1307–22. doi:10.1007/s00167-011-1588-8. Epub 2011 Jul 6. Review.
7. Cho HS, Oh JH, Han I, Kim HS. The outcomes of navigation-assisted bone tumour surgery: minimum three-year follow-up. J Bone Joint Surg Br. 2012;94(10):1414–20.
8. Cui G, Wang Y, Kao TH, Zhang Y, Liu Z, Liu B, Li J, Zhang X, Zhu S, Lu N, Mao K, Wang Z, Zhang X, Yuan X, Dong T, Xiao S. Application of intraoperative computed tomography with or without navigation system in surgical correction of spinal deformity: a preliminary result of 59 consecutive human cases. Spine (Phila Pa 1976). 2012;37(10):891–900. doi:10.1097/BRS.0b013e31823aff81.
9. Hawi N, Liodakis E, Suero EM, Stuebig T, Citak M, Krettek C. Radiological outcome and intraoperative evaluation of a computer-navigation system for femoral nailing: a retrospective cohort study. Injury. 2014;45(10):1632–6. doi: 10.1016/j.injury.2014.05.039.
10. Hojo Y, Ito M, Suda K, Oda I, Yoshimoto H, Abumi K. A multicenter study on accuracy and complications of freehand placement of cervical pedicle screws under lateral fluoroscopy in different pathological conditions: CT-based evaluation of more than 1,000 screws. Eur Spine J. 2014;23:2166–74.
11. Iwana D, Nakamura N, Miki H, Kitada M, Hananouchi T, Sugano N. Accuracy of angle and position of the cup using computed tomography-based navigation systems in total hip arthroplasty. Comput Aided Surg. 2013;18(5-6):187–94. doi:10.3109/10929088.2013.818713. Epub 2013 Jul 17.
12. Jeys L, Matharu GS, Nandra RS, Grimer RJ. Can computer navigation-assisted surgery reduce the risk of an intralesional margin and reduce the rate of local recurrence in patients with a tumour of the pelvis or sacrum? Bone Joint J. 2013;95-B(10):1417–24. doi:10.1302/0301-620X.95B10.31734.
13. Mason A, Paulsen R, Babuska JM, Rajpal S, Burneikiene S, Nelson EL, Villavicencio AT. The accuracy of pedicle screw placement using intraoperative image guidance systems. J Neurosurg Spine. 2014;20(2):196–203. doi:10.3171/2013.11.SPINE13413. Epub 2013 Dec 20. Review.
14. Matityahu A, Kahler D, Krettek C, Stöckle U, Grutzner PA, Messmer P, Ljungqvist J, Gebhard F. 3D navigation is more accurate than 2D navigation or conventional fluoroscopy for percutaneous sacroiliac screw fixation in the dysmorphic sacrum: a randomized multicenter study. J Orthop Trauma. 2014;28:707–10.
15. Miki H, Yamanashi W, Nishii T, Sato Y, Yoshikawa H, Sugano N. Anatomic hip range of motion after implantation during total hip arthroplasty as measured by a navigation system. J Arthroplasty. 2007;22(7):946–52.

16. Miki H, Kyo T, Sugano N. Anatomical hip range of motion after implantation during total hip arthroplasty with a large change in pelvic inclination. J Arthroplasty. 2012;27(9):1641–1650. e1. doi:10.1016/j.arth.2012.03.002. Epub 2012 Apr 20.
17. Ochs BG, Gonser C, Shiozawa T, Badke A, Weise K, Rolauffs B, Stuby FM. Computer-assisted periacetabular screw placement: comparison of different fluoroscopy-based navigation procedures with conventional technique. Injury. 2010;41(12):1297–305. doi:10.1016/j.injury.2010.07.502. Epub 2010 Aug 21.
18. Parratte S, Argenson JN. Validation and usefulness of a computer-assisted cup-positioning system in total hip arthroplasty. A prospective, randomized, controlled study. J Bone Joint Surg Am. 2007;89(3):494–9. THA.
19. Ritacco LE, Milano FE, Farfalli GL, Ayerza MA, Muscolo DL, Aponte-Tinao LA. Accuracy of 3-D planning and navigation in bone tumor resection. Orthopedics. 2013;36(7):e942–50. doi:10.3928/01477447-20130624-27.
20. Saidi K. Potential use of computer navigation in the treatment of primary benign and malignant tumors in children. Curr Rev Musculoskelet Med. 2012;5(2):83–90. doi:10.1007/s12178-012-9124-0.
21. Sugano N, Nishii T, Miki H, Yoshikawa H, Sato Y, Tamura S. Mid-term results of cementless total hip replacement using a ceramic-on-ceramic bearing with and without computer navigation. J Bone Joint Surg Br. 2007;89(4):455–60.
22. Sugano N, Takao M, Sakai T, Nishii T, Miki H. Does CT-based navigation improve the long-term survival in ceramic-on-ceramic THA? Clin Orthop Relat Res. 2012;470(11):3054–9. doi:10.1007/s11999-012-2378-4.
23. Ughwanogho E, Patel NM, Baldwin KD, Sampson NR, Flynn JM. Computed tomography-guided navigation of thoracic pedicle screws for adolescent idiopathic scoliosis results in more accurate placement and less screw removal. Spine (Phila Pa 1976). 2012;37(8):E473–8. doi:10.1097/BRS.0b013e318238bbd9.
24. Wong KC, Kumta SM. Computer-assisted tumor surgery in malignant bone tumors. Clin Orthop Relat Res. 2013;471(3):750–61. doi:10.1007/s11999-012-2557-3.
25. Wong KC, Kumta SM. Joint-preserving tumor resection and reconstruction using image-guided computer navigation. Clin Orthop Relat Res. 2013;471(3):762–73. doi:10.1007/s11999-012-2536-8.
26. Wong KC, Kumta SM. Use of computer navigation in orthopedic oncology. Curr Surg Rep. 2014;2:47. eCollection 2014. Review.
27. Zwingmann J, Hauschild O, Bode G, Südkamp NP, Schmal H. Malposition and revision rates of different imaging modalities for percutaneous iliosacral screw fixation following pelvic fractures: a systematic review and meta-analysis. Arch Orthop Trauma Surg. 2013;133(9):1257–65. doi:10.1007/s00402-013-1788-4. Epub 2013 Jun 8.

Chapter 7
Bone Tumor Navigation in the Pelvis

Lee Jeys and Philippa L. May

Abstract Pelvic and sacrum bones are highly complex in shape that is why they are one of the most challenging surgeries to achieve in oncologic orthopedics. Traditional resection and reconstruction are done "freehand" that is highly inaccurate. Conventionally, surgeons rely on twodimensional images from the pelvis. In this kind of surgeries it is achieved negative but also wide resections margins to be removed with a surrounding margin of healthy tissue so as to ensure the complete resection of the tumor. The complexity of pelvic surgeries relies on the size of the tumors that use to be huge, the difficulty to access, close proximity to vital structures and multiplanar complexity. It makes impossible to design onedesignfitsall prosthesis that is why this kind of surgeries overturn to computer assisted surgery and navigated guideline because it has identifiable bony prominences to use as reference points for resection. Preoperative navigation enables physicians to explore the tumor area before the operation and learn about the possible way outs of the resection. Intraoperative navigation simplifies surgeries reducing the risk of damaging vital structures and measure depth of penetration of the instruments, guiding the surgeon within the anatomical structures during the whole procedure. Although computer navigation assisted surgery in the Pelvis is in its relative infancy it is a useful asset that results on decreasing revision rate, decreasing need of amputation and saving nerves roots.

Keywords Computed assisted surgery • Preoperative planning • Allograft reconstruction and musculoskeletal tumors

L. Jeys, MB, ChB, MSc (Ortho. Eng), FRCS (✉)
FRCS Royal Orthopaedic Hospital, Birmingham, UK
e-mail: lee.jeys@nhs.net

P.L. May, BMedSci (Clin Sci), MBChB
College of Medical and Dental Sciences, University of Birmingham,
Edgbaston B15 2TT, UK
e-mail: pxm931@bham.ac.uk, phili_may@live.cp.uk

L.E. Ritacco et al. (eds.), *Computer-Assisted Musculoskeletal Surgery: Thinking and Executing in 3D*, DOI 10.1007/978-3-319-12943-3_7

Introduction

The pelvis and sacrum remain one of the most challenging locations for surgery in musculoskeletal oncology. The complex three-dimensional anatomy, proximity of vital structures, consistency of tumor and variable position of the patient during the procedure all contribute to the difficulty of surgical resection of pelvic and sacral tumors. Computer assisted sarcoma surgery has already improved surgical outcomes with regard to local recurrence, revision rates, amputations and nerve root damage despite being in its relative infancy within orthopedic tumor surgery [1, 2].

Osteogenic Pathology of the Pelvic Girdle

Pelvic and sacral tumors make up approximately 25 % of all chondrosarcomas and Ewings tumors but less than 8 % of osteosarcoma cases. The major tumor types seen that affect the pelvis are primary bone tumors but also locally invasive tumors from surrounding structures and metastases. Some less common tumors that have a predisposition to the pelvis and sacrum are chordomas, arising from remnant notochord, and benign tumors such as osteoblastomas, giant cell tumors and sacrococcygeal teratomas.

Primary Bone Tumors

Osteosarcoma, a malignant bone tissue tumor, is the most common primary bone tumor. It occurs most frequently in teens and young adults, and is the eighth most common form of childhood cancer, comprising 2.4 % of all malignancies in paediatric patients, and approximately 20 % of all primary bone cancers. Less than 8 % of osteosarcomas occur in the pelvis [3]. Ewing's sarcoma is a small round blue cell tumor, often located in the shaft of long bones and in the pelvic bones. It also occurs most frequently in children and young adults. Chondrosarcoma is a malignant growth of cartilage cells which often occurs as a secondary cancer by malignant degeneration of pre-existing benign tumors of cartilage cells such as enchondromas within bone and is primarily found among older adults. There is an average of 131, 96 and 55 new cases of osteosarcoma, chondrosarcoma and Ewing's sarcoma respectively diagnosed each year in England [4]. These malignancies tend to present late owing to their insidious growth and non-specific presentations and the ability of the pelvis to accommodate large tumors before they become noticeable to the patient. Though these tumors do not contribute a high volume of cases, the patients are typically young and therefore the loss of function is all the more devastating. The operations involved are also long, complex, may require personalised implants and have a mean inpatient stay of 28 days in our institution. Recurrence rates are high, as are rates of complications such as amputation, infection, prosthesis failure and nerve damage, all of which

comes at great cost, both in terms of financial implications to the institution and morbidity for the patient.

Sacral Tumors

Tumors of the sacrum are rare. Primary benign and malignant tumors of the sacrum may arise from bone or neural elements. Six percent of all malignant bone tumors involve the sacrum, including chordomas (50 % of cases), lymphomas (9 %) and multiple myelomas (9 %), Ewing's sarcoma in children (8 %), chondrosarcomas in adults, and osteosarcomas [5]. Sacral tumors, like pelvic tumors, usually remain clinically silent for a long time. The most common initial symptom is local pain due to structural weakness, mass effect and compression [6]. Lateral extension of sacral tumors across the sacroiliac joints causes local joint pain and invasion into gluteus maximus and piriformis muscles leads to pain and decreased hip extension and external rotation power. Nerve root compression causes radicular pain radiating into buttocks, posterior thigh or leg, external genitalia, and perineum. At a later stage, motor deficit, and eventually, bladder/bowel and/or sexual dysfunction is noted [7]. Sacral tumors are especially difficult to resect and invariably neurological dysfunction results as nerve roots are disturbed. If the tumor is lateral, this may be avoided but there is a risk of damaging the sacroiliac joints and affecting the weight-bearing capacity of the pelvic girdle.

Metastases

Metastatic disease is the most common malignancy of bone; prostate, breast, lung, kidney, and thyroid cancer account for 80 % of skeletal metastases [8]. The pelvis is the second most common site of bone metastases after the spine [9]. The management of metastatic lesions may be curative or palliative and involves a wide array of treatment modalities including chemotherapy, radiotherapy and surgery. Not all metastatic lesions of the pelvis require surgical stabilization; lesions not directly involving the hip joint, pathological fractures not involving the acetabulum, and avulsion fractures of the anterior superior/inferior iliac spines, iliac crest, and pubic rami do not compromise pelvic stability [10]. In contrast, diffuse involvement of the pelvis, pelvic discontinuity and bony destruction of the periacetabular area warrant surgical treatment [11]. It may seem counter-intuitive to put palliative patients through high risk surgery, but the goal of palliation is to relieve the patient's suffering and improve quality of life. Therefore, according to the patient's condition, surgical treatment is recommended under the following conditions: (a) severe symptoms which are not alleviated by immobilization of the limb, analgesic drugs and anti-tumor therapy; (b) no pain relief or unsatisfactory recovery of function of the affected extremity after radiotherapy; and (c) pathologic fracture of the ipsilateral femur or adjacent site requiring simultaneous treatment [12].

Challenges Faced During Pelvic Surgery

The pelvis is a highly challenging area to operate upon which requires great skill and experience to achieve successful results. The reasons for this difficulty are explored in the following section.

Size

Pelvic tumors, particularly primary pelvic tumors, can grow very large before they are picked up. Figure 7.1 demonstrates a large pelvic tumor invading into local structures. Typical symptoms of bone tumors such as pain and stiffness may be attributed to more common pathologies such as hip osteoarthritis, swelling may be impalpable due to the considerable overlying muscle bulk and symptoms of nerve compression (such as sciatica or incontinence) are highly non-specific. Therefore pelvic tumors can be extensive at diagnosis.

Anatomy

The pelvic bones have a complex anatomy both in their three-dimensional structure and their relationship to one another. The pelvis forms a ring, therefore encompasses a full 360°. The pelvis is also relatively inaccessible, particularly when compared to the long bones, and it is large. Therefore pelvic surgery often involves moving the patient intraoperatively to gain access. This coupled with the complex multiplanar structure makes pelvic surgery very challenging.

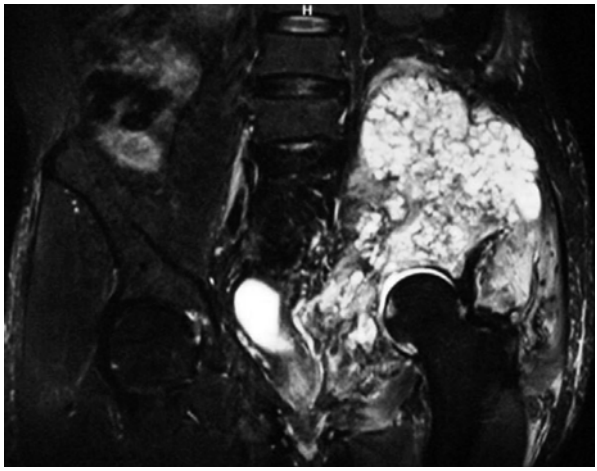

Fig. 7.1 Low grade chondrosarcoma of the pelvis

Consistency

Bone malignancies have variable consitencies, but often have cystic elements which may burst during the removal of the tumor. The tumor is also weaker than the surrounding healthy bone and may fracture upon removal. This makes it more difficult for the surgeon to remove the entire tumor en bloc and avoid tumor spill.

Margins

In order to reduce the risk of recurrence, it is accepted practice throughout oncology to achieve negative but also wide resection margins; that is, the tumor is removed with a surrounding margin of healthy tissue to ensure the entire tumor has been excised. This is very difficult to achieve during pelvic bone tumor surgery due to the size of the tumors being removed, difficulty of access, close proximity of vital structures and the multiplanar complexity of the structures involved. In addition, the late presentation of these tumors often allows the tumor to have invaded into local structures such as the pelvic veins or organs. Figure 7.2 demonstrates a pelvic chondrosarcoma in close proximity to the bladder, but with a clear plane for resection, Fig. 7.2a demonstrates a tumor invading into the bladder wall. Wide excision would be impossible in the case in Fig. 7.2a without a partial cystectomy. Additional difficulty occurs when a tumor has close anatomical relations to joints. It is common practice to preserve the joint architecture and articular surfaces during surgery to provide a better functional result, but often this is hampered by the desire to achieve a wide excision margin. Figure 7.3 shows intra-lesional, marginal, wide and radical resection margins. In patients with musculoskeletal malignancy the ultimate aim is to perform a wide-local resection and achieve adequate disease-free margins. Inadequate resection margins (intra-lesional or marginal) are frequently obtained [13]. The importance of achieving adequate surgical margins

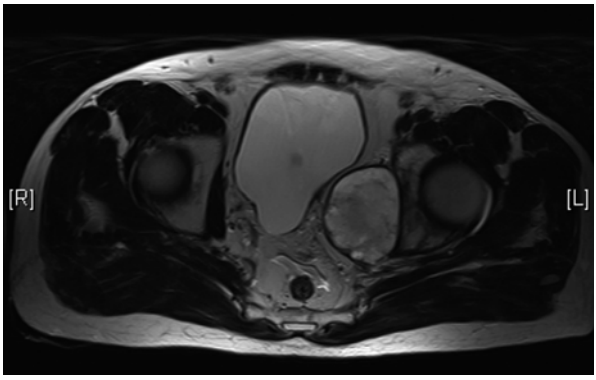

Fig. 7.2 Axial MRI scan of a pelvic chondrosarcoma with the cystic area and very thin soft tissue margin between the tumor and bladder

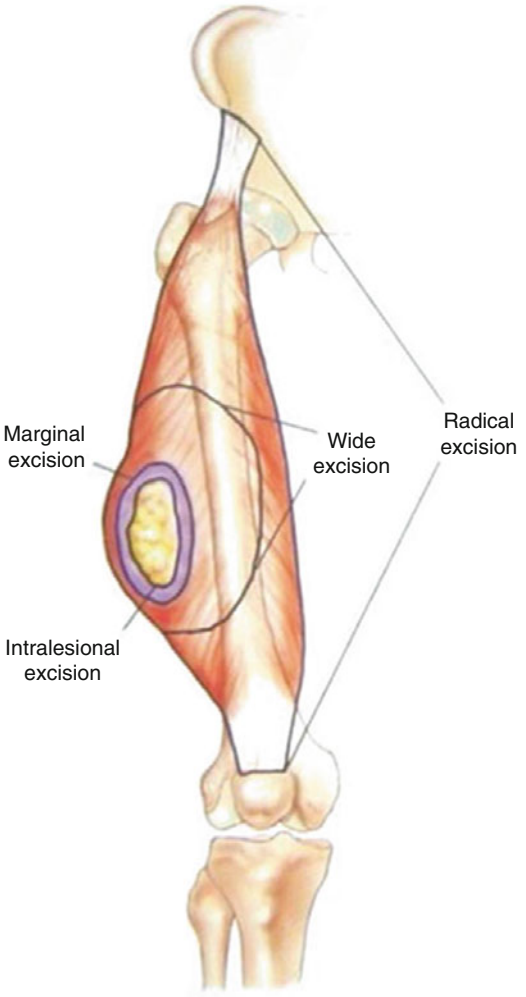

Fig. 7.3 Diagram depicting resection margins. In pelvic bone tumors, wide excisions are required to decrease recurrence rates

with these tumors is highlighted by the fact that local recurrence rates of up to 70 %and 92 % have been reported for pelvic tumors following marginal and intralesional resections respectively [13, 14].

Reconstruction

Unlike the long bones, it is impossible to design a one-design-fits-all prosthesis to implant following pelvic tumor resection. In order to achieve a successful reconstruction, the prosthesis must fit the resection margins exactly to preserve the

mechanics of the pelvic girdle. Debate rages as to whether the pelvic ring needs closing by reconstruction with most surgeons favoring not to close the ring. The complexity of the pelvis makes designing and fitting functional reconstructions that are durable and allow patients maximum function incredibly challenging. Poorly fitting prostheses result in damage to existing healthy bone and revision surgery, which is all the more complex for the deranged anatomy caused by the original tumor and primary surgical procedure. The long term survival of the reconstruction by endoprostheses is 75 % [15] and 85 % for massive allograft reconstruction [16].

Complications

Patients with malignancies of the pelvis are at a higher risk of treatment failure than other patients with similar tumors located in a limb [17]. Treatment failure can include recurrence, prosthesis failure, amputation and nerve damage. All of these problems stem from the difficulty in achieving adequate resection margins, and difficulty with reconstruction and large dead space. All major series have reported complication rates of in excess of 50 % following reconstruction. The complication rates following resection without reconstruction are lower and may still produce good functional results.

Function

The primary aim of pelvic tumor surgery is to remove the tumor completely to prevent recurrence. However, a key secondary aim is the need to preserve the function of the patient as much as possible. The functions to keep in mind are; transfer of weight from the upper axial skeleton to the lower limbs, especially during movement; providing attachment for muscles and ligaments used in locomotion; protecting the abdominal and pelvic viscera.

Suitability of the Pelvis for Navigation

The pelvis particularly lends itself to computer-assisted surgery as it has multiple easily identifiable bony prominences to use as reference points. Accurate registration is important as it allows the computer to build up a picture of the patient's anatomy in space and therefore allows for direct correlation between the two-dimensional imaging studies and the three-dimensional surgical field by point to point and surface matching. This facilitates accurate orientation, tumor location and reconstruction thereby reducing the surgeon's margin for error. The anterior superior iliac spines (ASIS), anterior inferior iliac spines (AIIS), posterior superior iliac

spines (PSIS), the top of the iliac notch or any other easily identifiable anatomical landmarks can be used for registration. The registration error should be <1 mm before proceeding with resection.

However, where the shape of the pelvis aids registration, it hinders the practicality of performing the surgery. Pelvic tumors are often very large and may require resection in multiple planes due to the unique geometry of the pelvis. There are also many critical structures that must be avoided during pelvic surgery, such as the sciatic nerve and the iliac vessels as they pass through the sciatic notch, the bladder and the peritoneum. The use of navigation can significantly reduce the risk of damage to vital structures by allowing the surgeon to know their location relative to the osteotome, as well of the depth of penetration of the instruments. This is particularly useful in the sacrum, where uninvolved sacral nerve routes can often be spared, improving the patient's neurological outcome after surgery.

Evolution of Surgical Techniques

All surgery requires extensive planning with knowledge of the patient's and the tumor's anatomy to enable a suitable implant to be designed. Since the advent of CT and MRI scanning, incredibly detailed three-dimensional representations of the tumor and surrounding anatomy can be isolated and explored before the operation. However, translating this information from view screen to intraoperative field can be difficult [17], resulting in inadequate resection margins or excessive removal of healthy tissue. Both of these scenarios result in unfavorable outcomes for patients. Inadequate resection margins (intra-lesional and marginal) frequently lead to local recurrence [14]. Excessive removal of bone causes difficulties to arise when trying to fit the implant or allograft. If this is not accurately done, there is a risk of non-union, disrupted biomechanics and implant failure.

Conventional techniques involve resection and reconstruction done 'freehand', with the scans available for reference. This has been shown to be highly inaccurate in a revealing study by Cartiaux et al. [18]. In this study, four experienced surgeons were asked to resect three different tumors on model pelvises under ideal conditions and the resection margins were measured. The probability of a surgeon obtaining a 10 mm surgical margin (5 mm tolerance above and below) was 52 %. This highlights the drawback of conventional surgical techniques within the pelvis.

Surgery using computer navigation has been used for a number of years to aid surgical precision in various branches of orthopedics, including spinal surgery, lower limb arthroplasty, and trauma [19–21]. In more recent years, there have been reports on the use of computer navigation assisted surgery for the resection of musculoskeletal tumors. Computer navigation assisted tumor surgery in the pelvis is in its relative infancy, therefore there have been huge improvements in a short time period. Initial attempts made use of spinal navigation software for intra-operative monitoring [22, 23]. These case reports demonstrated accurate excision and complete tumor clearance, however called for better CT and MRI imaging for the pre-planning stage to improve intraoperative precision.

Wong et al reported fusing CT and MRI images prior to tumor surgery, a technique used by neurosurgical and otorhinolaryngeal procedures. CT scans show intricate bony details well, whereas MRI is superior when examining intraosseous and extraosseous extensions of the tumor into the surrounding soft tissue. Therefore, integrating the two imaging modalities enables a more complete exploration of the tumor anatomy and better pre-operative planning [24]. They were also able to integrate functional imaging studies such as PET scans and angiography to further improve precision.

Cho et al. described improving intraoperative registration by preoperative implantation of four Kirschner wires—one in each of the two iliac crests and one in each of the two posterosuperior iliac spines—as fixed markers [25]. This is important when matching the patient's anatomy on the operating table with that on the scans, as subtle variations in orientation can affect accuracy of resection. It is also important to note that in patients with pelvic tumors, the normal anatomy and bony landmarks of the pelvis may be distorted or involved with the tumor. By implanting artificial landmarks at pre-defined sites and matching them with the scans, these difficulties can be overcome.

So et al. reported increased registration accuracy with CT-fluoro matching as opposed to point-to-point matching [26], and Cheong and Letson used both [17].

Although these studies have shown promising results, with more accurate resections and reconstructions being performed and improved implant positioning, it is recognized these conclusions are based on small case series and varied anatomical tumor sites [17, 22–26].

A study by Jeys et al. comprises the largest published series of the use of computer-assisted navigation in musculoskeletal tumors, and more specifically the largest series of primary pelvic and sacral bone tumors resected with navigation [1]. The results showed a significant reduction in intralesional excision rates from 29 % prior to the introduction of navigation to 8.7 % (n = 2) with clear bone resection margins achieved in all cases. At a mean follow-up of 13.1 months (3–34) three patients (13 %) had developed a local recurrence, whereas previous series had shown a local recurrence rate of 26 %. The conclusions from this and recent studies are that computer navigation is a safe technique with no complications specifically related to its use. To reduce the risk of errors, image-to-patient registration error should be less than 1 mm in all patients [1] to ensure accurate matching of the patients' intraoperative anatomy with the fused preoperative images. To minimize this registration error the time between imaging and surgical resection must be short [24].

How to Do It

Image Correlation

Accurate up to date MRI and CT scans are need to obtained prior to surgery. CT scans of the pelvis should <1 mm high resolution slices and the MRI should be 3–5 mm slices. Preferably the MRI and CT scan should include the whole pelvis and lower spine. The CT scan is used to delineate the bony anatomy and the MRI

to identify the extent of the tumor and important soft tissue structures. Additional imaging techniques, such as CT angiography and PET-CT can also be incorporated into the pre-operative plan. The technique depends on whether intra-operative CT based navigation is being used or prior image correlation is being used; the rest of the description is for the latter. The pelvis lends itself to accurate image correlation given its complex 3D shape. Most of the systems will allow automatic correlation, but this can be time consuming and inaccurate; the authors therefore recommend manual correlation with automatic fine tuning. Generally using the acetabulae to match the anatomy on the CT and MRI scans is a useful starting point on the coronal scans, the Sacro-illiac joints in the axial plane and the spinal canal in the sagittal planes. At least 2 MRI sequences or planes should be used to correlate with the CT scan. Generally the author favours the use of axial and coronal STIR sequences for planning of the tumor, however, peritumoral oedema can be misleading and may result in greater bone resection than required. The STIR sequences should always be cross referenced to the T1 weighted images to allow accurate planning of the tumor location. Once the surgeon is happy that the image correlation is good, the automatic matching can be undertaken to check and improve accuracy.

Once the images have been correlated the tumor can be identified to the computer in a process known as segmentation. Again, automatic segmentation is possible with most software, but the author favours manual segmentation. The automatic segmentation works on differential signal intensity and will often segment peritumoral oedema, vessels and other non-tumor structures with similar signal intensity to the tumor. Therefore a 'slice by slice' manual segmentation on two planes is recommended. Once the images have been correlated and the tumor segmented, then the user will often remove the rest of the information from the MRI volume, leaving simply the bony anatomy and tumor segment visible at surgery. Image correlation and tumor planning generally will take approximately 15 min and is the most important step in pre-operative planning so great care should be taken.

Resection Plane Planning

It is vital that the surgeon realizes the goal of the surgery is to remove the tumor with an adequate margin of healthy tissue and that computer navigation simply allows the surgeon to execute the pre-operative plan. In some tumors it may be safe to resect the tumor with a narrow margin of less than 5 mm, however, the surgeon should remember that registration error may account for up to 1 mm of discrepancy at surgery and the thickness of the saw blade may cause discrepancies of 2 mm. Therefore, generally the authors recommend a resection margin of at least 10 mm of normal bone around the tumor. In the sacrum it is possible to plan resection planes into the sacral foramen, which will allow preservation of the nerve routes in that foramen. Some systems allow the planning for screw and implant trajectories, which can be extremely useful at surgery to achieve accurate joint line reconstruction with implants, ensure there is no cortical breach with

stems and avoid damage to nerve routes with screws. In general, the author prefers multiplanar resections, especially with custom designed implants to preserve bone and ensure stable fixation.

Registration Points

The pelvis has a plethora of bony landmarks, which can be used for point to point registration. Typically the posterior superior iliac spine (PSIS), anterior superior iliac spine (ASIS) and anterior inferior iliac spine (AIIS) can be easily located at surgery. Even if these points are not being routinely exposed at surgery, stab incisions and percutaneous registration can be used as they are normally readily palpable. Other points can be used and vary with each case, but typically the iliac tubercle, pubic symphysis, sciatic notch, sacral foramen and acetabular tear drop can be used as readily identifiable points for point to point registration at surgery. The wider the spread of the registration points used in AP, lateral and sagittal planes will help to reduce the initial registration error and at least 4 points should used ideally. A registration error of 10–15 mm is acceptable initially, as this can be reduced to less than 1 mm with surface registration. The position of the patient at surgery, exposure and body habitus should all be taken into account when planning registration points (e.g. using the ASIS would be inappropriate if the patient is to be positioned prone for a sacral resection). Once point to point registration is completed then surface matching is used to reduce the registration error to <1 mm. This is done by taking 50–100 random points from the bone surface. Care should be taken to avoid areas where the tumor has spread outside the bone to avoid contamination, that the probe makes good contact with bone (and not soft tissue covering the bone) and that the points are spread out over as big an area of the bone as possible. The latter point can be sometimes difficult in a sacral resect from the posterior only approach, however, by exposing bilateral posterior superior sacro-illiac spines or making small percutaneous approaches remote from the operative field, this difficulty is easily overcome.

Design of Custom Made Implants

Given the detailed pre-operative planning that has been undertaken, the design of custom made implants is facilitated by navigation. The planned resection planes can be exported to engineers to design a custom made implant for the patient. If the software allows it, generally the engineers like to work with STL files or MIMICS software. If the programme does not allow exports, the authors generally measure the angles and distances of the resection planes from anatomical points to allow the engineer to reproduce the plan off exported screen shots.

The engineer will then create a virtual model of the desired custom implant on CAD-CAM software. The residual bone or implant can then be exported by the engineers and the STL file can be re-imported into the navigation software and compared for accuracy to the pre-operatively planned resection planes. The authors find that

telephone/video conferencing is useful with the engineers to ensure the design of the implant is correct. The advantage of navigation is that it facilitates multiplanar tumor resection, and the engineers can then design an implant matching this interface, which is more inherently rotationally stable than the previous uniplanar design. The author has found that new manufacturing techniques including additive layer manufacturing (3D printing) has allowed very complex implants to be custom manufactured for the patient, which has improved implant design and delivery times.

Non custom implants such as the Coned hemipelvic replacement (Stanmore Implants Worldwide) or LUMiC (Implantcast) can more accurately be positioned using navigation as the trajectory and size of the stem can be determined pre-operatively. Providing the patient tracker is not resected with the tumor and the plane of the acetabulum is planned pre-operatively, at operation, after resection of the tumor, the implant can be accurately placed to reconstruct the joint line with appropriate inclination and anteversion, which can be very difficult without navigation.

Tracker and Camera Positioning

Most navigation systems use 'line of sight' infrared communication between three points to triangulate the position of the patient intra-operatively. If the camera on the navigation machine's view of the trackers is blocked by the surgeon, assistant or another object, then the navigation will not work and there will be a warning displayed to alert the surgeon which tracker cannot be seen by the camera. The three points used by navigation are:

(a) A patient tracker – this is a tracker, which must be placed on the bone, which is due to be partially, or wholly resected. It does not have to be fixed to the part of the bone which is resected and is generally best positioned on the part of the bone which remains. This because after the bone has been resected, navigation can still be used to gain further information (joint line, confirmation of accuracy of resection etc). Once the bone on which the tracker is placed has been osteotomised the navigation will no longer be accurate if used on the specimen bone, which is separated from the bone where the tracker is. As the computer will only see it as a whole bone, the order of the osteotomies during surgery is vital to ensure the final osteotomy is the one which separates the part of the specimen from the tracker bone. Patient tracker position is therefore vital; it must be securely fixed to the bone with a minimum of 2 pins but ideally 3 pins. If the patient tracker moves during the operation, the navigation will become less accurate and if this is noticed then the surgeon should check the stability of the patient tracker fixation and re-register the patient if it has moved. The navigation camera must be able to see the patient tracker throughout the entire procedure, therefore, using a mobile position of the patient (e.g. floppy lateral position) the patient tracker position must visible to the camera in the extremes of positioning and the sensors must be pointing towards the camera. Fortunately the sensors and camera have a wide angle of field of view, accommodating most positions, however,

if the camera loses sight of the tracker during the procedure then the camera should be moved to 'see' the tracker, rather than the patient tracker.

(b) Navigation Camera – The camera is located on an arm of the navigation machine. On most systems this camera is mobile radially to the machine and also in the perpendicular axis allowing easy positioning and sight of the trackers. Intra-operatively if there is a poor view of the trackers the arm or machine can be moved into a better position without the need for re-registration of the patient.

(c) Instrument tracker/Pointer – The third point is made up of a pointer or tracker attached to an instrument, which has to be registered to the system either via a vector calibration device or by a registration point on the patient tracker. This can be done by scrub staff/assistant before the patient tracker is attached to the patient to save time intra-operatively. Intra-operatively the pointer can be used to identify the position of the tumor or set points required at surgery such as resection planes. The angle of the osteotomy or trajectory of a stem can be assessed using the pointer.

Navigated Instruments

The Stryker system allows calibration of any straight or angled instrument, to which a tracker can be attached and that will fit into the vector calibration device. Therefore osteotomes, burrs, saws and other instruments used during surgery can be recognized by the navigation, thus allowing precise knowledge of where the tip of a sharp instrument is in the bone or space. The authors have found this immensely useful when undertaking osteotomies of the sacrum from the posterior approach and will routinely undertake sacral osteotomies up to S1/2 from a posterior only approach rather than a combined approach prior to navigation. Knowledge of where the sharp end of the instrument is located increases the safety of the operation reducing the risk of inadvertent vascular injury.

Reduced Soft Tissue Exposure

An unanticipated advantage of the use of navigation in the pelvis is that if using navigated instruments less exploratory approaches are required, meaning that the retroperitoneum does not necessarily need exposing if undertaking a periacetabular osteotomy from the lateral ilium. As the tip of the osteotome can be accurately estimated (<1 mm) then routinely exposing and mobilizing the iliac vessels is not required providing the tumor is not intimately related to them. The author believes the reduction in the retroperitoneal dissection helps to prevent bleeding, reduces potential post-operative dead space and ultimately reduces the risk of infection. When using a planar (e.g. osteotome) or angled instrument care should be undertaken to ensure that the tracker can be seen by the navigation when being used in the orientation required. This sounds like an obvious point, but the author has frequently calibrated an instrument in the past, only to find the tracker is pointing 90° to the navigation and it cannot be 'seen' !!!

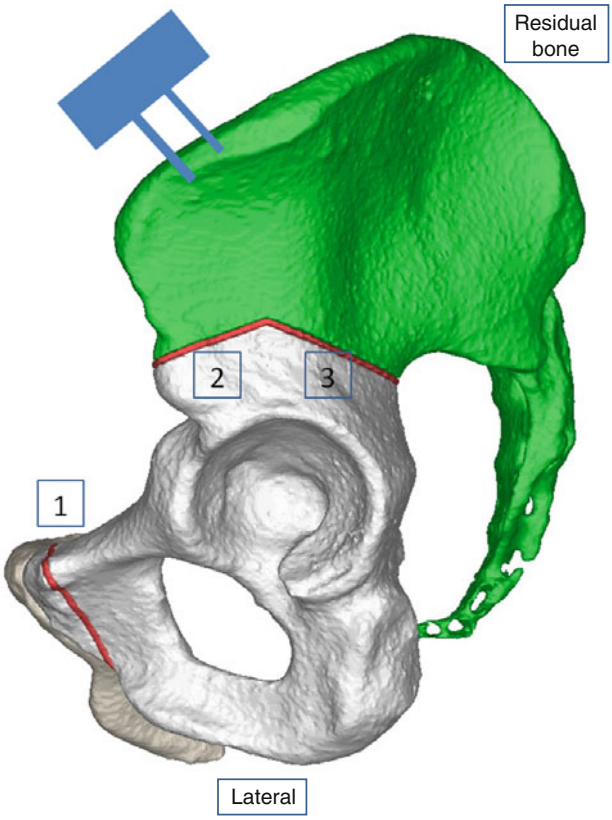

Fig. 7.4 If the green area is the residual bone anticipated after resection and the blue represents the patient tracker and the lower pelvis is to be resected in the midline, then the correct order of osteotomy would be (1) midline at the symphysis (2) superior illium and (3) inferior illium. This would reduce the risk of inaccuracy of the navigation. The author recommends marking the osteotomy planes with a diathermy prior to any osteotomy to give a reference line in case of navigation inaccuracy

Order of Osteotomy at Resection

As referred to earlier if an osteotomy either partially or wholly separates the resection specimen from the bone where the patient tracker is attached, then the navigation will be inaccurate and misleading. Therefore, careful consideration to the order of the osteotomy must be given. For most pelvic resections 3 osteotomies will be required (Fig. 7.4).

Sources of Error

It is vitally important that the surgeon appreciates the possible sources of error when undertaking navigated cases. The first source of error is in image correlation; the surgeon must ensure that the images are carefully correlated or else the basic plan of the operation is wrong from the outset.

The second source of error is poor planning of the tumor on the MRI scans. The surgeon must take into account the greatest possible extent of the tumor and

determine whether peri-tumoral oedema represents tumor or not. If the surgeon fails to properly segment the tumor in planning intralesional margins may occur.

The third source of error is inaccurate planning of tumor resection planes. The surgeon must ensure that an oncologically safe margin is planned, normally 5–10 mm from the tumor. Just because navigation is accurate does not mean that narrow surgical margins are acceptable.

The fourth source of error is inaccurate registration. The surgeon should not proceed using navigation unless a registration error of <1 mm is possible. Large registration errors are typically due to poor exposure or recognition of the anatomical landmarks used for registration or landmarks which are too close together.

The fifth source of error is due to movement of the patient tracker during surgery. Occasionally the patient tracker will be knocked or hit, or if the pins are not securely fixed, it may move slightly during surgery. If this happens then the navigation will become inaccurate and re-registration is required.

The final source of error is interference with the infrared beams between the trackers. This has been reported with the use of plasma screen televisions in theatre or by having the navigation machine too close or far away from the trackers. An ideal distance is 6–10 feet from the machine. If inaccuracies are noticed or the camera is having difficulty 'seeing' the trackers, turning off any possible electrical sources of interference may be helpful.

The majority of errors when undertaking navigation are due to poor planning from the surgeon and are easily avoided.

Benefits of Bone Tumor Navigation in the Pelvis

There are many benefits to capitalizing on recent advances in technology. Bone tumor navigation has been shown to be a safe, effective technique that has promising early results in decreasing revision rate, decreasing the need for amputation and saving nerve roots [1]. In addition to these improved outcomes, bone tumor navigation allows for more complex resections by allowing intraoperative monitoring of patient position and improved cutting precision.

This increased accuracy also allows for better fitting implants with better biomechanics, as demonstrated in Fig. 7.5. This improves prosthesis function and decreases abnormal loading, thereby increasing prosthesis life-span and improving patient satisfaction.

Importantly, computer navigation achieves reduced intra-lesional resection rates [13, 14, 27]. However, it seems that recurrence is impossible to eradicate as even with clear margins Wong et al and Cho et al reported local recurrence rates of 25 % and 20 % respectively. High grade, thin soft tissue margins and large size denotes poor prognosis in pelvic and sacral tumors.

The extra time that it takes to plan a navigated case is rarely wasted as the surgeon gets a much better appreciation of the anatomy of the tumor and plans the case more carefully by spending extra time with 3D images of the tumor, being generally better informed about the pitfalls of the surgery pre-operatively.

Fig. 7.5 Resected acetabulum due to osteosarcoma using computer-assisted navigation. The resected specimen and implant match precisely

The downside of new technologies is that they are costly and time consuming. It is generally agreed amongst surgeons that the time component will improve as surgeons become more practiced. Also, the use of computer navigation systems negates the need to establish resection margins intra-operatively, which could eventually result in reduced operation times. It is still early days, therefore cost-effectiveness remains to be evaluated, however, if it proves to reduce complications and locally recurrent disease this will undoubtedly prove worth the cost, particularly as techniques develop and materials decrease in price.

References

1. Jeys L, Matharu GS, Nandra RS, Grimer RJ. Can computer navigation-assisted surgery reduce the risk of an intralesional margin and reduce the rate of local recurrence in patients with a tumour of the pelvis or sacrum? Bone Joint J. 2013;95-B(10):1417–24.
2. Wong KC, Kumta SM. Computer-assisted tumor surgery in malignant bone tumors. Clin Orthop Relat Res. 2013;471:750–61.
3. Ottaviani G, Jaffe N. The epidemiology of osteosarcoma. In: Jaffe N, Bruland O, Bielack S, editors. Pediatric and adolescent osteosarcoma. New York: Springer; 2009.
4. Bone Sarcomas: incidence and survival rates in England – NCIN Data Briefing. 2010. National Cancer Intelligence Network. 9 3 2014. Ref Type: Online Source.

5. Unni K. Dahlin's bone tumors: general aspects and data on 11,087 cases. Philadelphia: Lippincott-Raven; 1997.
6. Mavrogenis A, Patapis P, Kostopanagiotou G, et al. Tumors of the sacrum. Orthopedics. 2009;32:342–56.
7. Payer M. Neurological manifestation of sacral tumors. Neurosurg Focus. 2003;15:E1.
8. Coleman R. Metastatic bone disease: clinical features, pathophysiology and treatment strategies. Cancer Treat Rev. 2001;27:165–76.
9. Ruggieri P, Mavrogenis A, Angelini A, et al. Metastases of the pelvis: does resection improve survival? Orthopedics. 2011;34:236–44.
10. Wunder J, Ferguson P, Griffin A, et al. Acetabular metastases: planning for reconstruction and review of results. Clin Orthop Relat Res. 2003;415(Suppl):187–97.
11. Jacofsky D, Papagelopoulos P, Sim F. Advances and challenges in the surgical treatment of metastatic bone disease. Clin Orthop Relat Res. 2003;415(Suppl):14–8.
12. Du Z, Zang J, Tang XD, et al. Experts' agreement on therapy for bone metastases. Orthop Surg. 2010;2:241–53.
13. Ozaki T, Flege S, Kevric M. Osteosarcoma of the pelvis: experience of the Cooperative Osteosarcoma Study Group. J Clin Oncol. 2003;21:334–41.
14. Fuchs B, Hoekzem N, Larson D. Osteosarcoma of the pelvis: outcome analysis of surgical treatment. Clin Orthop Relat Res. 2009;467:510–8.
15. Campanacci D, Chacon S, Mondanelli N, Beltrami G, Scocianti G, Caff G, Frenos F, Capanna R. Pelvic massive allograft reconstruction after bone tumor resection. Int Orthop. 2012;36(12): 2529–36.
16. Hwan S, Hyun G, Kim H, et al. Computer-assisted sacral tumor resection: a case report. J Bone Joint Surg A. 2008;90:1561–6.
17. Cheong D, Letson G. Computer-assisted navigation and musculoskeletal sarcoma surgery. Cancer Control. 2011;18:171–6.
18. Cartiaux O, Docquier P, Paul L, et al. Surgical inaccuracy of tumor resection and reconstruction within the pelvis: an experimental study. Acta Orthop. 2008;79:695–702.
19. Amiot L, Lang K, Putzier M, et al. Comparative results between conventional and computer-assisted pedicle screw installation in the thoracic, lumbar and sacral spine. Spine. 2000; 25:606–14.
20. Grutzner P, Suhm N. Computer aided long bone fracture treatment. Injury. 2004;35:57–64.
21. Anderson K, Buehler K, Markel D. Computer assisted navigation in total knee arthroplasty: comparison with conventional methods. J Arthroplasty. 2005;20:132–8.
22. Hufner T, Kfuri MJ, Galanski M. New indications for computer-assisted surgery: tumor resection in the pelvis. Clin Orthop Relat Res. 2004;426:219–25.
23. Krettek C, Geerling J, Bastian L, et al. Computer aided tumor resection in the pelvis. Injury. 2004;35:79–83.
24. Wong K, Kumta S, Antonio G, et al. Image fusion for computer-assisted bone tumor surgery. Clin Orthop Relat Res. 2008;466:2533–41.
25. Cho HS, Kang HG, Kim HS, et al. Computer-assisted sacral tumor resection. A case report. J Bone Joint Surg. 2008;90:1561–6.
26. So T, Lam Y, Mak K. Computer-assisted navigation in bone tumor surgery: seamless workflow model and evolution of technique. Clin Orthop Relat Res. 2010;468:2985–91.
27. Jeys L, Grimer R, Carter S, et al. Outcomes of primary bone tumors of the pelvis- the ROH experience [abstract]. J Bone Joint Surg [Br] Orthop Proc. 2012;94-B:39.

Chapter 8
Bone Tumor Navigation in Limbs

German L. Farfalli and Luis A. Aponte-Tinao

Abstract Computer assisted navigation surgery is an asset for oncologic surgeries. Every tumor is different in size and shape and surgical precision have a significant impact on the final oncologic outcome. Development in graphics enables to combine images of Computed Tomography (CT) and Magnetic Resonance Images (MRI) into a three-dimensional virtual scenario. Therefore, virtual scenario allows physicians to perform three-dimensional reconstructions, observe the patient's morphology and preoperatively plan the procedure.

One of the advantages is that planning can be executed during the surgery using surgical navigation. Navigated surgery is outstanding because guides surgeons during the procedure; intraoperative simulation guides the path in order to perform a high quality operation, more accurate and secure, reducing the error margin and the mean time during the procedure. The results explained in this chapter are optimistic. Only 4 out of 78 patients procedures were not carried out due to technical problems occurred during the first year of implementation. Eight percent of the patients had a local recurrence. Moreover, of the 78 cases, 65 were malignant and of this group of patients 6 (10 %) died of disease. The overall survival of the group of patients suffering of malignant tumors was 91 % at 4 years and disease free survivals was 81 % at 4 years.

Keywords Freehand navigation • Computer aided orthopaedic surgery (CAOS) • Total knee arthroplasty • Custom jigs • Passive/active robots

Introduction

Since the end of the 90s decade computer aided orthopaedic surgery (CAOS) has been a useful and accurate tool for trauma, spine surgery and in the implantation of hip and knee prosthesis [1–4]. Subsequently, other studies showed that the use of this technology for the placement of a prosthesis, improve alignment of the implant, but long term clinical outcomes were similar to those obtained in patients operated

G.L. Farfalli, MD • L.A. Aponte-Tinao, MD (✉)
Orthopaedics and Traumatology, Hospital Italiano de Buenos Aires,
Potosi 4247, Buenos Aires C1199ACK, Argentina
e-mail: German.farfalli@hospitalitaliano.org.ar; luis.aponte@hospitalitaliano.org.ar

L.E. Ritacco et al. (eds.), *Computer-Assisted Musculoskeletal Surgery: Thinking and Executing in 3D*, DOI 10.1007/978-3-319-12943-3_8

without navigation [5]. These results makes that navigation assistance in hip and knee prosthesis has fallen into disuse.

Different is the situation in oncologic patients, since the every tumor is different, and surgical precision can have a great impact on the final oncologic outcome [6]. Therefore, in a resection of a bone tumor, the osteotomy must be outside tumor margins but, at the same time, is important to respect as much as possible of non-affected bone tissue.

A didactic example is what happens in racing. Placement of prosthesis with computer assistance navigation assistance, it would be as if a pilot of the formula one needs a GPS to manage in a standard circuit. While in tumor resections, the example would be like a rally driver, who runs in a desert without roads. If it is not assisted by a GPS, it has greater risk not to finish race for not knowing the correct path.

Advances in the area of computer graphics have also allowed combine images of computed tomography with magnetic resonance image, generating three-dimensional reconstructions able to represent the bone and tumor morphology with great precision and clarity [8–12].

The ability to generate accurate 3-d images has allowed make a three-dimensional scenario where the surgeon can preoperative plan the tumor resection. In addition, this plan can be executed during the surgery using a surgical navigation [9–12]. In the same way that a system of global positioning (GPS) allows to orient a person in a way unknown to him, a scenario of intraoperative simulation would guide the path that will follow the cutting of a saw or an osteotome, during the surgical procedure.

Indication

Indications of CAOS initially focused to pelvic tumors [13]. Currently and with advances in virtual planning and intraoperative execution with navigation, indications extend to multiple situations like tumors located at the extremity. In our experience main indications for the use of CAOS in tumors located at the extremity are:

1. Resection of a pelvic or scapular tumor [13],
2. Biplanar segmental resections (intercalary or transepiphyseal) [14].
3. Multiplanar metaphyseal resections and reconstructions, using structural bone allograft, cut with same morphology of the resected bone [15].
4. Any osteoarticuar resections of the extremities with the intention of reconstruct the affected bone with osteoarticular bone allograft, cut with same size and rotation of the resected bone [14].
5. CAOS assessment for the placement of a tumor endoprosthesis to avoid errors in rotation [7, 16].
6. Assistance for tumor biopsies or intralesional curettage, in a difficult location [7, 16].

Preoperative Preparation

There are some steps required for the use of CAOS:

1. Acquisition of high resolution images.
2. Magnetic resonance (MRI) and computer tomography image fusion (CT).
3. Transform images into a three-dimensional model (segmentation).
4. Perform a preoperative planning in a virtual 3D scenario that will allow us to calculate an accurate oncologic margin, defining cutting plane.

Acquisition of Images

The first step to perform is the acquisition of images. Therefore, each case is evaluated with a multi-slice CT scan and nuclear magnetic resonance of the entire bone affected by the. High resolution images are recommended to detect small skip lesions that can be excluded in low resolution images. Tomography image acquisition is as follows: array of 512×512 pixels, size of pixel average: 0.5 mm, thickness 0.5 mm cuts every 0.5 mm, with a focus on the area of interest (bone tumor). We always use the use of 64 tracks or more. With respect to the MRI, we recommend the use a resonator of 1.5 T or more, acquiring images in time T1 and T2 with a 256×256 matrix pixels, with a pixel average size: 0.7 mm and cuts of 1 mm thick each 1 mm, with focus magnified in our area of interest (bone tumor). Set images, was stored in DICOM digital format.

Magnetic Resonance and Computer Tomography Image Fusion

Since the coordinate system of the CT scan does not coincide with the MRI, this step should perform the union of both segmented volumes of images: CT and MRI. In addition, this procedure can must be performed with specific software. The operator manually can observe if the axial, coronal, and sagital plane have a proper correspondence.

Segmentation of Images

After the fusion process, proceed to the three-dimensional reconstruction of the structures of interest: bone tumor. Once obtained the image files, these are imported in medical imaging software provided by the browser that the surgeon has available. With these programs, we proceed to reconstruct three-dimensional

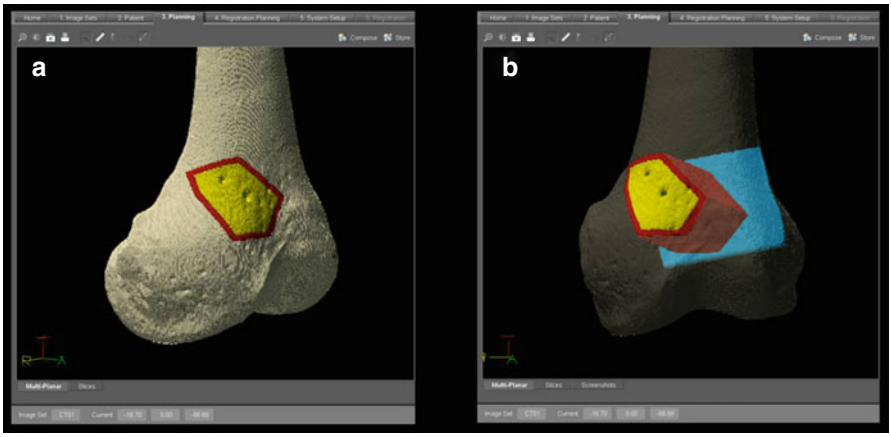

Fig. 8.1 (**a**) Preoperative planning. Chondrosarcoma multiplanar osteotomy resection. (**b**) Transparency allows us to see planes proyections in 3D

shape of the patient's bone, coloring segment by segment bone surface from CT images. On the other hand, the tumor volume is also segmented and reconstructed from magnetic resonance imaging, since tumor limits cannot be determined with accuracy with CT images.

Virtual 3D Preoperative Planning

With all the proceed images, the planning of each case is performed by a team of experts in orthopedic oncology. It consists of determining the tumor resection using virtuals planes, which must follow the saw or the osteotome during surgery (Fig. 8.1). You always have to consider the thickness of the saw or osteotome, since this can vary from 2 to 3 mm in the thickness of the virtual plane. According to tumor invasion, the tumor resection is planned using different virtual configurations resective osteotomies. Types of osteotomies planned virtually are divided into uniplanar, biplanar, and multiplanar (more than 2 planes). Tumor margin have to be determined according to the type of tumor, grade, response to chemotherapy and local extension of the lesion.

Technique with Pearls and Pitfalls

Once all plan is set, at the operation room, the navigation computer is best positioned opposite the surgeon approximately 5 feet away from the patient. The camera is located over the patient and directed downward at 45°. After surgical exposure, two 3 mm Apex pins are placed on the affected bone at least 3 cm away

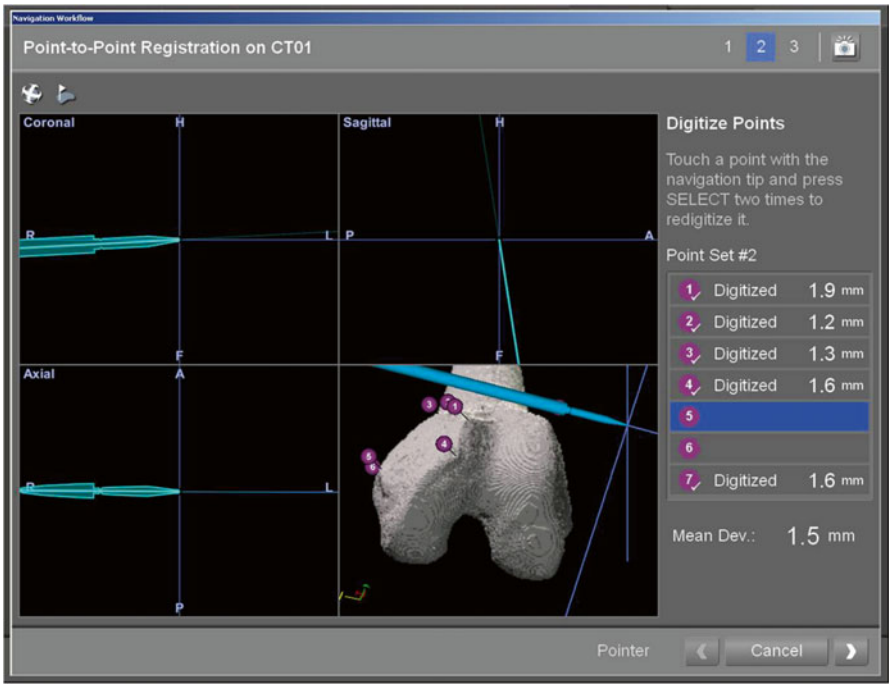

Fig. 8.2 Point to point registration

to the osteotomy programmed line in an area not affected for the tumor based in the preoperative planning. A navigation tracker is fixed to the pins. An image-to-patient registration to match precisely the operative anatomy and preoperative virtual CT images is performed by paired points (Fig. 8.2) and surface points (Fig. 8.3). In terms of surgical steps, 4 or at least 3 landmark points are identified in the affected bone based in the surgical exposure and anatomic visible points. Then, surface mapping of the bone is performed to reduce any mismatch between preoperative images and the patient's anatomy, using at least 80 surface registration points in unaffected bone. After registration, the surgeon must double check with the navigation pointer if the surface of the patient`s bone in real time correlates on the virtual preoperative images. Afterwards, using the navigation pointer the osteotomies are marked in the surface of the bone (Figs. 8.4 and 8.5). The directions of the bone cuts are determined with the pointer and the osteotomies are performed with an oscillating saw or an osteotome.

Finally, another advantage that has this procedure, is the reconstruction of the bone defect, using computerized assistance. This is mainly accomplished when the reconstruction is done with bone allografts. The procedure is to reproduce the same planned cuts used during tumor resection, about the Allograft. This way can the defect can be reconstructed with more precision than the conventional way (allograft tailored by hand without any guidance), as if they were pieces of a puzzle.

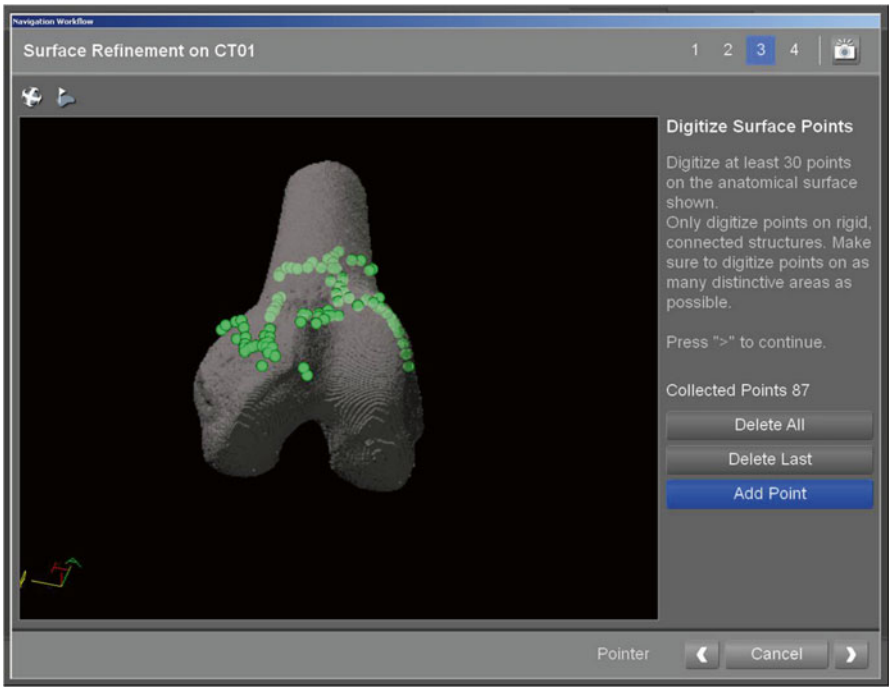

Fig. 8.3 Surface refinement registration

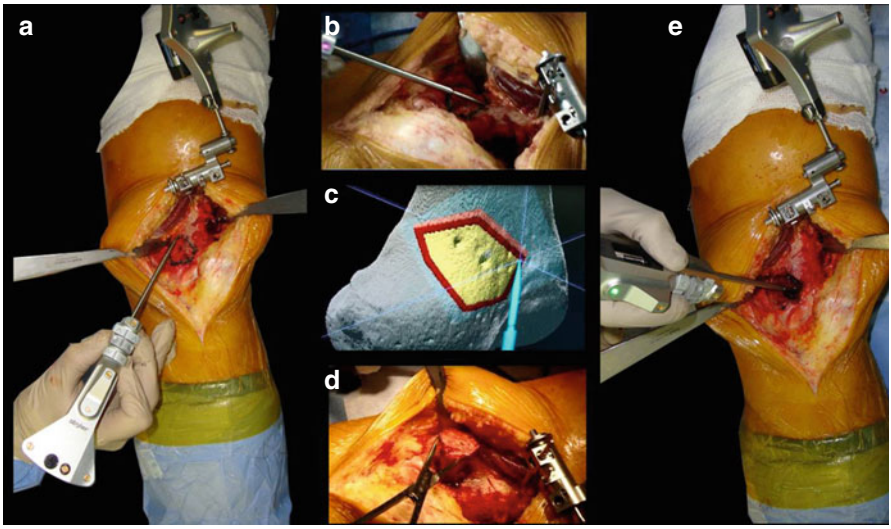

Fig. 8.4 (**a**–**c**) Pointer marking multiplanar osteotomy, (**d**) Bone tumor resection, (**e**) Bone defect after resection

Fig. 8.5 Bone tumor navigation

Results

For this review, we analyzed our first 78 cases performed during the first 2 years of the utilization of this technology. All patients were followed for at least 2 years after surgery.

In four of the 78 patients (5 %) the navigation was not carried out due to technical problems (1 pelvis, 1 humerus and 2 femurs). In two cases the crash was secondary to software problems. In the remaining two cases the crash was secondary to hardware problems. One of the software technical crash happens in a case was the computer does not recognize one letter of the patients last name (the spanish ñ). The remaining software crash was that we tried to navigate the position of the osteosynthesis plate for the reconstruction, and the information to perform this exceeds the capacity of the computer navigation system. The hardware failures were related to broken trackers undetected during the procedure. All failures occurred during the first year of the utilization of this technology.

The mean time for navigation procedures during surgery was 31 min (range 11–61). However, time was improved during the learning curve. Therefore, the latest computer assisted surgeries, were faster than the first ones. We observe than in pelvic tumors the mean time for navigation procedure as 41 min (range 23–61), but the mean time for navigation procedure in extremities tumors was 27 min (range 11–54).

Of the 78 cases where the navigation was performed, the median registration error was 0.6 mm (range 0.3–1.1). This range of registration error was constant during time, from the first navigation through the last one.

We performed histological examinations of all specimens and they showed a clear bone tumor margin in all patients. Six cases of the 78 patients in which the

navigation was performed had a local recurrence (8 %). According to the location of the local recurrences, we observed that 4 cases of the 17 pelvic tumors underwent a local relapse (23 %), and only 2 cases of the 60 tumors located in the extremities, had a local recurrence (3 %). Although, of the 78 cases, 65 were malignant lesions, and of this group of patients, 6 died of disease (10 %). The overall survival of the group of patients with malignant tumors was 91 % at 4 years (CI 95 %: 84–98 %), and disease free survival was 81 % at 4 years (CI 95 %: 70–92 %).

Conclusions

Virtual navigation in bone sarcomas of the extremities is a procedure where the surgeon resect tumors with a margin similar to the preoperative planned, without sacrificing healthy tissue uncompromised by the tumor. Also, this procedure seems to no take an excessive intraoperative time. Other important issue is that this method allows performing different types of resective osteotomies, which are very difficult to perform freehanded. Therefore, other important tool is that it allows making cuts in the bone allograft that facilitates and increases the congruence of the allograft with bone defect created during tumor resection.

References

1. Mavrogenis AF, Savvidou OD, Mimidis G, Papanastasiou J, Koulalis D, Demertzis N, Papagelopoulos PJ. Computer-assisted navigation in orthopedic surgery. Orthopedics. 2013;36(8):631–42.
2. Stulberg SD, Loan P, Sarin V. Computer-assisted navigation in total knee replacement: results of an initial experience in thirty-five patients. J Bone Joint Surg Am. 2002;84-A Suppl 2: 90–8.
3. Suhm N, Messmer P, Zuna I, Jacob LA, Regazzoni P. Fluoroscopic guidance versus surgical navigation for distal locking of intramedullary implants. A prospective, controlled clinical study. Injury. 2004;35(6):567–74.
4. Blakeney WG, Khan RJ, Wall SJ. Computer-assisted techniques versus conventional guides for component alignment in total knee arthroplasty: a randomized controlled trial. J Bone Joint Surg Am. 2011;93(15):1377–84.
5. Burnett RS, Barrack RL. Computer-assisted total knee arthroplasty is currently of no proven clinical benefit: a systematic review. Clin Orthop Relat Res. 2013;471(1):264–76.
6. Ayerza MA, Farfalli GL, Aponte-Tinao L, Muscolo DL. Does increased rate of limb-sparing surgery affect survival in osteosarcoma? Clin Orthop Relat Res. 2010;468(11):2854–9.
7. Cheong D, Letson GD. Computer-assisted navigation and musculoskeletal sarcoma surgery. Cancer Control. 2011;18(3):171–6.
8. Satcher Jr RL. How intraoperative navigation is changing musculoskeletal tumor surgery. Orthop Clin North Am. 2013;44(4):645–56.
9. Ritacco LE, Milano FE, Farfalli GL, Ayerza MA, Muscolo DL, Aponte-Tinao LA. Accuracy of 3-D planning and navigation in bone tumor resection. Orthopedics. 2013;36(7):e942–50.
10. Wong KC, Kumta SM. Computer-assisted tumor surgery in malignant bone tumors. Clin Orthop Relat Res. 2013;471(3):750–61.

11. Milano FE, Ritacco LE, Farfalli GL, Bahamonde LA, Aponte-Tinao LA, Risk M. Transfer accuracy and precision scoring in planar bone cutting validated with ex vivo data. J Orthop Res. 2015;33(5):699–704.
12. Ritacco LE, Milano FE, Farfalli GL, Ayerza MA, Muscolo DL, de Quirós FG, Aponte-Tinao LA. Bone tumor resection: analysis about 3D preoperative planning and navigation method using a virtual specimen. Stud Health Technol Inform. 2013;192:1162.
13. Jeys L, Matharu GS, Nandra RS, Grimer RJ. Can computer navigation-assisted surgery reduce the risk of an intralesional margin and reduce the rate of local recurrence in patients with a tumour of the pelvis or sacrum? Bone Joint J. 2013;95-B(10):1417–24.
14. Aponte-Tinao L, Ritacco LE, Ayerza MA, Luis Muscolo D, Albergo JI, Farfall GL. Does intraoperative navigation assistance improve bone tumor resection and allograft reconstruction results? Clin Orthop Relat Res. 2015;473(3):796–804.
15. Aponte-Tinao LA, Ritacco LE, Ayerza MA, Muscolo DL, Farfalli GL. Multiplanar osteotomies guided by navigation in chondrosarcoma of the knee. Orthopedics. 2013;36(3): e325–30.
16. Wong KC, Kumta SM. Use of computer navigation in orthopedic oncology. Curr Surg Rep. 2014;2:47. Review.

Chapter 9
Direct Navigation of Surgical Instrumentation

O. Andres Barrera and H. Haider

Abstract Hip and knee arthroplasty have a big impact on population health and economics due to the large number of procedures and their relative high costs. Joint replacements are complex surgeries, which require skillful surgeons and numerous mechanical instruments. When many such instruments make contact with the patient's tissue, they are bound to add to the overall infection risk.

Newer patient-specific instruments address part of this burden but introduce new challenges due to the extra manufacturer planning, surgeon approval and custom jig manufacturing steps and their associated scalability and potential liability issues. Alternatively, real-time direct navigation of bones and bone resection instrumentation, which we call here Navigated Freehand Cutting (NFC), can help reduce implant-specific jigs for arthroplasty. It could also lead to cheaper, faster, easier and perhaps even better surgical procedures, by reducing the risk of infection.

In this chapter we briefly contrast standard mechanical instrumentation for arthroplasty with modern variations and alternative approaches, including conventional navigation techniques (i.e. navigated jigs) and active and passive robotics. We also describe the progress citing various bench and cadaveric experiments on our approach of Navigated Freehand Cutting.

Keywords Navigated freehand cutting (NFC) • Freehand navigation • Computer aided orthopaedic surgery (CAOS) • Total knee arthroplasty (TKR) • Custom jigs • Passive/active robots

O.A. Barrera, PhD (✉)
Orthopaedic Surgery and Rehabilitation, University of Nebraska Medical Center, 6825 Pine St, Suite 120, Omaha, NE 68106, USA
e-mail: abarrera.research@gmail.com

H. Haider, PhD
Orthopaedics Biomechanics & Advanced Surgical Technologies Laboratory, Department of Orthopaedic Surgery and Rehabilitation, University of Nebraska Medical Center, Omaha, NE, USA

L.E. Ritacco et al. (eds.), *Computer-Assisted Musculoskeletal Surgery: Thinking and Executing in 3D*, DOI 10.1007/978-3-319-12943-3_9

Introduction

In the last two decades, hip and knee arthroplasty has proven to be a very successful surgical procedure to relieve pain, improve physical function, and provide high level of satisfaction for patients suffering from osteoarthritis. Currently, there are over 300,000 THR (total hip replacements) and 500,000 TKR (total knee replacements) per year in the USA alone. Projections point to a large increase in the number of arthroplasty procedures, with THR to nearly double and TKR to rise nearly seven times these numbers per year by 2030 [1]. The numbers of revision surgeries are similarly expected to rise. Arthroplasty surgery is relatively expensive (ranging between $15K and $60k per procedure in the United States, for example). With this volume and cost, they have a big impact on population health and economics.

However, standard joint replacements are still relatively complex procedures, which require skillful surgeons and a vast set of mechanical instruments, cutting blocks/jigs, and implant trial components (often totaling >100 pieces in a set), typically housed in various sterilize-able trays. This makes those (gold standard) instrument sets "implant specific" with jigs/fixtures typically suitable for one implant brand/model. Implant manufacturers typically offer multiple sets of instruments to each hospital, for use with their implant system models. These numerous and complex instruments require intense surgeon training for proper use. They also increase costs to the hospital for sterilization and other logistics, and increase engineering and production costs to the manufacturer. Moreover, with technological improvements over the years preventing other failure modes, infection has lately risen to be one of the dominant TKR failure factors [2]. A large number of instruments in contact with patient's tissue is bound to be a contributing factor for the overall infection risk.

Newer patient specific instruments address part of this burden but introduce challenges due to the extra (manufacturer planning, surgeon approval, custom jig manufacturing) steps and associated scalability and potential liability issues.

If surgical site bones and bone resection instrumentation (e.g. powered handpieces) can be navigated directly in real time, thus reducing (or completely eliminating) implant specific jigs and cutting blocks for arthroplasty, cheaper, faster, easier, and may be even better surgical procedures may result by reducing the risk of infection and potential other benefits. This has been the goal of our research and development. Our prototype technology provides surgeons with real-time, meaningful graphical information, while tracking bones and cutting instruments in 3D.

In this chapter we briefly contrast and critique the modern variations of and alternative approaches to standard mechanical instrumentation for arthroplasty. We therefore briefly visit conventional navigation techniques (i.e. navigated jigs), and active (autonomous) and passive (haptically hand/image guided) robotics including hand-navigated rotating burrs for uni-compartmental arthroplasty. We finally dwell on describing the progress, and citing various bench and cadaveric experiments on our Freehand Navigation of power tools approach.

Past and Current Alternatives for Conventional Arthroplasty Techniques

Variations of Conventional Jigs

While conventional arthroplasty techniques (using cutting blocks and jigs) have been very successful, various technologies have attempted to simplify the surgical procedure, to improve implant alignment, and to reduce outliers. Most innovations presented various improvements to what essentially remained implant-specific jigs. For example, computer aided orthopedic surgery (CAOS) and conventional navigation offer moderately better accuracy with fewer outliers in total knee arthroplasty (TKA). Most navigation systems for TKA (Ci, OrthoPilot, Stealth Navigation, Stryker Navigation, Vector-Vision, etc.) help to align (navigated/tracked) cutting blocks that are similar to conventional cutting jigs [3–7]. The navigated cutting blocks thus add a subset of new instruments. These systems are frequently criticized because they usually require significant initial capital investment, and add extra surgical time for registration, involve invasive pins, and add clutter to the surgical operating space [8–11].

Other approaches do reduce the total amount of instrumentation, such as patient specific (custom) jigs or technologies like Zimmer's iAssist. These however can still be considered implant specific instrumentation. Custom jigs are implant-specific jigs made by rapid prototyping, based on a pre-surgical plan over patient imaging studies: While the actual implementation varies from one manufacturer to another, the basic concept is that of creating a plastic jig (with slots and holes for instrument and screws/nails) conforming (matching) in shape to a 3D bone model generated from the patient specific CT data. The main advantages are potentially reducing overall surgical time, instrumentation count, and allowing surgeons to more easily switch between different implant models and even manufacturers since they do not need to be re-trained on how to use a full set of conventional mechanical instruments. On the negative side, this technology can isolate surgeons from some of the process, as generation of the bone model(s) and the creation of the first surgical plan, and manufacture of the custom jigs are often done by third party companies, although the surgeon contributes in choices and ultimately approves the surgical plan to be implemented. The process of bone generation, planning, and manufacturing jigs can take a few weeks, compromising the scalability of the technology. Moreover, it has been reported that the jigs do not always fit the bones properly (imperfect match) allowing the custom jig to lock onto the bone in more than one specific way, which could lead the surgeon to believe the jig is aligned properly when in fact it is not. The following are some examples of commercially available patient specific instrument (custom jigs): MyKnee by Medacta, Patient Specific Instrumentation by Zimmer, Prophecy knee guides by Wright Medical, ShapeMatch by OtisMed -now Stryker-, Signature Knee by Biomet, TruMatch by DePuy, Visionaire Patient Matched Instrumentation by Smith and Nephew.

Zimmer's iAssist [12] provides the surgeon with a set of small communication pods equipped with accelerometer sensors onboard and a prescribed procedure that allows them to accurately place the cutting blocks on the bone. This omits the need for invading the IM canal, or using extra equipment as in the case of navigated jigs. Nevertheless, even this technology still requires implant specific jigs, and requires multiple steps which may still be considered cumbersome by some surgeons.

Arthroplasty Without Jigs

In the early nineties, the first commercial robotic surgery systems for jig-less arthroplasty appeared: Robodoc[1] by Integrated surgical Systems/CA (now Curexo) [13–15]. Different configurations of the robotic system allowed milling of the bone to precisely place implant components without the need of attaching an implant specific cutting block to the bones.

Such **active robotic** systems as (Robodoc above) and Caspar (by OrthoMaquet/Germany [16]) introduced standardized three dimensional planning techniques and eliminated the need for implant specific jigs by transferring the plan and execution to the software driving the robot. Both systems above drove fast rotating burrs, so the bone resection process was more like milling than saw cutting. They were expected to improve bone cutting precision [17], but they also increased operating room (OR) time, added investment cost, operational and procedural cost, and occupied valuable OR space. The result was that those systems suffered delays in regulatory approval and even afterwards, were never embraced by the surgical community, and so therefore did not succeed or grow commercially. Other active robotic approaches help in the positioning of conventional-like guides and blocks for use with standard hand held surgical powered tools: Praxim[2] [18].

More recently, **passive robots** (Mako,[3] who also acquired Acrobot [19], and which is now owned by Stryker/NJ) became available for arthroplasty. These systems again hold a fast rotating burr at the end of a robotic arm, but the same end haptically senses the surgeons intended 3D position of the cutting tool, and the robotic system actuates/moves the tool in the intended direction. If the surgeon deviates from the pre-surgical plan, and is about to cut intended bone, the robotic arm resists (does not move) into those (out-of-bounds) positions. Although typically smaller in size than active robots, passive ones present the same drawbacks but add an extra limitation: Their current forms are suitable only for unicondylar knee surgery and hips, but not total knee replacements.

Lastly, a recent addition to commercial arthroplasty technology is NavioPFS (by BlueBelt[4]). This system uses an off the shelf optical tracker to navigate in real time the

[1] www.robodoc.com.

[2] www.praxim.fr.

[3] www.makoplasty.com.

[4] www.bluebelttech.com.

target bones (tibia and femur) and the cutting instrument: again a rotating burr. In this case, the burr is hand held and moved totally manually, but the cutting end is shielded or the burring speed attenuated or stopped if the surgeon deviates from the surgical plan. While NavioPFS allows planning and surgery without the use of mechanical jigs, it also favors sculpting of the bone and so more naturally to unicondylar implants (like Mako, described previously) and cannot be used for total knee replacements.

The Navigated Freehand Cutting Approach

Navigated Instruments

The approach we have proposed [20] and have called the Simplified Orthopaedic Surgery (SOS) system is a totally freehand navigated bone cutting technology, with usual orthopaedic powered tools such as sagittal and reciprocating saws and drills/reamers. The system was initially designed for and tested on the more challenging total knee replacement surgery, but is compatible with other arthroplasty procedures and other bone osteotomies. It enables surgeons to reshape the bones to fit the implants optimally (based on a pre-surgical plan) without the need for implant specific mechanical jigs, without expensive and cumbersome robots, and even without external navigation tracker equipment (optional).

This system enables the navigation of freehand-held bone cutting instruments (power saws and drills) with real-time 3D graphical feedback guidance provided to the surgeon. The dynamic feedback is shown on a small color LCD touch screen mounted onboard the hand held tool (Fig. 9.1), to allow the surgeon to remain focused on the surgical site, on a dual computer monitor (Fig. 9.6), or on a separate large computer monitor in the operating room. Moreover, through bi-directional wireless communication during cutting, the user can control what is required of the main system through menus on the touch screen device.

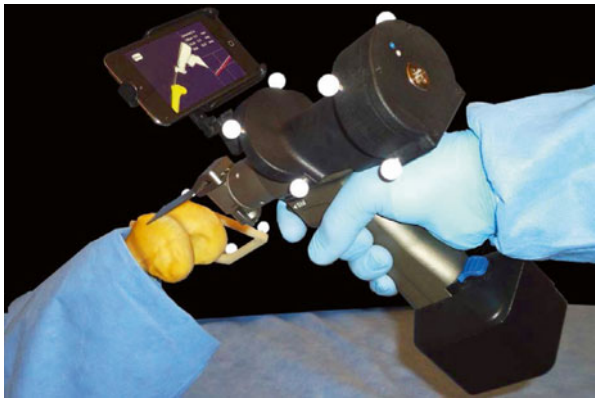

Fig. 9.1 Surgeons feedback presented on a small LCD touch screen mounted onboard the hand held tool

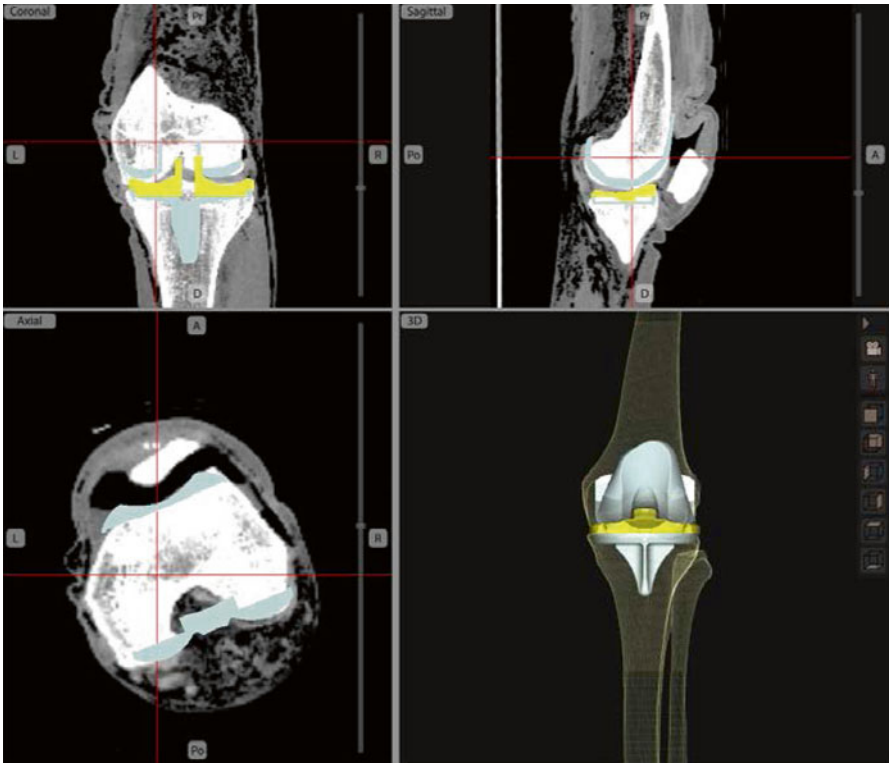

Fig. 9.2 Planning based on CT (SOS screen capture)

Planning Surgery

Being currently (CT) image based, SOS provides fully integrated software tools and interfaces in one application to reconstruct three-dimensional models from raw data of Dicom CT studies (Fig. 9.2).

Once the patient specific bone models are created by SOS, the graphical user interface provides tools for the user to define anatomical landmarks, and to choose an implant from a database with multiple implant brands, models and sizes, including design characteristics and 3 dimensional implant models originating from manufacturer computer aided design (CAD) data. The surgical plan can be based on any of the conventional TKR alignment techniques based on the mechanical axis and joint line, and rotationally based on the Epicondylar axis [21], or Posterior condyle alignment, or Whiteside's Line [22] (Fig. 9.3). Moreover, the user can fine-tune the plan by freely moving the tibial and femoral TKR component models on the screen relative to the bones. This allows the user to optimize other parameters such as articular surface matching/coverage, and to avoid notching or overhand of the femoral component say.

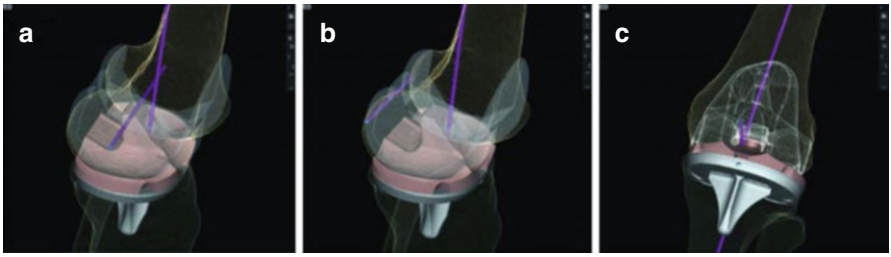

Fig. 9.3 Alignment: (**a**) Epicondyle axis; (**b**) Posterior condyles; (**c**) Whiteside line (SOS screen capture)

Navigated Power Tools

SOS uses a commercial tracker (NDI Polaris Spectra) and custom tibial and femoral reference frames to navigate the bones. However, unlike a conventional navigated jig system, SOS also directly tracks the powered cutting instruments in 3D via reference frames. After a quick registration process, the system is able to sense the location of both the bones and instruments relative to their reference frames, and therefore SOS can track the location of the bones and instruments in real time, indicating to the user how and where to cut. Customized wireless electronics embedded in the power tools allows SOS to slow down and/or stop the cutting/drilling if the user deviates from the surgical plan, which prevents the bone from being cut improperly. The surgeon can optionally empower this functionality, and adjust the cutting accuracy envelopes they allow themselves in each degree of freedom separately (Fig. 9.4).

Simplified 2D Guidance

In addition to the dynamic 3D virtual environment, SOS also provides a simplified (and more condensed) 2D guidance component. Inspired by flight simulators, the 2D guidance component displays a horizon line representing the plane of the cut, as well as lines representing the tip and back of the blade (see Fig. 9.5): When all three components coincide, it means that the potential bone cut is correct (tool is aligned properly with the cut), so that the user can proceed with the cutting. Similar guidance is shown for reciprocating saw (with vertical as opposed to horizontal lines) and drill (with cross-wired bulls-eye like target instead of lines).

Smart Views

During a procedure, the surgeon may prefer to see a particular perspective of the virtual environment (3D view), based on a certain combination of orientations of the patient model and the instrument. For example when aligning the oscillating saw to

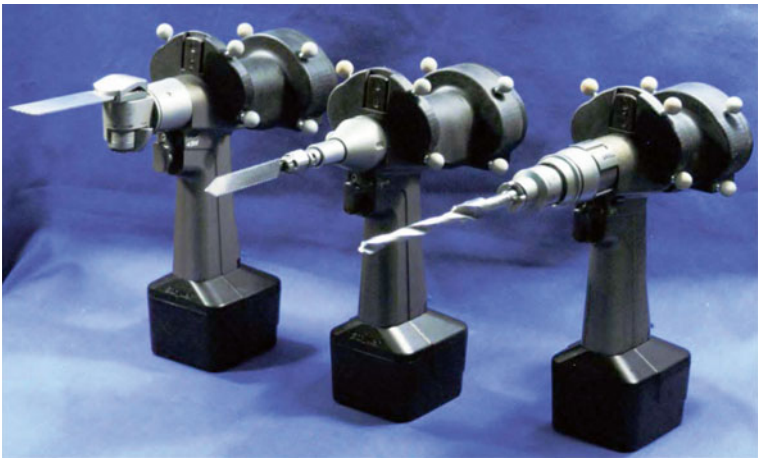

Fig. 9.4 Navigated power tools

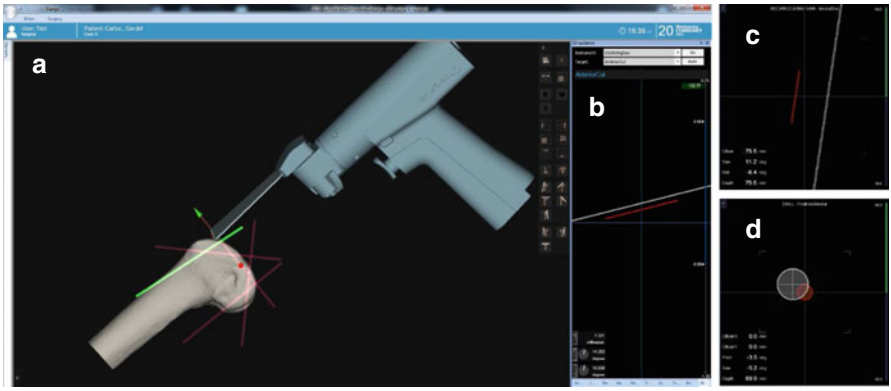

Fig. 9.5 Real time feedback for surgical guidance: (**a**) Full 3D guidance view for the oscillating saw; (**b**) 2D guidance for Oscillating saw; (**c**) Sample of 2D guidance for Reciprocating saw; (**d**) Sample of 2D guidance for Drill

make the anterior cut for a femoral component, the user would favor a lateral view of the bone so the guidance planes would appear like straight lines (see Fig. 9.5). This would be preferred by most users compared to a distal or anterior view, where the model of the saw would obstruct the view of the bone and the planar cut guidance plane. Although surgeons may desire to have control over the view, they normally do not want to be encumbered by manipulating system controls or interacting with any computer during a procedure.

Therefore, the SOS system is optionally configured to sense the context and the intended cut of the surgeon by real-time computations of the handheld tool motions and approach and proximity to a certain cut. The system then automatically and

Fig. 9.6 Navigated Freehand Cutting system, early elementary prototype used on Study1

dynamically changes the graphical environment view (perspective angle) to the most suitable default or relevant perspective view of the surgical scene previously chosen by the surgeon. The system naturally allows the surgeon to manually select any view/perspective the surgeon may desire. However, anticipating what the surgeon is about to do based on the relative position and orientation of instruments and bones contributes to a user adaptable/configurable knowledge based system.

Experimental Case Studies

Different versions of the system described above have been built and bench tested to evaluate feasibility of the concept and assess usability and accuracy. Two of the most comprehensive studies are cited here and summarized here:

Study 1: Navigated Freehand Cutting Experiments with Seven Independent Surgeons [23]

For this study, seven independent orthopaedic surgeons at different stages of their career have participated in testing. A distal femur was simulated on a surgical table by identical replicas molded from synthetic material of similar cutting-feel as real bone. An early elementary prototype version of the system described above was used to navigate the bone specimen and an oscillating bone saw fitted with passive reference frames. It was programmed with the ideal locations of the five distal femur plateau cuts for a widely used TKR system. Each surgeon performed five timed experiments in a 1-day session (Fig. 9.6).

The surgeons varied in speed but showed a steep learning curve, with 10.2 ± 4.3 min average cutting time (see Fig. 9.7). This was even faster than measured in our previous

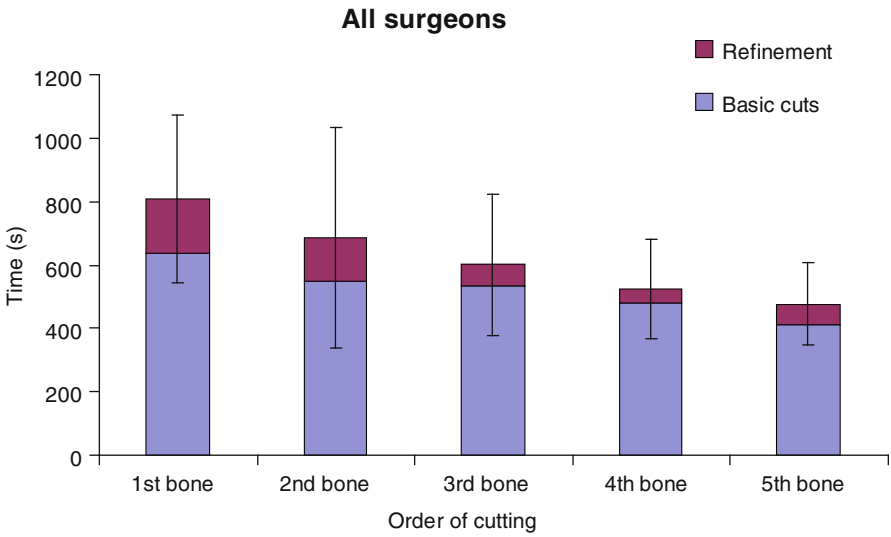

Fig. 9.7 A graph shows times of bone cutting for all surgeons, broken down and averaged according to the order in which the bones were cut. Values are expressed as mean and SD

studies [24], which were in-turn faster than with conventional instruments, promising savings in surgeon and OR tourniquet times. From the thousands of digitized surface points on each cut-surface, the average overall average surface roughness Ra was 0.19 mm, and the average difference between the highest-50-peaks and lowest-50-valleys was <1.2 mm. These also confirmed previous measures, that the cut surface smoothness was reproducible and adequate, especially for cemented cases.

Although tightness of how the implant fitted the bone prior to cementation was not targeted for this cemented implant, 21 out of 35 bones were tight on the implant-trial, and others slightly loose (without cementation). The worst looseness was in the implant "flexional" sense with average <1.6°, and <1 mm in translation. Average implant alignment error was 1.2°, and always <4.7° sagittally, <3.6° frontally and <2° axially. Linear-translation errors averaged 1.4 mm, and <4.2 mm everywhere, with some systematic undercutting of the distal plateau evident, attributed to surgeon being conservative and not following the computer guidance all the way for fear of overcutting. Digitization and 3D analysis of all cut-surfaces echoed the above results, showing the extreme-outliers to be the chamfers which were deliberately treated as less important and therefore were less intricately cut by most surgeons (Fig. 9.8).

The results showed high reproducibility of the cuts and a narrow envelope of alignment error. Alignment with SOS in previous studies was measured to be much superior to cutting with conventional TKR cutting blocks, and this was echoed here with a wide range of independent surgeons. Qualitative feedback from the surgeons surpassed our expectations, even with the bare-minimum level of technology used. We anticipate significant further improvements with the inclusion of novel smart software/hardware techniques on the same system.

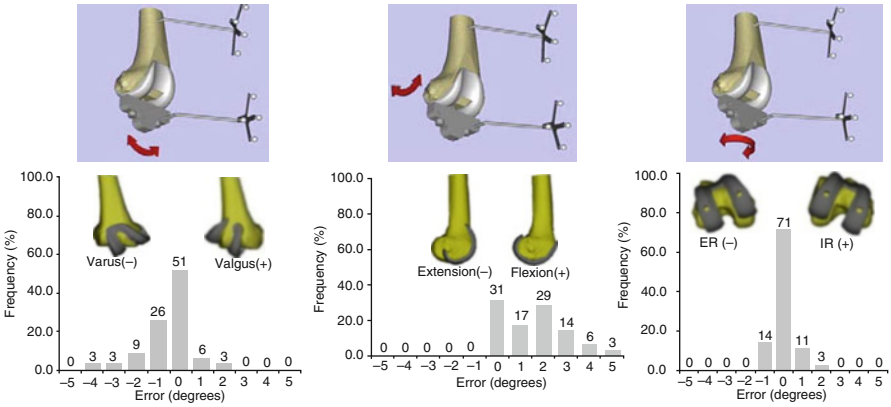

Fig. 9.8 Study 1: Frequency and magnitude of errors in coronal, sagittal and rotational alignment (*ER* external rotation, *IR* internal rotation)

Study 2: Experimenting with Cadavers [25]

This study pushed Navigated Freehand Cutting (NFC) further by using the technique to perform complete total knee replacement (TKR) surgeries (including implant cementing of tibia and femur) on cadaveric leg specimens.

A single surgeon performed a series of surgeries with cruciate sacrificing TKR implants which are considered more challenging for a freehand cutting approach due to the extra number and complexity of cuts needed around a posterior stabilizing post recess when present. A later prototype version of the SOS system was used, with real time graphics to indicate where/how to cut the bone without jigs. The system comprised a navigated smart oscillating saw, reciprocating saw and drill without any of the conventional jigs typically used in TKR (Fig. 9.9).

The tasks performed included pre-surgical planning, incision, placement of navigation pins & markers on tibia and femur, bone registration, marking and cutting, cut surface digitization (for quality assessment), implant placement and cementing, assessment of implant fit and location, and pin removal and wound closing.

The overall average surgery time was 1 h and 20 min. The cutting process took the most time (31 % of total time) followed by cementing and bone registration (14 % and 12 %, respectively). Surface smoothness of the bone cuts on human cadavers was better than what was previously obtained for synthetic bone (Fig. 9.10).

The results indicated that Navigated Freehand Cutting (NFC) technology could be used on patients, as surgical time, implant alignment, cut quality, and other metrics were consistent or better than those of conventional approaches, even with this prototype system. New computer-human interfaces under development are expected to reduce cutting, registration and digitization times, and promise faster overall surgery. We speculate that NFC is no longer a dream, no longer just feasible, but is on the way to clinical trials not too far in the future.

Fig. 9.9 Surgeon cutting a femur with and navigated oscillating saw

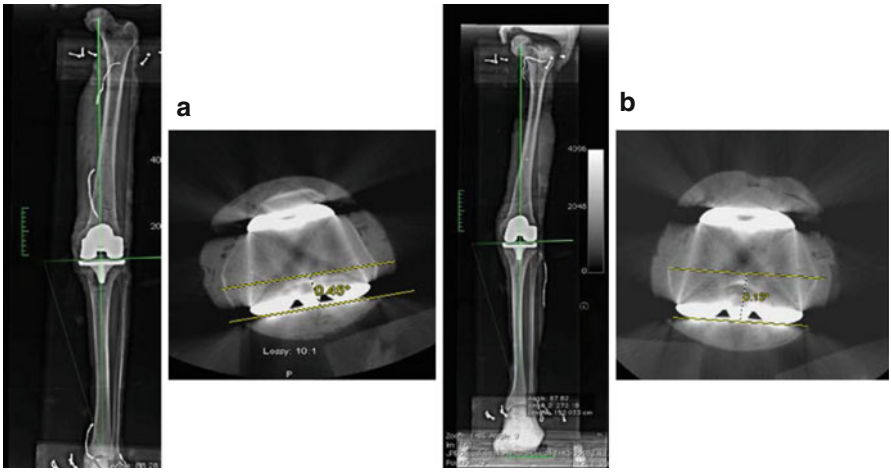

Fig. 9.10 Final implant alignment after full TKR. (**a**) Specimen 1: 1.8° Valgus, 0.45° I-Rotation; (**b**) Speciment 2: 1.5° valgus, 0.13° I Rotation

Fig. 9.11 OTT (On Tool Tracking) functional prototype at the University of Nebraska Medical Center

Futuristic Versions of Smart Navigated Instruments

With the objective of simplifying the system and reducing the footprint of the NFC tracking system (currently NDI Polaris), the University of Nebraska Medical Center is designing and implementing "On-Tool Tracking" (OTT) [26], a novel miniaturized tracking system that mounts onto the cutting instruments (Fig. 9.11). OTT is a wireless device that provides stereo navigation with miniature cameras onboard, laser projection onto the bone, motor control, and a touch-screen user interface.

In addition to reducing footprint in operating room, OTT avoids line-of-sight concerns (the tracker 'travels' with the tool, close to the bone), improve xy/z ratio due to the cameras proximity to the reference frames (RF), and minimize damage to the bone by RF pins due to smaller size and lighter RFs.

Concluding Remarks

Joint replacement surgery is highly successful, but is still a complex and relatively expensive procedure that requires a great level of training and expertise. The large set of implant-specific instruments conventionally required in arthroplasty is a key factor in the costs, intricacy, and adds to the infection risk. While newer approaches like computer aided orthopedic surgery (CAOS) and navigation offer modestly better accuracy with fewer outliers in total knee arthroplasty (TKA), most such systems for TKA help to align cutting blocks that are essentially similar to the conventional cutting jigs, thereby adding a subset of new instruments.

Other technologies like custom jigs, active and passive robots contribute with reducing complexity and instrumentation count. Nevertheless, these technologies can isolate surgeons from some of the surgical process, add extra steps to the procedure,

take valuable space in the OR, and require large capital investment and maintenance costs, and in many cases are not suitable for total knee replacement surgery.

Navigated freehand cutting (NFC), the technology presented above, promises to finally make TKR easier, faster, cheaper and equal or better than the conventional jigs (the current gold standard).

References

1. Kurtz S, Ong K, Lau E, Mowat F, Halpern M. Projections of primary and revision hip and knee arthroplasty in the united states from 2005 to 2030. J Bone Joint Surg Am. 2007;89:780–5.
2. Bozic KJ, Kurtz SM, Lau E, et al. The epidemiology of revision total knee arthroplasty in the United States. Clin Orthop Relat Res. 2010;468:45–51.
3. Stulberg SD, Loan P, Sarin V. Computer-assisted navigation in total knee replacement: results of an initial experience in thirty-five patients. J Bone Joint Surg Am. 2002;84-A Suppl 2:90–8.
4. Intelligent Orthopaedics, Minimally Invasive Surgery for P.F.C. Sigma and P.F.C. Sigma RP Knee Systems Surgical Technique. DePuy International Limited, Cat No: 9095-31-000 Version 1, 2005.
5. Wixon RL. Extra-medullary computer-assisted total knee replacement: towards lesser invasive surgery. In: Stiehl JB, Konermann WH, Haaker RGA, editors. Navigation and robotics in total joint and spine surgery. Germany: Springer; 2004. p. 311–8.
6. Konermann WH, Kister S. CT-free navigation including soft-tissue balancing: LCS-TKR and VectorVision systems. In: Stiehl JB, Konermann WH, Haaker RGA, editors. Navigation and robotics in total joint and spine surgery. Germany: Springer; 2004. p. 354–65.
7. Medtronic Navigation. Medtronic navigation orthopaedic surgery solutions brochure. 2005. 9670819 Rev02.
8. Chauhan SK, Scott RG, Breidahl W, Beaver RJ. Computer-assisted knee arthroplasty versus a conventional jig-based technique. A randomised, prospective trial. J Bone Joint Surg Br. 2004; 86:372–7.
9. Harvie P, Sloan K, Beaver RJ. Three-dimensional component alignment and functional outcome in computer-navigated total knee arthroplasty: a prospective, randomized study comparing two navigation systems. J Arthroplasty. 2011;26:1285–90.
10. Matziolis G, Krocker D, Weiss U, Tohtz S, Perka C. A prospective, randomized study of computer-assisted and conventional total knee arthroplasty. Three-dimensional evaluation of implant alignment and rotation. J Bone Joint Surg Am. 2007;89:236–43.
11. Molli RG, Anderson KC, Buehler KC, Markel DC. Computer-assisted navigation software advancements improve the accuracy of total knee arthroplasty. J Arthroplasty. 2011;26: 432–8.
12. Scuderi GR, Fallaha M, Masse V, et al. Total knee arthroplasty with a novel navigation system within the surgical field. Orthop Clin North Am. 2014;45:167–73.
13. Pransky J. ROBODOC – surgical robot success story. Ind Robot. 1997;24:231–3.
14. Lanfranco AR, Castellanos AE, Desai JP, Meyers WC. Robotic surgery: a current perspective. Ann Surg. 2004;239:14–21.
15. Lang JE, Mannava S, Floyd AJ, et al. Robotic systems in orthopaedic surgery. J Bone Joint Surg Br. 2011;93:1296–9.
16. Siebert W, Mai S, Kober R, Heeckt PF. Technique and first clinical results of robot-assisted total knee replacement. Knee. 2002;9:173–80.
17. Song EK, Seon JK, Yim JH, Netravali NA, Bargar WL. Robotic-assisted TKA reduces postoperative alignment outliers and improves gap balance compared to conventional TKA. Clin Orthop Relat Res. 2013;471:118–26.
18. Plaskos C, Cinquin P, Lavallee S, Hodgson AJ. Praxiteles: a miniature bone-mounted robot for minimal access total knee arthroplasty. Int J Med Robot. 2005;1:67–79.

19. Cobb J, Henckel J, Gomes P, et al. Hands-on robotic unicompartmental knee replacement: a prospective, randomised controlled study of the acrobot system. J Bone Joint Surg Br. 2006;88:188–97.
20. Haider H, Barrera OA, Garvin KL. Minimally invasive total knee arthroplasty surgery through navigated freehand bone cutting: winner of the 2005 "HAP" PAUL AWARD. J Arthroplasty. 2007;22:535–42.
21. Berger RA, Rubash HE, Seel MJ, Thompson WH, Crossett LS. Determining the rotational alignment of the femoral component in total knee arthroplasty using the epicondylar axis. Clin Orthop Relat Res. 1993;286:40–7.
22. Whiteside LA, Arima J. The anteroposterior axis for femoral rotational alignment in valgus total knee arthroplasty. Clin Orthop Relat Res. 1995;321:168–72.
23. Haider H, Barrera OA, Mahoney CR, et al. Navigated freehand bone cutting for TKR surgery: experiments with seven independent surgeons. Poster N°196 at AAOS-2008. San Francisco; 2008.
24. Barrera OA, Haider H, Walker PS, Sekundiak TD, Garvin KL. Freehand navigation cutting for TKR surgery without jigs: Assessment of distal femoral cuts vs. Conventional jigs. Presented at the 4th CAOS International Annual Meeting. Chicago, US; 2004.
25. Haider H, Barrera OA, Hartman CW, Garvin KL. Can the future bring TKR without implant specific instruments? Presentation at ISTA-2011. Bruges, Belgium; 2011.
26. Haider H, Al-Shawi I, Barrera OA, et al. On-tool tracking (OTT) system for navigated free-hand cutting (NFC). Invited talk at ISTA-2014. Kyoto, Japan; 2014.

Chapter 10
Navigation in Spinal Surgery

Joseph H. Schwab

Abstract Intraoperative navigation is used because it improves the accuracy by which screws are placed in the spine. Physicians who approve this technique are divided into two groups, some argue that fluoroscopic is best for its lower costs, whereas other group claims that computer tomography images for navigation decreases radiation exposure for surgeons and improves accuracy. Although "freehand" method is been demonstrated to be quite accurate in experienced hands it is comparable with intraoperative navigation. Throughout this chapter it can be claimed that all methods used today seem to improve precision over traditional "freehand" technique. Intraoperative navigation is needed in cases where accuracy is of great importance, for instance when resecting tumour navigation is used to ensure that the entire tumour is removed or that the resection margins are outside of the tumour. Moreover, navigation allows to perform clearer bony cuts and complete tumour resection since it can be seen the entire tumour area. The advantages such as decrease in radiation exposure and safety during procedures must be weighed against the high costs of purchasing equipment that suits for 3D navigation. Nevertheless, screws perforating the bone can cause trouble, for example if a screw is contacting a major blood vessel or nerve. In these cases navigation may be of clinical benefit. However, no study has yet to be performed that demonstrates a cost benefit for the use of navigation.

Keywords Freehand technique • Intraoperative navigation • Preoperative CT • Fluoroscopic guidance

Introduction

The use of intra-operative navigation continues to evolve. Advocates of navigation point to improved accuracy of pedicle screw placement as a primary reason for its use. Within the group of advocates some argue for fluoroscopic guidance of instrumentation and others favor computed tomography as the means to navigate. Those

J.H. Schwab, MD, MS
Department of Orthopaedics, Massachusetts General Hospital,
55 Fruit Street, Suite 3800, Boston, MA 02114, USA
e-mail: jhschwab@mgh.harvard.edu

L.E. Ritacco et al. (eds.), *Computer-Assisted Musculoskeletal Surgery: Thinking and Executing in 3D*, DOI 10.1007/978-3-319-12943-3_10

who favor CT guidance point to decreased radiation exposure to the surgeon [3] and improved accuracy [8] as reasons for its use while those that favor fluoroscopic guidance highlight lower costs. Navigation seems to improve the accuracy with which instrumentation can be placed when compared to free hand technique. However, this relative improvement is surgeon specific and the use of navigation is certainly not necessary in most cases as free hand techniques have been shown to be quite accurate in experienced hands [7]. One could argue that revision cases would benefit most from navigation particularly when one is placing implants into or through an area that has undergone a successful posterior fusion where the anatomic landmarks are distorted. Three other areas seem to fit naturally with navigation including percutaneous techniques as well as minimally invasive techniques and in areas where the target is quite narrow such as the cervical spine [6, 10, 13]. Navigation can play a useful role in cases where instrumentation is not being used as well. For instance, when one is removing a tumor, navigation can be used to assure that all of tumor is removed or that the resection margins are kept outside of the tumor [9]. When navigation is used in these cases it can allow for more accurate bony cuts or more complete tumor resection particularly when one is in an area where direct visualization is not possible. This chapter will review many of these concepts and show examples of how navigation can be used in a less conventional way.

Preoperative Preparation

Surgeons planning on using navigation will of course need to consider how best to use it and why. Depending upon the type of navigation used, the surgeon will need to assure all relevant equipment and expertise is available. In some cases navigation requires a pre-operative computed tomographic image to be formatted in a way compatible with the navigation software be used. In other cases and intra-operative computed tomogram is obtained. In some cases a pre-operative MRI is married to an intra-operative CT to maximize soft tissue imaging. These situations require planning to assure that the images are formatted appropriately.

One must remember that navigation equipment need not be expensive or particularly new to be useful. A plain radiograph or fluoroscopic image can provide enough information to assist in many techniques. Intraoperative fluoroscopy is likely the most commonly used form of image guidance and it has many advantages including availability, relatively low cost and familiarity. One downside is the radiation exposure to the surgeon which can become a concern when radiation doses accumulate over the years [14]. Some fluoroscopy machines are able to produce three dimensional displays of the operative target which improves accuracy of screw placement, but, again, with increased radiation exposure [4].

The use of computed tomography (CT) as a means to navigate in spine surgery started with the use of pre-operative CT. The data from the CT images was integrated into a software program that allowed for navigation of instruments. One of the issues noted with pre-operative CT is that the CT was taken while the patient

was supine and the operation was typically performed while the patient was prone. Furthermore, the lack of three dimensional imaging in the operating room prevented a detailed assessment of the hardware placement. These issues should be considered when one is preparing to use navigation.

Software exists that facilitates the marriage of pre-operative magnetic resonance images with computed tomography (either pre-operative or intra-operative CT can be used). This can prove useful when one is interested in soft tissue detail such as when a tumor invades outside the bone or during a bone biopsy when the lesion is not readily seen on CT. Typically the MRI would need to be processed in advance of the surgery and so one must plan for this event.

Templating is a tried a true form of preparation in arthroplasty and orthopaedic trauma surgery as well as in deformity surgery. Navigation can allow for templating in spine surgery as well. In this case the surgeon can decide pre-operatively the size and trajectory of the implants to be used using software. A phantom of the implant can then be left in place to be used as a template for insertion of the real device. Similarly, one can determine where they would like to make a bony cut using pre-operative planning software. Then the cuts or a phantom of the cuts can be left in place to allow the surgeon to mimic them intra-operatively.

Technique with Pearls and Pitfalls

In general it is vital to understand that navigation cannot teach you anatomy or how to place implants into the spine. One must be comfortable operating on the spine prior to using navigation. There are several obvious reasons for this but perhaps the most practical issue relates to the fact that navigation technology can fail. If the technology you are using is not working for whatever reason, then you must be able to function without it. If the navigation fails completely, then one is left with more conventional means of surgery such as using anatomic landmarks to place screws. A more sinister situation arises when the navigation seems to be working well but it is not calibrated properly. This situation the surgeon has to be able to discern there is a problem based on other signals such as tactile feedback or recognizing that the normal anatomy is not matching what the navigation is showing. If the surgeon fails to recognize this problem then disaster can strike where an instrument is placed somewhere the surgeon wishes it had not.

I will present three cases hoping to illustrate how one might use navigation in practice. The first case is of a 50 year old woman who has recurrent giant cell tumor of the upper thoracic spine. She has had a sub-total resection in the past and has been managed with Denosumab for several years. She tolerated the RANKL inhibitor well until recently when it was discovered that she had developed a stress fracture in her femur. The stress fracture forces the discontinuation of Denosumab and so revision surgery is revisited. She has no symptoms and so she is keen to avoid a large surgery if possible. Her previous surgery involved a posterior as well as an anterior approach with subsequent instrumented fusion (Fig. 10.1). The tumor is

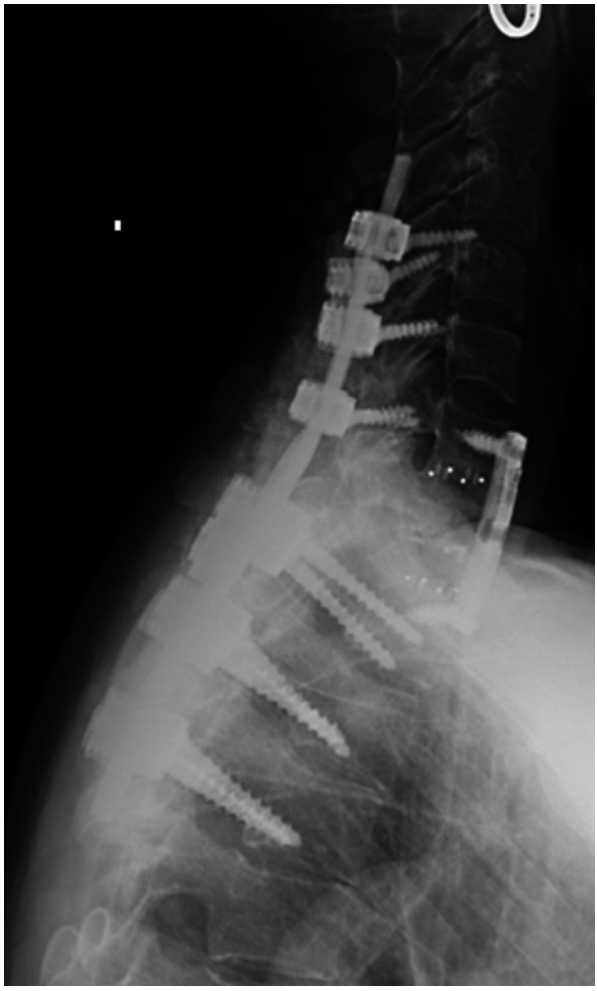

Fig. 10.1 This lateral radiograph demonstrastes anterior and posterior spinal instrumentation after excision of giant cell tumor of T1

localized to the right laminae of T1 as well as the vertebral body as seen on MRI (image not shown). The lesion is also well seen on computed tomography (Fig. 10.2). She has a solid fusion and to access the laminae in a conventional way would involve removing the hardware as well as taking down the fusion mass. However, the tumor is accessible via a direct posterior lateral approach. One could approach it via long posterior lateral incision or through a small incision. A smaller incision would limit one's ability to visualize the tumor and so navigation was chosen to help with identifying the tumor by incorporating an intra-operative CT image. This tumor is ideal for CT identification owing to its lytic nature which is readily seen on CT.

After positioning the patient in the operating room an intra-operative CT was obtained and the patient's tumor was mapped prior to making the skin incision. The navigation helped to determine the optimal position for the incision (Figs. 10.2 and 10.3). In this case the smaller incision was ideal for a tubular retractor system (Fig. 10.4). Again, the

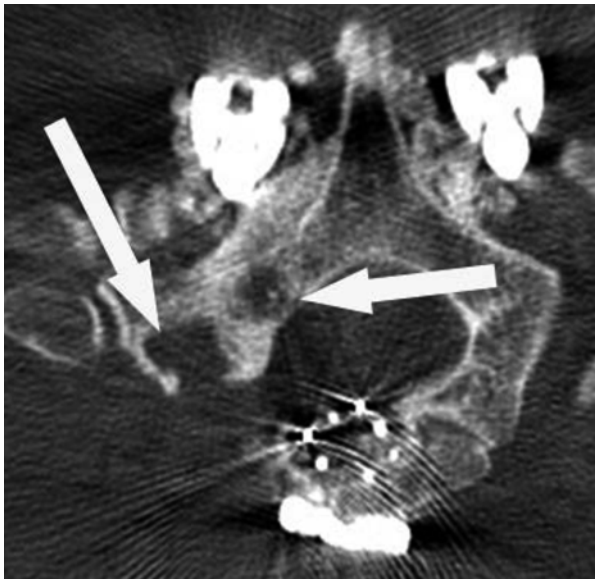

Fig. 10.2 This axial CT demonstrates lytic changes in the posterior elements of T1 (*arrows*)

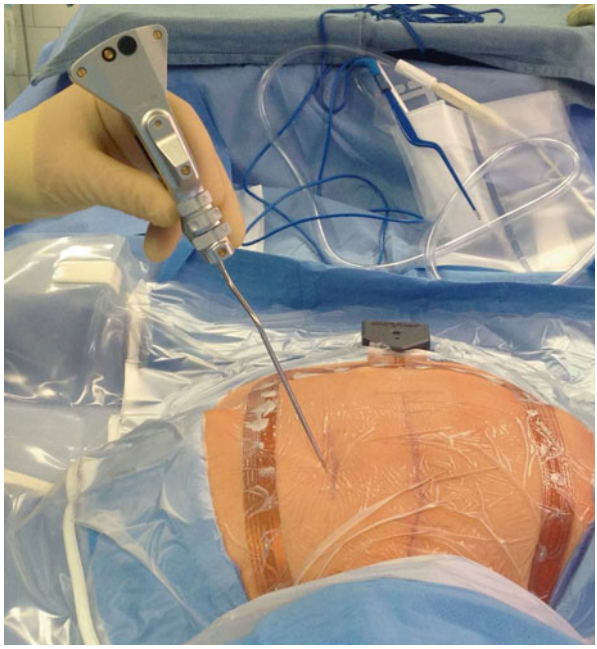

Fig. 10.3 This intra-operative photograph shows the navigation probe being used to help localize the lytic disease so that the incision can be made precisely at the level of the tumor

navigation allowed for the use of a smaller incision by helping to determine the best trajectory needed to access the tumor while avoiding the hardware already in place. Once the incision was made the navigation helped to guide the burr used to remove the tumor. The navigation probes were used frequently during the surgery to determine

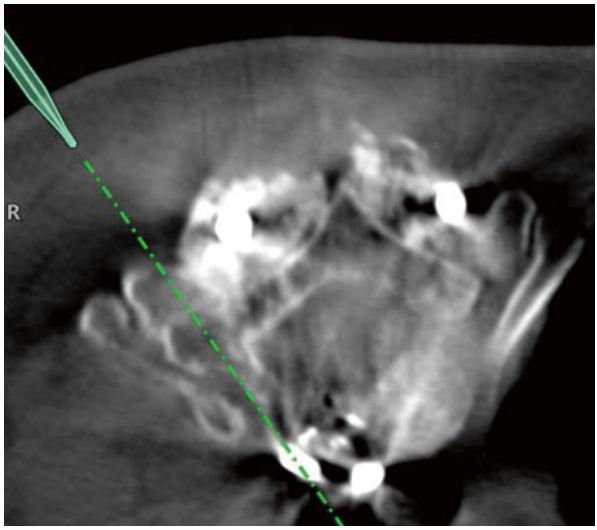

Fig. 10.4 This intra-operative navigation image shows the head of the probe over the lytic area in the bone. The probe appears to be in the subcutaneous tissues however, the probe is actually on the skin rather in the tissue

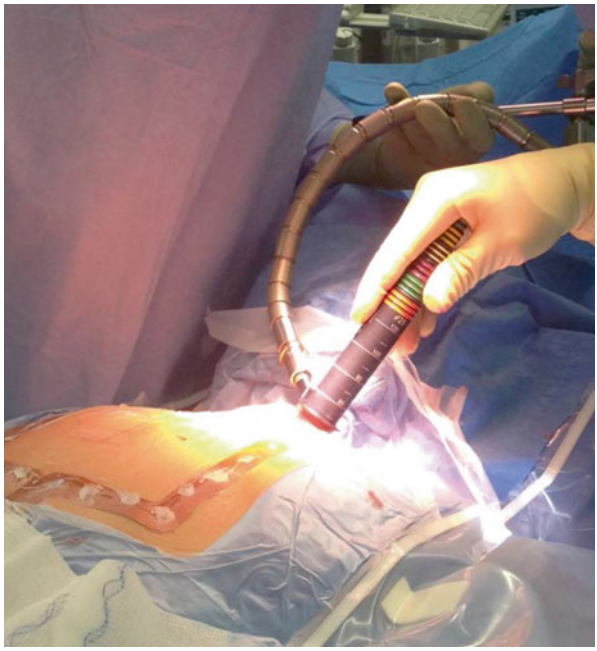

Fig. 10.5 This intra-operative photograph shows the placement of a tubular retractor system through a small incision centered over the T1

exactly how much bone/tumor to remove (Figs. 10.5, 10.6, and 10.7). A post-operative CT demonstrates the extent of resection most clearly (Fig. 10.8).

Another situation where navigation can be useful is where percutaneous implants are utilized. Fluoroscopic images are the standard method by which to insert these screws and it is a reliable method. However, CT based navigation is also quite useful

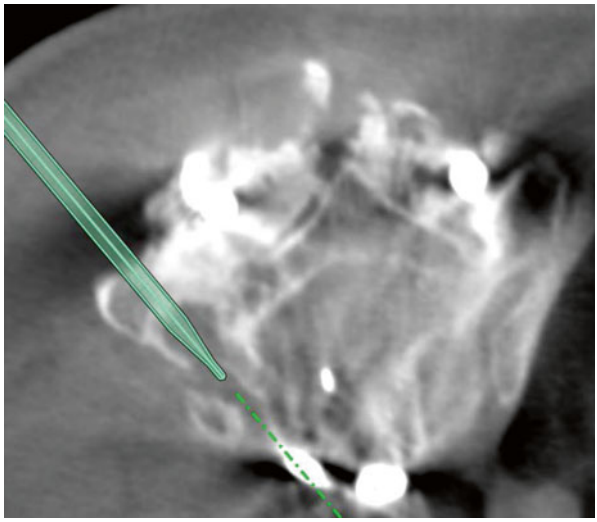

Fig. 10.6 This intra-operative navigation image shows the probe in the area of the lytic disease. In this case the area proximal to the tip of the probe has been removed with the drill. The navigation probe provides information regarding how much more bone should be removed as well as how close one is to the spinal canal. It also allows one to avoid the posterior instrumentation

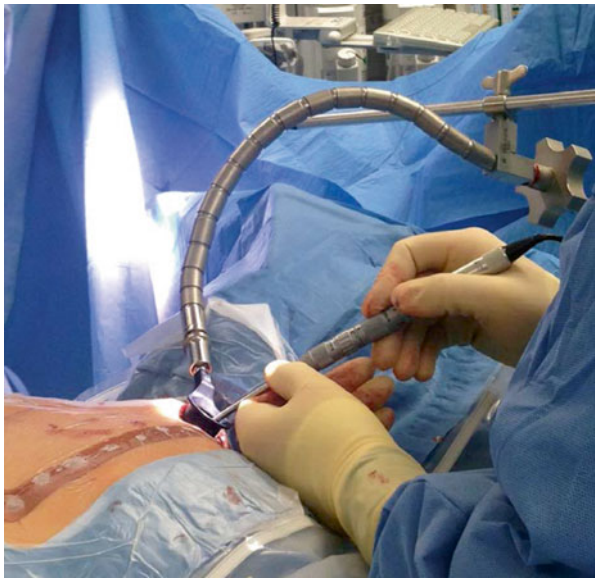

Fig. 10.7 This intra-operative photograph shows the drill being used to remove bone through the tubular retractor system

and can decrease operative time and radiation exposure to the surgeon.23883830 Fluoroscopy guided percutaneous screw placement requires the insertion of a guide wire over which the screw is inserted (Figs. 10.9, 10.11, 10.12, 10.13, and 10.14). Screws can be placed reliably using this method. One or dual C-arms can be used to obtain biplaner fluoroscopic images. Alternatively, three dimensional fluoroscopic images can be obtained with more specialized equipment.

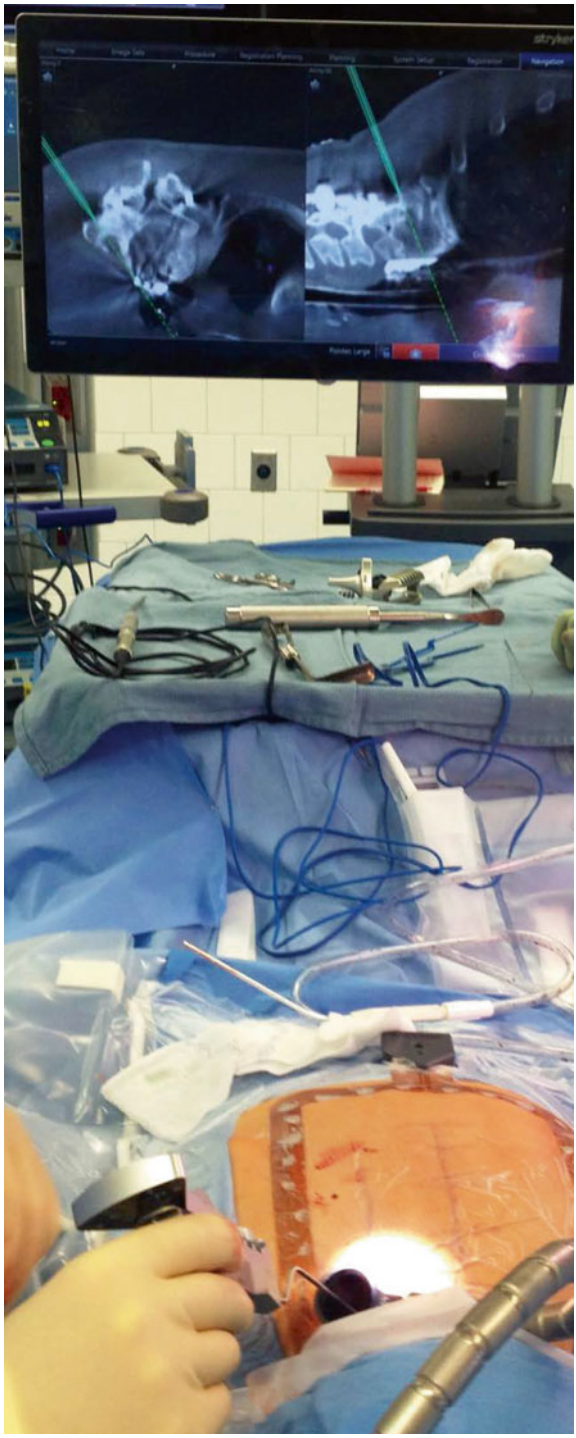

Fig. 10.8 This intra-operative photograph shows the navigation probe within the tubular retractor system. It also shows the navigation image in the same field allowing the reader to appreciate where the probe is relative to the lytic disease in the spine

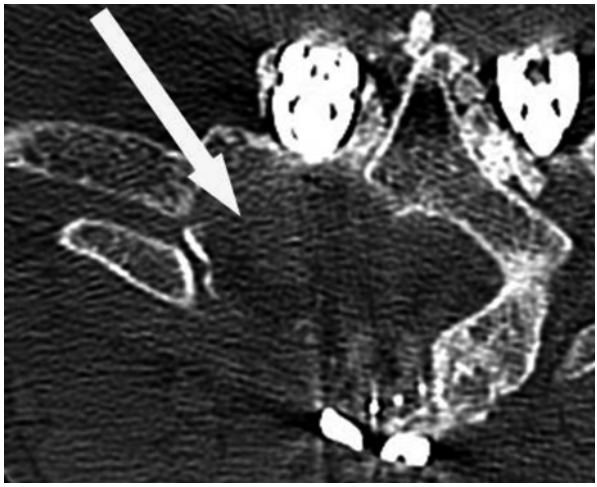

Fig. 10.9 This is a post-operative axial CT which shows complete removal of the lytic area (*arrow*) and surrounding bone in T1

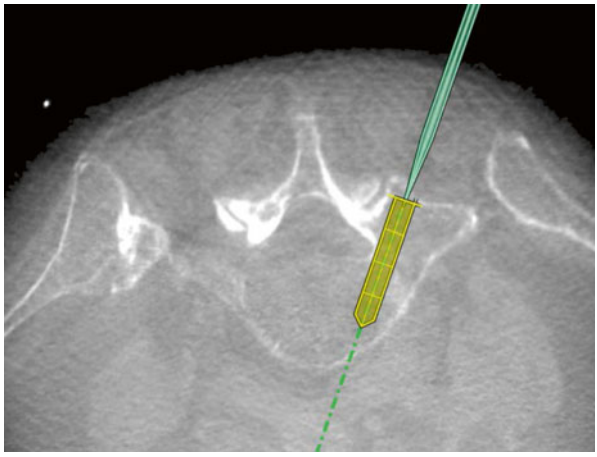

Fig. 10.10 This intra-operative navigation image reveals the navigation probe with a phantom screw attached to it's tip so that it can be used as a template

Complications

There are some complications associated specifically with navigation. One of the biggest concerns about using navigation relates to its accuracy. The accuracy of one method of navigation may be inherently different than another and are therefore embedded in to the system. This level of inaccuracy is predictable and therefore less dangerous. It is the unpredictable inaccuracy that is dangerous. Most navigation systems (at least those that allow tracking of instruments) must have a tracking device that remains fixed. If the tracking device is disturbed during surgery, then the instrument may not be where it appears to be on the screen. This can lead to errors

Fig. 10.11 This anterior/posterior fluoroscopic image reveals a Jamshidi needle in a thoracic pedicle

Fig. 10.12 This lateral fluroscopic image shows a guide wire in the pedicle and vertebral body of a thoracic vertebrae

Fig. 10.13 This lateral fluroscopic image shows a pedicle screw that has been placed over a guide wire

in placement of instruments and/or instrumentation. Again, this is avoidable if one is diligent about the tracker's position. However, one must also continue to utilize more conventional means to assess instrument position. For instance, if the operation is an open operation than one can use normal anatomic landmarks for screw placement as a means to check the accuracy of navigation. If the navigation screen shows the phantom in the pedicle but the surgeon sees that the instrument is heading into the spinal canal, then, of course, there is a problem. More subtle inaccuracies can also be a problem particularly when one is trying to place instruments into a small area such as the pedicles in the cervical spine.

Another area that is a problem when using navigation relates to percutaneous pedicle screw placement. Regardless of the system used, it is important for the surgeon to be careful not to bury the pedicle screws into the facet joint of the non-fused segment. This can be avoided by carefully monitoring the trajectory of the screw during placement. One must enter the pedicle more laterally to allow the facet to continue to move normally. If a screw is placed through the facet joint, then one might expect that joint to wear out more quickly. Another issue regarding percutaneous pedicle screws is how deeply to place the head of the screw. In open cases one generally tries to avoid hubbing the screw head into the facet above. However, when one is placing percutaneous screws one usually relies on tactile feedback to know

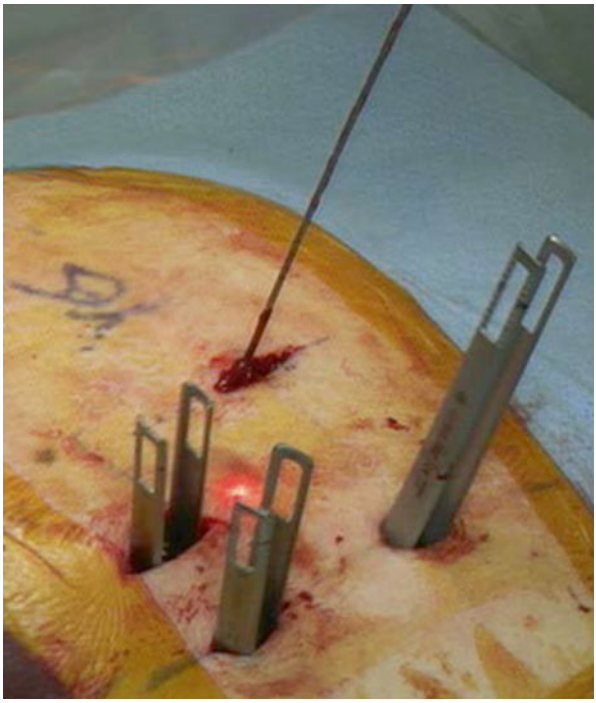

Fig. 10.14 This intra-operative image shows guide wire which has been placed in preparation for a screw. Three screws have already been placed with their extended tulip heads showing through the skin

when the screw is seated. Using this method of feedback would often lead the surgeon to hub the screw head into the facet above which is not desirable and may lead to adjacent segment degeneration. Either use the navigation to judge the depth of the screw in the bone or use tactile feedback to hub the screw but then back it off a few turns.

Another issue with percutaneous screws involves guide wires. When guide wires are used it is very important to monitor the length of the wire. The wires can become soiled with blood and this may lead to them becoming trapped within the hollow core of either the tap or the screw driver. If this occurs the wire may be inadvertently advanced along with the instrument. It is important to avoid this as wires can be driven into the thoracic or abdominal cavity leading to potential injury. This is not an issue when one does not require a guide wire. If the screws can be "navigated" without a wire, then this is of course not an issue.

Failure of arthrodesis is another potential issue with percutaneous fixation. If one is hoping to achieve an arthrodesis, then one must be very careful in deciding how to obtain this. There may be situations when arthrodesis is not necessary. For instance, a patient with an unstable pathologic fracture secondary to advance lung cancer may not require a fusion. Some factures require only temporary fixation and the screws can be removed later so fusion is not necessary. However, if arthrodesis is desired then one might consider an interbody fusion along with the percutaneous screws.

Results

Image guidance has been used principally to improve the accuracy by which screws are placed in the spine. The risk of screw perforation has been decreased with image guidance with one analysis reporting rates of 14.3–9.3 % [12]. All methods used today seem to improve accuracy over traditional "free hand" techniques [11]. Three dimensional imaging such as from 3-d fluoroscopy and or CT based systems seem have an advantage over 2-d fluoroscopic based systems in terms of accuracy [2, 5]. However, the benefit of 3-D fluoroscopy must be weighed against the risk of higher radiation exposure [4]. The downside to using 3-D navigation rests in the initial investment of purchasing the equipment. Although the data support the use of navigation in terms of improving accuracy, it is unclear if this improvement provides meaningful clinical benefit. Most of the screw perforations are not cause for concern. Certainly, there are situations where screws perforating the bone can cause trouble such as if a screw is contacting a major blood vessel or nerve. In these cases navigation may be of clinical benefit. However, no study has yet to be performed that demonstrates a cost benefit for the use of navigation.

Aside from placement of screws, navigation can be useful in localizing tumors. Navigation can theoretically facilitate obtaining negative margins by helping one stay outside of the tumor. Alternatively, one can use navigation to assess whether the entire tumor has been removed by using intra-operative CT based navigation [1]. The same is true for corrective osteotomies of the spine. However, as with oncologic indications, the data is sparse or not existent.

Conclusion

In conclusion, spinal navigation has provided an improvement in the accuracy of screw placement which would seem to be of use particularly in areas where pedicles are small or abnormal such as in the cervical spine or in congenital scoliosis. There also seems to be a benefit for using navigation in orthopaedic tumor surgery. The data on navigation are mostly retrospective and no level 1 evidence exists supporting its use. Having said that, navigation is being used more and more often and the technology is likely to improve and its costs to decrease over time making the application more likely to be accepted into common practice.

References

1. Bandiera S, Ghermandi R, Gasbarrini A, Barbanti Brodano G, Colangeli S, Boriani S. Navigation-assisted surgery for tumors of the spine. Eur Spine J. 2013;22 Suppl 6:S919–24.
2. Bourgeois AC, Faulkner, AR, Bradley YC, Pasciak A, Barlow PB, Gash JR, Reid WS Jr. Improved accuracy of minimally invasive transpedicular screw placement in the lumbar spine with three-dimensional stereotactic image guidance: a comparative meta-analysis. J Spinal Disord Tech. 2014 [Epub ahead of print].

3. Klingler JH, Sircar R, Scheiwe C, Kogias E, Kruger MT, Scholz C, Hubbe U. Comparative study of C-arms for intraoperative 3-dimensional imaging and navigation in minimally invasive spine surgery part II – radiation exposure. J Spinal Disord Tech. 2014 [Epub ahead of print].
4. Klingler JH, Sircar R, Scheiwe C, Kogias E, Kruger MT, Scholz C, Hubbe U. Comparative study of C-arms for intraoperative 3-dimensional imaging and navigation in minimally invasive spine surgery part II – radiation exposure. J Spinal Disord Tech. 2014 [Epub ahead of print].
5. Liu YJ, Tian W, Liu B, Li Q, Hu L, Li ZY, Yuan Q, Lu YW, Sun YZ. Comparison of the clinical accuracy of cervical (C2-C7) pedicle screw insertion assisted by fluoroscopy, computed tomography-based navigation, and intraoperative three-dimensional C-arm navigation. Chin Med J. 2010;123(21):2995–8.
6. Luo TD, Polly DW Jr, Ledonio C, Wetjen NM, Larson AN. Accuracy of pedicle screw placement in children</=10 years using navigation and intraoperative CT. J Spinal Disord Tech. 2014 [Epub ahead of print].
7. Miekisiak G, Kornas P, Lekan M, Dacko W, Latka D, Kaczmarczyk J. Accuracy of the free hand placement of pedicle screws in the lumbosacral spine using a universal entry point: clinical validation. J Spinal Disord Tech. 2015 [Epub ahead of print].
8. Patton AG, Morris RP, Kuo YF, Lindsey RW, Patton AG. Accuracy of fluoroscopy vs. computer assisted navigation for the placement of anterior cervical pedicle screws. Spine. 2015 [Epub ahead of print].
9. Satcher Jr RL. How intraoperative navigation is changing musculoskeletal tumor surgery. Orthop Clin North Am. 2013;44(4):645–56.
10. Schwab JH, Gasbarrini A, Cappuccio M, Boriani L, De Iure F, Colangeli S, Boriani S. Minimally invasive posterior stabilization improved ambulation and pain scores in patients with plasmacytomas and/or metastases of the spine. Int J Surg Oncol. 2011;2011:239230.
11. Tian NF, Huang QS, Zhou P, Zhou Y, Wu RK, Lou Y, Xu HZ. Pedicle screw insertion accuracy with different assisted methods: a systematic review and meta-analysis of comparative studies. Eur Spine J. 2011;20(6):846–59.
12. Tian NF, Xu HZ. Image-guided pedicle screw insertion accuracy: a meta-analysis. Int Orthop. 2009;33(4):895–903.
13. Uehara M, Takahashi J, Mukaiyama K, Kuraishi S, Shimizu M, Ikegami S, Futatsugi T, Ogihara N, Hashidate H, Hirabayashi H, Kato H. Mid-term results of computer-assisted cervical pedicle screw fixation. Asian Spine J. 2014;8(6):759–67.
14. Yu E, Khan SN. Does less invasive spine surgery result in increased radiation exposure? A systematic review. Clin Orthop Relat Res. 2014;472(6):1738–48.

Chapter 11
Knee Prosthesis Navigation

Andrea Ensini, Michele d'Amato, Paolo Barbadoro, Claudio Belvedere, Andrea Illuminati, and Alberto Leardini

Abstract Total Knee Arthroplasty (TKA) represents an effective technique to treat advanced and debilitating knee arthritis. However at long term follow-up the risk of TKA failure still remains a concern. Nowadays the major causes of failures and patient's dissatisfaction, in addition to infection, are a prosthesis that remains instable or is not well aligned on sagittal, transverse or coronal plane. All these situations, in fact, could lead to anterior knee pain, arthrofibrosis, wear or loosening. Therefore, was developed the Computer-Assisted Surgery (CAS), a device that helps the surgeon to position the prosthesis component in a much more accurate way than the conventional instrumentation. In fact, via intra-operative anatomy-based tracking of the tibio-femoral joint, CAS allows more precise bone cuts, more accurate prosthesis components implantation, more controlled soft tissue balance and targeted Mechanical Axis restoration. The aim of this chapter is to present and explain which are the main surgical landmarks of CAS, so how it works and how it could help the surgeon being much more precise with bone cuts and control instantly how the resections could influence the final alignment and the stability of the prosthesis.

Keywords Total Knee Arthroplasty • Computer-Assited Surgery • Knee alignment

Introduction

In case of advanced knee arthritis, Total Knee Arthroplasty (TKA) represents an effective and reproducible surgical technique. But at long term follow-up the risk of TKA failure and subsequently revision still remains a concern. In order to improve

A. Ensini, MD (✉)
1st Clinic Orthopaedic and Traumatology, Istituto Ortopedico Rizzoli,
Via di Barbiano 1/10, Bologna 40136, Italy
e-mail: andrea.ensini@ior.it

M. d'Amato • P. Barbadoro
Division of Orthopaedic Surgery, Rizzoli Orthopaedic Institute, Bologna, Italy
e-mail: miki.damato@gmail.com

C. Belvedere • A. Illuminati • A. Leardini
Movement Analysis Laboratory, Rizzoli Orthopaedic Institute, Bologna, Italy

L.E. Ritacco et al. (eds.), *Computer-Assisted Musculoskeletal Surgery: Thinking and Executing in 3D*, DOI 10.1007/978-3-319-12943-3_11

the functionality of the knee and increase its survival, an accurate positioning of the prosthesis components and a good soft tissue balance have always been considered the primary target to reach [1]. The correct rotational alignment of the femoral component is also critical because determines patellar groove position and flexion gap stability. An improper alignment can also induce anterior knee pain, arthrofibrosis and torsional stress on the tibial component that could lead to wear or loosening [2–6]. For all these reasons Computer-Assisted Surgery (CAS) was introduced in TKA surgery [7, 8]. In fact, via intra-operative anatomy-based tracking of the tibio-femoral joint (TFJ), CAS allows more precise bone cuts, more accurate prosthesis components implantation, more controlled soft tissue balance and targeted Mechanical Axis (MA) restoration.

To perform a well balanced TKA two surgical technique are possible. Some surgeons prefer to use the measured resection technique in which the bone landmarks, such as the transepicondylar or the posterior condylar axes, are used to determine the femoral component rotation, leaving the soft tissues balancing after trial component implantation. Others surgeons prefer instead the gap balancing technique in which the femoral component is positioned parallel to the resected proximal tibia with each collateral ligament equally tensioned [9].

In this chapter we will not analyze which of the two technique is better. The reader must know that which CAS is possible performing both of them using the same landmarks.

Here are the main surgical landmarks:

- Posterior condylar axis: The line connecting the posterior condyles, which was used as a reference for primary TKAs before 1986 (the same posterior osteotomy from both femoral condyles) [2, 10].
- Surgical transepicondylar axis: the line connecting the lateral epicondylar prominence and the sulcus of the medial epicondyle, were the deep fibers of the medial collateral ligament are attached [4]. It is perpendicular to the mechanical axis of the femur and perpendicular to the mechanical axis of the tibia when the knee is flexed to 90°. It was defined as a reference for the rotation of femoral component in TKA when other landmarks cannot be used [4], particularly in prosthetic revisions and in primary TKA with dysplasia of the distal femur [4]. Sometime it is difficult to identify accurately [2, 10].
- Clinical transepicondylar axis: the line connecting the lateral epicondylar prominence and the most prominent point of the medial epicondyle, were the superficial fibers of the medial collateral ligament are attached. It is difficult to identify the prominence of the medial epicondyle. This is externally rotated relative to the posterior condylar axis, about 3.5° (±2°) for varus or neutral knees, more externally rotated 4.4° (±1.8°) for valgus knees [5, 10].
- Posterior condylar angle: the angle between the posterior condylar axis and the surgical transepicondylar axis [4]. There is an internal rotation of the posterior condylar axis respect to the surgical transepicondylar axis. Berger et al. [4] demonstrated a mean of this angle of 3.5° (±1.2°) of internal rotation for males and a mean of 0.3 (±1.2°) for females [10].

– Anteroposterior axis (Arima axis or Whiteside line): a line through the deepest part of the patellar groove anteriorly and the center of the intercondylar notch posteriorly. Easily identified intraoperatively with the knee flexed. The best reference for the rotation of femoral component in valgus TKA to avoid patellar instability. After 1986 was used as a reference for rotational alignment of the femoral component for primary TKAs. The femoral surfaces were resected in a line perpendicular to the anteroposterior axis to establish rotational alignment of the femoral component. This line results approximately 4° (3–5°) externally rotated with respect to the posterior condylar axis [2]. The resection of the posterior condyles results in slightly more resection of the medial femoral condyle than the lateral condyle in the normal knees; resection of the medial condyle is much more than the lateral condyle in the valgus knees [2, 6, 10].

In TKA based on measured resection technique is recommended to place the femoral component parallel to the transepicondylar axis, perpendicular to the anteroposterior axis, or approximately 3–4° externally rotated relative to the posterior condylar axis.

In TKA based on gap balance technique is recommended to use an implant specific tensioners or two laminar spreaders placed below the posterior condiles to equally tension the collateral ligaments with the knee at 90 degrees of flexion. The AP femoral cutting block is then applied and, checking the navigation system, rotated until it is parallel with the resected proximal tibia.

Some authors [5] considered the anteroposterior axis difficult to define in arthritic knee, for trochlear wear and inter-condylar osteophytes, in case of severe trochlear dysplasia and in some varus knee. They considered the surgical transepicondylar axis, as good landmark for rotational alignment of the femoral component when the proximal tibia cut is performed at right angles to its mechanical axis [10].

Double checking the rotation by using the anteroposterior axis and the transepicondylar axis should ensure a correct rotation of the femoral component in most total knee replacements [5, 10].

Pre-operative Preparation

An accurate clinical examination of the deformity of the knee, and specific preoperative X-ray analysis are essential to perform an accurate surgical plan in navigated TKA.

The clinical examination of the deformity can take all the best solutions for the single patients; for this reason the deformity not only must be considered in the coronal plane but also in the sagittal and transversal plane. The evaluation of the deformity in the coronal plane is most important factor to consider in the pre-operative evaluation, in fact the amount of this deformity will affect the amount of surgical correction. Moreover the manual correction of the deformity has to be considered: in case of correctable deformity, probably with well aligned femoral and tibial bone

cuts alone could be possible to obtain a well aligned limb; on the other hand, when the deformity is fixed, some degree of soft tissue release could be considered. When a medio-lateral laxity as well as those related to the bone defect is present, a more constrained prosthetic implant could be considered [11]. Also the deformity on the sagittal plane must be considered during pre-operative planning. In severe flexion contracture, not related to bone anterior impingement, a more distal femoral cut than posterior could be considered associated to a reduction of the tibial posterior slope or an extension of the femoral component. All these procedures can correct this kind of deformity avoiding a gap unbalancing related to an eventually excessive resection of the proximal tibia. In case of genu recurvatum a reduction of the extension gap could correct this deformity, but a more constrained prosthesis design could be sometime considered. The deformity on the transversal plane are difficult to recognize, often are related to previous femoral or tibial fractures, and in this cases a pre-operative CT of the lower limb could be useful to plan their correction.

The X-ray evaluation is performed by means a weight bearing lower limb radiograph in antero-posterior (AP) projection, a particular of the knee in antero-posterior and latero-lateral (LL) projections, and a merchant view of the knee. Compared to the conventional technique, with navigation it is not necessary to measure the femoral valgus angle, because the distal femoral cut is directly planned on the femoral mechanical axis; but it is useful to measure the deformity of the knee measured on a lower limb AP radiograph. Moreover, if a natural inclination of the slope for the tibial cut is used, the inclination of the tibial plateau in the LL view has been measured to replicate it intra-operatively with navigation [10].

Technique with Pearls and Pitfalls

Navigation was introduced in TKA surgery in order to obtain better accuracy in component alignment. This better accuracy is obtained through some steps that have to be executed with a lot of accuracy. During learning curve it is necessary perform all the steps with endurance so that the results of this procedure are acceptable and the surgeon does not discouraged. The original scopes of surgical navigation, as described in the previous chapters, are:

- to plan intra-operatively the positioning of the components,
- to verify, during all the steps of surgery, the accuracy of all the resections performed, and verify in real-time if they match with our plan to assess the pre-operative and post-operative knee kinematics.

All actual surgical navigation systems are able to perform these phases during TKA, and it is possible to apply these systems both with “measured resection technique” and “gap balancing technique” [10]. Below these techniques are described using the Stryker Knee Navigation System, version 4.0 through the following steps:

1. Initial setting
2. Anatomical survey

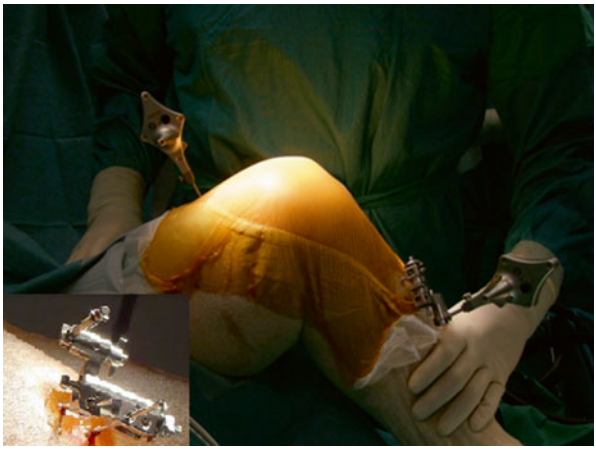

Fig. 11.1 Ortholock anchored to the femur and to the tibia with two bi-cortical pins

3. Intra-operative planning
4. Jigs navigation
5. Verification of resections
6. Soft tissue balancing
7. Final kinematics

Initial Setting

Before to start with surgery it is necessary to insert the patient data: age, sex, etiology and degrees of knee deformity, prosthesis model....

When a surgeon approaches the surgical navigation, he has to set up his personal surgical profile: if he prefers starting with resections of the femur or tibia, and how thick they should be; moreover he can define the posterior slope and which kinematics curves to record.

Before to start with surgical approach the supports for tibial and femoral trackers has to be fixed to the distal femur and to the proximal tibia. This specific device, called Ortholock, need to be anchored to the femur and to the tibia with two bi-cortical pins, and allows very good visualization by the camera without interfering to the surgical approach [10] (Fig. 11.1).

Anatomical Survey

This is one of the basic step of navigation, specially in the systems imageless based; in fact all the surgical femoral and tibial references have defined by digitizing some anatomical landmarks. The accuracy of these references is strictly related to the accuracy of our landmarks digitization. Moreover it is very important to know how the

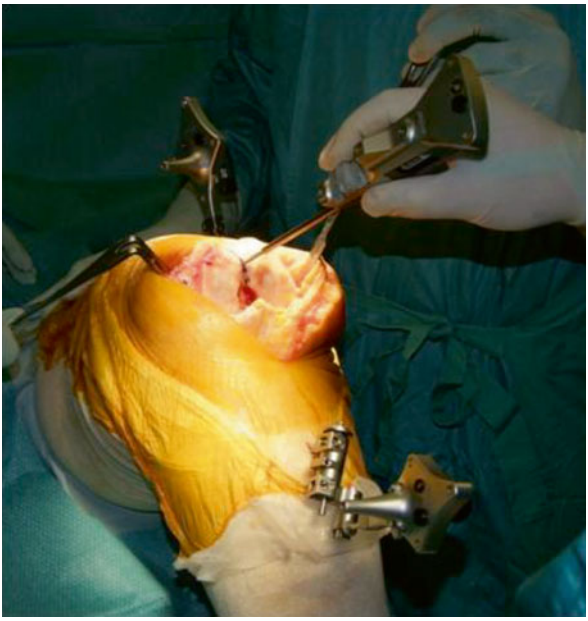

Fig. 11.2 The femur center is digitized with the pointer's tip at the center of the trochlear sulcus anterior, above the intercondylar notch

reference axis and plane has been defined by the software [10]. Below the femoral and tibial references has shown about the Stryker Knee Navigation System, Version 4.0.

Femur Anatomical Survey

By digitizing femoral landmarks the following axes and references are defined:

- Mechanical femur axis
- Femoral rotation axis
- Reference for resection level in the distal and posterior femur
- Reference for anterior notching
- Reference for automatic sizing, implant positioning, and for medio-lateral overhang

The mechanical femur axis is defined by the line from the hip center and the knee center. The hip center is calculated through a slow and smooth circumduction of the hip avoiding pelvic motion, while the femur center is directly digitized with the tip's pointer at the center of the trochlear sulcus anterior just above the intercondylar notch (Fig. 11.2). The mechanical femur axis so defined is the reference for varus/valgus and flexion/extension alignment.

The femoral rotation is defined as the average rotation axis calculated by the digitized transepicondylar axis (medial and lateral epicondyle), and Femoral AP axis. The medial and lateral epicondyles are directly digitized with the tip's pointer respectively at the sulcus of the medial epicondyle and onto the most prominent point of the lateral epicondyle. The femoral AP axis is calculated by aligning the

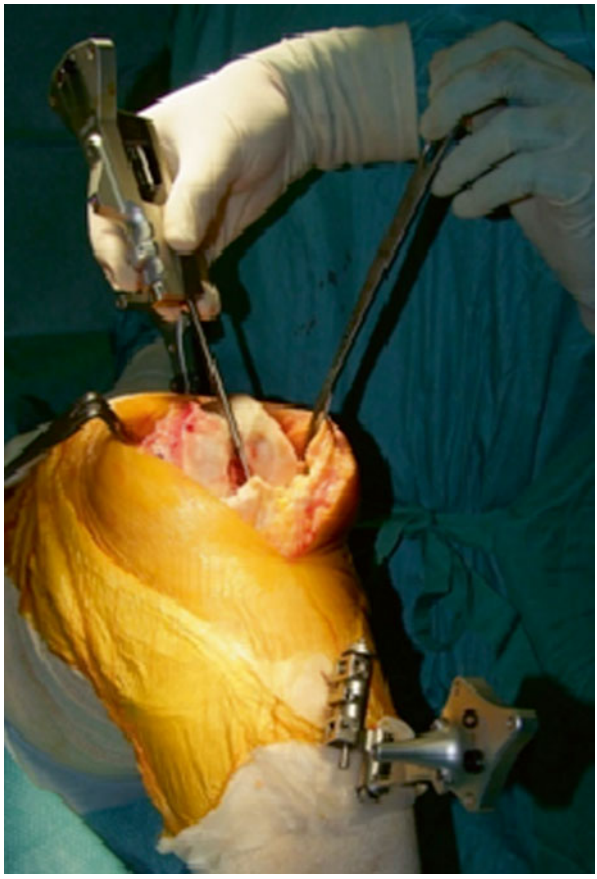

Fig. 11.3 The femoral AP axis is calculated by aligning the pointer's axis with the most posterior point of the trochlea and the most anterior point of the intercondylar notch

pointer's axis with the most posterior point of the trochlea and the most anterior point of the intercondylar notch, also referred to as Whiteside's line [2, 6] (Fig. 11.3).

The reference for the distal femur resection level is the most prominent distal point of the digitized condyle. It is important, that the most distal aspect of the condyle has been included in the points cloud digitized in order to avoid wrong resection thickness. The same procedure is performed to calculate the reference for the posterior resection level.

The reference for the anterior notching is defined during point acquisition of the anterior aspect of the distal femur. The points cloud of this digitization has include the portion of the anterior aspect below the expected saw blade exit points, to avoid wrong calibration of the level of anterior notching.

The reference for automatic sizing and femoral implant positioning, as in conventional technique, are the anterior cortical bone and the posterior femoral condyles. The purpose of the calculations is to achieve the best anterior match while keeping the implant size as small as possible. Moreover with the required digitization of the medial and lateral overhang femoral regions the software will provide, in numerical value, the average medial/lateral overhang or uncovered bone cut [10].

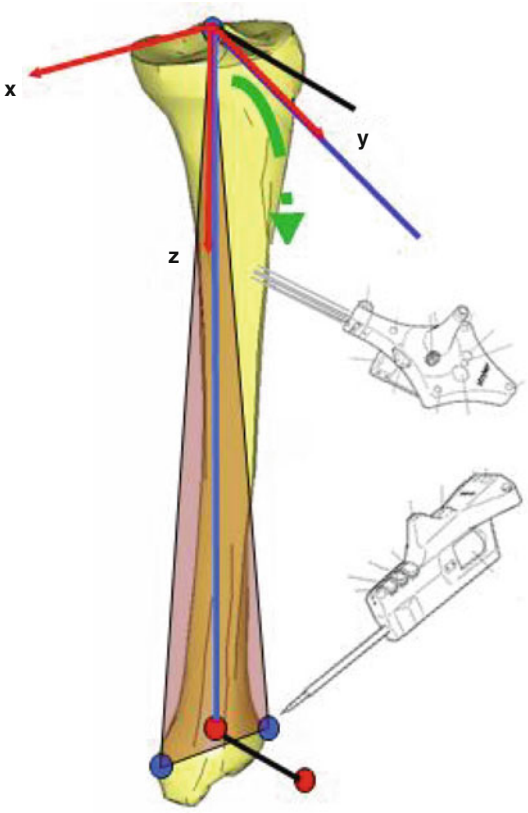

Fig. 11.4 The mechanical tibia axis is the reference for varus/valgus and flexion/extension alignment

Tibial Anatomical Survey

By digitizing tibial landmarks the following axes and references are defined:

- Mechanical tibia axis
- Tibial rotation axis
- Reference for resection level in the proximal tibia

The mechanical tibia axis is defined by the line from the tibia center and the calculated ankle center. The tibia center is directly digitized with the tip's pointer onto the middle of the interspinous sulcus anteriorly near the anterior mid footprint of the ACL attachment, while the ankle center is calculated by dividing the digitized transmalleolar axis according to the ratio of 56 % lateral to 44 % medial. The transmalleolar axis is the line between the most prominent point of the medial and lateral malleolus directly digitized with the tip's pointer. The mechanical tibia axis so defined is the reference for varus/valgus and flexion/extension alignment (Fig. 11.4).

The tibial rotation axis is calculated by aligning the pointer's axis with the midpoint of the posterior cruciate ligament (PCL) and the medial third of the tibial tuberosity. This axis is the reference for rotational alignment of the tibial component.

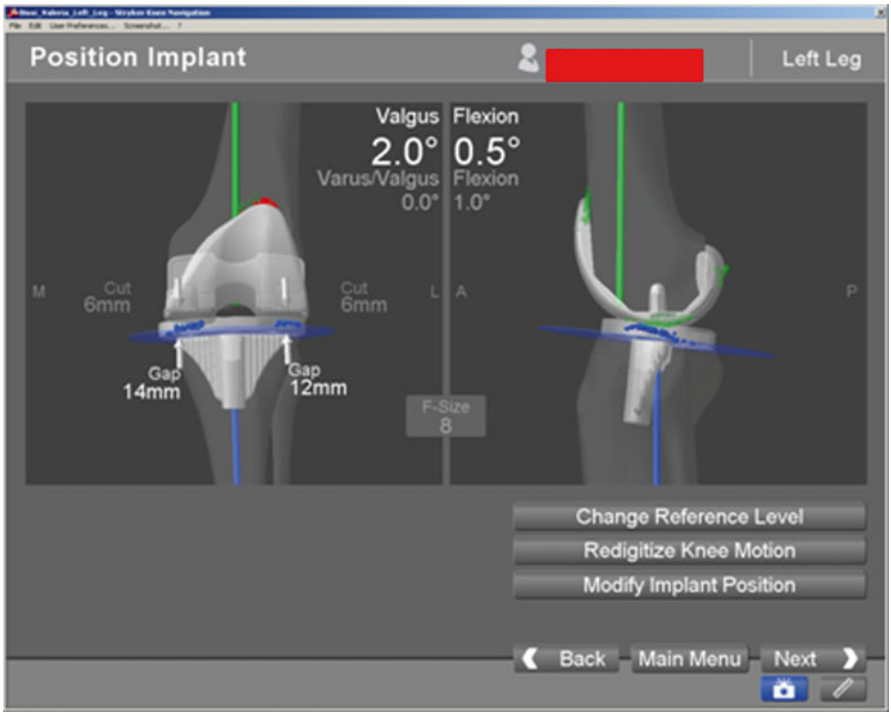

Fig. 11.5 The valgus and flexion can be changed during navigation

The reference for the proximal tibial resection level is the most recessed point of the digitized compartment. It is important, that the lowest aspect of the compartment has been included in the points cloud digitized, and that the pointer does not to digitize below the lowest anatomical point, in order to avoid wrong resection thickness [10].

Intra-operative Planning

After completion of patient registration, the software will calculate the size and position for the best fitting implant and place it on the virtual femur. Varus/valgus and rotational alignment are set to 0° respectively to the calculated mechanical axis, and to the average rotation axis calculated by the digitized transepicondylar axis (medial and lateral epicondyle), and femoral AP axis. The distal and posterior condyles are reconstructed in accordance to the principles of measured resection technique. If the gap balance technique is preferred, is possible changing the plan of the rotation of the femoral component after the distal femur resection and proximal tibia resection are performed. Once the intra-operative planning is displayed on the screen, the surgeon can decide whether to accept or modify it, changing femoral size or position. As described in Figs. 11.5 and 11.6, it is possible to change the

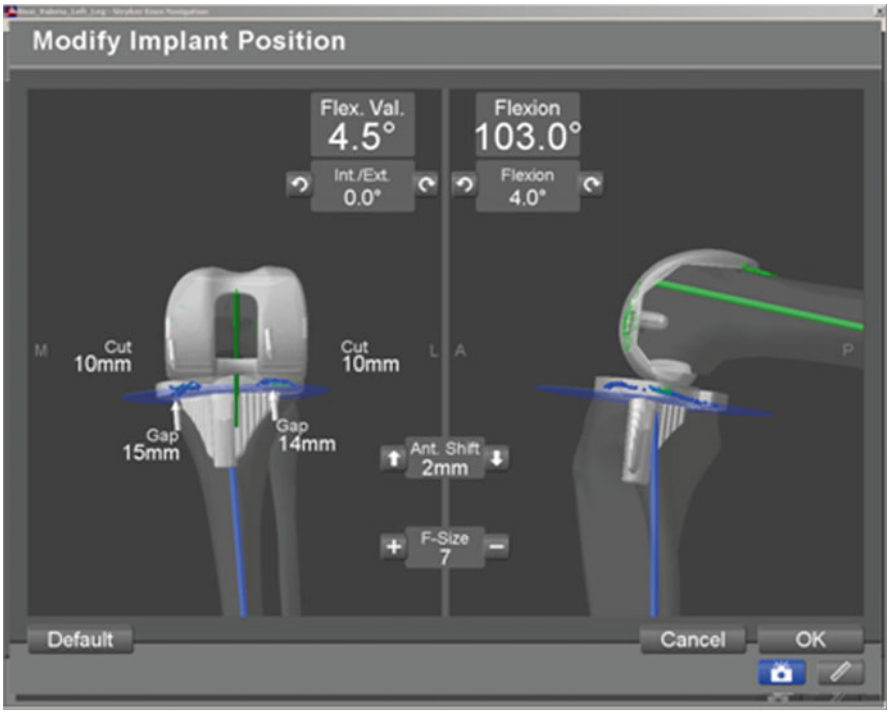

Fig. 11.6 The shift in craniocaudal or anteroposterior direction and the femoral size may be changed during navigation

orientation of the femoral component, to shift it in craniocaudal or anteroposterior direction, and to change the femoral size. Whenever a change in the position or in the size of the femoral component is performed, it is possible to verify the result of this change respect to the gap balancing, if it is caused an anterior notching, or if there is a medio-lateral overhang of the component respect to the bone.

During this phase to keep in mind the pre-operative deformity is crucial, because the surgeon can adjust the intra-operative planning to correct the deformity; for example, in a severe flexion deformity a greater distal femoral cut with reduction of femoral flexion can be planned respect to a standard posterior cut. At the end of this phase the "Planned Femoral Implant" dialog appears on the screen, summarizing size, alignment and position of the calculated femoral implant [10].

Jigs Navigation

When the intra-operative planning has been ended, the surgeon starts with cutting jigs navigation following his preferred technique. In this case the "free-hand technique" will be shown because it could provide a fast and accurate positioning of the

cutting guides after a little bit of practice. This technique provides the manual orientation of the jig controlled directly on the monitor by the first operator, while an assistant fixes the jig with drilling pins (Fig. 11.7).

Usually the distal femoral resection is performed at 0° respect to the femoral mechanical axis, with 0–5° of flexion, in order to avoid anterior notching of the femoral cortex, and with 8 mm of resection depth from the most distal femoral condyle, to restore the thickness of the distal part of the femoral component; in this case a Scorpio NRG implant (8 mm of thickness) has been used. In some particular cases the amount of the distal femoral resection can be modified: when a patella baha is present, it is recommended to reduce the amount of this resection, and to increase the proximal tibial resection; while in a flexed knee it is recommended to increase this resection respect to the femoral posterior cut and to reduce the femoral flexion.

The femoral rotation, and the AP positioning of the 4-in-1 cutting block is performed by the "navigated drill templates for AP alignment" (Fig. 11.8). The navigated drill templates can replace the conventional AP sizer. By this dedicated jig it is possible to check the position of the femoral component as previously planned matching the position of the yellow line (jig orientation) to the green (planning orientation) lines. If a gap balance technique is preferred, is possible performing the tibial cut first, and then, with the medial and lateral collateral ligaments in tension, align the posterior femoral cut to the proximal tibial cut. Before fixing the jig the system confirms the presence or not of anterior notching. In this case it is possible to translate anteriorly the guide, checking the posterior resection that could be too large.

The proximal tibial resection is performed at 0° respect to the tibial mechanical axis, with 0–10° of posterior slope trying to restore the natural slope of the tibial plateau as measured on the LL knee radiograph, and with about 10 mm of resection depth from the most normal tibial condyle (Fig. 11.9).

The tibial rotation can be navigated following the orientation calculated during the anatomical tibial survey, but it is also possible to align the tibia by using the trial components, and leaving the tibial component to self align respect to the femoral trial [10].

Verification of Resections

The real advantage of navigation is the possibility to check in real-time every single step during surgery, and so to have the possibility to change the orientation of all osteotomies. Sometime, as demonstrated by Bäthis et al. [3] can be differences from the guide orientation and the correlate bone cut, and this difference is very difficult to see with only a visual inspection. With navigation this checking is provided through numerical data and not only by the experience of the surgeon [10].

The verification of osteotomies orientation during navigation is performed with a dedicated "resection plane probe". Once all these bone cuts will be recorded gap monitoring will be possible with apposite distractor or more easily with trial component (Fig. 11.10).

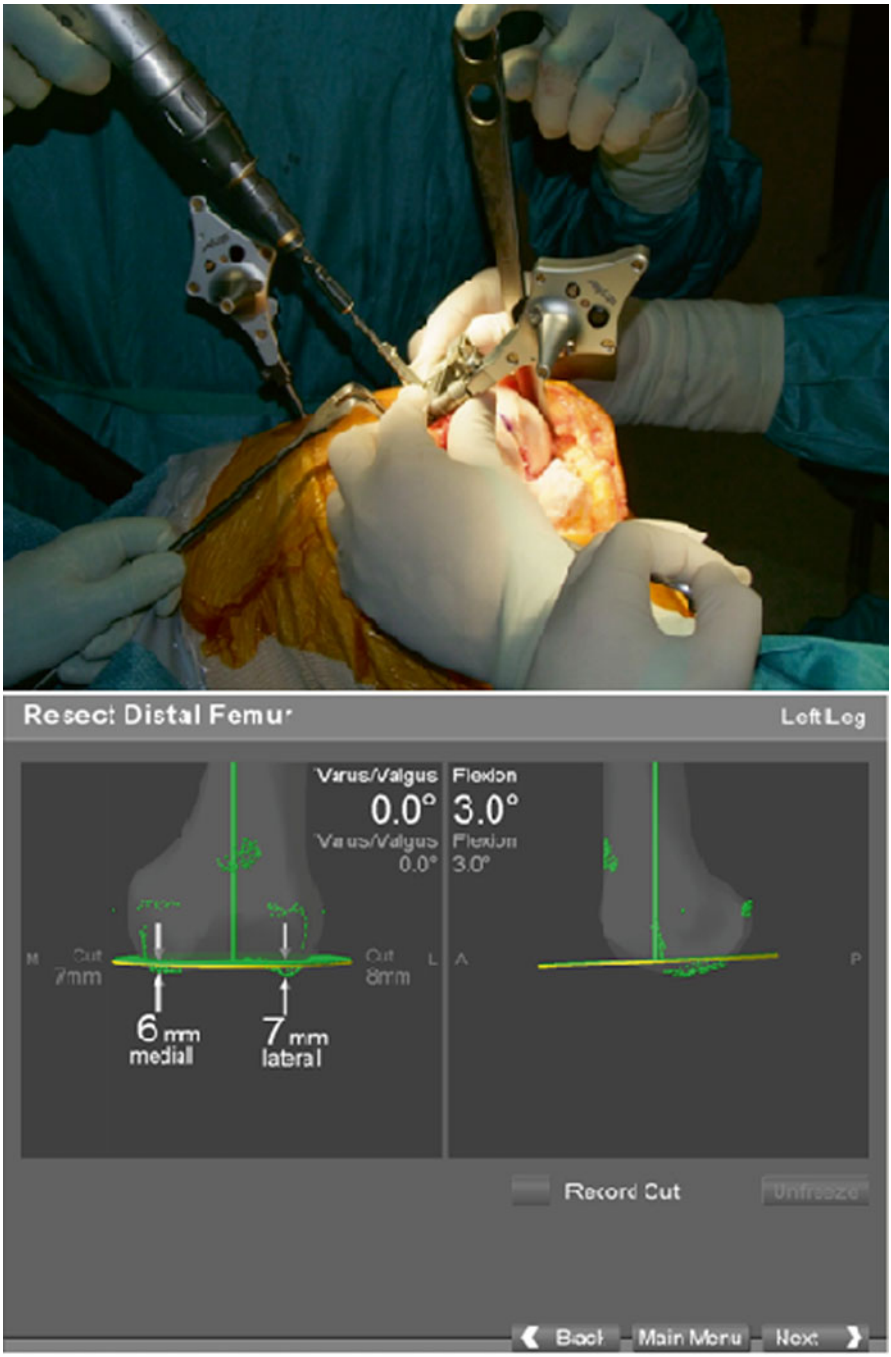

Fig. 11.7 The orientation of the jig is controlled directly on the monitor by the first operator, while an assistant fixes the jig with drilling pins

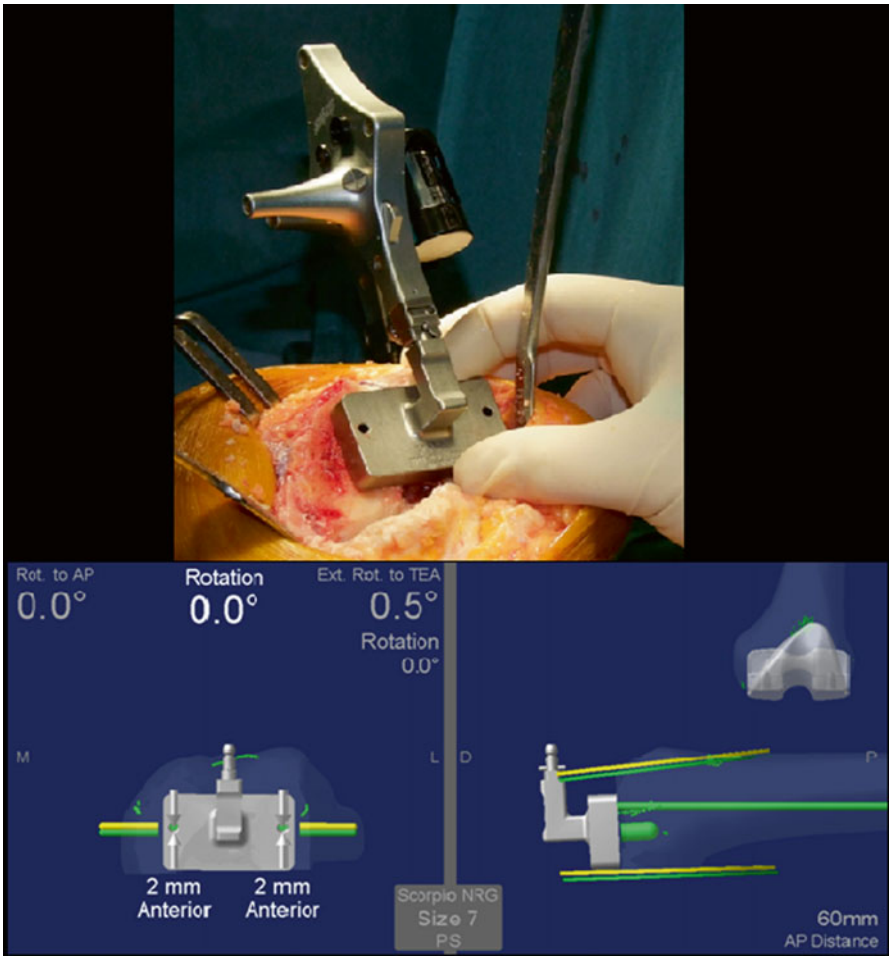

Fig. 11.8 The femoral rotation and the AP positioning of the 4-in-1 cutting block is performed using the navigated drill templates for AP alignment

Soft Tissue Balancing

The soft tissue balancing, usually is performed in two steps.

The first step is performed after the landmark calibration and pre-operative knee kinematics. In this phase all the osteophytes are removed from the femur and the tibia in order to check if the knee deformity is fixed or correctable. In the first case the deformity is not related only to the bone defect but also to medial or lateral soft tissue contracture, and therefore some amount of soft tissue release is performed. With navigation, it is possible to perform a calibrated medial or lateral soft tissue release avoiding excessive laxity of the collateral ligaments (Fig. 11.11). When the complete correction of the deformity is obtained the intra-operative planning is performed.

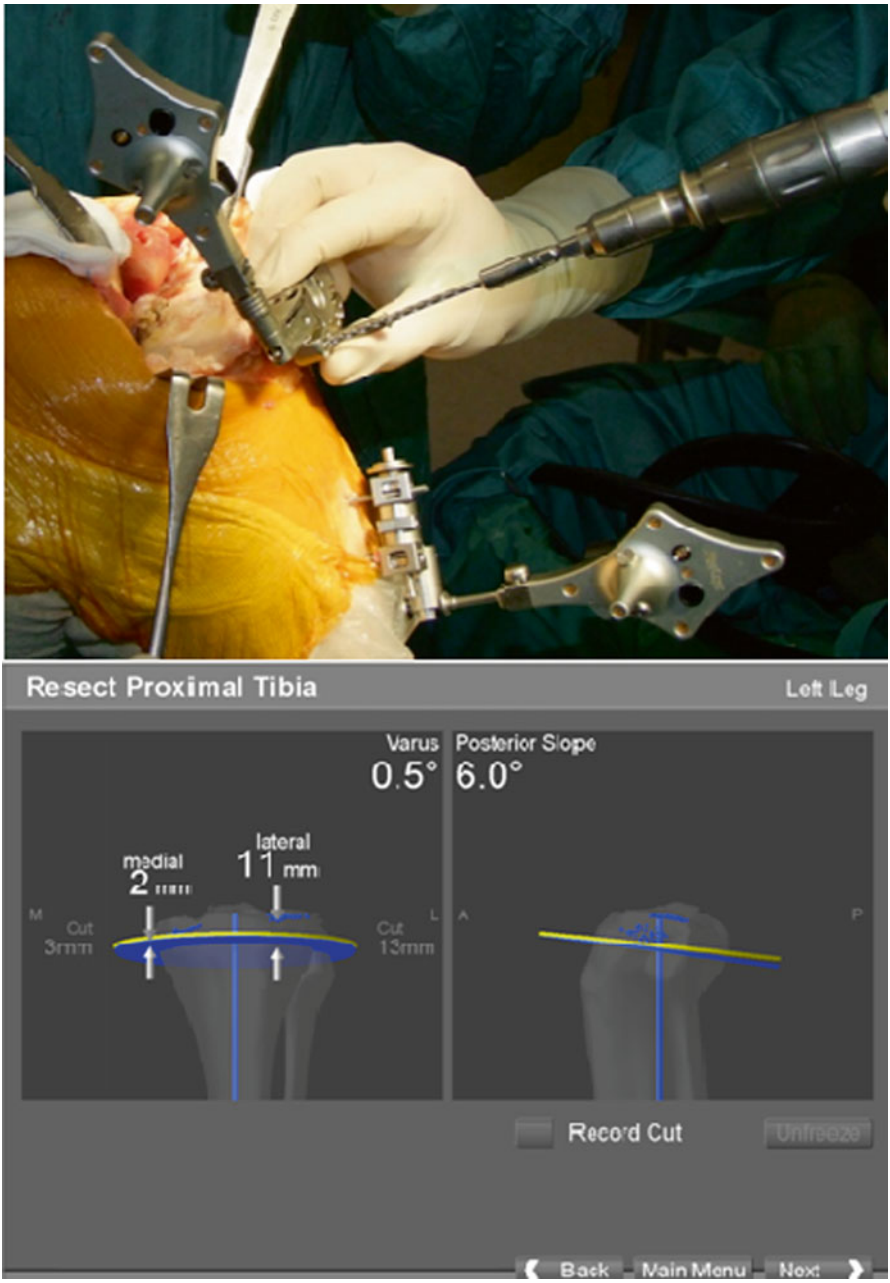

Fig. 11.9 The proximal tibial resection is performed at 0° respect to the tibial mechanical axis, with 0–10° of posterior slope to restore the natural slope of the tibial plateau with 10 mm of resection depth from the normal tibial condyle

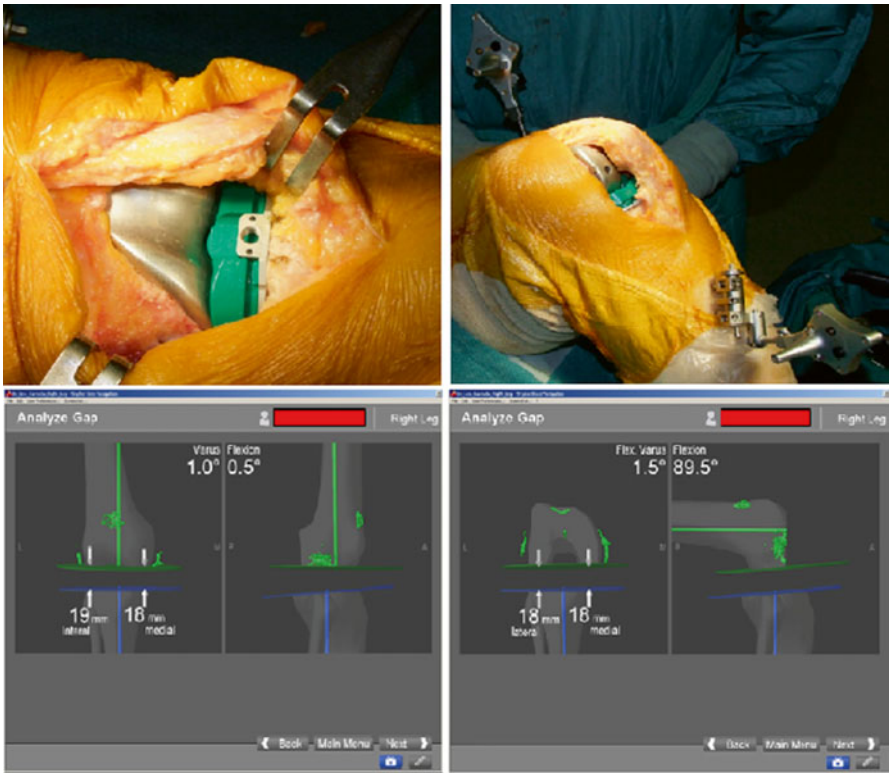

Fig. 11.10 Verification of resections using the resection plane probe

The second step of soft tissue release is performed with trial components. Usually when the release has been performed in a right way, as above showed, and the planning has been observed, this second phase is not necessary in the gap balance technique. In the measured resection technique, if some of deformity remains after trial component positioning, some soft tissue release is possible following the navigator [10].

Final Kinematics

When all the definitive components has been cemented, the final knee kinematics is recorded (Fig. 11.12). It is possible to record the final alignment in extension, the knee kinematics during flexion and the collateral ligaments tension during flexion, and to compare the final results with the pre-operative. It is possible to perform some further soft tissue release, because sometime the alignment of the definitive components could be different respect the trial components [12]. At the

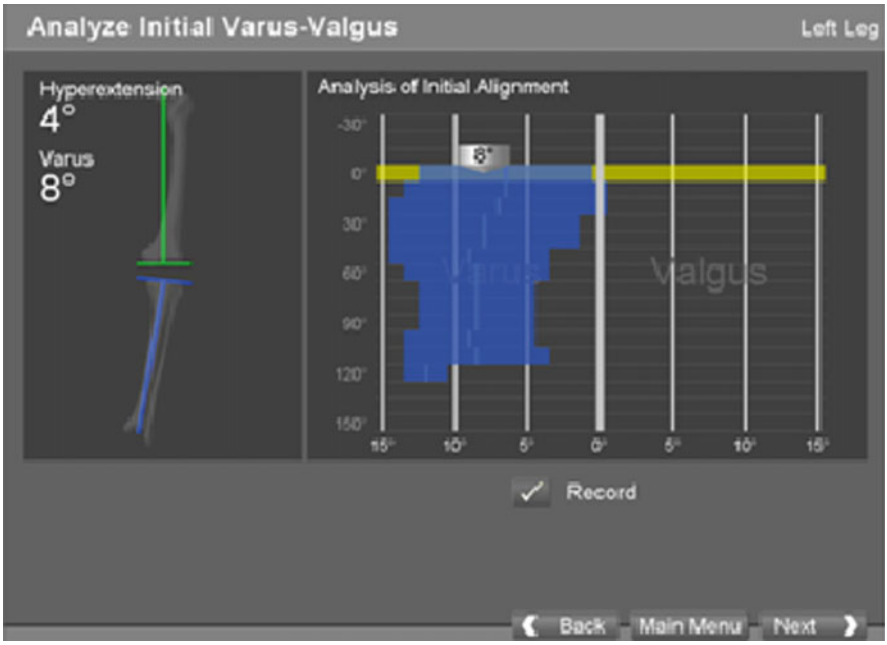

Fig. 11.11 Calibrated medial - lateral soft tissue release

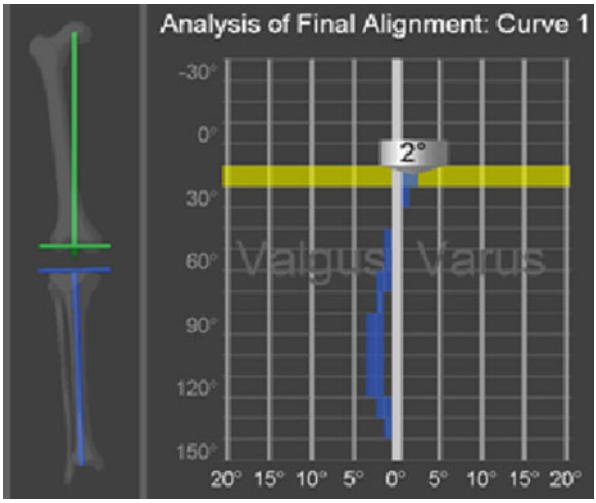

Fig. 11.12 Recording of final kinematics

end all the data related to the pre-operative deformity, to the planning, to the bone cuts orientation, and to the final kinematics are recorded in the final report. The report of these data is useful both for clinical research, or as a document in medical-legal issues [10].

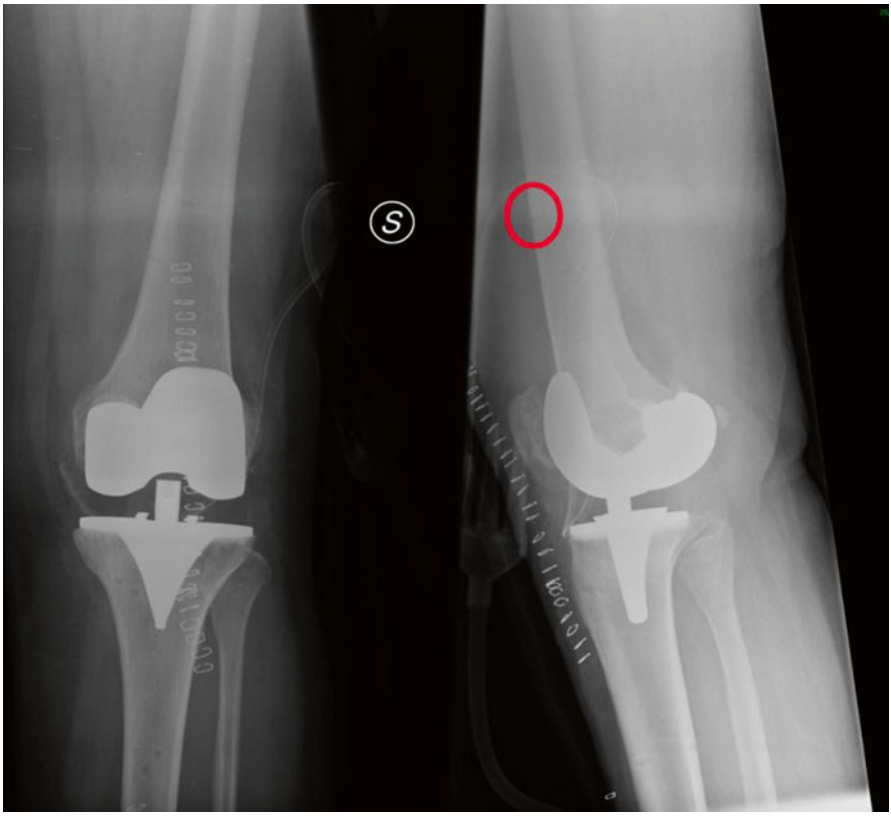

Fig. 11.13 Weakening due to pins drilled into the femur

Complications

Nowadays it has been largely proven in literature that Total Knee Arthroplasty performed with Computer-Assisted Surgery leads to better implant positioning and to neutral mechanical axis in a higher percentage of cases if compared to the Conventional Technique [12, 13]. On the other hand the surgical navigation is not free from complications. The most important complication reported in literature is the longer surgical time (about 17 min) needed [14], which is supposed to be associated with more blood loss and consequently higher transfusion rate, and to higher risk of infection due to longer exposure. But these complications are not supported by the literature [15]. Conteduca and Kalairajah even reported a lower transfusion rate in the navigated group [16, 17]. Other complications are instead related to the specific navigation system used: in fact the tracker's pins drilled into the femur or into the tibia creates an area of weakening of the bone that could lead to fracture. In our experience only once we observed this complication (Figs. 11.13, 11.14 and 11.15). We hypothesize that this complication occur especially if the pins are drilled

Fig. 11.14 Frontal view of fracture as a complication of drilling the pins into the femur

near the posterior or the anterior cortex, and could be avoided if the pins are drilled in the middle of the shaft.

Results

Nowadays it has been largely proven in literature that Total Knee Arthroplasty (TKA) performed with Computer-Assisted Surgery (CAS) leads to better implant positioning and to neutral mechanical axis in a higher percentage of cases if compared to the Conventional Technique (CI) [12, 13]. It is expected that this improved accuracy will lead to better clinical results and reduced revision rates [18]. Despite that, only few studies have compared CAS versus CI technique in terms of clinical outcomes and revision rate at mid-term [18–21] or at long-term follow-up [14].

For all these reasons, in 2002 we began a prospective, randomized, controlled study which compared 60 TKA operated using CAS and 60 TKA using the CI technique. The results of that study showed a better component alignment using navigation,

Fig. 11.15 Sagittal view of fracture as a complication of drilling the pins into the femur

but similar clinical outcomes if compared to the CI at 2 years follow-up [22]. Ten years later all those patients available at follow-up were clinically (using KOOS and KSS scores) and radiographically assessed, showing no statistically significant differences. Furthermore, the two groups were analyzed in terms of revision rate, and despite 5 revisions were observed in CI group and only 2 revisions in CAS groups, still no differences were shown using the Kaplan Meier survivorship.

Our results are consistent with the majority of literature, in fact Lützner et al. [18], Tolk et al. [19] and Blakeney et al. [21] showed in their works no clinical differences between CAS or CI at mid-term follow-up. Kim et al. [14] analyzed 520 TKA operated using CAS technique and 520 TKA using CI technique at 10 years follow-up, and didn't notice any difference between the two groups. Only very few studies reported clinical differences between the two techniques, in favor to CAS, like the work of Hoffart et al. [23].

Conclusions

Concluding, the benefits of a more accurate positioning of the components using the navigation remains a matter of debate.

We think that the advantages the navigation could bring nowadays are not completely understood or exploited. And the superimposability of the results between the Conventional Technique and the Navigation at long term follow-up is probably due to the incorrect goal we are looking for. In fact in the past we assumed that a neutral MA is associated to better biomechanics and longer survivorship. But all these studies were in-vitro or based on mathematic models. Probably more accurate biomechanical studies of the knee are necessary to better understand how the kinematics of the knee in vivo works, because maybe a final mechanical axis of 0° is not the best solution for every patient.

References

1. Ritter MA, Faris PM, Keating EM, Meding JB. Postoperative alignment of total knee replacement. Its effect on survival. Clin Orthop Relat Res. 1994;299:153–6.
2. Arima J, Whiteside LA, McCarthy DS, et al. Femoral rotational alignment, based on the anteroposterior axis, in total knee arthroplasty in a valgus knee. J Bone Joint Surg Am. 1995;77(9):1331–4.
3. Bäthis H, Perlick L, Tingart M, et al. Intraoperative cutting errors in total knee arthroplasty. Arch Orthop Trauma Surg. 2005;125(1):16–20.
4. Berger RA, Rubash HE, Seel MJ, et al. Determining the rotational alignment of the femoral component in total knee arthroplasty using the epicondylar axis. Clin Orthop Relat Res. 1993;286:40–7.
5. Poilvache PL, Insall JN, Scuderi GR, et al. Rotational landmarks and sizing of the distal femur in total knee arthroplasty. Clin Orthop Relat Res. 1996;331:35–46.
6. Whiteside LA, Arima J. The anteroposterior axis for femoral rotational alignment in valgus total knee arthroplasty. Clin Orthop Relat Res. 1995;321:168–72.
7. Bäthis H, Perlick L, Tingart M, Lüring C, Grifka J. CT-free computer-assisted total knee arthroplasty versus the conventional technique: radiographic results of 100 cases. Orthopedics. 2004;27(5):476–80.
8. Decking R, Markmann Y, Fuchs J, Puhl W, Scharf HP. Leg axis after computer-navigated total knee arthroplasty: a prospective randomized trial comparing computer-navigated and manual implantation. J Arthroplasty. 2005;20(3):282–8.
9. Daines BK, Dennis DA. Gap balancing vs. measured resection technique in total knee arthroplasty. Clin Orthop Surg. 2014;6(1):1–8.
10. Catani F, Zaffagnini S. Knee surgery using computer assisted surgery and robotics. Berlin: Springer; 2013. p. 27–42.
11. Meding JB, Keating EM, Ritter MA, Faris PM, Berend ME. Genu recurvatum in total knee replacement. Clin Orthop Relat Res. 2003;416:64–7.
12. Matziolis G, Krocker D, Weiss U, Tohtz S, Perka C. A prospective, randomized study of computer-assisted and conventional total knee arthroplasty. Three-dimensional evaluation of implant alignment and rotation. J Bone Joint Surg Am. 2007;89(2):236–43.
13. Thienpont E, Fennema P, Price A. Can technology improve alignment during knee arthroplasty. Knee. 2013;20 Suppl 1:S21–8.
14. Kim YH, Park JW, Kim JS. Computer-navigated versus conventional total knee arthroplasty a prospective randomized trial. J Bone Joint Surg Am. 2012;94(22):2017–24.
15. Mohanlal PK, Sandiford N, Skinner JA, Samsani S. Comparision of blood loss between computer assisted and conventional total knee arthroplasty. Indian J Orthop. 2013;47(1):63–6.

16. Conteduca F, Massai R, Iorio R, Sansotto E, Luzon D, Ferretti A. Blood loss in computer-assisted mobile bearing total knee arthroplasty. A comparison of computer-assisted surgery with a conventional technique. Int Orthop. 2009;33:1609–13.
17. Kalairajah Y, Simpson D, Cossey AJ, Verrall GM, Spriggins AJ. Blood loss after total knee replacement: effects of computer-assisted surgery. J Bone Joint Surg Br. 2005;87:1480–2.
18. Lützner J, Dexel J, Kirschner S. No difference between computer-assisted and conventional total knee arthroplasty: five-year results of a prospective randomised study. Knee Surg Sports Traumatol Arthrosc. 2013;21(10):2241–7.
19. Tolk JJ, Koot HW, Janssen RP. Computer navigated versus conventional total knee arthroplasty. J Knee Surg. 2012;25(4):347–52.
20. Hoppe S, Mainzer JD, Frauchiger L, Ballmer PM, Hess R, Zumstein MA. More accurate component alignment in navigated total knee arthroplasty has no clinical benefit at 5-year follow-up. Acta Orthop. 2012;83(6):629–33.
21. Blakeney WG, Khan RJ, Palmer JL. Functional outcomes following total knee arthroplasty: a randomised trial comparing computer-assisted surgery with conventional techniques. Knee. 2014;21(2):364–8.
22. Ensini A, Catani F, Leardini A, Romagnoli M, Giannini S. Alignments and clinical results in conventional and navigated total knee arthroplasty. Clin Orthop Relat Res. 2007;457:156–62.
23. Hoffart HE, Langenstein E, Vasak N. A prospective study comparing the functional outcome of computer-assisted and conventional total knee replacement. J Bone Joint Surg Br. 2012; 94(2):194–9.

Chapter 12
Local Tumor Ablation Using Computer-Assisted Planning and Execution

Jasper G. Gerbers, E.D. Dierselhuis, and P.C. Jutte

Abstract Image-guided tumor ablation was developed as a surgical technique to provide a minimally invasive alternative to open procedures. Over the years multiple methods have been developed to destruct the tumor tissue. Modern techniques include the use of heating and cooling systems (thermoablation), such as radiofrequency ablation (RFA), microwave ablation (MWA) and cryoablation. Local ablation has quickly become the preferred method of treatment of benign bone tumors as osteoid osteoma and a valuable tool in the treatment of painful metastases.

The next step, application to larger or more aggressive tumors, relies highly on accurate planning and execution of the procedure. Now with advances in imaging, computer assisted planning and instrument guidance, local ablation of tumor tissue can have a larger role in the orthopedic oncologic field. Planning can be done in 3D using estimated ablation shapes. Software simulation heat flow and calculation optimal needle placement are in development but are currently unproven. Use of computer assistance during the procedure can decrease ionizing radiation exposure and be used to accurately position ablation devices.

Keywords Radio-frequency Ablation • Computer Assisted Surgery • CAS ablation

J.G. Gerbers (✉) • E.D. Dierselhuis • P.C. Jutte
Department of Orthopedics, University Medical Center Groningen, Groningen, The Netherlands
e-mail: j.g.gerbers@umcg.nl

L.E. Ritacco et al. (eds.), *Computer-Assisted Musculoskeletal Surgery: Thinking and Executing in 3D*, DOI 10.1007/978-3-319-12943-3_12

Introduction

Image-guided tumor ablation was developed as a surgical technique to provide a minimally invasive alternative to open procedures. As the anatomical boundaries are not disturbed, this type of treatment can be classified as local, or in-situ, ablation. Over the years multiple methods have been developed to destruct the tumor tissue. Historical examples are mechanical destruction through the use of large bore needles and injections of chemicals such as ethanol through hollow needles. Modern alternatives are the use of heating and cooling systems (thermoablation), such as radiofrequency ablation (RFA), microwave ablation (MWA) and cryoablation. Thermoablation relies on the principle of cell death through thermo extremes (local temperature less than −40 °C or more than 60 °C). Local ablation has quickly become the preferred method of treatment of benign bone tumors as osteoid osteoma and a valuable tool in the treatment of painful metastases.

The next step, application to larger or more aggressive tumors, relies highly on accurate planning and execution of the procedure. Now with advances in imaging, computer assisted planning and instrument guidance, local ablation of tumor tissue can have a larger role in the orthopedic oncologic field. Planning can be done in 3D using estimated ablation shapes. Software simulation heat flow and calculation optimal needle placement are in development but are currently unproven. Use of computer assistance during the procedure can decrease ionizing radiation exposure and be used to accurately position ablation devices.

Radiofrequency Ablation

The mechanism of action is the generation of an alternating electromagnetic (EM) field, putting molecules into motion. Friction of these molecules (resistance) leads to heat production, transferred to neighboring cells by conductivity. With temperatures above 46° coagulation necrosis occurs with higher temperatures shortening required treatment time. At 60 °C almost instantaneous cell death occurs. Temperatures above 105 °C can leads to boiling, vaporization and char formation. This can lead to a less extensive ablation as tissue heat conductivity is lost and should thus be avoided. Early treatment used monopolar electrodes with limited reach. Development of cooled electrodes, pulsed RF, umbrella or multiprobe techniques increased the effective ablation area.

Monitoring the process can be either done by measuring tissue impedance or temperature, depending on the system used. Some devices have internally cooled tips to prevent overheating, thereby withholding scar formation due to needle backheating and providing a more efficient ablation. Others have used umbrella type

needles to efficiently distribute heat, although its efficacy in bone has not yet been adequately demonstrated.

Microwave Ablation

MWA is a more recently developed minimal invasive technique, used for treatment of solid organ tumors and bone tumors as well. As in RFA, heat is produced to cause tissue necrosis, although working mechanisms are different. In MWA, a probe is used to create an EM field of typically 900–2500 MHz. This leads to resonance of mostly water (H_2O) molecules, kinetic energy rises, leading to an increase in temperature of tissue. Penetration of microwaves is less dependent of tissue characteristics compared to radiofrequency. Therefore, it is expected that it is more efficient and has the potential to generate a larger ablation zone. It requires the presence of water molecules however, so the efficacy in bone is being discussed.

Cryoablation

Extreme cold can also lead to cell death, hence cryoablation. Sub-zero temperatures have a twofold effect: first, ice formation leads directly to intracellular mechanical destruction and dehydration due to increased extracellular osmolality. Second, endothelial damage leads to a decrease in blood flow, making cells more susceptible to necrosis.

Although cryotherapy was merely used as adjuvants to open surgery, more recently a closed loop system has been developed to treat painful bone metastases with cooling probes. Gas within the distal tip of the probe expands rapidly, leading to a prompt temperature drop. Due to this phenomenon – known as the Joule-Thompson effect – temperatures as low as −100 °C are reached within seconds. Since ice formation can be well observed by CT-scanning, it is believed that monitoring is more reliable compared to RFA and MWA. Therefore, especially lesions close to vulnerable structures might be indicated to be treated by cryoprobe ablation.

Indications

Indications currently include small benign tumors as osteoid osteoma, larger benign tumors, for example chondroblastoma and osteoblastoma, atypical cartilaginous tumors (primary or recurrence) and pain palliation in metastases.

Preoperative Preparation

While the technique of ablation can differ, the preoperative preparations are mainly the same. After acquisition of the 3D datasets the tumor is segmented. This process gives a volumetric value to the tumor volume and measurements of its basic shape. After that potential heat- or cold-sinks and critical structures are identified. Arteries and veins close to the ablation site can cause heat or cold loss in the surround tissue, carrying away the energy. Other sinks can be fluid pockets, for example synovial, that have different thermoconduction and heat capacity than the surrounding tissue. The spinal chord, peripheral nerves and cartilage are vulnerable to heat damage. Multiple studies indicate that potentially irreversible damage already occurs in these tissues above 45 °C at short heating times [1–3]. As the ablation zone, depending on technique is often not symmetrical, needle angulations can used to avoid heating of critical structures. As an extra safety step, temperature monitoring probes can be placed in the proximity of critical structures. Larger vessels are however protected by the heat sink effect.

Based on the specifications of the technique of ablation and chosen instrument, as the kill range and ablation shape, a planning can be constructed. In our experience this is mostly done manually using planning software. The goal is to obtain, within the constraints of safe approaches, a complete ablation with the least amount of probes required.

Experimental research mainly in the field of liver ablations has given rise to optimization algorithms for probe placement, a possible future improvement over manual planning. First was the development of modelers and solvers based on the geometric shape of the ablation zone [4, 5]. While some models build in deformation of the zones due to proximity of heat sinks these models do not simulate heating and cannot easily incorporate different power delivery protocols, differences in thermal diffusion over tissues and actual heat loss by perfusion and vessels. Computational models have been developed but are still computationally expensive and still lack proper experimental validation. Full planning of heat flow and optimal needle placement currently remains difficult.

Most of this research has also been performed for other tissues than bone. Consequently there are only some studies available that tried to model heat flow in bone. This is important as bone has a low conductivity and poor thermal conduction compared to lung, kidney or liver tissue [6]. RFA is more affected by this then MWA and it means that liver RFA heat models cannot be directly used in bone ablation modelling. An advantage is that there are less heat sinks and that they are more aligned in bone tissue [7]. Furthermore histological analysis of liver vessels shows that vessels under 3 mm diameter show luminal thrombosis (blocking of the vessel and thus cessation of blood flow) and vascular wall necrosis [8].

Rachbauer et al. demonstrated the lower thermal conduction in cortical bone, an exposed tip of 3 cm ablated a sphere of 1 cm in cortical bone and 3 cm in cancellous bone [9]. DePuy et al. showed that this insulating effect enables the safe use of RFA near the spinal canal [10]. Bitsch et al. recommend a 10 mm safe margin from the periost to nerve structures if the probe is placed close to the bone surface [11]. The largest experimental study, by Greenberg et al., looked at the temperature gradient

in cortical and cancellous bone in ablation of small tumors [7]. It found higher ablation temperatures in cancellous bone than cortical bone; furthermore it demonstrated that temperature achieved depends on the lesion size. Finally it gives two basic formulas for calculating heat flow in the osteoid osteoma model. All but the study of DePuy et al. did not stimulate normal perfusion physiology in the experiment [10]. More research into modelling of heat flow in bone is required. Until then estimations of ablation extend are used.

Thermal ablation requires regional anesthesia or general anesthesia for the larger ablations. Smaller RFA procedures can sometimes be performed under local anesthesia with or without moderate sedation.

Technique (with Perils and Pitfalls)

The treatment of small lesions as osteoid osteoma is generally done using CT-guided positioning. CT-guidance is not a real time positioning technique. The radiologist or orthopedic surgeon places the probe and makes an image run. The 2D slices are then interpreted by the user and based on this 2D-3D translation and anatomical orientation, the position of the probe is adjusted.

For the treatment of larger lesions which require precise probe centration or multiple probes are more accurate means of orientation is required. With the development of image fusion and instrument tracking this is possible. The first multimodal computer assisted navigation systems for interventional procedures were described in the literature in the beginning of the late 90s. These were dedicated or adapted stereotactical systems. Soft tissue matching and tracking is difficult as the needle displaces tissue, potentially breaking the match. As bone is a rigid body this is less of a problem. The procedure can be performed with standard orthopedic imagebased navigation systems if they support cone-beam CT image acquisition and matching. A basic workflow is displayed in Fig. 12.1.

Workflow:

1. Fiducials or patient trackers are placed for patient tracking. In the OR this can be done under fluoroscopic guidance, placing two rigid pins in an anatomically safe location. Generally navigation accuracy using trackers is better than with fiducials.
2. System set-up, the registration and check of instruments and patient tracker
3. An acquisition scan is performed
4. Fusion with the planning data/the planning is created.
5. Real-time guidance of the instruments using navigated drilling-guides or drills

With the expanding use of local ablation in metastasis surgery it can be used as a step in an open procedure for example for stabilization of highly vascularize metastatic lesions. In this case a normal image based setup procedure can be performed using standard landmark and surface matching.

Post-operative control scans after local ablation can best be performed using MRI. MRI T1 and T2 sequences without contrast clearly show the halo, the ablated

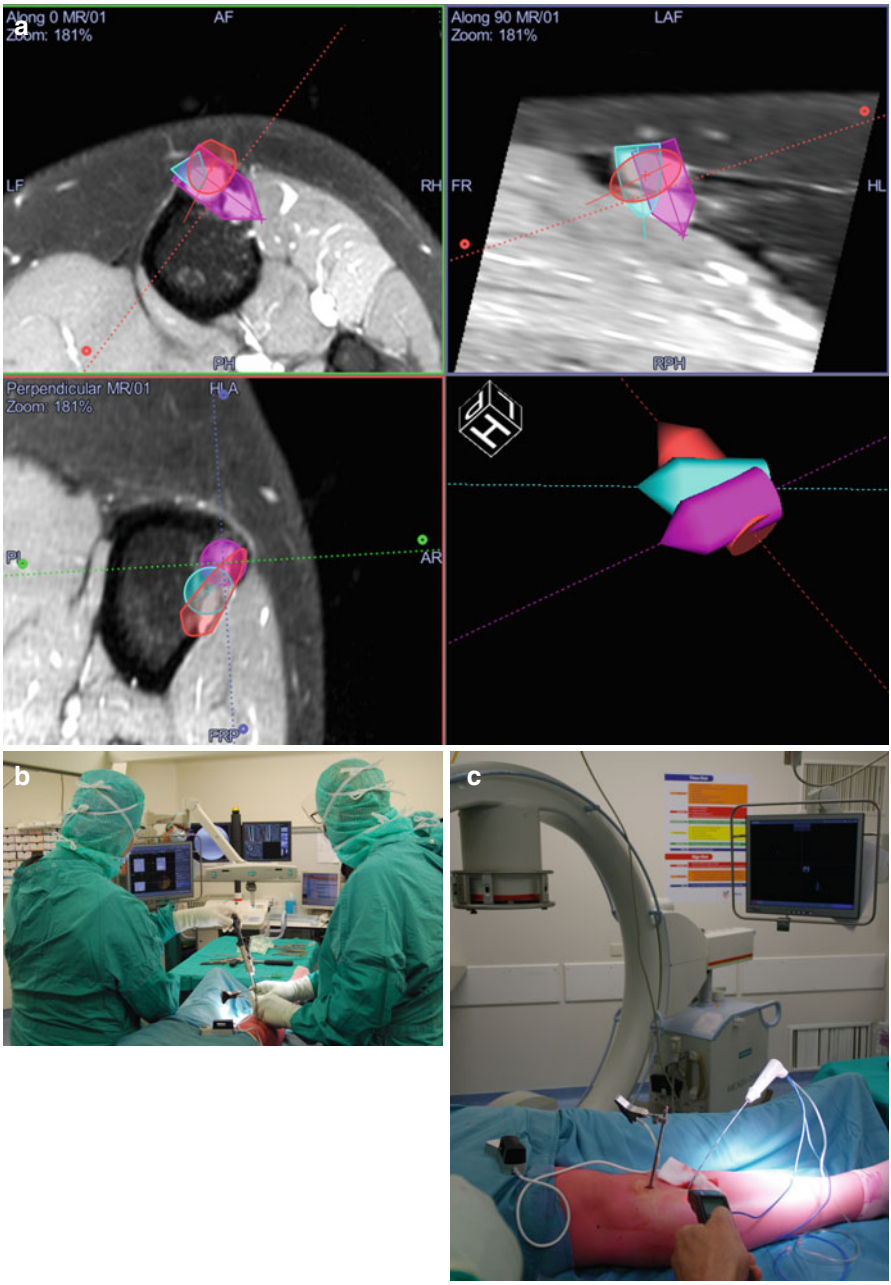

Fig. 12.1 (**a**) Demonstration of pre-operative planning on MRI of needle placement for a tumor on the anterior side of the tibia using conservative (*cortical bone*) treatment ranges. Three probe placements were needed for this tumor. (**b**) Per-operative workflow. The CAS screen on the left is in target mode for one of the probe locations. The surgeons are locating this planned position using the pointer tool. The iso-c screen in the back shows the intra-operative CT-scan that was used for CAS matching and MRI/CT fusion. (**c**) The probe in situ during a run. The patient tracker is visible proximally of the probe. The iso-c arm (*left*) and CAS (*right*) are in the back. Temperature of the skin, cooled using wet gauzes is monitored using an infrared thermometer

Fig. 12.2 Post-operative MRI slice (T1-TSE) of an ablated atypical cartilaginous tumor clearly shows a halo sign around the lesion

area where dead tissue resides. Figure 12.2 demonstrates the halo on a post-operative MRI scan after RFA ablation.

While navigation provides orientational guidance of the probe, the radiologist or the surgeon still has to accurately place the needle. With the development of robotic systems both orientation and execution can be performed by the computer. The first studies comparing robotic to standard CT-guided needle placement in soft tissue find a quicker needle placement time, good accuracy and slightly lower mean ionizing radiation use [12–14]. However, most papers describe robots that work with real-time CT navigation or a feedback loop of imaging and adjusting, this because of the limitations of soft tissue navigation. Decreasing procedural radiation exposure is hard using this workflow. Currently, as far as we know, no papers have been published on robotic guided needle placements in bone.

MRI guidance requires specialized non-magnetic equipment and is still expensive. Furthermore due to interference RFA treatment and image acquisition cannot be performed at the same time. MR thermometry sequences are available and can be an interesting method of intra-procedural monitoring, especially combined with robotics, but currently MRI guidance is not a routine method of guidance in orthopedic surgery. In our experience, MRI directly after CT-guided ablation does not reliably show ablation extent.

Current perils and pitfalls of the computer assisted local ablation technique:

- Requirement of CT based navigation means radiation exposure
- Currently no means of modelling the local ablation in preplanning outside basic geometric matching
- Navigated local ablation requires a high initial investment both in time and money
- Currently no easy means of monitoring ablation progression and local temperature
- MRI guidance currently expensive and not compatible with most RFA systems

Complications

RFA has proven to be a safe technique, although some complications have been reported. Mostly, they are due to heat effects in surrounding tissues, such as burning of the skin or cellulitis. However, if load bearing areas are ablated, there is an increased risk of spontaneous fracturing. The technique is contraindicated in patients with pacemakers and potentially other digital implants. By nature, MWA has the potential to lead to complications comparable to those caused by RFA, although they are not described in orthopedic literature, probably because of lack of reports on MWA. Even if cryoablation as adjuvant to intralesional surgery increases the risk of postoperative fracturing, this is not observed when modern cryoprobes are used in the palliative setting for bone metastases.

Results

Local ablation has quickly become the preferred method of treatment in osteoid osteoma. While outcome studies show a lower first procedure success rate, this is acceptable because of the much lower invasiveness associated with percutaneous treatment. In a pilot study of 20 patients the use of RFA has demonstrated the potential to completely eradicate cartilaginous tumour cells [15]. The authors describe that the positioning needs to be improved to increase treatment effectiveness. RFA has further been applied with success to chondroblastoma, osteoblastoma and other benign and intermediate grade tumors.

There are currently no studies on positioning accuracy and precision in orthopedic patients comparing CT-guidance to computer assisted probe placement. However multiple reports have been published on the successful use of computer navigation in RFA procedures [16–18]. Imagebased computer navigation has already been proven in providing highly accurate instrument positioning.

With the increased use of CT navigation for the positioning of probes, radiation exposure can be a potential problem. In a study comparing radiation dose for RFA procedures in 66 cases Cheng et al. found a reduction of mean radiation dose using intra-operative cone beam CT both with and without navigation compared to radiology suite-based CT [17]. Treatment was equally effective over the three treatment arms.

Conclusion

Local thermal ablation is a technique that is already successfully deployed in the orthopedic oncologic field. In its current role RFA shows that minimally invasive procedures can be effective and safe for benign and intermediate grade tumors. Two issues remain for a larger therapeutic role. One is the accurate positioning of the probe and the other is monitoring. With computer assistance local ablation becomes possible on larger lesions that require multiple ablation sites and high positional trueness. Furthermore it can help reduce ionizing radiation exposure.

Recommended Reading

- **Radiofrequency tumor ablation: principles and techniques**.
  Goldberg SN. Radiofrequency tumor ablation: principles and techniques. Eur J Ultrasound. 2001;13(2):129–47.
- **Step by step instructions and video in a RFA procedure for an osteoid osteoma**
  Cheng EY, Naranje SM. Radiofrequency ablation of osteoid osteoma with use of intraoperative three-dimensional imaging and surgical navigation. JBJS Essent Surg Tech. 2014;4(4):e22.

References

1. Good CR, Shindle MK, Griffith MH, Wanich T, Warren RF. Effect of radiofrequency energy on glenohumeral fluid temperature during shoulder arthroscopy. J Bone Joint Surg Am. 2009;91(2):429–34.
2. Letcher FS, Goldring S. The effect of radiofrequency current and heat on peripheral nerve action potential in the cat. J Neurosurg. 1968;29(1):42–7.
3. Yamane T, Tateishi A, Cho S, Manabe S, Yamanashi M, Dezawa A, et al. The effects of hyperthermia on the spinal cord. Spine. 1992;17(11):1386–91.
4. Dodd III GD, Frank MS, Aribandi M, Chopra S, Chintapalli KN. Radiofrequency thermal ablation: computer analysis of the size of the thermal injury created by overlapping ablations. Am J Roentgenol. 2001;177(4):777–82.
5. Butz T, Warfield SK, Tuncali K, Silverman SG, Van Sonnenberg E et al. Pre- and intraoperative planning and simulation of percutaneous tumor ablation. Medical Image Computing and Computer-Assisted Intervention–MICCAI 2000;1935;317–326.
6. Brace CL. Radiofrequency and microwave ablation of the liver, lung, kidney, and bone: what are the differences? Curr Probl Diagn Radiol. 2009;38(3):135–43.
7. Greenberg A, Berenstein Weyel T, Sosna J, Applbaum J, Peyser A. The distribution of heat in bone during radiofrequency ablation of an ex vivo bovine model of osteoid osteoma. Bone Joint J. 2014;96-B(5):677–83.
8. Lu DS, Raman SS, Vodopich DJ, Wang M, Sayre J, Lassman C. Effect of vessel size on creation of hepatic radiofrequency lesions in pigs: assessment of the “heat sink” effect. Am J Roentgenol. 2002;178(1):47–51.
9. Rachbauer F, Mangat J, Bodner G, Eichberger P, Krismer M. Heat distribution and heat transport in bone during radiofrequency catheter ablation. Arch Orthop Trauma Surg. 2003;123(2–3):86–90.
10. Dupuy DE, Hong R, Oliver B, Goldberg SN. Radiofrequency ablation of spinal tumors: temperature distribution in the spinal canal. Am J Roentgenol. 2000;175(5):1263–6.

11. Bitsch RG, Rupp R, Bernd L, Ludwig K. Osteoid osteoma in an ex vivo animal model: temperature changes in surrounding soft tissue during CT-guided radiofrequency ablation 1. Radiology. 2006;238(1):107–12.
12. Abdullah BJJ, Yeong CH, Goh KL, Yoong BK, Ho GF, Yim CCW, et al. Robot-assisted radiofrequency ablation of primary and secondary liver tumours: early experience. Eur Radiol. 2014;24(1):79–85.
13. Cornelis F, Takaki H, Laskhmanan M, Durack J, Erinjeri J, Getrajdman G, et al. Comparison of CT fluoroscopy-guided manual and CT-guided robotic positioning system for in vivo Needle Placements in Swine Liver. Cardiovasc Intervent Radiol. 2014; [Epub ahead of print].
14. Koethe Y, Xu S, Velusamy G, Wood BJ, Venkatesan AM. Accuracy and efficacy of percutaneous biopsy and ablation using robotic assistance under computed tomography guidance: a phantom study. Eur Radiol. 2014;24(3):723–30.
15. Dierselhuis EF, van den Eerden PJ, Hoekstra HJ, Bulstra SK, Suurmeijer AJ, Jutte PC. Radiofrequency ablation in the treatment of cartilaginous lesions in the long bones: results of a pilot study. Bone Joint J. 2014;96-B(11):1540–5.
16. Okada K, Myoui A, Hashimoto N, Takenaka S, Moritomo H, Murase T, et al. Radiofrequency ablation for treatment for osteoid osteoma of the scapula using a new three-dimensional fluoroscopic navigation system. Eur J Orthop Surg Traumatol. 2014;24(2):231–5.
17. Cheng EY, Naranje SM, Ritenour ER. Radiation dosimetry of intraoperative cone-beam compared with conventional CT for radiofrequency ablation of osteoid osteoma. J Bone Joint Surg Am. 2014;96(9):735–42.
18. Cheng EY, Naranje SM. Radiofrequency ablation of osteoid osteoma with use of intraoperative three-dimensional imaging and surgical navigation. JBJS Essent Surg Tech. 2014;4(4):e22.

Part III
Custom Implants

Chapter 13
Patient-Specific Instruments in Orthopedics

Paul Laurent

Abstract Patient-Specific Instruments have revolutionized the way of approaching an orthopedic intervention. They progressively invaded the operative rooms from the 2010s to assist the surgeons during total knee arthroplasties. Nevertheless, they have been invented much earlier in the middle of 1990s for rare applications. Their manufacturing has evolved deeply. From subtracting milling at its beginning, instruments are now manufactured by material addition. This chapter reminds the history of patient-specific instruments, the manufacturing evolution, and their slow acceptation by the medical field. Instruments for knee arthroplasty will be described, as well as the report on the controversy about their claimed accuracy and usefulness. Finally, innovative applications will be exposed showing the high potential Patient-Specific Instruments can bring.

Keywords Patient-Specific Instruments • History • Current applications • 3D printing technology

Introduction

Personalized medicine is today a reality. Patient-specific drug treatments based on genetics analysis are now available permitting significant improvements in treatment efficacy. The arrival of computers in medicine has opened new possibilities producing a tremendous step forward in radiology and, as a direct consequence, in surgery. Orthopedics was a pioneer in the field benefiting from the higher resolution images and the ease to extract bone contours from a standard computed tomography acquisition. Computerized assistances were then developed to perform preoperative planning, bringing the possibility of analyzing pathologies in three-dimensions. The understanding of the bone shape or its deformation has permitted to anticipate bone cuttings to restore a normal anatomy.

P. Laurent, PhD, Ir
3-D-Side, Fond des més, 4, Louvain-La-Neuve 1348, Belgium
e-mail: Laurent.Paul@3dside.eu; lp@3dside.eu

L.E. Ritacco et al. (eds.), *Computer-Assisted Musculoskeletal Surgery: Thinking and Executing in 3D*, DOI 10.1007/978-3-319-12943-3_13

The transfer toward the operative room has also benefitted from computers. Robots and navigations systems have been put on the market to reliably reproduce the planning, making surgery safer and more accurate. In the recent years, new intra-operative assistances have arose with a strong trend toward simplification.

This chapter will introduce the concept of Patient-Specific Instruments (PSI) and the recent advances in their surgical applications. Firstly, the history of PSI will be detailed, from their invention in Aachen, to these days. Secondly, we will approach knee arthroplasty which is today the main use of PSI. Finally, recent and innovative applications will be presented to understand the potential they bring in the operative room.

PSI History

The general belief is that PSI have been created only few years ago by implant manufacturers to provide cutting jigs for knee arthroplasty. Personalization of orthopedic surgical treatments arose much earlier in the middle of the 90s. This belief is certainly due to their slow acceptation that made them a minor evolution. Indeed, at this period, robotics and optical navigation systems were considered the future of computer assistances for orthopedic surgeries. The claimed accuracy was highly promising, new sensors were appearing and several clinical applications were investigated. The community of scientists and surgeons was very enthusiastic in developing these new intelligent systems. Some improvements were still required to widely spread the technology. The main concern was related to the intra-operative time dedicated to the assistances. The computation power and display devices available at this moment were sufficient to achieve their objectives, but not as efficiently as desired. Other minor concerns were the size of the machines in the operative room, the important additional costs and the relative low ergonomics of the systems which required complex interactions with computerized systems. The technology was highly dependent of the expected increase in computation power and miniaturization.

Based on these considerations, a team of researchers (Radermacher, Rau, Staudte, et al.) at Helmholtz Institute for Biomedical Engineering (Aachen University, Germany) has developed an alternative to fully computerized systems. They proposed a “relatively simple, low cost solution that facilitates exact safe and fast implementation of planned surgery on bone structures, eliminates the need for continual radiographic monitoring and avoids overburdening surgery with complex equipment and time consuming procedures” [29]. By molding the shape of the target bone structure into a generic template, they have created “Individual Templates”, that are today known as Patient-Specific Instruments. The bone-specific surface provided a mean to find the physical correspondence between a pre-operative 3D bone model and the actual bone structure in the operative room. The spatial correspondence was physically embedded into the template during the manufacturing stage instead of creating it in the operating room. The positioning was straightforward and did not require a matching of bony structures nor time-consuming computations. They have

described the whole process from image processing to the sterilization for the first time in 1994 in a conference paper [31]. Cervical spine decompression and triple pelvic osteotomies were the first proposed clinical applications, followed by pedicle screw placement and total knee arthroplasty few years later [29].

The manufacturing process of the individual templates was fast and quite easy. First, a Computerized Tomography (CT) was used to extract the shape of bone structures and create a 3D reconstruction. Then, a pre-operative planning was performed to virtually execute the surgery using a dedicated software installed on a DISOS workstation [28]. The instruments were manufactured by subtractive manufacturing using a desktop milling machine. Milling technique was preferred to additive manufacturing because the latter was much expensive at the moment (3000 euros for a bone model) [24]. The instrument was sterilized by standard autoclave at 135 °C. According to the authors, less than 1 h was needed from the data transmission to the use of PSI in the operative room. This delay seems optimistic since the sterilization process itself lasts more than 1 h (30 min for automatic washing, 1 h for manual wrapping and steam sterilization).

In the operative room, the PSI were combined with additional hardware to achieve specific tasks. They were equipped with interfaces to adapt a handle that allows an easy manipulation. Some drill guides or conventional osteotomy guides could be inserted and bone pins could be used to rigidly fix the PSI on the bony structure. They also acted as an interface between the bone and the usual standard template.

The PSI have been widely tested by the Aachen team to assess their accuracy and impact on time during the surgery. The early reported results on accuracy of PSI applied on bone replicas were encouraging. Positioning measurements have shown an angulation error below 0.6° in the spine and the tibia and 1° in the femur [30]. Converting angles into distance, the error was found below 1 mm on tibia and spine, while a maximum of 1.6 mm error was found for a femoral head drilling. Cadaveric experiments have been led and showed clinically acceptable results in spine [35] with a few number of errors above 2 mm when compared to the conventional method. It should be noted that a software failure has caused important errors. It emphasizes that computer assistances are subject to software computations and can lead to severe errors.

In matter of time, studies have shown a shorter duration of the surgery in two different applications. A cadaveric experimentation has demonstrated that PSI decreased the time to find the entry point of the drilling in a vertebra pedicle [35]. For triple pelvic osteotomies on actual patients, the whole surgery time has been decreased by 23 % to gain 35 min [36]. This improvement is easily understandable by the “plug and play” characteristic of the instrument. The user places the instrument in the correct position and connects standard devices to achieve the desired task. The decrease of intra-operative irradiation thanks to a lesser use of fluoroscopy is also an added-value of the technology. It has been shown that it is significantly decreased when using PSI [4]. The clinical impact has also been reported, but conclusions are less clear because of rare clinical cases that makes the production of comparative data difficult.

Surprisingly, although all their positive aspects, PSIs have disappeared quite rapidly. The main reason is that PSI technology seemed to be very demanding, with the need for having a specific workstation with specific software, a skilled technician and the milling machine. This kind of machine was mainly dedicated to the industry and was rarely user friendly to be used by a newbie. The conceivers claimed that a surgeon can use the system within few minutes to create a patient specific instrument. Some stages still required the presence of a technician to be present to perform the pre-operative planning, design the instrument and set up the machine.

In the meantime, navigation systems have become the standard option for computerized assistances in many applications (knee, hip and shoulder arthroplasties, spine instrumentation, ilio-sacral screw placement). Navigation being intensively pushed by the implant manufacturers, strong innovations such as bone morphing has been developed, contributing to its promotion. It has appeared to be more flexible and stand alone with the ability to plan the surgery on the machine that will be used during the surgery. Early clinical results were enforcing these considerations with an excellent accuracy for several joint arthroplasties.

PSI for TKA

During several years, navigation systems, provided by specific manufacturers (praxim, brainlab, Amplitude, Medtronic, stryker,…) was used to perform knee, hip and shoulder arthroplasties. These companies provided surgeons with virtual 3D models of the implants to adapt the pre-operative planning to the intended implant. With the success of navigation systems, implant manufacturers have developed their own solutions. Progressively, implant manufacturers have put on the market navigation systems to place their own implants. The announced accuracy of these systems made it a gold standard spreading the technology around the world.

However, controversy has arose progressively on the actual added value for the patient. Some clinical papers were discussing on the supposed benefits relative to the involved costs in terms of investment and consumables. Furthermore, the global accuracy of such system had reached a plateau at approximately 1 mm. This incompressible residual error found its source in the camera resolution and in the matching process. Other drawback of the method was the time to create the link between the patient and its preoperative images. The acquisition process of points was time consuming and could even fail leading to long wasted minutes to set-up the system. Finally, as described by the Aachen Team, the size of the machine and screen interactions could be painful for the user and the team.

Based on these considerations, in the middle of the 2000s, PSI for total knee arthroplasty have been reworked. Advances in the additive manufacturing technology have brought an alternative to milling manufacturing. This emerging technology, also called rapid prototyping and more widely known as 3D printing, was continuously improved. Its resolution and accuracy were by far sufficient to be used in a surgical context as well as new biocompatible and sterilizable materials were

developed. The technology being more popular, its cost decreased largely making it an affordable solution.

In 2006, the first paper about the technique and the feasibility was published [17]. The authors reported the principle of the required planning and their first use of "patient-specific templating" on cadavers and plastic bones. They also reported a short cost-efficacy study. The feasibility of surgery using PSI has been assessed on 45 plastic and cadaver knees. The different components of this technique (planning, material, 3D machine) have been found suitable to carry out the required tasks. Their findings about accuracy were encouraging since a low error was shown. The maximum error was 2.3° for rotations and 1.1 mm for translations. There are some limitations on these accuracy measurements since they are partially reported (no sagittal alignment for the femur, translations are not well described) and also were not systematic (only 6 postoperative CTscan, randomly selected). The intra-operative time has been decreased when compared to the conventional method, but significance was not mentioned. The cost analysis has concluded that the PSI were not as costly as standard templates. However, in their analysis, the authors have taken into account the manufacturing cost of the standard instruments, a cost that is supported by the implant manufacturer. Furthermore, the sterilization costs of conventional instrumentation seem overestimated while the production costs for PSI were astonishingly low (200$) and the cost for the specific software was not mentioned. Despite these limitations, this first experimental paper has definitely raised a new field for knee arthroplasties.

The concept was relatively simple. CT or MRI data were transferred to the company by using a secured server on sending a CD-ROM. The preoperative planning consisted in determining the optimal positioning of the implant with respect to the bony specificity. The planning started with landmarks acquisition by an operator who was responsible for finding the correct anatomical point that will construct a local reference coordinate system. Once the referential determined, the implant size and position were chosen, defining de facto the cutting trajectories. The result was sent back to the surgeon who was usually provided with an interface (web, file, in 2D or false 3D) to verify the conformance of the planned surgery with the patient's needs. Some distance and angle measurements were also provided. The surgeon had the possibility to accept or reject the pre-operative planning. In case rejection, the planning was adapted by the operator. Once approved, the 3D planning was validated, standard templates were individualized with patient's bone surfaces embedding flat surfaces or slots to perform cuttings, alternatively drilling guides to position a standard ancillary. The instruments were manufactured by Selective Laser Sintering as follow. A laser draws a 2D shape on top of a polyamide powder container. The polyamide is instantaneously melted under the action of high energy provided by the laser. A hardened 2D shape is then obtained. A thin layer of powder is then sprayed on top of the container, over the 2D shape. The laser draws a new 2D shape that melts the free powder to the previous layer. The process is repeated layer by layer until the 3D model is completed. After intensive free powder cleaning, the instruments were packed, labelled and sent to the surgeon's institution to be sterilized by standard steam autoclave before entering into the intra-operating room.

Two different approaches have been implemented for the preoperative planning: CT- or MRI-based. CTscan is usually preferred because of its availability in most institutions and a presumed higher resolution for bony landmarks. The main drawback of CTscan is the radiation exposure that may cause radio-inducted cancers. On the other hand, MRI represents a safer modality providing an excellent image of cartilage that may be used as contact surface for the PSI. In terms of costs, the CTscan compares favorably to the MRI. Accuracy of both philosophies have been investigated by several authors [33, 39, 42] yielding to diverging conclusions.

White et al. have extracted bone structures from MRI and CTscan and manufactured replicas using Selective Laser Sintering. They have compared measures taken from the replicas and the actual bone. Obtained data are highly surprising with deviation up to 11 mm between the MRI model and the actual bone. These impressive errors should result from an improper segmentation of the MRI since manual editing and several semi-automated segmentations were required to extract the bone contours. Conclusions drawn from this experiment may not be representative of the reality.

Rathnayaka et al. and Van den Broeck et al. compared virtual bone models derived from CTscan and MRI with a model considered as gold standard. Rathnayaka et al. have acquired their gold standard by a mechanical contact scanner. Van den Broeck et al. have generated their reference by a high resolution optical scanner. They have matched MRI and CTscan models to the reference and computed the average distance between both models. Both studies have shown non-significant differences between MRI and CT concluding that both modalities were equivalent in terms of accuracy. Rathnayaka et al. have investigated the accuracy on 5 different target zones. Interestingly, MRI has produced a significantly higher error on the distal extremity of bone, zone of interest for patient-specific instruments. According to these latter two studies, both modalities can safely be used to create patient-specific instruments provided that the segmentation method is accurate and reproducible.

Once the feasibility established, implant manufacturers have implemented the technology and proposed PSI associated to their implant. OtisMed Corporation (later bought by Stryker) was the first to commercialize the technology in 2008. First published results seemed very poor with a wide range of obtained angles on the femur as well as on the tibia [21]. However, the reported figures were measured against the mechanical axis while the concept of the OtisMed prosthesis and associated instruments was to restore the initial anatomy rather than a neutral alignment. Thus, this study does not report actually accuracy error of the instruments, since the target angles were unknown.

This paper has been criticized in a letter to the editor [40] invoking that one author of this study was involved in a pre-commercial evaluation led by OtisMed. They also report that they have pursued their experience in using the OtisMed PSI, treating 650 patients within the next 14 months. Without providing any figures, authors conclude that this system is much more reliable and accurate that Klatt et al. has reported. The letter to the editor has been followed by a ‘In Reply’ [19] that

was more a personal clarification than a scientific criticize. A second published paper has reported 48 patients treated by using PSI showing encouraging results [18]. A satisfying accuracy was obtained in most cases except 3 % where instruments did not fit perfectly to the bony structure. It has been established that the error found its source into the preoperative planning that was inaccurately executed by the technical operator. A last paper in the early life of PSI was published in 2008 [22]. After an initial cadaveric experiment, authors reported an interesting experience using PSI to guide pins that will align the standard cutting block. The accuracy was reported to be within 2.3°, but there was any explanation about which angle has been measured nor about the methodology. This incomplete analysis of accuracy demonstrates the lack of standardization in the postoperative assessment of accuracy.

In the few years following 2008, PSI has become a real trend to quickly replace the navigation system. The main advantage is that the investment is minimal for the hospital (no heavy investment to acquire the machine) and the learning curve is very short (intuitive usage). The accuracy of the manufacturing was very good since the resolution was 0.2 mm, a way lower than the resolution of optical navigation systems.

The year 2012 has seen several published studies to assess PSI accuracy for knee arthroplasty. A meta-analysis summarizing this specific literature [37] has concluded that PSI may improve accuracy of implant positioning even if the quality of obtained data are inconsistent. Furthermore, the clinical aspect was not observed at this time, basing the judgment on the fact that an implant accurately positioned implied a satisfying clinical outcome.

This conclusion has then been revised by several studies showing that PSI were not necessarily improving implant positioning [1, 25]. These studies were among the first to negatively conclude on PSI. Authors have compared groups of patients treated using either the conventional technique or the PSI. The postoperative measurements have shown more outliers in the PSI group than in the conventional group. A more recent meta-analysis [38] has shown that alignment over several reference planes were not improved using PSI. The authors conclude that the system is of no clinical benefit for the patient.

Recently, a new turn has been observed. The French chapter of CAOS international has had a conference where the usage of PSI has been discussed. Interesting questions have been raised leading to a new trend. First of all, it has been emphasized that the preoperative planning must be strictly supervised by the surgeon. The preoperative planning is crucial in the success of implant positioning by using PSI. The operator who is virtually positioning the implant obeys to a systematic procedure. The accuracy, repeatability and reproducibility of the method is questionable as sensitivity analysis tends to demonstrate. The planning designer must provide the surgeon with efficient tools to visualize the acquisition of reference axes. Doing so, the surgeon is able to check if point acquisition reflects the reality of the involved bones. Also, implant positioning must be controlled by the surgeon himself to ensure there will be no unsatisfying result such as anterior femoral step or undesired tibial slope. In the current days, the planning is largely

underestimated, leading to potential misconception that are not related PSI accuracy.

Secondly, the instrument design has been criticized. It has been observed that instrument could reach several positions on the bony surface because of primary instability. Instrument could also slip from the target surface because of poor intrinsic in-place locking. Finally, mechanical constraints during K-wires or pins insertion can cause an instrument movement. These potential pitfalls can explain the unsufficient accuracy results described in the literature.

Surgeons should keep in mind that the overall system requires a high attention at all stages, from the images acquisition to the intra-operative use. If one link is weak, the resulting accuracy may be strongly affected. Even if these requirements are met, evidence of any clinical added value for the patient must still be proven.

Current Innovative Applications

PSI for knee arthroplasty has favored the growing popularity of additive manufacturing and made it affordable for medical use. The resurgence of PSI has bring back all the advantages described by Radermacher et al. But many others were also gained: production costs were decreased, resolution was improved and manufacturing process was located into certified medical facilities. This new picture of the market has permitted the development of numerous applications to treat complex bone pathologies or correct skeletal abnormalities.

Spine Instrumentation

Scoliosis correction is a challenging surgery requiring a high accuracy in inserting screws into pedicles that can be narrow and deformed. It is the reason why spine instrumentation has benefitted from the latest innovations such as navigation systems and, lastly, PSI. The latter has known extensive developments to reach clinical usage in early 2009 [23, 43]. It has shown excellent results with a significantly decreased pedicle perforation rate. Since then, research projects have been launched to further develop the concept, improving the design of instruments, leading to an increased stability [15]. Surprisingly, commercial applications are not widely available.

Degenerative spine correction is a similar application where the deformation can be first corrected by performing a bone resection and fixing the spine in an anatomical position. A specific planning determines the optimal positioning of the spine while preserving the spinal cord. A PSI is then manufactured to guide the saw blade during osteotomies. The PSI can either be molded onto the bone model using medical acrylic (Fig. 13.1) or virtually design and manufactured by additive manufacturing.

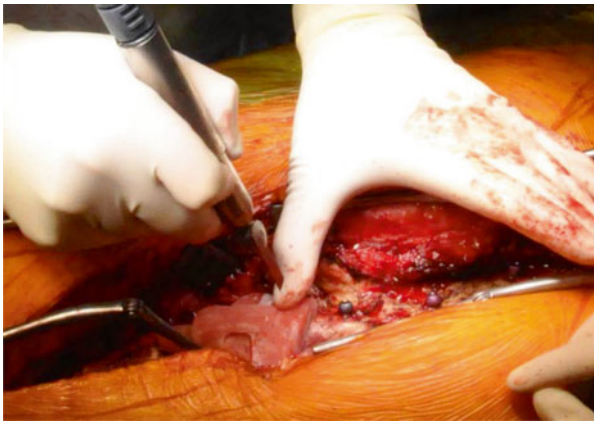

Fig. 13.1 Instrument (pink shape) molded on the bone model using acrylic. The instrument presents a flat surface indicating the target osteotomy

Joint Arthroplasties

Several joint arthroplasties are now benefitting from PSI to be planned and positioned. Several research projects have led to commercial products. For the shoulder arthroplasty, Imascap (Brest, France) has developed a software to give the surgeon the ability to perform its virtual pre-operative planning. This software is now proposed by Tornier (Montbonnot Saint-Martin, France) as the Blueprint® solution. Imascap has also developed and brought onto the market a PSI to transfer the planning into the operative room.

Hip prosthesis is also benefitting from PSI to increase accuracy of implant positioning. Several research projects are validating the concept [20, 34, 43]. Increased accuracy has been proven when using the PSI, showing that the technology may be useful in a clinical situation. However, there is no commercial application to date even if a patent has been registered in 2013 and a clinical study launched in the next few months.

The situation is more advanced for ankle arthroplasty were developments have been validated and transferred to a commercial product. Wright Medical has put on the market the Prophecy® Inbone® to position their prosthesis. Berlet et al. [3] have observed a high repeatability in positioning the instrument, leading to a final implant positioning within $\pm 3°$ when compared to the planned position. However, the solution is not an actual positioning instrument and clinical data are not available yet.

Bone Tumor Surgery

In tumor surgery, surgical excision must be highly accurate to ensure the total removal of the pathologic tissue without infraction of the tumor. Other way, a local recurrence of the tumor can arise leading to a failure of the initial treatment. The conventional method has shown unsufficient clinical results with a local recurrence

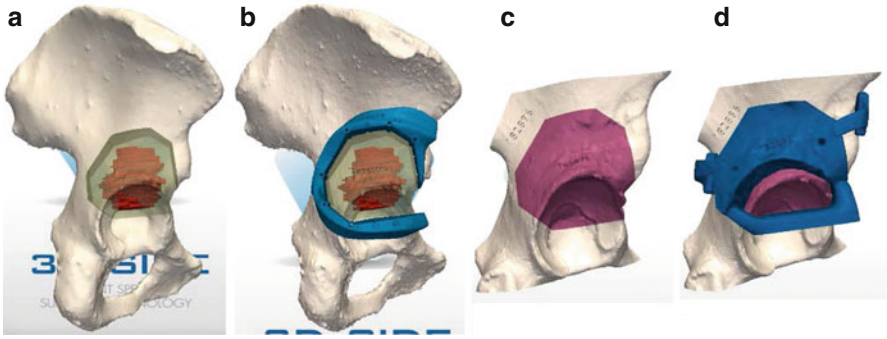

Fig. 13.2 Preoperative planning of a tumor surgery. (**a**) Shows the cutting trajectories around the tumor, including a safe margin. (**b**) Shows the instrument designed to resect the tumor. Allograft selection can be performed virtually (**c**) according to reconstruction needs. An instrument can also be designed to actually cut the allograft (**d**)

rate observed in 28–35 % in case of pelvic tumors [9]. These clinical results have been confirmed by in vitro experiments leading to intralesional resections on plastic pelves [5, 6]. Preoperative assistances have been developed to plan the tumor removal. Tumor extension is delineated on the MRI and merged with the CTscan to combine anatomical and functional data. Based on the generated 3D view, cutting trajectories are chosen including a user-defined safe Margin (Fig. 13.2) [26]. When needed, a reconstruction strategy can be planned as well, using either a frozen allograft [27] or a commercial implant. The transfer into the operating theater was made possible by using a customized optical navigation system. The overall accuracy of the process has been assessed on plastic pelves [5]. A significant improvement has been shown with a reduced error during bone cuttings from 11.2 mm down to 2.8 mm ($p<0.001$). The system has been used to surgically treat a small number of patients [14]. The technique has been more widely described by Docquier et al. the creators of the overall system [13].

The previously described resurgence of PSI has conducted the developers of the assistances to move toward this new accessible technique. PSI have been tested on plastic pelves to assess the feasibility of tumor resection and estimate their accuracy [7]. The mean accuracy was below 2 mm, showing a significant improvement when compared to the conventional method and a non-significant improvement regarding the optical navigation. Since then, PSI have been used on actual patients to treat several bone (Figs. 13.3 and 13.4). Their excellent accuracy has permitted to decrease the target safe margin from 10 mm (standard desired safe margin) down to 4 mm in some cases. The objective of decreasing the target safe margin is crucial since it allows the preservation of important anatomical structures such as joints, ligament insertions or nerves.

A spin-off company from the Université catholique de Louvain (3D-Side, Belgium) has been launched to put the technology on the market. To date,

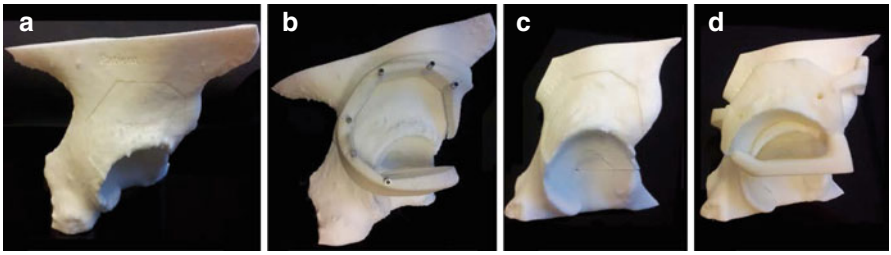

Fig. 13.3 Bone models and instruments manufactured. Bone models from the patient (**a**) and from the allograft (**c**) can be manufactured and sterilized. Instruments positioning are checked before the surgery to ensure a satisfying use (**b**, **d**)

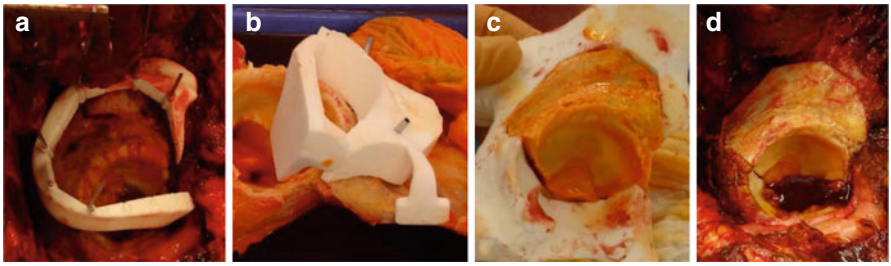

Fig. 13.4 Instruments use during the surgery. The instrument for resection is positioned onto the bone and fix using KWires (**a**). The process is repeated for the allograft (**b**). After allograft cutting, the accuracy is checked on the allograft model (**c**). Finally, the cut allograft is impacted in the defect (**d**). A perfect fit is obtained with contact for each of the 7 cutting planes

55 patients have been successfully treated in several European countries. Clinical series have been reported in the literature showing good oncological results [2, 16]. No local recurrence linked to a bone contamination has been observed postoperatively even if the post-operative follow up is too short to draw strong conclusions. A local recurrence has arose because of a contaminated soft tissue margin. R0 safe margins have been systematically obtained except in one case where the tumor has been morselized to urgently extract it from the patient who was suffering from severe bleeding and poor cardiovascular conditions. A further cost-efficiency study will be led to assess a potential financial benefit of the technique regarding the prevented cost of local recurrence.

Corrective Osteotomies

Patients who have suffered from a bone fracture usually recover a fully normal limb function. In some cases, a non-anatomical bone fusion can be observed yielding to a limited function of the involved limb. When the limitation prevents a

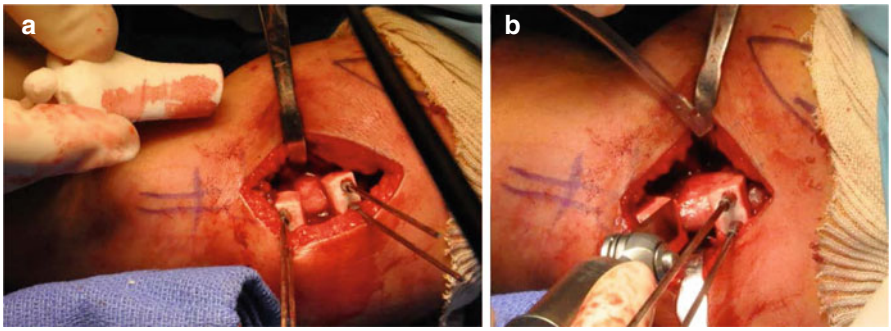

Fig. 13.5 Instrument is positionned onto the bone surface (**a**). KWires are inserted into the cylindric guides to fix them. A flat surface guides the saw blade (**b**)

normal everyday life, a corrective surgery is indicated. The required correction is often a complex biplanar bone cutting representing a solid angle. By using a conventional manual method, the obtained correction is often suboptimal, leading to an over- or a sub-correction. A 3D simulation of the cuttings is highly helpful to visualize the initial position and estimate the appropriate correction that should be brought.

Some companies (Materialise, 3D-side, Cartis) and academic research projects propose a 3D analysis showing a reconstruction of the bone and proposing a strategy to restore a normal anatomy [11, 12, 41]. The retained surgical option is transferred into the operating room by using PSI. Three different approaches can be adopted.

The first method is based on a PSI that serves as hole driller and saw guide. Firstly, holes are drilled into the involved bone, representing the trajectories of future screws. Secondly, the PSI is used to cut the bone thanks to a slot guiding a saw blade. The PSI is removed from the bone and the reconstruction is performed by inserting a dedicated plate and the pre-drilled screws. This technique requires the use of 3D models from screws and plates of an implant manufacturer during the preoperative planning. Also, the technique does not allow any change in plate and screws sizes.

In the second philosophy, the PSI is positioned onto the bone and fixed in place by using two-by-two parallel k-Wires. The PSI indicate the osteotomy to be performed, guiding the saw blade (Fig. 13.5). After bone cutting, the k-Wires are parallelized to obtain the correct limb alignment as planned preoperatively. This second solution is not dependent from any implant manufacturer and thus any osteosynthesis material can be used to make the osteosynthesis.

Finally, the third method consists in determining a single cut that may correct the anatomy. A PSI allows to perform the cutting and drilling the future screws trajectories. Finally, a patient-specific plate, including a solid angle portion corresponding to the correction that will be brought, is designed to realign the bone segments into an anatomic position. The plate is manufactured by additive manufacturing and implanted during the surgery.

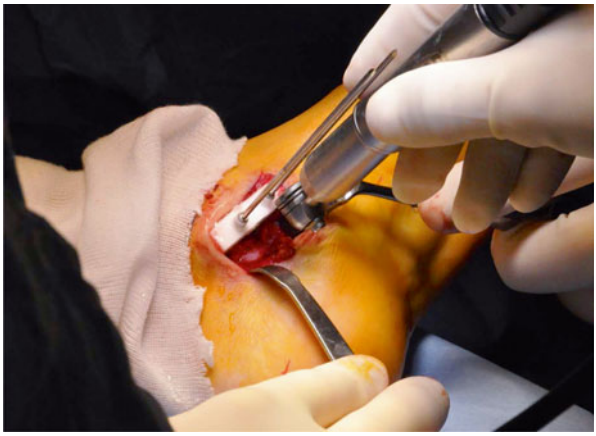

Fig. 13.6 The instrument indicates the osteotomy to perform. The depth control is achieved thanks to a physical stop that prevents the blade from going into the safe joint

Other Applications

Synostosis

This pathology, abnormal fusion between two bones, usually affects the calcaneo-navicular or the talocalcaneal junctions. It occurs in approximatively 1 % of the population, specifically in young people. The treatment is a surgical resection in the coalition zone, removing sufficient portion of bones. The recurrence rate is relatively high because of unsufficient resection. In case of breakage of the healthy joint, hidden by the bones, the foot can be painful. Accuracy can be improved by performing a simulation of the resection and actually create it using a PSI (Fig. 13.6). The planning permits to ensure a complete resection of the degenerative joint. The depth control preventing breaching the healthy joint can be achieved if the saw depth is determined at the stage of preoperative planning. This technique has been reported, as well as early clinical results on 9 patients [10]. No recurrence has been observed at last follow-up.

Paprovsky Pathology

This pathology is a degenerative process of the hip that can lead to incapacity of walking for the patient. In many cases, the hip cannot be restored properly since bone loss is too extensive to accept a standard hip implant. This surgery was among the first to benefit from PSI. A synthetic metallic implant was designed to fill the hip defect and restore a normal anatomy. The implant is manufactured using additive manufacturing, usually in titanium or Cobalt-chromium alloys. The manufacturing process produces porous surfaces, once in contact with patient's bone present excellent properties to accept bone ingrowth. Regarding the joint, a finishing is required to produce smooth surfaces allowing a normal function of the joint. An associated instrument is designed to perform an accurate resection and ensure an optimal

fitting of the implant with the anatomy. Mobelife, a spin-out from Materialise (Leuven, Belgium) has put this solution on the market in the years 2010. The main disadvantage of the methodology is the high cost of the manufacturing that leads to a very expensive solution for the surgeon. The medical benefit should be balanced against the economic profit that may incur. In some countries, the social system has accepted a reimbursement.

Ilio-Sacral Screws

Stabilization of joint dislocation or sacral fractures is usually performed by inserting screws through the sacro-iliac joint. The accuracy is crucial in this surgery to ensure a bone insertion without breaching sacral nerves. Recently, PSI have been clinically used in 16 patients [8]. Reported results were promising when compared with conventional fluoroscopic insertion. A significant improvement in accuracy has been shown. PSI are particularly suitable for this application since the surfaces of the iliac crest are highly discriminant allowing an easy positioning and an immediate stability of PSI.

Conclusion

Patient-Specific Instruments has deeply modified the orthopedic surgery, bringing new possibilities [32]. Supported by what is considered as the third industrial revolution, namely additive manufacturing, PSI have invaded the operative room. Emphasize must be put on the pre-operative planning which takes a crucial role. Firstly, it has to be as accurate as possible since the assistance is meant to replicate the planning on the actual bone. Secondly, the planning must first conform to the situation that will be met in the operative room. It implies that the surgeon anticipates how surgery will be performed several days or weeks before the actual surgery. For example, the surgical approach must be firmly defined since it has a strong impact on the instrument design or the contact surface with bone. Finally the planning must be performed using 3D data to define cutting or drilling trajectories in the 3D space. This new approach generates new tasks to perform and new tools to understand for the surgeon. That's why an engineer is often responsible for handling the computerized tools that produces the pre-operative planning. The cooperation between the surgeon and the engineer is thus critical to generate a planning that reaches the desired target and meets the medical requirements.

The story of PSI is very interesting to understand how a disruptive technology can be adopted. While it has shown to be of great help, accurate, safe and easy to use, Patient-Specific Instruments have not met the success that could have been forecasted. Proposed applications were scientifically interesting, but financially not mature enough to be widely pulled on the market by customers. When implant manufacturers have adopted the technology, a large push has been observed. Then,

the technique has been quickly and widely approved at first, surfing over a positive wave. A large amount of literature has been published concluding that PSI was the best option, without any supporting data. This statement has rapidly been destroyed by evidence-based medicine and the clinical observation that from the patient's side, no benefit was shown. Today, it seems that the expectations curve is finding an inflection point with a resurgence in favor of PSI for total knee arthroplasty. The future of this application is certainly between a large enthusiasm and the total rejection. In particularly deformed bones or rare pathologies, PSI should be of great help, improving the understanding of the pathology and guiding the surgical gesture. In these days, PSI are still in use for this application since manufacturers are displaying amazing figures: Materialise, has manufactured 146.000 PSI in 2013. The evolution of this figure in 2015 should give an overview of the future trend for PSI.

References

1. Barrack RL, Ruh EL, Williams BM, Ford AD, Foreman K, Nunley RM. Patient specific cutting blocks are currently of no proven value. J Bone Joint Surg Br. 2012;94:95–9. doi:10.1302/0301-620X.94B11.30834.
2. Bellanova L, Paul L, Docquier P-L. Surgical guides (patient-specific instruments) for pediatric tibial bone sarcoma resection and allograft reconstruction. Sarcoma. 2013;2013:787653. doi:10.1155/2013/787653.
3. Berlet GC, Penner MJ, Lancianese S, Stemniski PM, Obert RM. Total ankle arthroplasty accuracy and reproducibility using preoperative CT scan-derived. Patient-specific guides. Foot Ankle Int. 2014;35:665–76. doi:10.1177/1071100714531232.
4. Birnbaum K, Schkommodau E, Decker N, Prescher A, Klapper U, Radermacher K. Computer-assisted orthopedic surgery with individual templates and comparison to conventional operation method. Spine. 2001;26:365–70.
5. Cartiaux O, Banse X, Paul L, Francq BG, Aubin C-É, Docquier P-L. Computer-assisted planning and navigation improves cutting accuracy during simulated bone tumor surgery of the pelvis. Comput Aided Surg. 2013;18:19–26. doi:10.3109/10929088.2012.744096.
6. Cartiaux O, Docquier P-L, Paul L, Francq BG, Cornu OH, Delloye C, Raucent B, Dehez B, Banse X. Surgical inaccuracy of tumor resection and reconstruction within the pelvis: an experimental study. Acta Orthop. 2008;79:695–702. doi:903404236.
7. Cartiaux O, Paul L, Francq BG, Banse X, Docquier P-L. Improved accuracy with 3D planning and patient-specific instruments during simulated pelvic bone tumor surgery. Ann Biomed Eng. 2014;42:205–13. doi:10.1007/s10439-013-0890-7.
8. Chen B, Zhang Y, Xiao S, Gu P, Lin X. Personalized image-based templates for iliosacral screw insertions: a pilot study. Int J Med Robot. 2012;8:476–82. doi:10.1002/rcs.1453.
9. Delloye C, Banse X, Brichard B, Docquier P-L, Cornu O. Pelvic reconstruction with a structural pelvic allograft after resection of a malignant bone tumor. J Bone Joint Surg Am. 2007;89:579–87.
10. De Wouters S, Tran Duy K, Docquier P-L. Patient-specific instruments for surgical resection of painful tarsal coalition in adolescents. Orthop Traumatol Surg Res. 2014;100:423–7. doi:10.1016/j.otsr.2014.02.009.
11. Dobbe JGG, du Pré KJ, Kloen P, Blankevoort L, Streekstra GJ. Computer-assisted and patient-specific 3-D planning and evaluation of a single-cut rotational osteotomy for complex long-bone deformities. Med Biol Eng Comput. 2011;49:1363–70. doi:10.1007/s11517-011-0830-3.

12. Dobbe JGG, Vroemen JC, Strackee SD, Streekstra GJ. Patient-tailored plate for bone fixation and accurate 3D positioning in corrective osteotomy. Med Biol Eng Comput. 2013;51:19–27. doi:10.1007/s11517-012-0959-8.
13. Docquier P-L. Computer-navigated bone cutting in the resection of a pelvic bone tumor and reconstruction with a massive bone allograft. JBJS Essent Surg Tech. 2011;1:1–13. doi:10.2106/JBJS.ST.K.00013.
14. Docquier P-L, Paul L, Cartiaux O, Delloye C, Banse X. Computer-assisted resection and reconstruction of pelvic tumor sarcoma. Sarcoma. 2010;2010:125162. doi:10.1155/2010/125162.
15. Ferrari V, Parchi P, Condino S, Carbone M, Baluganti A, Ferrari M, Mosca F, Lisanti M. An optimal design for patient-specific templates for pedicle spine screws placement. Int J Med Robot. 2013;9:298–304. doi:10.1002/rcs.1439.
16. Gouin F, Paul L, Odri GA, Cartiaux O. Computer-assisted planning and patient-specific instruments for bone tumor resection within the pelvis: a series of 11 patients. Sarcoma. 2014;2014:e842709. doi:10.1155/2014/842709.
17. Hafez MA, Chelule KL, Seedhom BB, Sherman KP. Computer-assisted total knee arthroplasty using patient-specific templating. Clin Orthop. 2006;444:184–92. doi:10.1097/01.blo.0000201148.06454.ef.
18. Howell SM, Kuznik K, Hull ML, Siston RA. Results of an initial experience with custom-fit positioning total knee arthroplasty in a series of 48 patients. Orthopedics. 2008;31:857–63.
19. Hozack WJ. In reply. J Arthroplasty. 2008;23:638. doi:10.1016/j.arth.2008.03.008.
20. Kitada M, Sakai T, Murase T, Hanada T, Nakamura N, Sugano N. Validation of the femoral component placement during hip resurfacing: a comparison between the conventional jig, patient-specific template, and CT-based navigation. Int J Med Robot. 2013;9:223–9. doi:10.1002/rcs.1490.
21. Klatt BA, Goyal N, Austin MS, Hozack WJ. Custom-fit total knee arthroplasty (OtisKnee) results in malalignment. J Arthroplasty. 2008;23:26–9. doi:10.1016/j.arth.2007.10.001.
22. Lombardi AV, Berend KR, Adams JB. Patient-specific approach in total knee arthroplasty. Orthopedics. 2008;31:927–30. doi:10.3928/01477447-20080901-21.
23. Lu S, Xu YQ, Zhang YZ, Li YB, Xie L, Shi JH, Guo H, Chen GP, Chen YB. A novel computer-assisted drill guide template for lumbar pedicle screw placement: a cadaveric and clinical study. Int J Med Robot. 2009;5:184–91. doi:10.1002/rcs.249.
24. McGurk M, Amis AA, Potamianos P, Goodger NM. Rapid prototyping techniques for anatomical modelling in medicine. Ann R Coll Surg Engl. 1997;79:169–74.
25. Nunley RM, Ellison BS, Zhu J, Ruh EL, Howell SM, Barrack RL. Do patient-specific guides improve coronal alignment in total knee arthroplasty? Clin Orthop. 2012;470:895–902. doi:10.1007/s11999-011-2222-2.
26. Paul L, Cartiaux O, Docquier P-L, Banse X. Ergonomic evaluation of 3D plane positioning using a mouse and a haptic device. Int J Med Robot. 2009;5:435–43. doi:10.1002/rcs.275.
27. Paul L, Docquier P-L, Cartiaux O, Cornu O, Delloye C, Banse X. Selection of massive bone allografts using shape-matching 3-dimensional registration. Acta Orthop. 2010;81:250–5. doi:10.3109/17453671003587127.
28. Radermacher K, Bliem R, Hennecke C, Staudte HW, Rau G. A desktop image processing system for computer-assisted orthopedic surgery (DISOS). Stud Health Technol Inform. 1996;29:675–80.
29. Radermacher K, Portheine F, Anton M, Zimolong A, Kaspers G, Rau G, Staudte HW. Computer assisted orthopaedic surgery with image based individual templates. Clin Orthop. 1998 (354):28–38.
30. Radermacher K, Portheine F, Zimolong A, Eichhorn C, Staudte H-W, Rau G. Image guided Orthopedic Surgery using individual templates. In Troccaz J, Grimson E, Mösges R, editors. CVRMed-MRCAS'97, Lecture notes in computer science. Berlin/Heidelberg: Springer; 1997. p. 606–15.

31. Radermacher K, Staudte HW, Rau G. Computer assisted orthopedic surgery by means of individual templates-aspects and analysis of potential applications. In DiGioia A, editor. Proceedings of the first international symposium on medical robotics and computer assisted surgery. Presented at the first international symposium on medical robotics and computer assisted surgery, Pittsburgh; 1994. p. 42–8.
32. Radermacher K. Renaissance of computer-assisted orthopedic surgery with individual templates: evolution or revolution? In: Haaker R, Konermann W, editors. Computer and template assisted orthopedic surgery. Berlin/Heidelberg: Springer; 2013. p. 11–21.
33. Rathnayaka K, Momot KI, Noser H, Volp A, Schuetz MA, Sahama T, Schmutz B. Quantification of the accuracy of MRI generated 3D models of long bones compared to CT generated 3D models. Med Eng Phys. 2012;34:357–63. doi:10.1016/j.medengphy.2011.07.027.
34. Sakai T, Hanada T, Murase T, Kitada M, Hamada H, Yoshikawa H, Sugano N. Validation of patient specific surgical guides in total hip arthroplasty. Int J Med Robot. 2014;10:113–20.
35. Schkommodau E, Decker N, Klapper U, Birnbaum K, Staudte H-W, Radermacher K. Pedicle screw implantation using the DISOS template system. In: Navigation and robotics in total joint and spine surgery. Berlin/Heidelberg: Springer; 2004. p. 501–5.
36. Staudte H-W, Schkommodau E, Honscha M, Portheine F, Radermacher K. Pelvic osteotomy with template navigation. In: Navigation and robotics in total joint and spine surgery. Berlin/Heidelberg: Springer; 2004. p. 455–63.
37. Thienpont E. Recent advances in knee surgery. The Knee. 2013 (20 Suppl 1):S1–2. doi:10.1016/S0968-0160(13)70002-4.
38. Thienpont E, Schwab PE, Fennema P. A systematic review and meta-analysis of patient-specific instrumentation for improving alignment of the components in total knee replacement. Bone Joint J. 2014;96-B:1052–61. doi:10.1302/0301-620X.96B8.33747.
39. Van den Broeck J, Vereecke E, Wirix-Speetjens R, Vander Sloten J. Comparing CT and MRI segmentation accuracy of long bones [WWW Document]. 2013. https://lirias.kuleuven.be/handle/123456789/413823. Accessed 11 Mar 2014.
40. Vernace JV, Bodenstab A. Letter to the editor. J Arthroplasty. 2008;23:637–8. doi:10.1016/j.arth.2008.03.007.
41. Victor J, Premanathan A. Virtual 3D planning and patient specific surgical guides for osteotomies around the knee: a feasibility and proof-of-concept study. Bone Joint J. 2013;95-B:153–8. doi:10.1302/0301-620X.95B11.32950.
42. White D, Chelule KL, Seedhom BB. Accuracy of MRI vs CT imaging with particular reference to patient specific templates for total knee replacement surgery. Int J Med Robot. 2008;4:224–31. doi:10.1002/rcs.201.
43. Zhang YZ, Chen B, Lu S, Yang Y, Zhao JM, Liu R, Li YB, Pei GX. Preliminary application of computer-assisted patient-specific acetabular navigational template for total hip arthroplasty in adult single development dysplasia of the hip. Int J Med Robot. 2011;7:469–74. doi:10.1002/rcs.423.

Chapter 14
Custom Implants

Paul S. Unwin and Abtin Eshraghi

Abstract Although Patient Specific Implants have been used over 60 years they have not gained enough popularity in orthopaedics field, they were used in rare diseases or complex reconstructions mainly. In the past, custom made orthopaedic bone and joint replacements also called Patient Specific Implants were much more expensive, time consuming and inflexible due to the little technology that surgeons and engineers relied on. When it came to compare the massive produced off the shelf implants and custom made implants it was easy to identify that off the shelf implants were less expensive, less time consuming, had more availability, had preoperative flexibility and difficulty of achieving precise placement. Nowadays, with modern desktops PCs preoperative planning has become easier and faster. Three dimensional virtual scenarios produce 3D virtual images in a matter of hours, and then it is possible to reconstruct the exact bone and the exact area where the tumour is located and build a custom made replacement to fit precisely in the defect bone. Nevertheless it is a challenge to lower the costs of machinery for 3D reconstructions. Furthermore what physicians are pointing with the use of custom made implants is to "fit the implant to the patient, and not the patient to the implant"; computed assisted surgeries, preoperative planning, and intraoperative navigation are assets in order to make custom made implants more common within orthopaedic surgeries.

Keywords Computer assisted surgeries • Off the shelf implants • 3D virtual images • Preoperative planning • Modelling implant body

Introduction

Personalized medicine has become a key focus for medical product development and the concurrent advancements in digital technologies have led to a resurgence in interest in patient specific implants. Available today are a diverse array of patient-specific devices from bioresorbable tracheal splint to patient specific orthopaedic

P.S. Unwin, BSc (Hons), MSc, PhD (✉) • A. Eshraghi, MEng
Stanmore Implants Worldwide Ltd, Centennial Park, Elstree WD6 3SJ, UK
e-mail: Paul.unwin@stanmoreimplants.com

L.E. Ritacco et al. (eds.), *Computer-Assisted Musculoskeletal Surgery: Thinking and Executing in 3D*, DOI 10.1007/978-3-319-12943-3_14

implants and even artificial limbs [26]. Although custom-made orthopaedic bone and joint replacements have been used successfully for over 60 years they have rarely gained popularity other than for very rare diseases or complex reconstructions. Although, in comparison to mass-produced off-the-shelf implants, custom-made devices account for less than 1 % of all devices implanted, they are an essential element in the orthopaedic surgeon's reconstruction armamentarium.

Custom-made also referred as patient-specific implants are typically used in two extreme orthopaedic reconstruction sectors, (i) limb salvage surgery for bone tumour and complex revisions of failed joint replacements and (ii) joint replacement surgery for complex primary arthroplasty and less severe revisions of failed standard joint replacements. Patient specific implants are designed based on the philosophy of 'fit the implant to the patient and not the patient to the implant.' However, due to the very nature of uniquely designed patient-specific implants there requires the implant designer to have expertise of thinking and executing in 3D.

As 3D technologies advance there are expanding opportunities to further enhance patient-specific devices to address unmet clinical needs and improve clinical outcomes. With increasing awareness of the clinical performance and long-term outcomes of mega-prostheses, the demand has increased and there are continual endeavours to push the boundaries further. Typically this relates to minimising the bony resections, sparing joints and soft tissue attachments. As the implant and associated bone interfaces become more sophisticated there is a corresponding increasing need to plan and execute sophisticated 3D processes. Hence, computer-assisted surgery is becoming essential and inextricable linked with the process of designing, manufacturing and precise placement of custom-made implants.

History

The history of custom-made bone and joint replacements dates back over six decades and throughout have had and continue to have an essential role in complex bone and joint reconstructive surgery. In the pioneering decades of the 1940s and 1950s, joint and bone reconstruction orthopaedic implants particularly those used in limb salvage were individually designed and manufactured [12]. Due to the rarity of tumour and complex reconstruction cases requiring the need of a custom implant, the design and manufacture of these implants was limited to a small number of institutions globally. The first mega prostheses, all of which were custom-made, were being designed in the early 1950s by Prof John Scales and his team of the Centre of Biomedical Engineering, Institute of Orthopaedics, Royal National Orthopaedic Hospital, Stanmore. Scales was one of the most influential pioneers in designing many of the worlds' firsts including distal femoral replacement (1952) and hemi-pelvic replacement (1961) [24]. The implants fabricated were in comparison to today's relatively simple, with bioengineers creating 3 dimensional designs based upon dimensions taken from bi-planar measurement radiographs utilising their knowledge, experience and the careful study of cadaveric bones. These

pioneering bioengineers were thinking and executing in 3D without the aid of computer technology. The 1970s saw the mass-productionisation of standardised 'off-the-shelf' joint replacements to meet the increasing demand of hip and knee arthroplasty and thus virtually restricting the use of custom implants to bone tumour limb salvage reconstruction.

In the late 1980s with the introduction of CAD-CAM technologies into the orthopaedic industry and concurrent with enhanced skeletal radiographic imaging, there was resurgence of interest in custom implants. This led to the formation of the International Society for the Study of Custom Prostheses (ISSCP, that later became International Society for Technology in Arthroplasty, ISTA). The society was founded in 1987 by a group of orthopaedists and scientists who were excited and enthusiastic about the application of 3D imaging techniques and CAD-CAM technologies. The membership of this society led the way in bringing computer-assisted surgery into orthopaedics and working out how to plan and execute in 3D. Leading advocates including Dr. David Stulberg from the USA, Dr. Peter Thumler from Germany, Prof Peter Walker from the UK and Professor Jean Aubaniac from France were keen to take a holistic approach engaging a wide range of disciplines to solve problems. There was a flurry of activity in designing and manufacturing femoral hip stems that included the remarkable Identifit system (Depuy, Warsaw IN) of making a polymer casting of the femoral cavity at surgery and manufacturing the stem within the next 45 min, whilst the patient was kept asleep. However, it became apparent that the key problem was fitting precisely the patient-matched uncemented femoral hip stems. To solve this problem the inspirational Robodoc®, a highly sophisticated imaging and robotically controlled milling system for precision surgery was developed by Dr Hap Paul and Dr William Bargar in the US [22].

However the patient-specific CAD-CAM hip stem resurgence was curtailed due in part to the commercial viability, the need for precise specialised imaging that was only available in a small number of centres, the learning curve to achieve repeatable precise fitment and the difficulty of showing improved clinical results. The CAD–CAM process still remains in use today primarily for the treatment of complex primary joint arthroplasty with conditions such as achondroplasic dwarfism and juvenile rheumatoid arthritis and is provided by specialist implant manufacturers such as Stanmore Implants Worldwide Ltd (UK) and Symbios (Switzerland). These patient-matched implants are typically designed based on radiographs and or CT scans of the recipient patient taking into account the presented anatomy and bony dimensions. Clinical results of patient specific CAD-CAM femoral hip stems have showed outstanding longevity. One study of primary uncemented CAD-CAM femoral hip stems followed up for between 11 and 17 years showed no incidence of aseptic loosening [17]. The authors considered that it was the designing the hip stem in 3D to fit and fill the proximal femoral canal that enabled initial implant stability that led to long-term osseointegration.

Recently, custom-made implants have become popularised through the media, with articles on the 3D printing revolution and the potential to produce 'the next generation of orthopaedic implants' or even 3D printing of the human body. The improvements in the precision and accuracy of surgery primarily through the use of

computer-assisted navigation, has enabled the designer greater freedom in the design of implants knowing that there are appropriate tools at the surgeons disposal to achieve the desired placement. Rapid Prototyping (RP) is taking the manufacturing sector by storm and more specifically the extremely exciting metallic alloy-based Additive manufacturing (AM) and is being recognised by the orthopaedic device manufacturers as a significant addition to the existing conventional manufacturing technologies. Murr et al. in their recent papers elegantly described the potential for AM in developing more advanced orthopaedic implants [18, 19]. AM is already showing the potential to kick-start the next generation of orthopaedic implant designs and is probably the most important innovation in implant technology since the introduction of hydroxyapatite coatings back in the late 1980s.

Background to Specialist Custom-Made Orthopaedic Implants

Limb salvage implants, also known as mega or massive implants, are those that replace shaft bone and may include one or more joints. Mega implants are most commonly used for the treatment of malignant bone tumours and increasingly more common for the revision of failed standard joint replacements. Bone tumours are very rare with an annual incidence of approximately 8 in 1 million. Most malignant bone tumours occur in the second and third decades of life with the commonest being osteosarcoma. Osteosarcoma most commonly occurs in the distal femur and the proximal tibia. The widely accepted method of surgical treatment is to excise the tumour with a wide margin and replace it with a metallic mega implant. In the young patients that have not reached skeletal maturity, expandable telescopic mega implants are used to maintain leg length equality [14, 23]. Young patients who survive their disease will have a normal life expectancy and therefore are expected to have the need for a functional metallic mega implant for over 70 years; a huge engineering challenge!

Mega implants are also successful in the treatment of complex revision of failed standard joint replacements, where the patient may have undergone multiple revision surgeries using conventional joint replacements that have subsequently failed resulting in major bone loss [13, 16]. Over the last two decades there has been major advances in mega implant design including improving fixation thus reducing aseptic loosening [6], mechanical breakages [20], the reliability of extendible mega implants [27] and reducing the risk of infection by modifying the implant surface with silver [28].

As limb salvage implants are some of the most sophisticated and complex to design due to the broad diversity. Key factors, including the following:

- patient age (range 2–99 years). The bones and in particular the joints of prepubescent patients are typically not ossified completely and the intra-medullary canal diameter can be as little as 5 mm in the humerus and tibia. Designing intramedullary stems is a balance between the mechanical strength of the stem and the extent to which the canal can be enlarged by reaming. At the other end of the

age spectrum, bones of the elderly become osteoporotic requiring consideration in stem design to minimise the risk of peri-prosthetic fractures.

- bone condition/indication (tumours, revisions, trauma, skeletal growth deformities). Following resection for bone tumour, the residue bone is typically normal unless it has been subjected to radiotherapy. In revision surgery either as a result of a failed standard joint replacement or a mega-prostheses the integrity and bone quality can be poor. There are also extremely rare bone disorders such as osteopetrosis and Gorham's disease that demand special attention when designing the implant and its associated instrumentation.
- life expectancy. Ranging from young patients who will survive cancer to hospitalised elderly patients. Young patients who will survive their disease may have upwards of 70 years of life and thus planning for inevitable revisions is a key consideration. In contrast, those with a short life expectancy the primary aim of the implant reconstruction is rapid rehabilitation and restoration of function.
- minimising musculoskeletal resection. Extensive bone and soft tissues resections can have significant impact on the patient's functional outcome. Joint sparing implant designs where the resections is within 30 mm of the joint retains the joint capsule and ligamentous structure thus retaining joint proprioception and natural joint function compared to those patient that have a joint sacrificed [7].
- functional expectations. Typically young patients desire to undertake activities of their peers and frequently wish to undertake sports or high demand activities. Those older wish to return to work and to have a normal family and social life. The extent of the resection, bone and soft tissue quality and co-morbidities have direct bearing on the functional ability and the device needs to be designed accordingly. For some patients a joint sparing intercalary replacement would be ideal whilst in others a knee arthrodesis may be warranted.
- skeletal locations. Bone tumours can arise all regions of the bones of the appendicular skeleton with the most common being the distal femur and the proximal tibia. Rarely tumours arise in the forearm bones and the distal tibia but the custom-made implant provider needs solutions to address these reconstructions. Modular off-the-shelf limb salvage systems do not extend beyond the more common skeletal locations.
- unusual bony anatomy. One of the greatest challenges for the implant designer is grossly deformed anatomy for example in achondoplasia. The biomechanical environment can be significantly modified and the designer needs to ensure the implant compliments the bone and soft tissue biomechanics as well as ensure that mechanical forces placed upon the implant do not adversely risk the patient.
- rarity of cases and lack of high quality clinical studies. In comparison to hip and knee arthroplasty there are few rigorous clinical studies of long-term performance that can aid the designer in establishing the validity of specific design elements.

The above is not an exhaustive list of consideration when designing custom-made implants within the 3 dimensional environment. Described below is the way that Stanmore Implants design patient specific implants and this may vary from the approaches other custom implant providers undertake.

Current Design Methods

The overall success of a custom implant is highly dependent on many factors as mentioned above, but understanding of the patient's musculoskeletal 3D geometry, its condition and the extent of the deformity is crucial. In addition, the current design envelope is not solely restricted to that of producing the custom implant but increasingly important are the tools that enables precise placement such as patient specific cutting guides, computer-assisted navigation and robotic assisted surgery (Fig. 14.1).

To affectively visualise and understand this important factor, we must adopt 3D imaging techniques such as CT and MRI scans. The image sets from these modalities can then be used to gauge the bone and soft tissue quality and generate 3D models of affected bone and cartilage.

Image Processing

Software packages such as Mimics® (Materialise, Leuven, Belgium) and ScanIP® (Simpleware Ltd, Exeter, UK) generate masks of the patient's bone, soft tissue and existing metalwork. This technique is often referred to as thresholding (Fig. 14.2). The Hounsfield units allow the software operator, in this case the implant design engineer to differentiate between areas of different density material to determine whether it is bone, soft tissue, PMMA cement, or existing implants which may be in-situ.

Often in revision scenarios where the implant in-situ is being removed, challenges in image processing and segmentation will arise. CT artefacts and scatter occur in the imaging due to the extreme heterogeneity of the metal and tissue in cross sections. If left ignored, these artefacts distort the image and make the segmentation impossible or inaccurate. The operator will require using a combination of image filtering techniques, anatomical knowledge, past experience to negate and compensate for these artefacts by manually thresholding each affected slice. This introduces an element of subjectivity and human error which, if accumulates over the whole length of the image, has the potential to affect the overall accuracy and reliability of the 3D models.

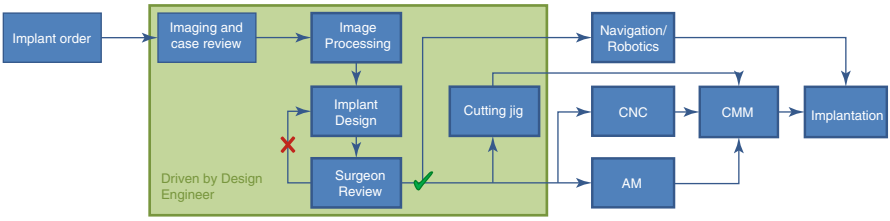

Fig. 14.1 Process workflow for custom implant design with interfaces to manufacture and precise placement technologies

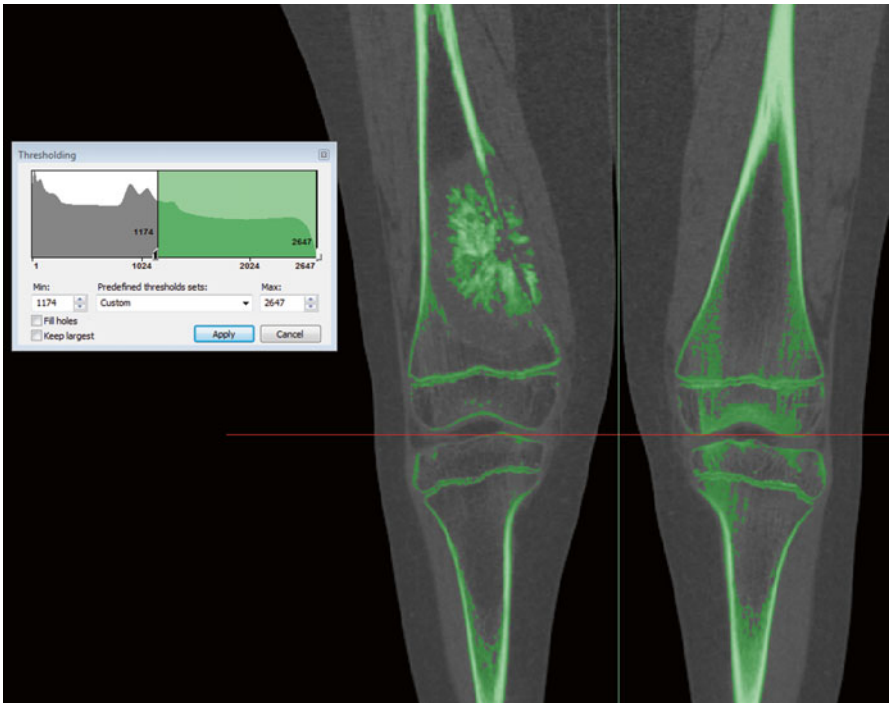

Fig. 14.2 Thresholding of bone in Materialise Mimics showing the bone tumour, the bone cortices and the growth plates in this skeletally immature patient

Once the imaging is sufficiently processed and the patient bone is sufficiently thresholded, the overall mask is then segmented into different bones (Fig. 14.3). This process is called segmentation and again, can be highly dependent and the operators skill and experience. These segmented masks can then be converted into 3D models of the bone (Fig. 14.4).

Implant Design

Pre-operative Planning

Once the 3D model of the bone is obtained, it allows for easier review of the patient's condition and rotating the view enables closer inspection of the details. Having been presented with this data, it is then the surgeon's responsibility to determine the oncological margins and associated resection levels. The surgeon communicates this with the design engineer through annotations on multiple images in various views. The design engineer will then translate these lines in to the 3D planning software representing the resection planes and segments the models further, in effect showing the plan, pre-resection and post resection (Fig. 14.5).

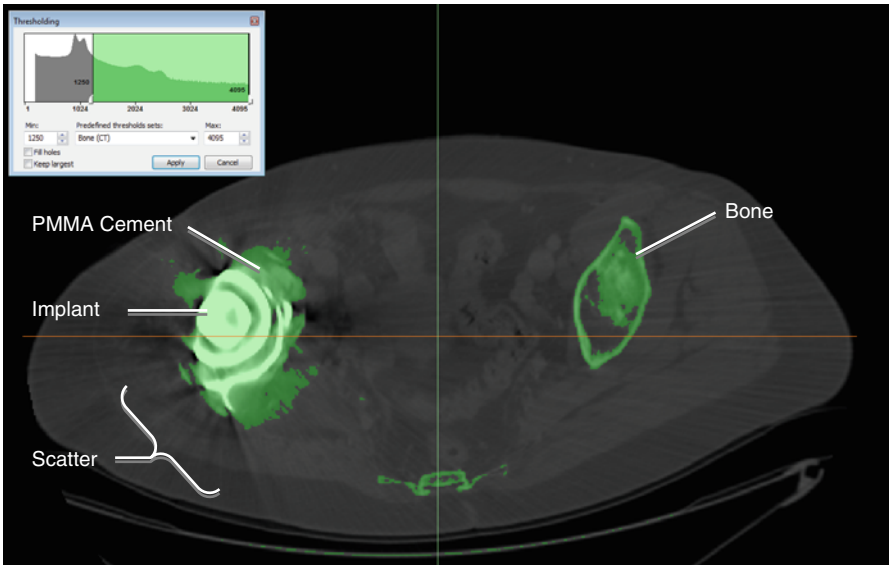

Fig. 14.3 Thresholding with artifacts and scatter caused by the implants in-situ

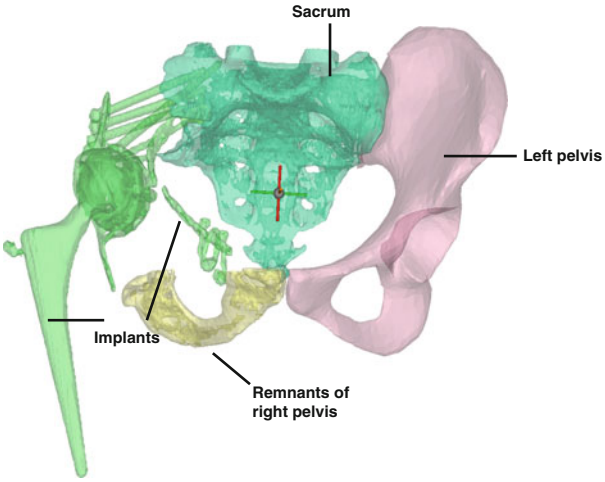

Fig. 14.4 The 3D models of the remaining pelvis, sacrum, implant and metal work

Modelling Implant Body

Once both the surgeon and engineer agree with the planning, the engineer can model the implant body. Many CAD techniques may be used from extruding and revolving, to more sophisticated sheet based and freeform modelling tools such as sweep along guides and cross sections (Fig. 14.6). In essence the engineer will create the implant body in the space that is left by the resection, usually as a simplified geometry of the bone being replaced.

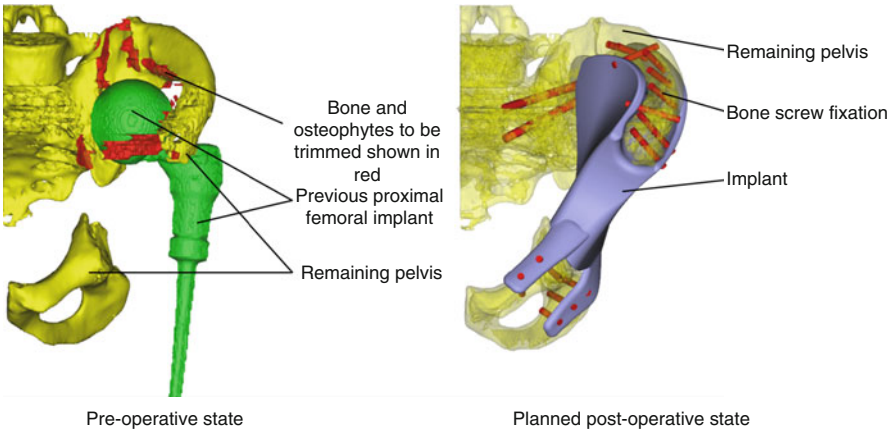

Fig. 14.5 Example of computer aided planning, showing the patients pre-operative state and the planned post-operative outcome

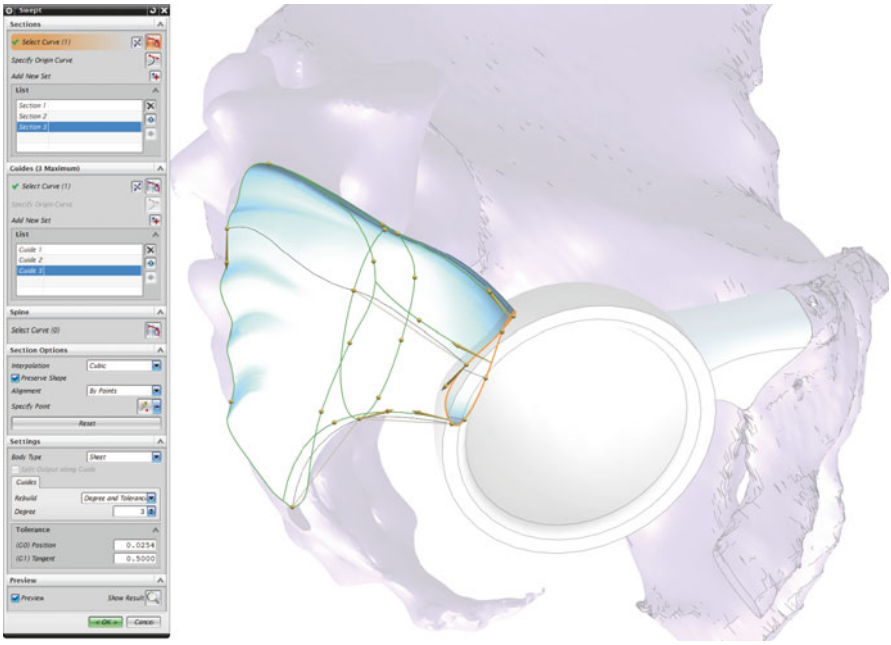

Fig. 14.6 Part of a Hemipelvis implant body being modelled in Siemens NX using the "Swept" tool

Modelling Fixation

The fixation of the device on to the bone and the interface between the two requires the design to be at its most precise. Typically when the resolution of images allow, fixation interfaces are designed to sit as close as 200 µm to the bone, without interference. The type of fixation used varies depending on the skeletal location, age of

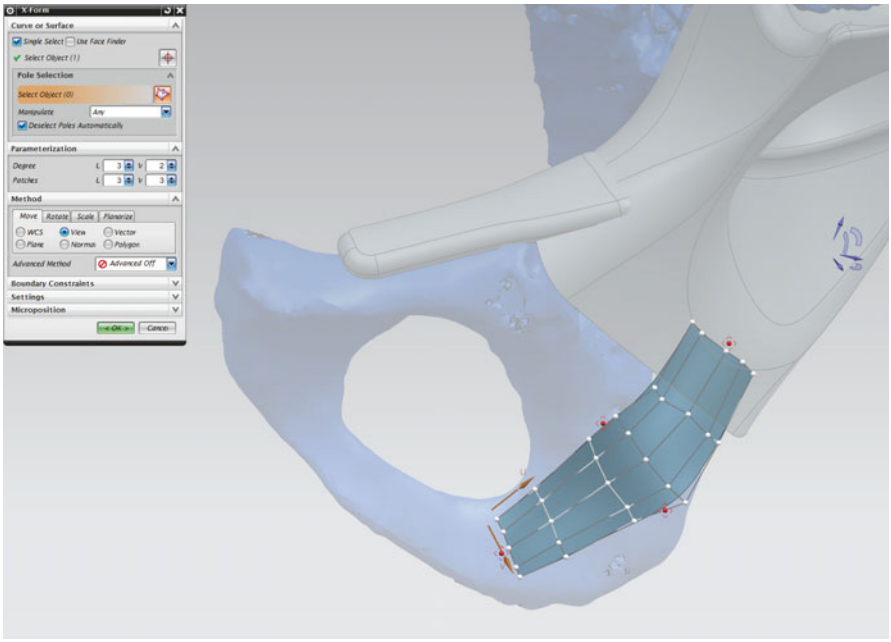

Fig. 14.7 Modelling extra-cortical plates to match contour of the bone in Siemens NX using the "X-Form" tool

the patient, quality and geometry of remaining bone, and the loading the implant body will sustain.

Both cemented and cemented intramedullary stems are often used when fixing into the medullary canals of long bones. However the choice between cemented and uncemented is largely dictated by the skeletal location, patient age, quality of bone and the surgeon's preference. For shorter fragments of bone, such as joint saving implants, short internal fins, and extra-cortical plates are often used. Bone screws are used to achieve immediate short-term fixation between the extra-cortical plates and bone. However as the bone grows across the interface and on to the HA coated implant and extra-cortical plates, the loading is transferred from the screws on to the plates. Extra-cortical plates are also used in pelvic and acetabular reconstructions, again with the aid of HA coating and bone to achieve sufficient fixation (Fig. 14.7).

Once the design process is complete, it is presented to the surgeon. The implant model is converted to a 3D portable document file (pdf) along with the model of the bone, allowing the surgeon to closely inspect the implant in relation to the bone. Any further changes are made and the design is finalised. At this stage the manufacturing drawings are detailed and ready for production.

Finite Element Analysis

Currently finite element analysis is not used to evaluate designs for patient specific cases. The many simplifications, unknowns and sources of error are all factors that, when combined, equate to unreliable results that add little value to the design process. The time consuming nature of meaningful FEA also makes it impractical for application to urgent patient specific limb salvage cases.

Manufacturing

The two most common manufacturing techniques for complex implants are through the more traditional CNC (Computer Numeric Controlled) techniques and the increasingly popular route of AM. The machining path is considered by the design engineer during the design process, as it could become a limiting factor in the design, if the degree of complexity of the design prevents it from being manufactured.

CNC Milling

The CAD model of the file is converted to numerical commands for CNC milling machines via a post processor. These commands then control the path of the tool, cutting away excess material from a bar of metal until the required shape of the implant is remaining. Multi-axis CNC machines allow for more complex shapes to be achieved without manual intervention by the operator. They also typically allow for an enhanced surface finish of complex surfaces than conventional 3 axes machines. Support structures to aid the stability of component whilst being machined are often modelled on to the implant to allow for further processes such as drilling of holes or manual finishing of the implant such as polishing.

ALM

ALM technology presents the designer with fewer limitations on the complexity of the design, as it allows for shapes to be fabricated layer by layer, using either a focused laser or electron beam to melt a layer of Ti-6Al-4 V or Co-29Cr-6Mo alloy powder. The selected layer portions which are melted are then added to the build direction until the final geometry of the implant is built. This manufacturing technique allows for the designer to explore new ways of achieving better fixation. For example, the placement of porous regions along the interface allows for greater possibility of bony in-growth on to the implant. Furthermore, by introducing porous

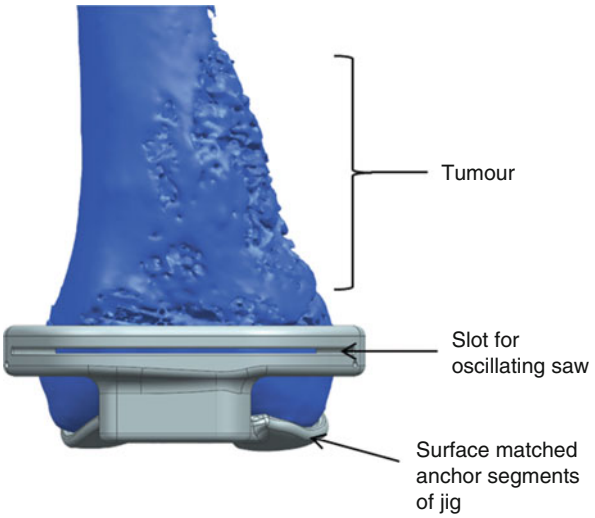

Fig. 14.8 A cutting guide for a distal femoral joint saver

scaffold and attempting to match the stiffness of the bone the engineer can attempt to prevent the phenomena of stress shielding. While ALM is a vital tool for manufacturing freeform and organic shapes, it still requires manual processing in the form of removing support struts, cleaning up holes and polishing.

Coordinate Measurement Machine (CMM)

As the complexity of implant designs increase, quality-control inspection and verification becomes more challenging using conventional methods. The latest CMM technology allows for 3D verification of the implant against the CAD model, enabling quality engineers to quickly and efficiently determine deviations from the model.

Patient-Specific Cutting Jigs

In order for surgeons to replicate difficult resection planes and osteotomies, the design engineer can produce patient specific cutting jigs. These jigs allow for the surgeons to achieve a cut in the exact position and orientation as planned during the design phase, ensuring a precise match between the remaining bone and implant. Correct positioning of the jig is achieved by designing the contact surface to match the exact contour of the bone, so the inside surface of the jig locks against the bone. Once positioned correctly, bone pins are inserted through a choice of holes in various positions into the bone in order to fix the jig in place. The jig features slots with boundaries that constrains the surgeons' oscillating saw to the plane of the planned resection (Fig. 14.8).

These jigs enable the surgeon to be much more adventurous with their planning and allows for multi-planar resections to be made considerably easier. This in turn

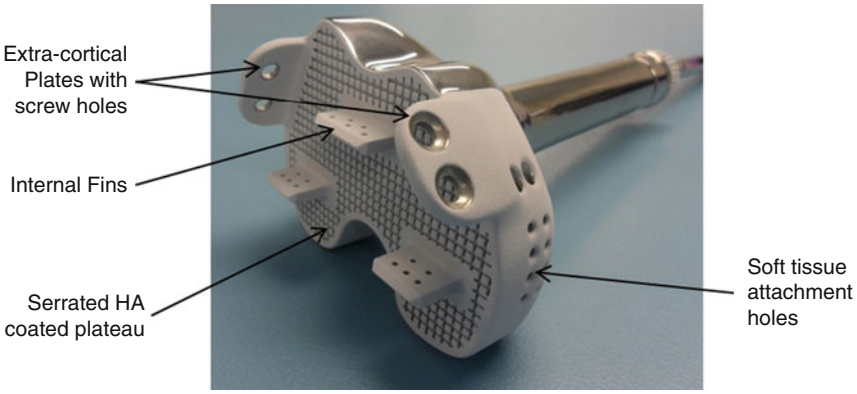

Fig. 14.9 Distal end of an anatomically-shaped distal femur joint saving implant

allows the designer to design more sophisticated implants. One particularly useful application of such jigs is for joint saving distal femoral implants (Fig. 14.9). With tumours that are relatively close to the joint, but not affecting the adjacent bone, surgeons tend to not only remove the affected bone, but also sacrifice the joint. However, provided that the surgeon can achieve an adequate resection margin from the tumour, the joint can be preserved and the design engineer can produce a design which features extra-cortical plates which encapsulate the remaining bone along the periphery, with additional internal fins and hydroxyapatite coating which encourage bony in-growth on to the implant. The cutting jigs prove their worth in this scenario, as even the slightest discrepancy between the planned resection and achieved cut means that the implant may not fit. This is due to the cross sectional profile of the bone varying considerably depending on the position and orientation of the cut.

Navigation and Robotics

The design engineer can also interface with navigation and robotic assisted surgeon equipment. It is crucial that the 3D geometry design is faithfully transferred and therefore it is essential that implant designers and navigation/robotic systems develop work closely together to have a common language and standard points of reference.

Stanmore Implants Worldwide Clinical Experience Using Additive Manufacturing

The first clinical application using selective laser sintering fabrication of a titanium alloy implant using the design processes described above was undertaken in November 2010. A 62 year old male with a malignant tumour of the pelvic wing

required an extensive resection. A 3 dimensional model was created from CT scans, from which the implant was designed. Key features of the implant design included extensive lattice structures at the bone interfaces, transverse sacral bolts and integral flanges anterior and posterior to fix the implant to the bone. The lattice structures were hydroxyapatite coated to encourage bone integration. The pelvic device was implanted with the aid of navigation. At 6 months, following an uneventful rehabilitation, the patient was fully weight bearing with a stick. At 24 months the patient remains active and reviewing the radiographs there was the appearance of bony ingrowth into the lattice structure. A further 13 hemi-pelvic replacements, all for oncology have been implanted. The pelvic resections were predominantly extensive (Types I+II, I+II+III and I-S). Most have incorporated multiple faceted resections and have been aided by navigation and/or patient specific cutting guides. Two cases required resection of the SI joint and the implants were designed with lattice structures to permit osseointegration along the joint interface. In November 2011, the first AM built scapula was implanted and this has been followed by a further 8 devices (8 oncology, 1 non-union). To date there have been no prosthetic related complications reported. This early use of Advanced Manufacturing as an additional manufacturing route for patient specific limb salvage implants has been very encouraging.

Discussion

Throughout the 60 years of orthopaedic bone and joint reconstruction there has been a continuing need for custom-made bone and joint implants in complex joint arthroplasty and limb salvage. Orthopaedics has capitalised on the digital revolution and has adapted technologies and advanced tools to enable implant design engineers working with surgeons collaboratively to visualise, plan and execute designs, manufacture implants and place them precisely. Although the clinical performance of custom-made implants can be outstanding plus their ability to addresses reconstruction problems that are beyond the scope of off-the-shelf implants, the use is very limited, with a range of objections cited. Objections cited include cost of the device, the amount of time required to meet critical surgical deadlines, availability, the lack of perioperative flexibility, and difficult of achieving precise placement. It is discussed here, that combined, the 3 dimensional computer-assisted design, visualisation manufacturing and navigational capabilities are addressing these objections. In addition, the advancements are kick-starting the development of the next generation of more functional implants, in a sector that over the last decade has seen little product improvements.

It is often claimed that the cost of custom-made implants are considerably more expensive than off-the-shelf implants. Although on an implant per implant this is typically true it is important to evaluate the total procedural costs from pre-planning through surgery and continue to include long-term performance and reduction in costly revision procedures. Throughout the design and production process cost-reduction actions are being pursued. The pre-planning and modelling processes can

now be swiftly undertaken with modern desktop PCs. Early PC-based 3D visualisation and rendering software packages were extremely slow typically taking hours or even days to build models whereas this can be undertaken in a matter of minutes. The complete array of design processes can now be achieved in hours rather than days. This not only impacts costs but also has a significant impact on reducing the overall time for supply of the device in time-critical tumour surgery. Plus the rapid transfer of huge digital data files of rendered implant and bone models enables designers and surgeons to work closely together irrespectively of where they are in the world.

In recent years due to the technology advances surgeons are pushing the boundaries seeking solutions for more extreme cases [29]. Implant designs have become more complex and this has led to a greater need for interfacing with navigation systems or for the design and production of patient specific cutting guides. The integration of the planning, design, manufacturing and navigation software permit the rapid and accurate transfer of 3D data has enabled the designers to produce sophisticated designs within the same time envelope as previous. Additive manufacturing (AM) is being hailed by the aerospace and automotive industries as a paradigm shift in fabrication offering unique capabilities and significant time and cost savings. The orthopaedic sector has been slow to adopt AM in part due to the regulatory pressures, the vast installed base of conventional manufacturing plant, its novelty, and economic viability. The Italian based Lima Corporate (Udine, Italy) have lead the way and offer a diverse range of AM fabricated acetabular shells. The advantages and cost savings of additive manufacturing have been misrepresented by comparing solely additive with conventional manufactured material costs. However, additive manufactured implant components typically require post-build precision conventional machining and more extensive cleaning processes. Cronskar in her thesis [9] and associated papers [10, 11] has eloquently described the advantages of using additive manufacturing in the production of custom-made implants. Their studies have shown that the finished item cost can be 35 % cheaper when compared with comparable subtractive manufactured components. It is key that additive manufacturing be recognised as an adjunct to the implant manufacturers' capabilities and not as an alternative. Additive manufacturing offers the opportunity to build structures that would be impossible via conventional subtractive methods irrespective of costs. For example building deep structured anisotropic lattices that have been designed specifically to encourage tissue ingrowth or the free-form fabrication of the implant/bone interface in order to preserve tissues and improve functional outcomes [15, 18].

The 'off-the-shelf' availability of modular reconstruction implants is a distinct advantage in trauma or periprosthetic fractures need to be reconstructed. In cases of primary bone tumour, severe failing standard joint replacements and joint arthroplasty in cases of complex bony anatomy, the need for immediate availability is rare. In virtually all cases there is adequate time for the surgeon and implant manufacturer to work together to produce the best reconstructive solution. Typical turnaround time for custom implant solutions is 3 weeks. This can be shortened if there is a time-critical need for example when a bone tumour is not responding to treatment and when there are cases of complex bony anatomy then the design and

planning phases may be protracted but rarely is the patient requiring urgent reconstructive surgery. Current modular reconstruction systems provide the surgeon with an array of components permitting options during surgery. In stark contrast, with a custom-made implant there are no or limited options at the time of surgery. In tumour reconstruction, pre-planning of the resections is an essential step and only in exceptional circumstances would surgeons deviate from the plan during the resection. Therefore a custom-made implant will provide the preferred solution as the implant will be designed to the skeletal dimensions of the patient keeping the resection to a minimum and the intra-medullary stems can be set to natural curvature of the recipient bone. The same can be said for reconstructions for complex bony anatomy but revising of failing joint and bone replacements poses the surgeon and engineers a series of 'what if' scenarios. Modular systems have the advantage that they can address most of the 'what if' scenarios for example bone integrity and quality around a failing hip stem. Visualising 3D images and the ability to produce polymeric rapid prototypes for closer assessment of the 3D bony geometry the experienced surgeon and designer can help to foresee potential complications. With adequate preplanning and assessment custom designs can provide surgeons with a degree of flexibility during the reconstructive surgery and if required a modular system can be on standby if unexpected complications are encountered.

Long-term clinical studies of precision-fitted patient specific femoral hip stems and patient specific distal femoral replacements have demonstrated no cases of aseptic loosening in the former [17] and remarkably low in the latter [6]. It has yet to be demonstrated that although the initial cost of accurately placed personalised implants can be higher than comparable off-the-shelf devices, the excellent long-term performance and associated reduction in implant-related failures and subsequent costly revision procedures may result in lower overall lifetime costs. It is considered that accurate placement of an anatomically matching designed implant is a major factor in achieving long-term implant survival. Studies have shown that freehand cuts in the pelvis may deviate as much as 11 mm from the desired target [2]. When designing custom made implants, this magnitude of error in the location and orientation of the resection plane, may cause the implant to not fit as intended or become completely unusable. This clearly necessitates for aids to help the surgeon achieve the desired and planned resection. Whilst a precision implant, designed to match the geometry of the patient may seem like an ideal solution, with increasing complexity of bone cuts, it becomes less likely that the surgeon can replicate the cut freehand as planned per the design software. It is essential that the 3D data transmissions between imaging, design, manufacturing in its various forms and navigation software does not corrupt or miscalculate the geometry. Studies have shown that there are concerns with the accuracy of imaging and in particular between various modalities [1]. Inaccuracies in the early phases will then be perpetuated through the whole process. In this complex 3D dimensional working environment where the digital technologies are evolving rapidly, data integrity is paramount. The positional accuracy of patient specific cutting guides has also been evaluated. Whilst some large studies have shown that there is accuracy improvement [5, 21], others were not able to demonstrate superior accuracy comparing

patient specific with conventional cutting blocks [3, 4, 8]. Slamin and Parsley [25] considered that it requires patient specific cutting guides to be used in combination with patient specific implants to enhance the overall implant performance. They also considered that the combined technology could shorten operating times and improve better implant placement. Our early experiences of using patient specific cutting guides with our custom implants does provide the surgeon with greater confidence and early indications show that implants are being positioned correctly but rigorous studies need to be undertaken to evaluate the accuracy and position and whether in the long-term this further enhances the functional longevity.

It is considered here that the acme of custom implants is dawning. The greatest opportunities lie by integrating and maximising the potential of the advanced 3D design and manufacturing processes with the computer-assisted precision placement techniques to further advance the performance of patient specific bone and joint replacements.

References

1. Asada S, Mori S, Matsushita T, Nakagawa K, Tsukamoto I, Akagi M. Comparison of MRI- and CT-based patient-specific guides for total knee arthroplasty. Knee. 2014. 21(6):1238–43. pii: S0968-0160(14)
2. Cartiaux O, Banse X, Paul L, Francq BG, Aubin CÉ, Docquier PL. Computer-assisted planning and navigation improves cutting accuracy during simulated bone tumor surgery of the pelvis. Comput Aided Surg. 2013;18(1–2):19–26.
3. Cavaignac E, Pailhé R, Laumond G, Murgier J, Reina N, Laffosse JM, Bérard E, Chiron P. Evaluation of the accuracy of patient-specific cutting blocks for total knee arthroplasty: a meta-analysis. Int Orthop. 2014;39(8):1541–52.
4. Chareancholvanich K, Narkbunnam R, Pornrattanamaneewong C. A prospective randomised controlled study of patient-specific cutting guides compared with conventional instrumentation in total knee replacement. Bone Joint J. 2013;95-B(3):354–9.
5. Cheng T, Zhao S, Peng X, Zhang X. Does computer-assisted surgery improve postoperative leg alignment and implant positioning following total knee arthroplasty? A meta-analysis of randomized controlled trials? Knee Surg Sports Traumatol Arthrosc. 2012;20(7):1307–22.
6. Coathup MJ, Batta V, Pollock RC, Aston WJ, Cannon SR, Skinner JA, Briggs TW, Unwin PS, Blunn GW. Myers Long-term survival of cemented distal femoral endoprostheses with a hydroxyapatite-coated collar: a histological study and a radiographic follow-up. J Bone Joint Surg Am. 2013;95(17):1569–75.
7. Cobb JP, Ashwood N, Robbins G, Witt JD, Unwin PS, Blunn G. Triplate fixation: a new technique in limb-salvage surgery. J Bone Joint Surg Br. 2005;87(4):534–9.
8. Conteduca F, Iorio R, Mazza D, Ferretti A. Patient-specific instruments in total knee arthroplasty. A review of current literature. Int Orthop. 2014;38(2):259–65.
9. Cronskär M. The use of additive manufacturing in the custom design of orthopedic implants. Thesis for the degree of Licentiate of Technology, Östersund; 2011.
10. Cronskar M, Rannar L-E, Backstrom M. Implementation of digital design and solid free-form fabrication for customization of implants in trauma orthopaedics. J Med Biol Eng. 2012;32(2):91–6.
11. Cronskar M, Backstrom M, Rannar L-E. Production of customized hip stem prostheses – a comparison between conventional machining and electron beam melting (EBM). Rapid Prototyping J. 2013;19(5):365–72.
12. Dunstan E, Tilley S, Briggs TW, Cannon SR. A customised replacement for polyostotic fibrous dysplasia of the upper femur. A 51-year follow-up. J Bone Joint Surg Br. 2005;87(1):114–5.

13. Höll S, Schlomberg A, Gosheger G, Dieckmann R, Streitbuerger A, Schulz D, Hardes J. Distal femur and proximal tibia replacement with megaprosthesis in revision knee arthroplasty: a limb-saving procedure. Knee Surg Sports Traumatol Arthrosc. 2012;20(12):2513–8.
14. Hwang N, Grimer RJ, Carter SR, Tillman RM, Abudu A, Jeys LM. Early results of a non-invasive extendible prosthesis for limb-salvage surgery in children with bone tumours. J Bone Joint Surg Br. 2012;94(2):265–9.
15. Lopez-Heredia MA, Goyenvalle E, Aguado E, Pilet P, Leroux C, Dorget M, Weiss P, Layrolle P. Bone growth in rapid prototyped porous titanium implants. J Biomed Mater Res A. 2008; 85(3):664–73.
16. Lundh F, Sayed-Noor AS, Brosjö O, Bauer H. Megaprosthetic reconstruction for periprosthetic or highly comminuted fractures of the hip and knee. Eur J Orthop Surg Traumatol. 2014;24(4):553–7.
17. Muirhead-Allwood SK, Sandiford N, Skinner JA, Hua J, Kabir C, Walker PS. Uncemented custom computer-assisted design and manufacture of hydroxyapatite-coated femoral components: survival at 10 to 17 years. J Bone Joint Surg Br. 2010;92(8):1079–84.
18. Murr LE, Gaytan SM, Medina F, Lopez H, Martinez E, Machado BI, Hernandez DH, Martinez L, Lopez MI, Wicker RB, Bracke J. Next-generation biomedical implants using additive manufacturing of complex, cellular and functional mesh arrays. Philos Trans A Math Phys Eng Sci. 2010;368(1917):1999–2032.
19. Murr LE, Gaytan SM, Martinez E, Medina F, Wicker RB. Next generation orthopaedic implants by additive manufacturing using electron beam melting. Int J Biomater. 2012; Article ID 24572. Epub 2012 Aug 21.
20. Myers GJ, Abudu AT, Carter SR, Tillman RM, Grimer RJ. Endoprosthetic replacement of the distal femur for bone tumours: long-term results. J Bone Joint Surg Br. 2007;89(4):521–6.
21. Ng VY, DeClaire JH, Berend KR, Gulick BC, Lombardi Jr AV. Improved accuracy of alignment with patient-specific positioning guides compared with manual instrumentation in TKA. Clin Orthop Relat Res. 2012;470(1):99–107.
22. Paul HA, Bargar WL, Mittlestadt B, Musits B, Taylor RH, Kazanzides P, Zuhars J, Williamson B, Hanson W. Development of a surgical robot for cementless total hip arthroplasty. Clin Orthop Relat Res. 1992;285:57–66.
23. Picardo NE, Blunn GW, Shekkeris AS, Meswania J, Aston WJ, Pollock RC, Skinner JA, Cannon SR, Briggs TW. The medium-term results of the Stanmore non-invasive extendible endoprosthesis in the treatment of paediatric bone tumours. J Bone Joint Surg Br. 2012;94(3):425–30.
24. Scales JT. Prostheses in the management of bone cancer. Br Med J (Clin Res Ed). 1983;287(6394):761–2.
25. Slamin J, Parsley B. Evolution of customization design for total knee arthroplasty. Curr Rev Musculoskelet Med. 2012;5(4):290–5.
26. U.S. FDA. Paving the way for personalised medicine. FDA's role in a new era of medical product development. U.S. Department of Health and Human Services. U.S. Food and Drug Administration. October 2013.
27. Unwin P. The mechanical reliability of non-invasive extendible implants: an engineering perspective. International Society of Limb Salvage. 16th General meeting. Beijing, 15th–18th Sept 2011.
28. Wafa H, Grimer R, Carter S, Tillman R, Abudu A, Jeys L. Retrospective evaluation of the incidence of early periprosthetic infection with silver-treated custom megaprostheses in high risk patients: case control study international society of limb salvage. 17th General meeting. Bologna, 11th–13th Sept 2013.
29. Wong KC, Kumta SM, Chiu KH, Cheung KW, Leung KS, Unwin P, Wong MC. Computer assisted pelvic tumor resection and reconstruction with a custom-made prosthesis using an innovative adaptation and its validation. Comput Aided Surg. 2007;12(4):225–32.

Chapter 15
Patient's Specific Template for Spine Surgery

Paolo D. Parchi, Gisberto Evangelisti, Valentina Cervi, Lorenzo Andreani, Marina Carbone, Sara Condino, Vincenzo Ferrari, and Michele Lisanti

Abstract Currently, Pedicle screws are positioned using a freehand technique or under fluoroscopic guidance. Although computer navigation has improved its accuracy over the last years, image guided navigation has still little use among physicians for orthopaedic surgeries. This is because computer assisted surgeries are very expensive, specially the required equipment, and also has difficulties related to use. The drill must be perfectly orientated following the navigator screen, which is no easy task to perform. A new asset for pedicle screw placement is to use a robotic platform, which reduces misplacement. However, it is too expensive and its learning curve can take a long time to be completed. In some cases this kind of technology must not be useful and practical. A third solution for pedicle screw placement is to use Patient's Specific Templates, which is less expensive and less complex to learn. This alternative is stable at a unique position, easy to use, easy to place (with high reproducibility), less invasive and more accurate. The time from design to production of one template is short, although it depends by the familiarization with the software used (time spent for the preoperative planning and the template design) and by the 3D printer used. Previously planned surgeries reduce costs and the time spent in the operating room during a procedure because surgeons can predict and perform the surgery before the real operation. Furthermore the use of patient's specific templates can save surgeons from potential errors, and consequently additional costs for the health system due to additional treatments or legal reasons.

Keywords Freehand technique • Fluoroscopic guidance • Robotic platform • 3D printers • Preoperative planning

P.D. Parchi, MSc, Phd (✉) • (✉) • G. Evangelisti, MSc • V. Cervi, MSc
L. Andreani, MSc, PhD • M. Lisanti, MSc
1st Orthpedic and Traumatology Division – Department of Traslational Research and New Technology in Medicine and Surgery, University of Pisa, Via Paradisa, 2, Pisa 56124, Italy
e-mail: paolo.parchi@unipi.it; gisberto85@hotmail.it; valentinacervi@virgilio.it; l.andreani@hotmail.it; lisanti@med.unipi.it

M. Carbone, MSc, PhD • S. Condino, MSc, PhD • V. Ferrari, MSc, PhD
EndoCAS – Department of Translational Research and of New Surgical and Medical Technologies, University of Pisa, Via Paradisa 2, Pisa 56124, Italy
e-mail: marina.carbone@endocas.org; sara.condino@endocas.org; vincenzo.ferrari@endocas.org

L.E. Ritacco et al. (eds.), *Computer-Assisted Musculoskeletal Surgery: Thinking and Executing in 3D*, DOI 10.1007/978-3-319-12943-3_15

Introduction

Pedicle screw fixation to stabilize spine fusion is the gold standard amongst posterior instrumentation techniques. However, screw positioning remains difficult, due to variations in anatomical shapes, dimensions and orientation, which can determine the inefficacy of treatment or severe damage to adjacent structures especially in thoracic and cervical surgery. Currently, pedicle screws are positioned using a free-hand technique or under fluoroscopic guidance, with error in the range 10–40 % depending on the skill of the surgeon [1–3]. Although the use of computer navigation has significantly improved the accuracy in screws placement in spine surgery, a meta-analysis of perforation risk for computer-navigated pedicle screw insertion estimated the overall risk as 6 % [4]. Moreover Image-guided navigation is used by a minority of surgeons, due to the high cost and difficulties related to use, with the need for a cumbersome localizer in the surgical setting and a registration procedure [5–8]. Furthermore, the image-guided technique requires correct positioning and orientation of the drill, following the navigator screen and keeping it stable during the drilling phase, a task which is not always simple to perform. An alternative promising technique for pedicle screw placement, which allows for automatic movement and fixing a hollow cylinder to guide the drill, relies on the use of a robotic platform [9, 10]. This technique significantly reduces screw misplacement but, as with almost all robotic solutions, it is expensive and its use requires a learning curve which can be lengthy. Indeed, for small hospitals which perform a limited number of spine stabilizations yearly, a robotic platform technique may not be practical.

A different image-guided approach, less expensive and less complex, is the use of patient's specific templates [11], which are similar to the approach used for dental implants or knee prosthesis. The first solution for pedicle screws placement based on patient's specific templates has been proposed by Van Brussel and Rademarcher at the ends of 90s [11, 12]. After this pioneering experience in the last 20 years several solutions have been proposed by several authors, aim of this chapter is to review all the papers published about the use of patient's specific templates in spine surgery. Each solution has been evaluated on the basis of the template design (single level/multi level, full contact/low contact, numbers of contact points …) and on the basis of the performed in-vitro/in-vivo trials.

General Concepts

In the literature over the years have been proposed many types of patient-specific surgical guides. In this section we try to analyze the various factors that can affect the use and efficacy of these surgical templates in the context of spinal surgery.

Fabrication Process (Biomodeling Process)

The surgical guides are manufactured using computer-aided design and rapid prototyping, and during surgery the pedicle screws are placed following predetermined entry points and orientation. Over the years several methods of template manufacture have been proposed ranging from milling, stereolithography to laser sintering technology. The accuracy in the whole process of creation of the template is an important factor that can influence the final result. Several steps can affect the accuracy of the template from the virtual construction to the production of the physical template. During construction of the 3D vertebral model, slice thickness and in-plane resolution of the CT scan and outline modeling are critical for creating an accurate template. The computer model then must be exported in STL format, and the STL format itself can reduce the accuracy of the template. When manufacturing the physical template using rapid prototyping, the rapid prototyping material can produce deformation. Although Rapid prototyping can reproduce complex designs with an high accuracy and versatility, all the rapid prototyping machines have a resolution limit.

Template Design

The template design is a key factor for its stability and usability in relation to soft tissue. The function of the personalized template is to guide a drill according to a preoperatively planned path. Therefore, the template should provide a correct and stable fit on the bony structures. To obtain a high accuracy and a high reproducibility of use between different operators it is necessary that for each vertebra there is only one stable position of the template (unique stable position).

As suggested from the studies of Berry and Merck the use of multi level designs is associated to a high error rate due to the changes in the relationship between each vertebral bodies from the CT acquisition to the surgical table [13–15]. To improve the accuracy for multi-level guides the CT-scan of spine has to be performed on patients lying in prone position to simulate similar facet joint relations as during the operating procedure [14, 15]. These problems are overtaken using a single level design in which the template fits only on one vertebra (articular processes, vertebral lamina, spinous process…) avoiding errors related to changes in spine position.

Up to now, the solutions proposed to guide pedicular screws can be divided in two main types on the basis of the relationship between template and the vertebral bone: (1) full contact templates (2) low contact templates.

Full Contact Designs

The template surface is created as the inverse of the vertebral posterior surface, thus potentially enabling a near perfect fit to the bone (lock-and-key solution); this kind of solution allow to have a perfect stability of the template on bone but it needs the perfect removal of all soft tissues which increases the invasiveness of the intervention [16–22]. The remaining soft tissue on the bone can introduce variations to the shape of the vertebrae. Therefore, it is important for the bone surface of the posterior lamina and the dorsal root of the spinous process to be stripped clean of any soft tissue avoiding alterations of the bone anatomy. Furthermore, reproducibility of the technique can be difficult, due to a lack of easy verification of correct or incorrect template positioning; to solve this problem some authors have suggested to use transparent materials [23].

Low Contact Designs

There are only small areas of contact between the template and the vertebral bone to reduce the problems related to the soft tissues removal [12, 13, 24–26]. In this kind of template is important an accurate choice of the location (anatomical landmarks) and the number of the supporting points are important to get the right balance between an easy placement in a unique position, a low invasiveness (soft tissue saving) and the template stability. The use of a small number of supporting points can determine the template instability and false-stable positions of the template, which consequently can lead to screws misplacement. It is also important the shape of the supporting points, some authors [13, 24, 27] suggest the use V- or U-shape knife edge supports other authors [25, 26] suggest the use of supporting points that reproduce the shape of the vertebral bone and a meticulous preparation of soft tissue at the level of the supporting points. Concerning the location of the supporting points most of the proposed solutions use of the spinous process as main reference to increase template placement accuracy on the vertebrae. Additional supporting points could be added to the vertebral laminae, to the articular processes and or to the transverse processes. As suggested from the study of Ferrari [25] to avoid the template instability it is necessary to use a redundant number of contact points and only when all the support points are perfectly in contact with the bone surface the template is in the right position. In this kind of templates during the surgical procedure it is important to avoid any tilting of the template, especially in the transversal plane. This can be achieved by a precise preparation of the soft tissues at level of contact-points on bone and applying a moderate pressure to the template to fix it on the vertebrae.

Clinical Studies

Aim of in this paragraph is to review the main clinical studies regarding the use of patient specific templates in spine surgery. There are few studies on humans, many of the studies are conducted on cadaver or in-vitro.

Cervical Spine

Due to anatomical issues, an accurate placement of screws in cervical spine and mid and upper thoracic spine is a difficult task. Its difficulty is related to the small dimensions of pedicles especially in these sites.

Transarticular C1-C2 fixation according to Magerl is a procedure not without risk, particularly for the vertebral artery, so in this context Goffin et al. presented cadaver studies and clinical results of a new technology with template and drill guide, designed to simplify and shorten the surgical act and enhance the accuracy of screw positions in the Magerl procedure [24]. Two series of cadaver studies were carried out. For the first series of five cadavers a template with clamps connecting only to the lamina of the second cervical vertebra, not considering the spinous process as interface, was tried out; for the second series of three cadavers the template was connected also to the spinous process. Two patients were then operated on using this technology. The results showed that the first device could not provide enough stability and accuracy because the rotational stability toward the lamina C2, without the spinous process, was insufficient and it led to an error in screw placement. Instead with the second template design both the entry points and screw trajectories were very satisfactory.

Berry et al. described the use of four different designs of personalized drilling guide templates produced by a selective laser sintering, to place 4 cervical screws, 32 thoracic screws, and 14 lumbar screws in four cadaveric spines [13]. The first design had three V-shaped knife edges that were positioned on the transverse and spinous processes, it was used to place screws in lumbar vertebrae. For the thoracic region, where the pedicles are narrower than in the lumbar region, the design was adapted by adding extra lateral supports and a threaded hole in which to fix a handle. When the authors found that even with the extra supports this design was unstable in the thoracic spine they produced e new design for the thoracic and cervical region. This third design had lateral cylindrical supports to fit on the posterior surface of the lamina, plus a posterior support to fit the spinous process. Surgeons observed that adding additional supports to enhance stability the third design had no failures, although the number of screws used in the cervical region was small. They concluded that templates can lead to successful screw placement, even in small pedicles, providing their design is optimized for the application area, e.g. with enhanced rotational stabilization.

Ryken et al. presented two studies regarding the design of personalized drilling guide for cervical pedicle screws implantation [20, 21]. The first study evaluated the feasibility of different rapid prototyping processes for manufacturing spine surgical templates, based on patient CT data and on predefined drilling trajectories [20], while the second study [21] was a laboratory investigation in which the designed guide was used for placing 3.5 mm pedicle screws in C3-7 vertebrae of 4 cadavers (20 templates). The drilling template fits the posterior surface of the cervical vertebra providing a larger contact surface. The surface of the template was created to be the inverse of the vertebral surface, potentially allowing the template to fit onto the vertebral surface in a lock-and-key fashion. Final placement of the screw was confined entirely within the pedicle in 19 of the 20 cases. The solution proposed

provided a good template stability, but it required the removal of soft tissue in order for the guide to come in contact with the vertebra bone structure.

Owen et al. presented a drill template for placement of a cervical pedicle screw in a single vertebral level [28]. A drill template with a predefined trajectory was constructed that was designed to match the posterior surface of the right side of the fifth cervical vertebra. Imaging and visual inspection confirmed accurate placement of cervical pedicle screw without cortical violation so the methodology is appeared to provide an accurate technique and trajectory and the feasibility of this patient-specific rapid prototyping technique was demonstrated.

Lu et al. presented the design process of two surgical guides for cervical vertebra C2 and lumbar vertebra L2, modelled in a surface-surface manner [16]. The template surface was created as the inverse of the vertebral posterior surface, thus potentially enabling a near-perfect fit. The guide is designed, as the most part of the solutions presented in the literature, considering the spinous process as major anatomical landmark. The accuracy of the drill templates was tested on 25 patients (14 male, 11 female, age 17–53 years) with cervical spinal pathology A total of 88 screws were inserted into levels C2–C7 with 2–6 screws on each patient [17]. Of these pedicle screws, 71 were in Grade-0, 14 in Grade-1, 3 in Grade-2, and no screw was in Grade-3. None of the cases had complications caused by pedicle perforation and especially there were no injury to the vertebral artery or to the spinal cord, nor was there a need for revision of pedicle perforation in any of the cases. As pointed out by the authors the use of this kind of template (full contact design) requires an accurate preparation of the bone surface, including thorough removal of the attached muscle and fat tissue without causing damage to the bony surface structure in order to ensure proper fit of the drill template on the lamina.

The anterior transpedicular screw (ATPS) technique merges the biomechanical merits of posterior transpedicular fixation with the surgical benefits of anterior approach only procedures, because it can increase initial construct stability in an anterior surgery which is believed to be best beneficial for some severe multilevel cervical instabilities. Therefore, accurate and biocompatible insertion of ATPS remains a challenge. To address this challenge, Fu et al. constructed a biocompatible drill template for ATPS insertion using 3D reconstruction, rapid prototyping production and reverse mold manufacture tecniques and they designed an in vitro study with 24 formalin-preserved cervical vertebrae (C2–C7) [22]. The authors found no significant differences between medial/lateral and superior/inferior deviations and they concluded that the patient specific drill template was easy to apply and accurate in assisting ATPS insertion.

Thoraco-Lumbar Spine

Low Contact Design Template

Van Brussel was the pioneer in the field of patient's specific template in spine surgery. In his papers about the use of patient specific surgical guides in cervical and lumbar spine he reported good results using a multiple knife-edge supporting

points template [12]. The surgical guides are produced by stereolithography. The authors evaluated two different template designs: a three contact points design (two on the transverse processes and one on the top of the spinal process), and a four point contact points design (two on the side faces of the spinal process rather than the top of it and the two on the transverse processes). The lumbar and cervical template designs are optimized by 3 series of cadaver studies including 18 cadaver's spines altogether. A total of 15 lumbar and 4 cervical templates are successfully applied in-vivo. In the spine high template stability was observed during application in vitro as well as in vivo. Soft tissue remainders did not compromise template stability and a unique position was found in all of the cases. All the screws that had been placed using the spinal templates were clinically successful. No cortex perforations were observed. None of the screw positions in the lumbar spine deviated more than 2 mm from the planned position at the screw ends. In the cervical spine all screws were placed with sub-millimeter accuracy. After their clinical trial the authors concluded that: (a) The contact area at the top of the spinal process must be smaller to minimize the posterior soft tissue removal (b) the use of a small contact area on the spinal processes requires the use of lateral bounds on the facet joints to add a sufficient stability to the template (c), the knife-edge support structures must be always perpendicular to the transverse processes to increase stability and to avoid sliding.

From the template design proposed by Van Brussel [12], Porada et al. developed a three V-shaped knife-edge supporting point template that was designed to rest on the surfaces of the transverse processes and on the spinous processes [27]. This template design had been tested on cadever (2 cadavers 14 pins) obtaining good results (no cortical pedicle perforation). As suggested by the authors the main limits of this design are the low template stability and the possible errors related to the soft tissue (using a tripod configuration it is very difficult to detect a false stable position if one of the three supporting points is not properly positioned because the other two supporting points could seem perfectly in contact with the bone).

In 2005 Berry et al. published a study in which four different template designs were tested [13]. The first design, similar to the design proposed by Van Brussel [12], had three V-shaped knife edges that were positioned on the transverse and spinous processes. Fourteen screws were placed in lumbar vertebrae using this template design without any cortex pedicle perforation. The first design was adapted for use in the thoracic region by adding extra lateral supports. Sixteen screws were placed in thoracic vertebrae using this design. The use of this template design in thoracic spine led to an high rate of screws misplacement (44 %) due to the template instability**.** The third design was produced for the thoracic and cervical regions when it was found that even with the extra supports the second design was unstable in the thoracic spine. This design had lateral cylindrical supports to fit on the posterior surface of the lamina, plus a posterior support to fit the spinous process. Four screws were placed in the cervical vertebrae and two in the thoracic vertebrae with this design. No screws were placed outside the pedicle. The last design tested is a multilevel design made to fit on two or three vertebrae at once on the transverse processes only. Fourteen screws were placed in the thoracic vertebrae with this multilevel design obtaining a high rate of screws misplacement (43 %).

The concept of a multi level template was newly proposed by Merc et al. [14]. A drill guide template was constructed with a surface designed to be the inverse of the dorsal part of facet joint. That was meant to enable a lock-and- key mechanism fitting the dorsal part of the facet to achieve minimal overlap. The parts of the template for each pedicle screw were connected to each other in the sagittal and transversal plane to achieve maximum stability of the template. Additionally, cylinders fitting a trajectory hole had been manufactured allowing temporary fixation of the drill guide with K-wires. The authors reported that the rate of cortical pedicle perforation associated to the use of this multi level design in thoracic spine is 11 % (versus 38 % of perforation rate in the free hand group). In another study published in 2014 the authors evaluated the in vivo error rate of pedicle screws implanted with the multilevel drill guides in comparison with the planned screws direction. Seventy-two screws were inserted in 11 patients. The post-operative CT evaluation showed that 19 screws (26 %) were implanted inaccurately [15].

Ferrari et al. in 2012 proposed a new multiple low contact points template design (Fig. 15.1) [25]. The main body of each template includes four main supporting points two at the level of the articular processes ("anterior shafts") and two at the level of the vertebral laminae ("posterior shafts") and a fitting area located on the sides of the spinous processes ("central shaft") that allows the simplification of the template alignment and that facilitates the template correct positioning. The internal surface of the central shaft is a little bit bigger in comparison with the spinous process surface because such as shaft, this one is added for the alignment of the template but it is not used to stabilize it. The base of each shaft is the complementary to the bone surface. The orientation of these shafts was chosen to maximize template stability. The template had been tested on porcine spine (Fig. 15.2). During the ex vivo animal

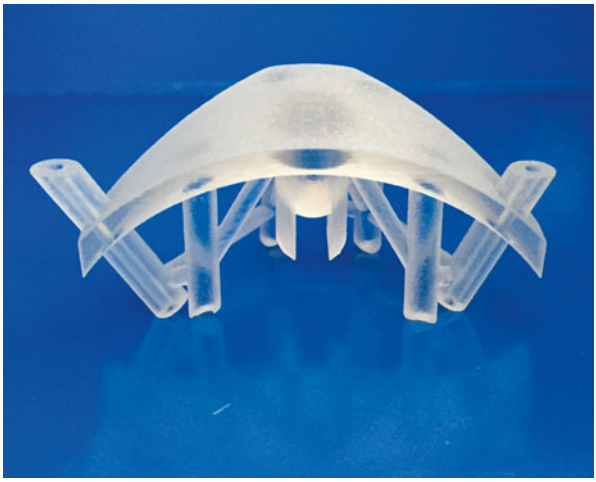

Fig. 15.1 Template Design. Ferrari et al. proposed a multiple low contact points single level template design

test sessions, the surgeon found that template alignment was easy, thanks to the fitting area on the side of the spinous process (Fig. 15.3). The positioning of the fitting area on the vertebral laminae and on the articular processes only required removal of the soft tissue under the bases, using an electric cutter. Sometimes the surgeon identified false-stable template positions because not all of the four fitting areas were actually in contact with the bone surface; thus, he proceeded to remove the remaining soft tissue (Fig. 15.4). The CT evaluation demonstrated that one of the 28 Kirschner wires

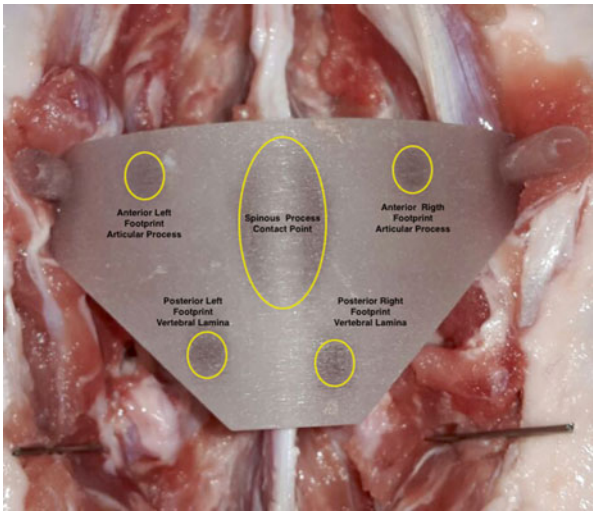

Fig. 15.2 Template Top View (ex-vivo study). There are 2 support points at the level of the articular processes ("anterior shafts"), 2 support points at the level of the vertebral laminae ("posterior shafts") and a a fitting area located on the sides of the spinous processes ('central shaft') that allows the simplification of the template alignment and that facilitates the template correct positioning

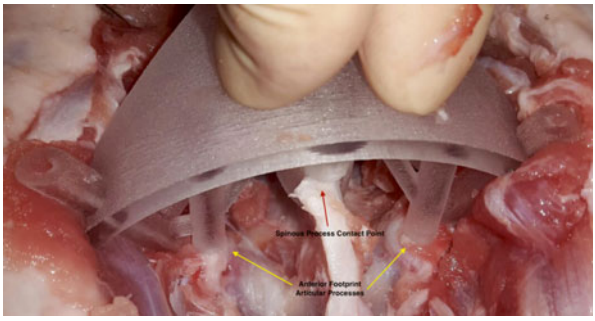

Fig. 15.3 Anterior Support Points on the Articular Processes [ex vivo study]. The presence of multiple contact points (4 or more) reduces the possibility to have a false-stable template positions; the template is well-placed only when all the fitting areas are in contact with the bone surface. In the case of the remaining tissue under the foot of a tripod, this can seem well-positioned because the other two feet are in contact with the bone

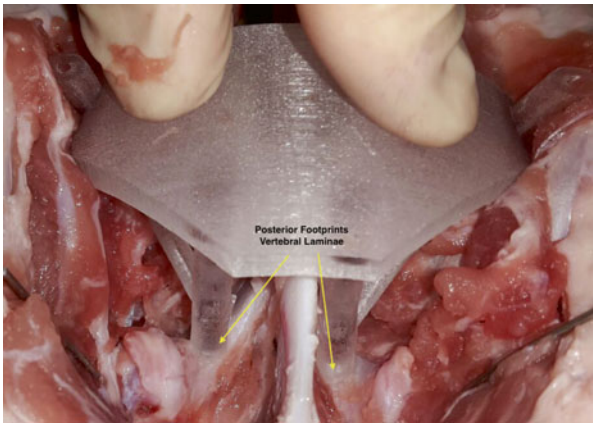

Fig. 15.4 Posterior Support Points on the vertebral laminae [ex vivo study]. The presence of multiple contact points (4 or more) reduces the possibility to have a false-stable template positions; the template is well-placed only when all the fitting areas are in contact with the bone surface

implanted using the template (3.5 %) had been incorrectly positioned (grade II pedicle cortex violation). The authors concluded that false-stable template positions are avoided using 4 or more fitting areas; the template is well-placed only when all four fitting areas are in contact with the bone surface. In the case of remaining tissue under the foot of a tripod, this can seem well-positioned because the other 2 feet are in contact with the bone.

Similar results have been reported by Tomnic et al. in 2014 with the use of multiple contact points design template in the thoracic spine (cadaveric study) [26]. The templates were specially designed to fit and lock on the lamina during the procedure anchoring at three sites – on the lamina at the base of the superior articular process on both sides and at the tip of the spinous process. The templates have a special metallic drill sleeve with inner hole corresponding to the drill bit diameter. These metallic sleeves also prevent formation of debris from the template itself during drilling. The CT Analysis showed that 13 out of 14 (92,9 %) screws were inside of pedicle trajectories without violation of pedicle wall with the tip inside of the vertebral body (Fig. 15.5). One screw violated medial pedicle wall in an "in-out-in" fashion.

Full Contact Template Design

To overcome the problems related to the template instability Sheng Lu et al. in 2009, proposed the use of a full contact design [18]. The template surface was created as the inverse of the vertebral posterior surface, thus potentially enabling a near-perfect fit (lock and key solution). This design had been tested on cadaver (6 lumbar spines) and on 6 patients with lumbar spinal pathology. 58 screws were inserted (36 in cadavers, 22 in patients) and no pedicle perforation was observed by postoperative CT scan. In another study published in 2012 the authors evaluate the

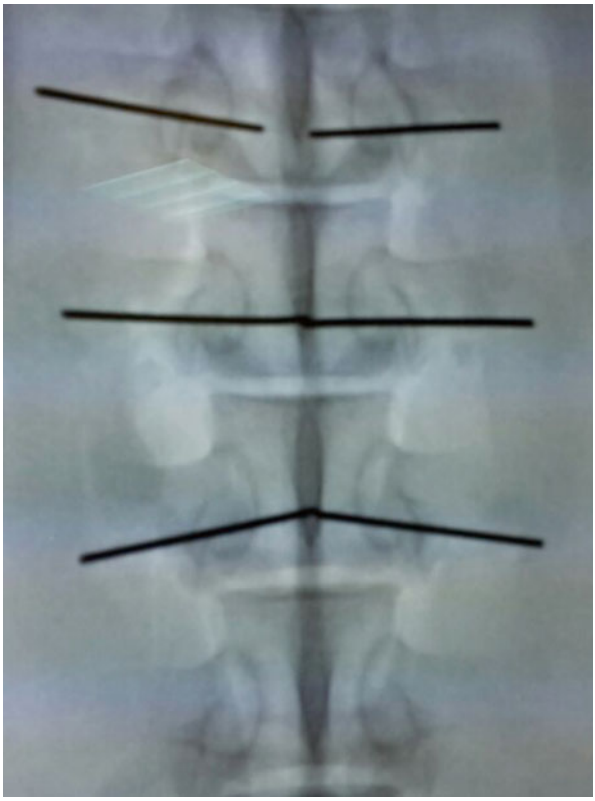

Fig. 15.5 The Template has been tested on an ex vivo animal test (porcine spine). The Postoperative Fluoroscopic Evaluation showed the correct a Kirschner wires alignment. The postoperative CT evaluation (performed after each test session) showed an error less than 1 mm in 93 % of the cases and between 1–2 mm in 7 % of the cases

accuracy of pedicle screws placement with the templates in a group of 16 patients with a thoracic scoliosis [19]. Of the 168 screws implanted 157 screws were considered intrapedicular, while 11 screws were considered to have a 0–2 mm breach without any pedicle screw brech more than 2 mm. As stressed by the authors to avoid screws misplacement a meticulous preparation of the bone surface was essential, including thorough removal of the attached muscle and fat tissue without damage to the bony surface structure.

The solution proposed by Sheng Lu [18] for the lumbar spine has been used by Ma et al. 2012 in the thoracic spine [22]. Twenty thoracic cadaver specimens were randomly divided into two groups the template group and the free-hand group. 480 pedicle screws were placed (240 screws for each group). In the template group, 224 screws were fully contained in the pedicles (Grade 0) and 16 screws exhibited pedicle wall violation (all of which were classified as Grade 1). In the free-hand group, 156 screws were fully contained in the pedicles (Grade 0) and 84 exhibited

pedicle wall violation. Screw misplacement in the template group were related mainly to an inadequate soft tissue preparation that led to a template wrong positioning. Accuracy of screw placement in the two groups was 93.4 % and 65 %, respectively. In the free-hand group, the accuracy of screw placement in the first five and the last five cadaver specimens was 55 and 75 %, respectively, whereas in the navigational template group the values were 91.6 % and 95 %, respectively (P [0.05]). Thus, there was an evident learning curve in the free-hand group that was not detected in the navigational template group.

To avoid the errors related to a template wrong positioning with the use of a full contact design Sugawara et al. in 2013 proposed to use three different templates for each level: a location template with 3-mm-diameter holes was made to mark the screw entry points on the lamina, a drill guide template to control the screw trajectory before screw insertion and a screw guide template to control screw insertion [29]. The authors tested this solution on study in 10 patients with thoracic or cervicothoracic spinal pathological entities. A total of 58 thoracic pedicle screws were inserted. Postoperative CT scans confirmed that no screws violated the cortex of the pedicles, and the mean deviation of the actual screw trajectory from the planned screw trajectory on the coronal plane at the midpoint of the pedicle was 0.87 ± 0.34 mm. Also with the use of three templates for each level the authors point out the importance of an accurate preparation of the soft tissues to ensure the perfect fit and lock of the templates on bone.

Discussion

Pedicle screw placement is usually performed using a free- hand technique, with high risk of screws malpositioning especially in cervical or thoracic spine or in presence of spine deformity. Robotic and image-guided solutions have been proposed to perform safer interventions, but the application is expensive and their use requires a learning curve that can be too long, particularly for small hospitals that perform a limited number of spine stabilization yearly [5–8]. Furthermore, surgical navigators require a cumbersome localizer in the surgical setting and a registration procedure to correctly position and orientation the drill following the navigator screen, and keep it stable during the drilling phase, a task which is not always simple to perform.

A different, less expensive, and less complex image-guided approach involves the use of patient's specific templates. An ideal Patient's Specific Template should be: stable in a unique position, easy to use, easy to place (with a high reproducibility), less invasive and very accurate. As emerged from the literature review each template should be designed to fit on one vertebra; all the multilevel templates manufactured until now, had low accuracy level due to the changes in the relationship between each vertebral bodies from the CT acquisition to the surgical table. The accuracy of placement mainly depends on the template design, the fitness between template and vertebra, and the surgical procedure. For the template design is important a right balance between template stability and ergonomics in relation to the soft

tissues. Templates that are designed as the inverse of the bone surface (full contact design) allow to obtain an high stability on bone (lock and knee mechanism) with an high level of accuracy at the clinical test but this kind of design needs a precise decortication of a large area of bone from soft tissues, which takes additional surgical time and increases the invasiveness of the procedure [16–22]. An inappropriate preparation of the soft tissues can result in a high level of error and screws misplacement. Templates that are designed to be fixed in its position by touching small parts of the dorsal elements of the spine in a few spots (e.g., V-shaped knife), had often limited or inappropriate accuracy due to the template instability [13, 24, 27]. As emerged from the study of Berry et al. the use of only three contact points can result in false-stable positions and it does not give to the surgeon the right feel in the use of the template [13].

Recent studies have re-proposed the use of small contact points or fitting areas, which are designed as the complementary likeness of the bone surface, not just a 'V shape' [25, 26]. This kind of design allows one to obtain template stability without increasing intervention invasiveness. It is important that the template design is optimized taking in account mechanical considerations to guarantee template stability, simple positioning and minimal intervention invasiveness. The presence of multiple contact points (4 or more) reduces the possibility to have a false-stable template positions; the template is well-placed only when all the fitting areas are in contact with the bone surface. In the case of the remaining tissue under the foot of a tripod, this can seem well-positioned because the other 2 feet are in contact with the bone. Nevertheless, in the case of multiple contact points, another foot would be far above the bone surface revealing a template false-stable position [25]. Regards the choice of the supporting points the majority of proposed designs using the spinous process as the main reference [13, 16–22, 24–27]; in our experience the spinous process is to be used as a reference point for the orientation and positioning of the template, but not as a support point for the presence of posterior ligaments that cover the bone [25]. The other supporting points can be fixed on the vertebral laminae, articular processes or transverse processes without great differences in terms of the template stability (the use of transverse processes requires a larger bone exposure), to increase the template stability it is important that the supporting points cover different planes to construct a stability area in which the center of gravity of the template must fall. The orientation of the supporting points has to choose to maximize template stability. For this reason, no tangential force must be imposed on the fitting areas to avoid the need for friction between the bone and the template to fix it and avoid sliding. Furthermore, the forces must be aligned with the shaft axes to prevent deformation, and consequently the deformation of the entire template. For these reasons the shafts should be positioned orthogonal to the bone surface [25].

As reported by the literature with the design optimization following the previous rules, the use of Patient's specific template to guide screws placement in spine surgery showed a high accuracy level.

The overall cost for the templates production is the sum of the cost of the software used to make the preoperative planning and to design the patient, the cost of

materials, the cost for the use of the 3D printer and the cost of the personnel dedicated to the template production. Often both the software used and the 3D printer are used in other researches and clinical works and this can eventually reduce the cost of the template. With respect to the costs related to the use of patient's specific templates those reported in literature are between 20 to 400 dollars [16–22, 24]. In our experience the cost to design and fabrication for a one level templates range from 50 to 100 euros and this cost progressively decreases at the increase of the numbers of the levels that have to be treated [25].

The time from design to production of one template range from few hours to several days and it depends by the familiarization with the software used (time spent for the preoperative planning and the template design) and by the 3D printer used. It is important to notice that all this time is spent before the surgery and it allow to reduce the surgery time and cost [16–22, 24, 25]. Furthermore the use of patient's specific templates will allow avoiding potential errors, and consequently additional costs for the health system due to additional treatments or legal reasons.

Conclusion

After the literature review we think that the template design should be based on the following considerations:

- The template must be fixed on the bone surface by small and thin-fitting areas, to avoid to increase the intervention invasiveness.
- Each fitting area must be positioned on easy-to-recognize bone zones, which are almost all exposed during the intervention.
- The template design must guarantee template stability during the intervention by forces that have to be applied on the template by the surgeon's hand.
- The template design must avoid the risk of wrong positioning due to the presence of residual soft tissue under the fitting areas.
- The template design must simplify alignment to avoid incorrect coupling of the fitting areas with the bone, and thus erroneous template fitting.

With an optimization of the design patient-specific template in spine surgery could offer several advantages:

- The use of the surgical guides allows to reproduce a precise preoperative planning with an high accuracy and it is important especially in the cervical and thoracic regions or in case of spine deformity when the radiographic landmarks can look distorted and obscured; the surgeon can decide location, orientation and the size of each screw based on the unique morphology of each vertebrae even before going to the operation table. The Preoperative CT/MRI evaluation allows to make a precise planning of the surgical procedure and this planning could be successfully transfer to surgical theatre using patient specific template instead of

navigation systems. With the exception of the multi level designs, there are no special requirements regarding patient positioning on the CT scanner bed because the template fits on the bone surface and the bone is not deformed if the patient decubitus is changed.

– Surgical templates are a simple solutions that require a very short learning curve [15, 22]. During the learning curve It is important to give to the surgeon, in addition to the surgical template the physical model of patient's spine, to check the right position of the template on the model before surgery. Lastly, the need for fluoroscopy during screw insertion is eliminated, which as a result considerably reduces the radiation exposure to the members of the surgical team.
– The use of surgical guides is relatively low cost solution. In contrast to the other computer assisted solutions proposed to guide screws placement in spine surgery, the use of patient specific templates eliminates the need for complex equipment and time-consuming procedures in the operation theatre, thus this technique reduces the duration of the surgical procedure and consequently of the overall cost of surgery. Because all the time spent to make the preoperative planning and to make the template is outside the surgical room. Furthermore the use of patient's specific templates do not require any registration procedures that is one of the main drawback of the most navigation/robotic systems.

Although there are few studies published in literature about the use of patient's specific template on human we think that this is a newly, low cost, promising computer assisted solution to guide screw placement in spine surgery. The main concerns regard the template accuracy and the standardization of their use and for these reasons further studies are necessary especially on humans.

References

1. Farber GL, Place HM, Mazur RA, et al. Accuracy of pedicle screw placement in lumbar fusions by plain radiographs and computed tomography. Spine (Phila PA 1976). 1995;20(13):1494–9.
2. Merloz P, Tonetti J, Eid A, et al. Computer assisted spine surgery. Clin Orthop Relat Res. 1997;337:86–96.
3. Wang VY, Chin CT, Lu DC, et al. Free-hand thoracic pedicle screws placed by neurosurgery residents: a CT analysis. Eur Spine J. 2010;19(5):821–7.
4. Shin BJ, James AR, Njoku IU, Härtl R. Pedicle screw navigation: a systematic review and meta-analysis of perforation risk for computer-navigated versus freehand insertion. A review. J Neurosurg Spine. 2012;17:113–22.
5. Amiot LP, Lang K, Putzier M, et al. Comparative results between conventional and computer-assisted pedicle screw installation in the thoracic, lumbar, and sacral spine. Spine. 2000;25(5):606–14.
6. Laine T, Lund T, Ylikoski M, et al. Accuracy of pedicle screw insertion with and without computer assistance: a randomised controlled clinical study in 100 consecutive patients. Eur Spine J. 2000;9(3):235–40.
7. Schwarzenbach O, Berlemann U, Jost B, et al. Accuracy of computer-assisted pedicle screw placement. An in vivo computed tomography analysis. Spine (Phila PA 1976). 1997;22(4): 452–8.

8. Ishikawa Y, Kanemura T, Yoshida G, et al. Clinical accuracy of three-dimensional fluoroscopy-based computer-assisted cervical pedicle screw placement: a retrospective comparative study of conventional versus computer-assisted cervical pedicle screw placement. J Neurosurg Spine. 2010;13(5):606–11.
9. Kantelhardt SR, Martinez R, Baerwinkel S, et al. Perioperative course and accuracy of screw positioning in conventional, open robotic-guided and percutaneous robotic-guided, pedicle screw placement. Eur Spine J. 2011;20(6):860–8.
10. Lieberman IH, Togawa D, Kayanja MM, et al. Bone-mounted miniature robotic guidance for pedicle screw and translaminar facet screw placement: Part I – Technical development and a test case result. Neurosurgery. 2006;59(3):641–50.
11. Radermacher K, Portheine F, Anton M, et al. Computer assisted orthopaedic surgery with image based individual templates. Clin Orthop Relat Res. 1998;354:28–38.
12. Van Brussel K, Vander Sloten J, Van Audekercke R, et al. A medical image-based drill guide for pedicle screw insertion: a cadaver study. J Biomech. 1998;31 suppl 1:39.
13. Berry E, Cuppone M, Porada S, et al. Personalised image-based templates for intra operative guidance. Proc Inst Mech Eng H. 2005;219(2):111–8.
14. Merc M, Drstvensek I, Vogrin M, Brajlih T, Recnik G. A multi-level rapid prototyping drill guide template reduces the perforation risk of pedicle screw placement in the lumbar and sacral spine. Arch Orthop Trauma Surg. 2013;133(7):893–9.
15. Merc M, Drstvensek I, Vogrin M, Brajlih T, Friedrich T, Recnik G. Error rate of multi-level rapid prototyping trajectories for pedicle screw placement in lumbar and sacral spine. Chin J Traumatol. 2014;17(5):261–6.
16. Lu S, Xu YQ, Zhang YZ, et al. A novel computer-assisted drill guide template for placement of C2 laminar screws. Eur Spine J. 2009;18(9):1379–85.
17. Lu S, Xu YQ, Lu WW, Ni GX, Li YB, Shi JH, Li DP, Chen GP, Chen YB, Zhang YZ. A novel patient-specific navigational template for cervical pedicle screw placement. Spine (Phila Pa 1976). 2009;34(26):E959–66.
18. Lu S, Xu YQ, Zhang YZ, et al. A novel computer-assisted drill guide template for lumbar pedicle screw placement: a cadaveric and clinical study. Int J Med Robot. 2009;5(2):184–91.
19. Lu S, Zhang YZ, Wang Z, Shi JH, Chen YB, Xu XM, Xu YQ. Accuracy and efficacy of thoracic pedicle screws in scoliosis with patient-specific drill template. Med Biol Eng Comput. 2012;50(7):751–8.
20. Ryken TC, Kim J, Owen BD, Christensen GE, Reinhardt JM. Engineering patient-specific drill templates and bioabsorbable posterior cervical plates: a feasibility study. J Neurosurg Spine. 2009;10(2):129–32.
21. Ryken TC, Owen BD, Christensen GE, Reinhardt JM. Image-based drill templates for cervical pedicle screw placement. J Neurosurg Spine. 2009;10(1):21–6.
22. Ma T, Xu YQ, Cheng YB, Jiang MY, Xu XM, Xie L, Lu S. A novel computer-assisted drill guide template for thoracic pedicle screw placement: a cadaveric study. Arch Orthop Trauma Surg. 2012;132(1):65–72.
23. Birnbaum K, et al. Computer-assisted orthopedic surgery with individual templates and comparison to conventional operation method. Spine. 2001;26(4):365–70.
24. Goffin J, Van Brussel K, Martens K, Vander Sloten J, Van Audekercke R, Smet MH. Three-dimensional computed tomography-based, personalized drill guide for posterior cervical stabilization at C1–2. Spine. 2001;26:1343–7.
25. Ferrari V, Parchi P, Condino S, Carbone M, Baluganti A, Ferrari M, Mosca F, Lisanti M. An optimal design for patient-specific templates for pedicle spine screws placement. Int J Med Robot. 2013;9(3):298–304.
26. Tominc U, Vesel M, Al Mawed S, Dobravec M, Jug M, Herman S, Kreuh D. Personalized guiding templates for pedicle screw placement. Information and Communication Technology, Electronics and Microelectronics (MIPRO), 2014 37th International Convention on, Opatija, Croatia. p. 249, 251, 26–30 May 2014

27. Porada S, Millner P, Chiverton N, et al., editors. Computer aided surgery with lumbar vertebral drill-guides, using computer aided planning, design and visualisation. Medical Image Understanding and Analysis (MIUA); 2001.
28. Owen BD, Christensen GE, Reinhardt JM, Ryken TC. Rapid prototype patient-specific drill template for cervical pedicle screw placement. Comput Aided Surg. 2007;12(5):303–8.
29. Sugawara T, Higashiyama N, Kaneyama S, Takabatake M, Watanabe N, Uchida F, Sumi M, Mizoi K. Multistep pedicle screw insertion procedure with patient-specific lamina fit-and-lock templates for the thoracic spine: clinical article. J Neurosurg Spine. 2013;19(2):185–90.

Part IV
Robotics

Chapter 16
The Use of ROBODOC in Total Hip and Knee Arthroplasty

Nathan A. Netravali, Martin Börner, and William L. Bargar

Abstract Total hip arthroplasty (THA) and total knee arthroplasty (TKA) are successful procedures in terms of restoring patient mobility and relieving pain. Several clinical studies have demonstrated the importance of restoring knee alignment in achieving long term clinical results. Similarly, successful hip replacement requires strong osseointegration, restoration of offset, leg length, and version to prevent complications. Computer navigation and robotic systems have been developed to increase implant placement accuracy and achieve improved long term results. ROBODOC was the first active robotic system created to be used in orthopaedic surgery. Its design is based on computer aided design (CAD) and computer aided manufacturing (CAM). Each case is preoperatively planned using CT scans and then ROBODOC precisely executes the plan on the bone. Initial studies, however, showed increased surgical time and blood loss. Subsequent improvements of the device have reduced or eliminated these concerns. Several clinical studies have demonstrated that ROBODOC's ability to place implants within the bone according to the preoperative plan is greatly improved over a conventional manual technique and that outliers have been virtually eliminated.

Keywords ROBODOC • Preoperative CT scan • Active robotics • Alignment • Outcomes

N.A. Netravali, PhD (✉)
Think Surgical, Inc., 47320 Mission Falls Ct, Fremont 94306, CA, USA
e-mail: nnetravali@thinksurgical.com

M. Börner, MD
Chairman of the Board, Dr. Erler Clinics, Kontumazgarten 4-18, Nuremberg 90429, Germany

Retired, Berufsgenossenschaftliche Unfallclinic (BGU) Frankfurt,
Frankfurt am Main, Germany
e-mail: Prof.Martin.Boerner@t-online.de

W.L. Bargar, MD, MMAE
Department of Orthopaedics, Sutter Joint Replacement Center, University of California at Davis School of Medicine, Sutter General Hospital, Sacramento, CA 95816, USA
e-mail: wbargar@jointsurgeons.com

L.E. Ritacco et al. (eds.), *Computer-Assisted Musculoskeletal Surgery: Thinking and Executing in 3D*, DOI 10.1007/978-3-319-12943-3_16

Introduction

Primary reconstructive joint surgery, including total knee arthroplasty (TKA) or total hip arthroplasty (THA), is commonly performed to relieve pain and restore function in patients with end-stage osteoarthritis of the affected joint. In the US, these procedures are growing rapidly, with 619,000 primary TKA's and 284,000 primary THA's performed in 2009 and these numbers are expected to potentially grow to over 3 million primary TKA's and 500,000 primary THA's by 2030 [19]. In terms of clinical outcomes, TKA is a successful procedure for pain relief and restoration of patient mobility with greater than 90 % survival rate at 10–15 years postoperatively [7, 11, 40]. Similarly, THA results in positive clinical outcomes with over 95 % survivorship at 10-year follow-up and over 80 % survivorship at 25-year follow-up [19, 27].

Numerous peer-reviewed published papers have identified knee alignment as the most important factor in achieving good long term clinical results [4, 9, 12, 17, 18, 22, 38, 39]. Similarly, a successful hip replacement requires strong osseointegration [7, 36] to prevent femoral osteolysis and correct placement of the femoral implant can reduce the risk of leg length discrepancy [10] and of dislocation due to impingement [25]. Implant manufacturers have developed complex manual instrumentation to address each of the above factors and help the surgeon place the implants where they planned. In addition to manual instruments, computer navigation and robotic systems have been developed to increase the accuracy of implant placement and reduce outliers with the overall goal of improved long term clinical results.

The first active robotic system for use in orthopaedic procedures was ROBODOC (Think Surgical, Inc., Fremont, CA) and was developed as a joint effort between the University of California–Davis and IBM's Thomas Watson Research Labs in New York from 1986 to 1992. ROBODOC was conceptualized by Howard A. Paul, DVM and William L. Bargar, MD as a method to improve the ingrowth of early cementless femoral components in total hip arthroplasty. Based on a traditional computer-aided design (CAD)-computer-aided manufacturing (CAM) system, ROBODOC consists of a computed tomography (CT)-based computer-aided robotic milling device that allows accurate preparation of the femoral bone and anatomic placement of the femoral component in primary cementless THA. Since the initial version, the application has been expanded to accommodate primary TKA and revision THA [3].

The first human cases using ROBODOC were performed at Sutter General Hospital in Sacramento, CA in November 1992 after canine clinical studies were successfully performed from 1989 to 1991. A randomized multicenter study in the U.S. of 136 hips in 119 patients took place from 1994 through 1998 to determine the safety and efficacy of using ROBODOC for cementless primary hip arthroplasty [43]. The results showed that the ROBODOC System statistically improved fit, fill, and alignment of the implant. There was no occurrence of intraoperative fractures and a 2-year follow-up revealed no statistical difference in Harris hip scores compared with the manual THA control group [2].

However, although this clinical trial demonstrated that ROBODOC had several benefits, there were still some issues with the system at the time. Operative times

were longer for the ROBODOC cases, which could be attributed to the learning curve associated with the novel system. Additionally, if the robot software detected an error or a motion in the operative bone, it automatically stopped. Restarting the procedure required additional steps to ensure operational safety, thus increasing operative time. There was also an increase in blood loss in the ROBODOC group when compared with the controls, which could be attributed to the increase in surgical time when using the system. This first generation of ROBODOC also required an additional surgery prior to the THA to place locator pins before the CT scan. These locator pins were used intraoperatively to register the bone within the robot's workspace. Although these potential issues did not result in any specific complications during the trial, they did raise some concerns.

Several improvements were then made to the system to directly address these issues. A new registration method was created that did not require the locator pins and the additional surgery. This pinless registration technique used a point-to-surface algorithm that matches bone surface points collected intraoperatively to the CT bone contours created preoperatively. Furthermore, cutting paths were optimized to reduce their time and the recovery system was improved to reduce the time recovered to re-register the bone.

A second multicenter US trial of the ROBODOC system using the new registration system was started in 2001. One hundred and fifteen (115) subjects were enrolled in the study at 4 clinical sites and the results showed that average blood loss in the ROBODOC group was 522 cc and surgical time was 125.5 min. These results were significant improvements over the results achieved during the first multicenter trial [2] in which average blood loss was 1189 cc and average surgical time was 258 min. This assisted in ROBODOC receiving 510(k) clearance for primary cementless total hip arthroplasty in the US in August of 2008. A new version of this active robotic system received 510(k) clearance for primary total hip arthroplasty and is currently being marketed in the United States by THINK Surgical, Inc. (Fremont, CA) as TSolution One™.

Preoperative Preparation

The ROBODOC System consists of ORTHODOC, a preoperative planning workstation and ROBODOC (Fig. 16.1): an electromechanical arm, electronic control cabinet with display monitor, operating software, tools and accessories. Each ROBODOC procedure requires a preoperative CT scan. A motion rod is scanned with the joint that allows the ORTHODOC software to detect if any patient motion occurred during the scan. Any movement adversely affects the ability to perform intraoperative registration due to image quality, decreasing the accuracy of implant placement.

Once the scan is complete, the CT data is used as input into ORTHODOC, which combines the individual slices to produce a series of 2D images for templating purposes. A 3D surface model of the operative bone is also created in ORTHODOC for intraoperative registration purposes. A sample ORTHODOC screen used for

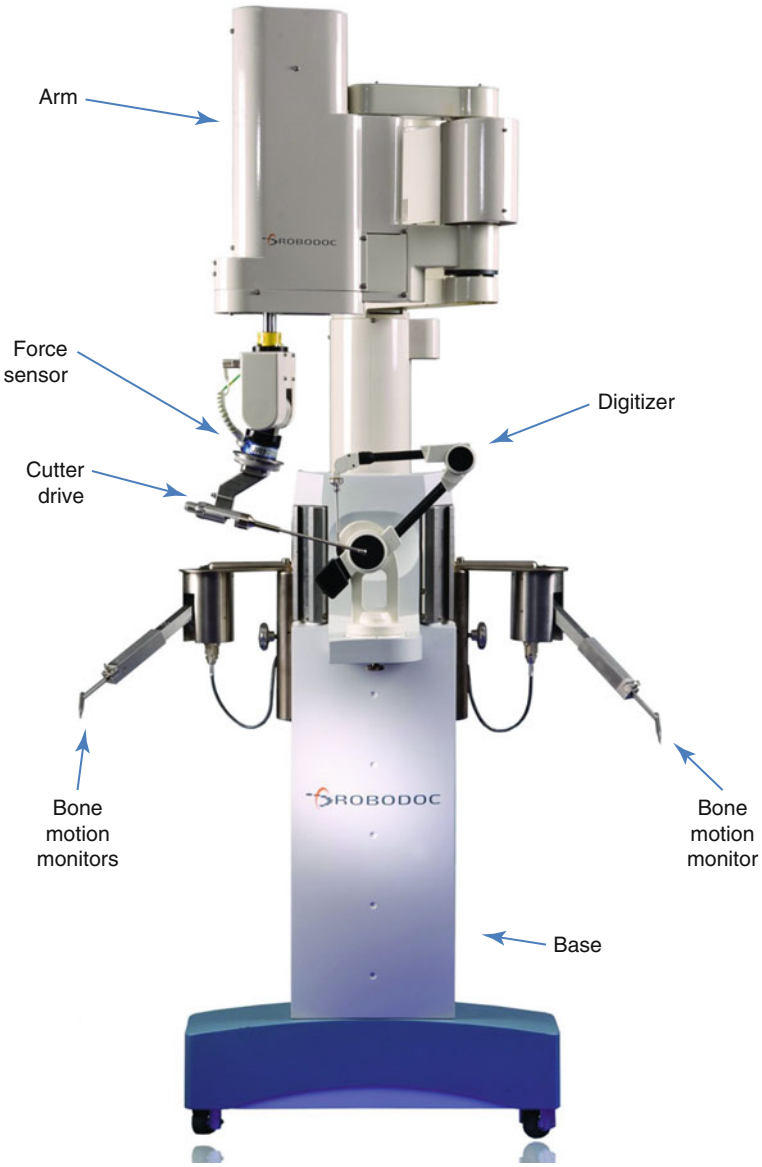

Fig. 16.1 The ROBODOC System (Think Surgical, Inc., Fremont, CA)

planning THA is shown in Fig. 16.2. ORTHODOC contains an open library of 510(k) cleared hip or knee replacement implants, depending on the application installed. The surgeon can select an implant model from this library and manipulate the 3D representation of the implant in relation to the bone to optimally place the implant. Once the surgeon is satisfied with the implant location, the data is written to a transfer media file for use with the ROBODOC during surgery.

Fig. 16.2 An example of the 3D planning workstation, ORTHODOC, for a THA case

Technique

In the operating room, surgical exposure during a ROBODOC surgery is the same as is done during a normal TKA or THA. Once the joint is exposed, fixation is required to ensure that the operative bones are immobilized with respect to the ROBODOC base. Fixation is specific to the indication (i.e., THA fixation fixes the proximal femur while TKA fixation fixes the distal femur and proximal tibia). Once fixation has been established, bone motion recovery markers are placed on the bone. Recovery markers are used to recover the 3D location and orientation of the bone in the event that the bone moves after it has been registered. Bone motion monitors (BMM's) are directly attached to the operative bones and can determine if a bone motion occurs. If a bone motion occurs during registration or cutting, the procedure is automatically paused by the system. This requires the bone be re-registered before the procedure may continue.

After the BMM's have been attached, the next step is to register the operative bone within ROBODOC's workspace. The current version of ROBODOC uses a widely accepted method of registration used in computer vision based on a point-to-surface technique. It requires the creation of a surface model of the bone from the preoperative CT scan using a semi-automated process in ORTHODOC and collecting, or digitizing, bone surface points on the patient intraoperatively.

During surgery, the surgeon uses a digitizer located on the ROBODOC system to collect points on the bone with respect to the ROBODOC arm coordinate system. The software directs the surgeon towards areas on the surface of the bone where points need to be collected. This method does not require the collection of specific anatomic points, but rather, the algorithm is designed to match the surface of the bone based on a variety of points in anatomic regions that are sufficiently

spread out. If the points are not well distributed, a software check will require the points to be recollected until they are sufficiently spread apart. If the calculated registration meets the accuracy requirements, the surgeon is asked to verify the results of the registration by digitizing specific points. The graphic display then indicates where each collected point lies relative to the CT surface model. If they are acceptable to the surgeon, he/she can accept the registration and proceed with the surgery.

The next step of a ROBODOC procedure is the milling of the bone using a rotary cutting tool (Fig. 16.3). The surgeon must ensure that the soft tissue is properly retracted prior to letting ROBODOC begin cutting of the bone. During the entire bone preparation procedure (Fig. 16.4), the surgeon is in control of the process and is in direct view of the operative site while ROBODOC is cutting. The surgeon has the ability to pause, stop, or abort the use of ROBODOC at any point via a hand-held controller. During the entire ROBODOC procedure, the surgeon is guided through the workflow through on-screen prompts and displays.

Once ROBODOC has finished preparing the bone, the software will prompt the surgeon to move ROBODOC away from the operating table. At this point, the surgeon removes the recovery markers and fixation system and proceeds with implant

Fig. 16.3 An example of a ROBODOC THA cutting tool and sleeve used to prepare the bone surface

Fig. 16.4 ROBODOC preparing the femoral canal during THA

fitting and insertion in the same manner as a manual hip or knee arthroplasty. Finally, the exposed joint can be closed per standard procedures.

Results and Complications

The ROBODOC system has been used in thousands of clinical cases for both THA and TKA. A summary of the reports in which ROBODOC was used for THA and TKA are presented Tables 16.1 and 16.2, respectively. The reports and their primary findings are discussed in the sections below. It should be noted that all of these studies were performed with a variety of different implants created by different implant manufacturers.

THA

As mentioned previously, the first human cases of ROBODOC were performed in 1992. Bargar et al. [2] describe the results of the first clinical trial using ROBODOC in the US along with the first 900 THA procedures performed in Germany. Under European law, all cases performed in Europe were performed after the system received CE mark. The US cohort was a controlled and randomized study with 65 ROBODOC cases and 62 manual control cases. There were no differences in functional outcomes in the two groups. Radiographic fit and component positioning was improved in the ROBODOC group but surgical time and blood loss were significantly greater in the ROBODOC group. The control group had three cases of

Table 1 Clinical studies using ROBODOC for THA

Study	Procedure	No. cases	Blood loss (cc)	OR time (min)
Bargar et al. (1998), US	THA	65/62	1,189/644cc[a]	258/134[a]
Bargar et al. (1998), Germany	THA	900/–	–	90/–
Honl et al. (2003)	THA	61/80	–	107/82[a]
Nishihara et al. (2004)	THA	75/–	–	–
Nishihara et al. (2006)	THA	78/78	527/694[a]	122/102[a]
Hananouchi et al. (2006)	THA	31/27	–	–
Schulz et al. (2006)	THA	143/–	–	–
Nakamura et al. (2009)	THA	75/75	591/–	129/–
Nakamura et al. (2010)	THA	118/–		120/108
Yamamura et al. (2013)	RTHA	19/–	1,235	267

All values presented are for ROBODOC/Conventional where available
[a]Indicates a significant difference

Table 16.2 Clinical reports using ROBODOC for total knee arthroplasty

Report	Procedure	# Robotic cases	# Conventional cases
Börner et al. [6]	TKA	100	N/A
Park and Lee [33]	TKA	32	30
Song et al. [42]	TKA	30	30
Song et al. [41]	TKA	50	50
Yim et al. [45]	TKA	117	N/A
Lio et al. [21]	TKA	31	29

femoral fracture while the ROBODOC group had none. In the German group, 870 of the cases were primary total hip arthroplasties with the remaining 30 bieng revision THA cases. The Harris hip scores rose from 43.7 preoperatively to 91.5 postoperatively and the learning curve for the system was demonstrated as the first case was 240 min, while the majority of cases were 90 min, on average. Complication rates were similar to conventional techniques, except the ROBODOC cases had no intraoperative femoral fractures.

Honl et al. [14] described their experiences using the ROBODOC system in 2003 in a randomized prospective clinical study. Of the 74 ROBODOC cases, 13 of them had to be converted to manual technique due to technical complications. Revision was required in two of the manual group and nine of the ROBODOC group. The ROBODOC cases took longer at 107.1 min on average, while the conventional cases only took 82.4 min on average. The ROBODOC group had significant improvements in limb-length equality and varus-valgus orientation of the stem. Additionally, the ROBODOC group had more heterotopic ossification at 6 months along with better Mayo clinical scores and Harris scores at 12 months. However, dislocation was higher in the ROBODOC group with 11 of the 61 cases reporting dislocation and eight of them requiring revision surgery compared to none in the conventional group. It should be noted that all of the revisions were for recurrent dislocations and pronounced limp. At revision, the authors found the abductor muscles were detached from the trochanter and implied that in those cases, the robot

damaged the abductor muscles, causing rupture. Since ROBODOC is designed such that the tool shall not deviate from the prescribed cut path, it appears as though there were issues with properly clearing the workspace prior to allowing ROBODOC to cut. These results were unrepresentative of what was found in nearly all other reports. When the revision cases were excluded, the authors found the Harris hip scores, prosthetic alignment, and limb length differentials were better for the ROBODOC group at both 6 and 12 months.

In 2004, Nishihara et al. evaluated the accuracy of femoral canal preparation using postoperative CT images for 75 cases of THA performed with the pin-based version of ROBODOC. The results showed that the differences between the preoperative plan and the postoperative CT were less than 5 % in terms of canal fill, less than 1 mm in gap, and less than 1° in mediolateral and anteroposterior alignment with no reported fractures or complications. They concluded that the ROBODOC system resulted in a high degree of accuracy. The same group published results in 2006 comparing THA's performed with ROBODOC to those prepared using manual rasping techniques. This was a prospective randomized study in which each of the ROBODOC and manual groups had 78 subjects. In terms of clinical outcome, the ROBODOC group resulted in significantly better Merle D'Aubigné hip scores at 2 years postoperatively. There were no intraoperative fractures in the ROBODOC group compared to 5 in the manual group. Furthermore, the manual group had greater estimated blood loss, an increased use of undersized stems, higher than expected vertical seating and unexpected femoral anteversion when compared to what was planned. The ROBODOC cases took 19 min longer than the manual cases and this was significant. Overall, the authors felt the benefits of improved fit, fill, and alignment and elimination of intraoperative fractures were clear advantages over manual cases with the only potential drawback of the ROBODOC system being a justification of cost, which needs longer term data for proper analysis.

Hananouchi et al. [13] decided to look at periprosthetic bone remodeling after THA to determine whether load was effectively transferred from implant to bone after using the ROBODOC system to prepare the femoral canal. The cohort included 31 hips in the ROBODOC group and 27 hips in the manual group and looked at dual energy X-ray absorptiometry (DEXA) to measure bone density. They found that significantly less bone loss occurred in the proximal periprosthetic areas in the ROBODOC group compared to the manual group, however, there were no differences in the Merle d'Aubigné hip scores. They concluded that the ROBODOC system reduced postoperative bone loss, at least for a straight-type stem with proximal porous coating and a polished distal taper.

A paper by Schulz et al. [40] reported on their experience of consecutive cases performed from 1997 to 2002. Of 143 total hip replacements performed in that time period, they obtained follow-up data for 97 cases. In nine of the cases, there were technical complications listed. These technical complications included five cases in which the BMM stopped cutting and re-registration was required. Although considered by Schulz et al. to be a complication, this is actually a safety system designed to prevent unwanted bone cuts and harm to the patient. The remaining four complications included two femoral shaft fissures requiring wire cerclage, one case of

damage to the acetabular rim from the milling device, and one defect of the greater trochanter that was milled. There were early postoperative complications in nine patients which included three hematomas, two superficial infections, three deep venous thromboses, and one dislocation. Two late complications included a Brooker type 3 heterotopic ossification that was removed 25 months postoperatively and a scar that had to be excised at 11 months. In terms of clinical results, they found that these complications, functional outcomes, and radiographic outcomes were comparable to manual techniques. It was only the technical complications that concerned them. However, it should be noted that three of the nine were due to locator pin implantation problems, which has since been removed from the ROBODOC system. Additionally, the femoral shaft fissures have not been reported in any other study with ROBODOC and the rate reported here was still comparable to manual technique.

Nakamura et al. [28] compared the locator pin-based registration ROBODOC system with the surface-based registration (DigiMatch) ROBODOC system in terms of postoperative alignment and functional outcomes. The study included 81 subjects who had THA performed with the pin-based system and 43 subjects who had THA performed with the surface-based registration system. The results showed that although the surface-based registration surgeries took 25 min longer than the pin-based surgeries, there was no significant difference in blood loss. There were no significant differences in complications between the two groups and the accuracy of stem placement was not significantly different. However, the postoperative Japanese Orthopedic Association (JOA) hip scores were significantly better in the surface-based registration group compared to the pin-based group. They concluded that the surface-based registration was safe and effective and eliminated the need for a prior locator pin implantation surgery thereby eliminating any related risks.

Nakamura et al. [29] subsequently published a prospective comparison between the ROBODOC assisted THA and a manual technique with 75 subjects in the ROBODOC group and 71 in the manual group. This was a 5 year follow-up study which looked at JOA clinical scores, leg length variance, and stress shielding of the bone. The results showed that at 2 and 3 years postoperatively, the ROBODOC group had better JOA scores, but by 5 years postoperatively, the differences were no longer significant. When looking at leg length inequality, the ROBODOC group had a range of 0–12 mm, while the manual group had a significantly larger range of 0–29 mm. The results also showed that at both 2 and 5 years postoperatively, there was more significant stress shielding of the proximal femur in the manual group compared to the ROBODOC group. This suggests greater bone loss in the manual group.

Yamamura et al. [44] were the first to document the use of ROBODOC in revision total hip arthroplasty. Specifically, the ROBODOC system revision module can be used to remove bone cement selectively from the femoral canal during a revision THA. This study included a cohort of 19 patients who underwent revision THA with the ROBODOC system. The follow-up ranged from 76 to 150 months and the authors looked at the amount of bone cement remaining postoperatively, how long it took to be weight bearing, and any complications. The results showed that all of

the bone cement was completely removed in all cases. Full weight bearing was possible within 1 week of surgery for 9 of the 19 cases and all of the cases within 2 months. There were no cases of perforation or fracture of the femur in any of the cases. Compared to other reports, in which the rate of intraoperative fractures varies from 2.3 to 50 % [8, 11, 20, 23, 26], the authors concluded that the ROBODOC system provided a distinct advantage over other techniques for cement removal since the cutting area could be assessed three-dimensionally prior to surgery.

TKA

The ROBODOC System was first used for TKA procedures in 2000 [30]. The first 100 TKA procedures using ROBODOC were performed at the Trauma Clinical of Trade Associations (BGU) in Frankfurt Germany by Professor Martin Börner [6]. All of the patients received the Duracon Total Knee (DePuy Orthopedics Inc., Warsaw, IN). The ROBODOC system was used to make cuts that allowed cementless implantation for both the tibia and femur in 76 of the first 100 patients. The remaining cases required cement for either the tibial component (16 cases) or both components (8 cases) due to poor bone quality. In 97 % of the cases, the alignment of the knee was restored to the planned ideal mechanical axis (0° error). The remaining three cases resulted in knee alignment being restored to within 1° of the ideal mechanical axis. The operative time for the first case was 130 min and decreased to between 90 and 100 min by the end of the first 100 cases. Of the first 100 cases, five were successfully converted to a manual procedure due to technical issues with the ROBODOC system.

Park and Lee [34] performed a prospective randomized study comparing ROBODOC-assisted TKA and manual TKA with 32 patients in the ROBODOC group and 30 patients in the manual group. They found that there were no differences in terms of clinical outcome when looking at Knee Society scores and postoperative range of motion (ROM). When looking at individual implant placement on postoperative X-rays, they found that there were significant improvements in femoral component position in the AP plane in the ROBODOC group, but no differences in the overall femorotibial angle between the two groups. They believed that this was due to soft tissue balancing that compensated for the inaccurate femoral implant position in the manual group. However, it was clear that the ROBODOC system greatly improved implant placement accuracy and precision. They did, however, run into five complications in the ROBODOC group, mostly resulting in soft tissue damage. These included skin damage due to an inadequate incision, a tendon rupture, a postoperative supracondylar fracture, a patellar fracture and a peroneal nerve injury in their early cases. These issues were resolved later in the study as the incision size was increased and smaller fixation pins were used to fixate the bones.

Song et al. [42] directly compared ROBODOC-assisted TKA and a manual TKA in the same subject using a prospective randomized study. Thirty patients underwent simultaneous bilateral TKA with a ROBODOC-assisted procedure in one

knee and a manual procedure in the contralateral knee. Postoperatively, the alignment of the knee and the individual components were determined along with clinical follow-up scores including the HSS and WOMAC scores. The results showed significantly fewer outliers in terms of alignment errors and nearly equivalent clinical outcome results for both HSS and WOMAC scores. The postoperative mechanical axis was improved to 0.2° ± 1.6° (mean ± SD) in the ROBODOC group and only 1.2° ± 2.1° (mean ± SD) in the manual group. Furthermore, the ROBODOC group had no outliers in mechanical axis, defined as an error ≥±3°, while the manual group had seven outliers. However, the ROBODOC-assisted surgeries took, on average, 25 min longer than the manual cases, but resulted in significantly less postoperative bleeding. There were no major adverse events related to the use of the robotic system reported.

Song et al. [41] more recently published another study comparing ROBODOC-assisted and manual TKA's. This study looked at 100 total subjects that were randomly divided into 50 receiving ROBODOC-assisted TKA and 50 receiving manual TKA. Once again, the primary objective was to create a postoperative mechanical axis with neutral (0°) alignment. The results showed that the postoperative mechanical axis was improved to 0.5° ± 1.4° (mean ± SD) in the ROBODOC-assisted group and 1.2° ± 2.9° (mean ± SD) in the manual group. The ROBODOC group had significantly fewer outliers (none), once again defined as error ≥±3°, compared to the manual group (12 outliers). The operative time was once again an average of 25 min longer in the ROBODOC cases but they once again resulted in significantly less blood loss. The clinical results (ROM, HSS scores, and WOMAC scores) showed no differences between the two groups. Additionally, this study compared the ability to balance the flexion and extension gaps after the bony cuts and soft tissue balancing were completed. The ROBODOC group resulted in only three outliers (defined as a difference in flexion and extension gap outside of 2 ± 2 mm (mean ± SD)) which were significantly fewer than the ten outliers found in the manual group. Additionally, the PCL tension was measured intraoperatively. The ROBODOC group resulted in 96 % of the knees having excellent tension and 4 % having poor tension, while the manual group only had 76 % of the knees with excellent tension and the remaining 24 % with poor tension. This difference between groups was statistically significant. The ROBODOC group experienced six local and five systemic complications compared to the manual group which experienced three local and eight systemic complications. These complications rates were not statistically different.

A comparison of alignment methods was performed by Yim et al. [45] using the ROBODOC system with a cohort of 117 subjects. They compared clinical outcomes using both a classical (56 subjects) and anatomical (61 subjects) alignment method for TKA to determine if there were any clinical or radiological differences in outcome. The classical method, as defined by Insall et al. [16] suggests making tibial and femoral cuts perpendicular to the mechanical axis of the tibia and femur resulting in a joint line that is perpendicular to the mechanical axis. The anatomical method, described by Hungerford et al. [15] suggested cutting the tibia in varus and the femur in valgus to create a joint line that is

parallel with respect to the ground. Yim et al. compared postoperative varus and valgus laxities, ROM, HSS and WOMAC scores, and radiological outcomes. There were no differences in any of the outcome measures they considered including mechanical alignment of the lower limb. They concluded that using the ROBODOC system eliminated any surgeon variability in technique and showed that both the classical and anatomical alignment methods result in comparable outcomes.

A study by Liow et al. [21] performed a prospective randomized study comparing 31 ROBODOC-assisted TKA's with 29 manual TKA's. They looked at how accurately each technique can restore the joint line and mechanical axis and additionally looked at clinical outcome measures. The results showed that there were no outliers (>3°) in postoperative mechanical axis in the ROBODOC-assisted group with 19.4 % of the subjects being outliers in the manual group. Additionally, there was a shift in joint line >5 mm in 3.23 % of the ROBODOC group compared with a shift in joint line >5 mm in 20.6 % of the manual group. With regards to clinical outcome, there were no significant differences between the groups in ROM, Oxford Knee Scores, Knee Society Scores, or SF-36 scores. They were able to conclude that the ROBODOC system clearly reduced the number of implant placement outliers, but had no effect on short term clinical outcomes. They felt that until an intermediate or long-term benefit is shown, conventional techniques may remain more cost-effective.

Conclusion

The clinical reports described above demonstrate that the ROBODOC system has been used in a number of primary total hip and knee arthroplasties and some total hip arthroplasty revisions. Overall, the reports agree on the fact that the ROBODOC system has greatly improved the ability to place implants within the bone according to the preoperative plan and virtually eliminated outliers.

The early versions of the ROBODOC system, especially for THA, had some issues that may have affected patient safety. This included the requirement of a prior surgery to implant locator pins, increased operative times, and increased blood loss. However, many of these issues were addressed and the results showed numerous improvements in terms of implant fit and fill, reduced leg length discrepancy, and few intraoperative femoral fractures.

The TKA system also had some early complications as reported by Park and Lee [33]. However, as they stated, some early modifications to the system seem to have alleviated those problems. The remaining studies demonstrated how the ROBODOC system can be used to eliminate alignment outliers and position implants exactly as planned. However, there is some debate as to what the ideal target should be for coronal plane alignment [24, 35]. Technologies like ROBODOC and other navigation systems may improve alignment, but this has not been shown to improve short-term results, suggesting that coronal plane alignment may not be related to postoperative outcome [37].

Although “the perfect position” for either a hip or a knee implant may not yet be known and will very likely depend on each individual, the ROBODOC system is capable of helping surgeons achieve this ideal. Each case must be individually planned preoperatively in ORTHODOC and ROBODOC executes the plan with precision that is not possible with conventional, manual techniques. ROBODOC may, in fact, be the tool to help determine ideal implant position since its use can help eliminate surgeon variability and allow various alignment techniques to be compared. In any case, surgical robots like ROBODOC have demonstrated that today’s technology is capable to assist in orthopaedics and it is likely that their use will continue to grow within the operating room and research.

References

1. Bargar WL, Bauer A, Börner M. Primary and revision total hip replacement using the ROBODOC System. Clin Orthop Relat Res. 1998;354:82–91.
2. Bargar WL. Robots in orthopaedic surgery: past, present, and future. Clin Orthop Relat Res. 2007;463:31–6.
3. Bathis H, Perlick L, Tingart M, Perlick C, Luring C, Grifka J. Intraoperative cutting errors in total knee arthroplasty. Arch Orthop Trauma Surg. 2005;125:16–20.
4. Börner M, Wiesel U, Ditzen W. Clinical experiences with Robodoc and the Duracon total knee. In: Stiehl JB et al., editors. Navigation and robotics in total joint and spine surgery. Berlin: Springer; 2004. p. 362–6.
5. Bobyn JD, Engh CA. Human histology of bone-porous metal implant interface. Orthopedics. 1984;7:1410.
6. Busch CA, Charles MN, Haydon CM, Bourne RB, Rorabeck CH, MacDonald SJ, McCalden RW. Fractures of distally-fixed femoral stems after revision arthroplasty. J Bone Joint Surg Br. 2005;87(10):1333–6.
7. Colizza WA, Insall JN, Scuderi GR. The posterior stabilized total knee prosthesis: Assessment of polyethylene damage and osteolysis after a ten-year-minimum follow-up. J Bone Joint Surg Br. 1995;77(11):1730–20.
8. Choong P, Dowsey MM, Stoney JD. Does accurate anatomical alignment result in better function and quality of life? Comparing conventional and computer-assisted total knee arthroplasty. J Arthroplasty. 2009;24(4):560–9.
9. Clark CR, Huddleston HD, Schoch EP, Thomas BJ. Leg-length discrepancy after total hip arthroplasty. J Am Acad Orthop Surg. 2006;14(1):38–45.
10. Egan KJ, Di Cesare PE. Intraoperative complications of revision hip arthroplasty using a fully porous-coated straight cobalt-chrome femoral stem. J Arthroplasty. 1995;10:S45–51.
11. Emmerson KP, Moran CG, Pinder IM. Survivorship analysis of the kinematic stabilizer total knee replacement: a 10- to 14-year follow-up. J Bone Joint Surg Br. 1996;78:441–5.
12. Griffin FM, Insall JN, Scuderi GR. Accuracy of soft tissue balancing in total knee arthroplasty. J Arthroplasty. 2000;15(8):970–3.
13. Hananouchi T, Sugano N, Nishii T, Nakamura N, Miki H, Kakimoto A, Yamamura M, Yoshikawa H. Effect of robotic milling on periprosthetic bone remodeling. J Orthop Res. 2007;25(8):1062–9.
14. Honl M, Dierk O, Gauck C, Carrero V, Lampe F, Dries S, Quante M, Schwieger K, Hille E, Morlock M. Comparison of robotic-assisted and manual implantation of primary total hip replacement: a prospective study. J Bone Joint Surg. 2003;85:1470–8.

15. Hungerford DS, Kenna RV, Krackow KA. The porous-coated anatomic total knee. Orthop Clin North Am. 1982;13:103–22.
16. Insall J, Scott WN, Ranawat CS. The total condylar knee prosthesis: a report of two hundred and twenty cases. J Bone Joint Surg Am. 1979;61A:173–80.
17. Jakopec M, Harris SJ, Rodriguez y Baena F, Gomes P, Cobb J, Davies BL. The first clinical application of a "hands-on" robotic knee surgery system. Comput Aided Surg. 2001;6: 329–39.
18. Jeffery R, Morris RW, Denham RA. Coronal alignment after total knee replacement. J Bone Joint Surg Br Ed. 1991;73:709–14.
19. Kurtz S, Ong K, Lau E, Bozic KJ. Impact of the economic downturn on total joint replacement demand in the United States. J Bone Joint Surg Am. 2014;96:624–30.
20. Lawrence JM, Engh CA, Macalino GE, Lauro GR. Outcome of revision hip arthroplasty done without cement. J Bone Joint Surg Am. 1994;76(7):965–73.
21. Liow MHL, Xia Z, Wong MK, Tay KJ, Yeo SJ, Chin PL. Robot-assisted total knee arthroplasty accurately restores the joint line and mechanical axis. A prospective randomised study. J Arthroplasty. 2014;29(12):2373–7.
22. Longstaff LM, Sloan K, Stamp N, Scaddan M, Beaver R. Good alignment after total knee arthroplasty leads to faster rehabilitation and better function. J Arthroplasty. 2009;24(4): 570–8.
23. Malkani AL, Lewallen DG, Cabanela ME, Wallrichs SL. Femoral component revision using an uncemented, proximally coated, long-stem prosthesis. J Arthroplasty. 1996;11(4): 411–8.
24. Matziolis G, Adam J, Perka C. Varus malalignment has no influence on clinical outcome in midterm follow-up after total knee replacement. Arch Orthop Trauma Surg. 2010;130: 1487–91.
25. Miki H, Sugano N, Yonenobu K, Tsuda K, Hattori M, Suzuki N. Detecting cause of dislocation after total hip arthroplasty by patient-specific four-dimensional motion analysis. Clin Biomech. 2013;28:182–6.
26. Morrey BF, Kavanagh BG. Complications with revision of the femoral component of total hip arthroplasty: a comparison between cemented and uncemented techniques. J Arthroplasty. 1992;7(1):71–9.
27. National Joint Registry for England and Wales. 7th annual report. Hemel Hempstead: National Joint Registry; 2010.
28. Nakamura N, Sugano N, Nishii T, Miki H, Kakimoto A, Yamamura M. Robot-assisted primary cementless total hip arthroplasty using surface registration techniques: a short-term clinical report. Int J Comput Assist Radiol Surg. 2009;4(2):157–62.
29. Nakamura N, Sugano N, Nishii T, Kakimoto A, Miki H. A comparison between robotic-assisted and manual implantation of cementless total hip arthroplasty. Clin Orthop Relat Res. 2010;468:1072–81.
30. Netravali NA, Shen F, Park Y, Bargar WL. A perspective on robotic assistance for knee arthroplasty. Adv Orthop. 2013: Article 970703.
31. Nishihara S, Sugano N, Nishii T, Miki H, Nakamura N, Yoshikawa H. Comparison between hand rasping and robotic milling for stem implantation in cementless total hip arthroplasty. J Arthroplasty. 2006;21(7):957–66.
32. Nishihara S, Sugano N, Nishii T, Tanaka H, Nakamura N, Yoshikawa H, Ochi T. Clinical accuracy evaluation of femoral canal preparation using the ROBODOC system. J Orthop Sci. 2004;9:452–61.
33. Park SE, Lee CT. Comparison of robotic-assisted and conventional manual implantation of a primary total knee arthroplasty. J Arthroplasty. 2007;22(7):1054–9.
34. Parratte S, Pagnano MW, Trousdale RT, Berry DJ. Effect of postoperative mechanical axis alignment on the fifteen-year survival of modern, cemented total knee replacements. J Bone Joint Surg Am. 2010;92:2143–9.

35. Paul HA, Bargar WL, Mittlestadt B, Musits B, Taylor RH, Kazanzides P, Zuhars J, Williamson B, Hanson W. Development of a surgical robot for cementless total hip arthroplasty. Clin Orthop Relat Res. 1992;285:57–66.
36. Pearle AD. Directions for future research. J Bone Joint Surg (Am). 2009;91 Suppl 1:159–60.
37. Perrilo-Marcone A, Barrett DS, Taylor M. The importance of tibial alignment: finite element analysis of tibial malalignment. J Arthroplasty. 2000;15:1020–7.
38. Ritter MA, Davis KE, Meding JB, Pierson JL, Berend ME, Malinzak RA. The effect of alignment and BMI on failure of total knee replacement. J Bone Joint Surg Am. 2011;93: 1588–96.
39. Schulz AP, Seide K, Queitsch C, von Haugwitz A, Meiners J, Kienast B, Tarabolsi M, Kammal M, Jürgens C. Results of total hip replacement using the Robodoc surgical assistant system: clinical outcome and evaluation of complications for 97 procedures. Int J Med Robot. 2007;3:301–6.
40. Sharkey PF, Hozack WJ, Rothman RH, Shastri S, Jacoby SM. Why are total knee arthroplasties failing today? Clin Orthop Relat Res. 2002;404:7–13.
41. Song EK, Seon JK, Yim JH, Netravali NA, Bargar WL. Robotic-assisted TKA reduces postoperative alignment outliers and improves gap balance compared to conventional TKA. Clin Orthop Relat Res. Published online first, 06 June 2012. doi:10.1007/s11999-012-2407-3.
42. Song EK, Seon JK, Park SJ, Jung WB, Park HW, Lee GW. Simultaneous bilateral total knee replacement with robotic and conventional techniques; a prospective, randomized, comparative study. Knee Surg Sports Traumatol Arthrosc. 2011;19(7):1069–76.
43. Spencer EH. The ROBODOC clinical trial: a robotic assistant for total hip arthroplasty. Orthop Nurs. 2006;15(1):9–14.
44. Yamamura M, Nakamura N, Miki H, Nishii T, Sugano N. Cement removal from the femur using the ROBODOC System in revision total hip arthroplasty. Adv Orthop. 2013: Article 347358.
45. Yim J-H, Song E-K, Shan MS, Sun ZH, Seon J-K. A comparison of classical and anatomical total knee alignment methods in robotic total knee arthroplasty: classical and anatomical knee alignment methods in TKA. J Arthroplasty. 2013;28:932–7.

Chapter 17
A Comparative Study for Touchless Telerobotic Surgery

Tian Zhou, Maria E. Cabrera, and Juan P. Wachs

Abstract This chapter presents a comparative study among different interfaces used to teleoperate a robot to complete surgical tasks. The objective of this study is to assess the feasibility on touchless surgery and its drawbacks compared to its counterpart, touch based surgery. The five interfaces evaluated include both touch-based and touchless gaming technologies, such as Kinect, Hydra, Leap Motion, Omega 7 and a standard keyboard. The main motivation for selecting touchless controlling devices is based on direct use of the hands to perform surgical tasks without compromising the sterility required in operating rooms (OR); the trade-off when working with touchless interfaces is the loss of direct force-feedback. However, based on the paradigm of sensory substitution, feedback is provided in the form of sound and visual cues. The experiments conducted to evaluate the different interaction modalities involve two surgical tasks, namely incision and peg transfer. Both tasks were conducted using a teleoperated high dexterous robot. Experiment results revealed that in the incision task, touchless interfaces provide higher sense of control compared with their touch-based counterparts with statistical significance ($p<0.01$). While maintaining a fixed depth during incision, Kinect and keyboard showed the least variance due to the discrete control protocol used. In the peg transfer experiment, the Omega controller led to shorter task completion times, while the fastest learning rate was found when using the Leap motion sensor.

Keywords Gaming technology • Robot assisted surgery • Touchless control scheme • Dexterous movement

T. Zhou • M.E. Cabrera • J.P. Wachs, BEdTech, MSc, PhD (✉)
School of Industrial Engineering,
315 North Grant St., West Lafayette 47907, IN, USA
e-mail: zhou338@purdue.edu; cabrerm@purdue.edu; jpwachs@purdue.edu

L.E. Ritacco et al. (eds.), *Computer-Assisted Musculoskeletal Surgery: Thinking and Executing in 3D*, DOI 10.1007/978-3-319-12943-3_17

Introduction

Minimally invasive surgery (MIS) has been gradually losing ground to teleoperated robot-assisted surgery (RAS) in certain types of procedures (e.g. colorectal, gynecologic and urologic) where the dexterity, precision, high-resolution, motion planning and execution capabilities of robotic applications surpass the restricted capabilities of laparoscopic control. One of the most popular examples is the widely adopted commercial teleoperated da Vinci robot. Its paradigm builds on complex loaded controls at the master console where the surgeon manipulates a sort of joystick or haptic device stabilized by mechanical linkages, and in turn, those movements are projected to the patient site. At the patient's side, a slave station drives robotic arms, including cameras and surgical tools, to mimic the surgeon's hand movements with its end effector's motions.

This setting for manual control is not exclusive to the da Vinci system, it is also found in several surgical systems for conducting different procedures with evident success (e.g. ZEUS, AESOP, Mazor, Raven II) [1]. However all these robotic solutions limit significantly the natural hand operational dexterity associated with skillful in-situ surgery: using bare-hands allows an increased mobility and natural expressiveness, not found in any standard control console [2–4]. Another critical problem of using touch-based interfaces is increasing the risk for bacterial transmission, spread and infection in the operating room, which has been previously associated with the use of keyboard and mice [5]. Those interfaces have been proved to be a vehicle of pathogen and contamination [6]. Since the surgeon who conducts the surgery is often in the same room (contrary to general belief that robotic surgery is teleoperated at a remote location), or close by within the hospital, the associated risks for infection spread are as high as using keyboards or mice [5].

A potential solution applied to this field of robotic surgery would involve the manipulation and control of virtual and physical tools based on free hand movements. This would allow surgeons to operate as if they were physically engaged with in-situ surgery. Gaming technologies offer an attractive alternative to touch based interaction, through interfaces and sensors such as the Kinect [7], Leap Motion [8] and MYO arm band [9]. Such devices offer a touch-less control scheme based on natural gesturing. Their main limitation, applied to surgery, is the lack of tactile feedback, an intrinsic feature existing in manual surgery. This drawback can be addressed using techniques which provide airborne force feedback [10, 11], tactile sensors mounted on the hands and fingers [12] or by leveraging in sensorial substitution with visual hints to convey contact force [13]. The latter is the venue pursued in this Chapter. The goal of this work is to offer a robotic control system that does not compromise surgical asepsis while allowing natural, unconstrained hand gestures in a surgical context; this is still a virgin area of research.

This chapter describes a comparative study among touch-based and touch-less gaming interfaces applied for telesurgery. With these interfaces, the aim is to map user movements, in the context of embodied interaction, to specific robotic

commands regarding position control or performing an action. Using body language as a form of control, represents an advantage since it is the main form of communication and task performance in the OR [14, 15]. The implementation of the system is based on the Taurus robot, shown in Fig. 17.1. Among its features, like dexterous movement of two 7-DOF arms and stereoscopical cameras for 3D vision, it can also hold tools, make incisions and transfer parts.

The comparative study includes gathering information from optical sensors (Kinect [7] and Leap Motion [16]) and pedals as the touch-less interfaces, and compare those to the performance delivered through touch-based interfaces such as keyboards, 3D joysticks (e.g. Hydra [17]) and haptic controllers (e.g. Omega 7 [18]). The measured metrics include deviation error when following a reference annotation, control variance, task completion time and number of errors within each trial.

The outline for the remaining sections of this work is as follows. In section "Related Work", an overview of related work and the state of the art is provided. The next section offers a general view of the system with a brief description regarding the processing modules. Following that is a description of the kinematic configuration space and the trajectory generation of the Taurus robot, along with the different mappings from the interfaces to the robot and other details regarding each interface. The experiments are described subsequently with their corresponding results in section "Experiments: Settings and Results". To finish, the conclusions followed by recommendations and future work.

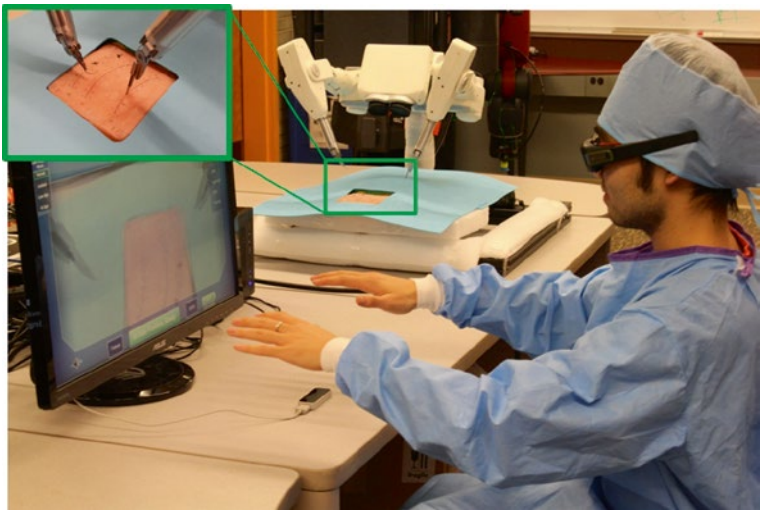

Fig. 17.1 The user seated at the master console of the Taurus robot-assisted surgery system. The Leap Motion sensor placed below can track two hands to control the position and orientation of each end effector. Inset shows a custom fixture for a scalpel mounted on the Taurus end-effector in one arm and in the other surgical tweezers

Related Work

With the aim of improving performance and success rates for MIS, the field has been incorporating new sensors and control based technologies, making way for a new field in robotic minimally invasive surgery (RMIS). The most recognized example is the da Vinci robot [1], which rely on having the surgeon operate using encumbered interfaces to guide the robot through the surgical procedure. This form of control is also found in other state-of-the-art robots since it often provides tactile sensory information through haptics to restore "the real feeling of touch" to the operating surgeon. However, at the same time, this modality of control leads to limited range of manual operation [19], sense of detachment [20] and arises problems with surgical asepsis [21]. Some of these limitations could be tackled using touchless interfaces as a potential solution. The current gap is the lack of tactile information, existing in those touch-based interfaces previously discussed.

Sensorial substitution methods offer an attractive alternative to direct force feedback. Using these methods, feedback is delivered through other alternative modalities which are available to the user [22]. One example is using the visual system in a surgical teleoperation setting to provide information about skin contact, depth of incision or tissue manipulation [13]. Another option is to provide airborne force-feedback using air bursts aimed at the user's hands [10]. A different approach to convey force is through ultrasound generated waves directly onto the users' bare hands [23]. These touchless feedback methods allow the use of new interfaces based on natural free gestures, widely used in other human-robot interaction applications currently [24]. The main benefits of commodity sensors like Kinect, Leap Motion or the MYO arm band, are lower costs than many haptic devices and their increasing popularity in gaming consoles. Such sensors are pervasive and widely used for real-time hand gesture recognition [25, 26].

Previous research has been exploring the use of touchless hand gestures as a form for interacting with robots in the OR. For example, Jacob et al. [21] developed a robotic scrub nurse which delivers surgical instruments based on real-time hand gesture recognition [21]. Kim et al. [27] used the da Vinci robot to compare task performance between touch-based control interfaces and Kinect. In the latter, high latency and errors were found in the Kinect based control, leading to underperformance compared to the alternatives. Additional work has been done in this direction without tangible results [28, 29]. Some other work has been focused on controlling devices other than robots in the OR. Hartmann and Schlaefer [30] used the Kinect sensor for automating the OR lighting [30]. In Wachs et al. [24] hand gestures were adopted for browsing radiological images [30, 31]. Mouth gestures were also tested as a way to control the da Vinci Robot [32].

None of the works described include a systematic evaluation of touch-based and touch-less interfaces for robotic surgery performance assessment. The current chapter describes: (a) the development of a touchless hand gesture based interface for controlling a surgical robot and validated through a mock procedure, and (b) a comparison between touch-based and touchless interfaces in a clinically relevant context with corresponding performance metrics. Technical and theoretical findings

are also reported related to the relationship between the user interaction space and the task space, and their effect in task performance.

System Architecture

The system architecture is presented in Fig. 17.2. Using one of the five interfaces available, the user performs gestures to control the Taurus' navigation to complete a given task. These gestures are part of the lexicon which maps specific instructions to gestures through image processing, segmentation and registration processes. Once the gesture is recognized, a motion trajectory is generated to replicate the user's motion in the robot space through a 3D projection and coordinate mapping of the user space. Subsequently, the trajectory is converted to robotic commands using the Robot Control Scheme module shown below.

While performing the task, the user is able to receive feedback from Taurus by both visual and sound cues. Using the stereo cameras mounted on the robot, a 3D image is generated and presented to the user, as well as information regarding stiffness, position and orientation of the tooltips. This information is presented to the user through color and sound feedback modalities. Based on this feedback, the user generates the subsequent set of commands to complete the task.

Taurus is a high fidelity telemanipulation robot with a 3D HD display developed by SRI (Menlo Park, CA). Taurus has two dexterous and compact arms which can be applied to the surgical setting; it enables surgical-like precision in a modular, portable frame. As shown in Figs. 17.3 and 17.4, it has two independently controlled manipulators with seven degrees of freedom each. One end-effector includes a custom fixture for mounting a scalpel, while the other functions as surgical tweezers.

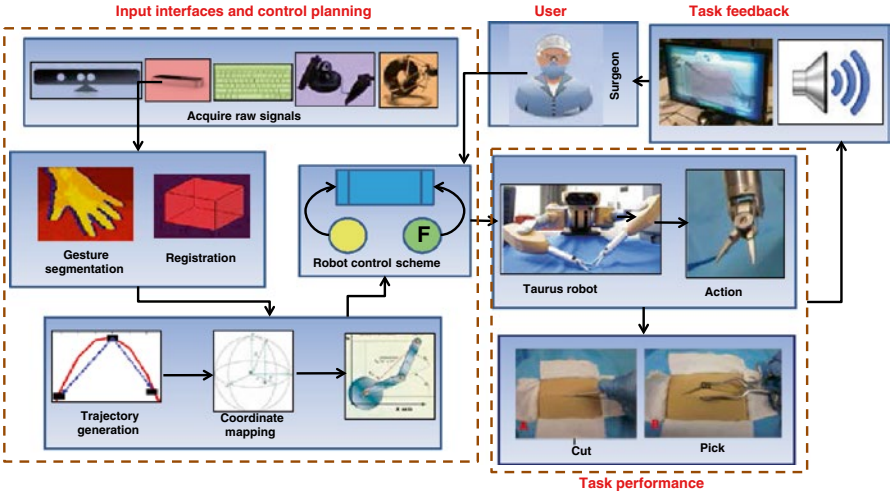

Fig. 17.2 System architecture

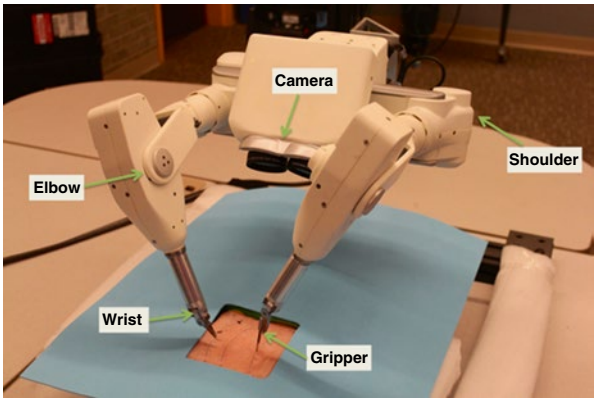

Fig. 17.3 Picture of Taurus with a scalpel mounted on the left gripper

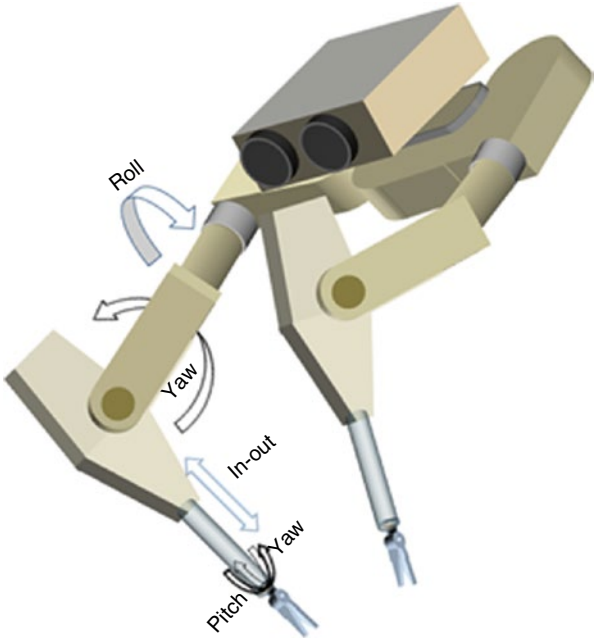

Fig. 17.4 The Taurus' manipulator degrees of freedom

Real-time visual feedback information is provided using a stereoscopic camera system and presented to the user in a 3D stereo display. The left and right views are accurately integrated using Nvidia's stereoscopic glasses 3D Vision 2.

Kinematic Configuration Space and Trajectory Generation

In order to control both the position and the orientation of each of Taurus' end-effector, packets are transmitted to the robot server at a rate of 250 packets per second. The kinematic configuration is determined by a homogeneous transform

4-by-4 matrix X (one for each arm), shown in Eq. (17.1), which contains a 3-by-3 sub-matrix on the upper left representing the rotation transform (from user to task space); on the upper right holds the 3-by-1 position vector with the coordinates for the end effector; and finally the last row is formed by a zero 1-by-3 matrix and a scaling factor.

$$X = \begin{bmatrix} X_{11} & X_{12} & X_{13} & x \\ X_{21} & X_{22} & X_{23} & y \\ X_{31} & X_{32} & X_{33} & z \\ 0 & 0 & 0 & 1 \end{bmatrix} \tag{17.1}$$

Each vector of the rotation matrix relates one axis of user coordinates to robot coordinates. The equations in Eq. (17.2) were used to compute the roll (α), pitch (β) and yaw (γ) angles and later on re-coded to real-world-coordinates by multiplying rotational operators, as shown in Eq. (17.3), using ROT as a rotation function along a specified axis and angle [33].

$$\begin{aligned} \gamma &= \arctan 2\left(X_{32} \middle/ X_{33} \right) \\ \beta &= \arctan 2\left(\frac{-X_{31}}{\sqrt{X_{11}^2 + X_{21}^2}} \right) \\ \alpha &= \arctan 2\left(X_{21} \middle/ X_{11} \right) \end{aligned} \tag{17.2}$$

$$\begin{aligned} Rot(\gamma, \beta, \alpha) &= ROT\left(\check{\mathrm{Z}}, \alpha\right) ROT\left(\check{\mathrm{Y}}, \beta\right) ROT\left(\check{\mathrm{X}}, \gamma\right) \\ &= \begin{bmatrix} c\alpha & -s\alpha & 0 \\ s\alpha & c\alpha & 0 \\ 0 & 0 & 1 \end{bmatrix} \begin{bmatrix} c\beta & 0 & -s\beta \\ 0 & 1 & 0 \\ s\beta & 0 & c\beta \end{bmatrix} \begin{bmatrix} 1 & 0 & 0 \\ 0 & c\gamma & -s\gamma \\ 0 & s\gamma & c\gamma \end{bmatrix} \end{aligned} \tag{17.3}$$

Where $c\alpha$ and $s\alpha$ are shorthand for (cos α) and (sin α) respectively. Due to mechanical constraints, Taurus cannot respond accurately to large rotation increments. Therefore, to assure safe operation, the maximum rotation increment was limited to 0.1°. Therefore, the following algorithm was implemented to perform a piecewise-linear approximation of the overall rotation angle.

```
Algorithm 17.1: Trajectory Generation
1: Input: Transform matrix X, step_length τ
2: α, β, γ=Extract_angles(X) // use equation (17.2)
3: τ=Get_current_frame_from_robot
4: αo, βo, γo=Extract_angles(τ) // use equation (17.2)
```

5: $N = \max\left(\frac{|\alpha-\alpha_o|}{\tau}, \frac{|\beta-\beta_o|}{\tau}, \frac{|\gamma-\gamma_o|}{\tau}\right)$ // number of iterations

6: $\Delta\alpha = \frac{|\alpha-\alpha_o|}{N}, \Delta\beta = \frac{|\beta-\beta_o|}{N}, \Delta\gamma = \frac{|\gamma-\gamma_o|}{N}$ // rotation step

```
7: For i=1 : N
8:        P=Construct_control_packet(Δα, Δβ, Δγ, τ)
9:        Send_to_Taurus(P)
10: End
```

Mapping Interfaces to Actions

Five interfaces were selected for the comparative study, among which there are three touch-based and two touchless. The touch-based interfaces included: a regular keyboard, a Hydra gaming controller [17] and Omega 7 haptics device [18]. A Leap Motion controller [16] and a Kinect [7] were used as the touchless interfaces. A picture of all interfaces is shown in Fig. 17.5.

A foot pedal was implemented along with all five interfaces to toggle the engage/disengage servo mechanism, which helped the operators switch the working space or stay idle. Also, the raw data gathered from the sensors was filtered using a

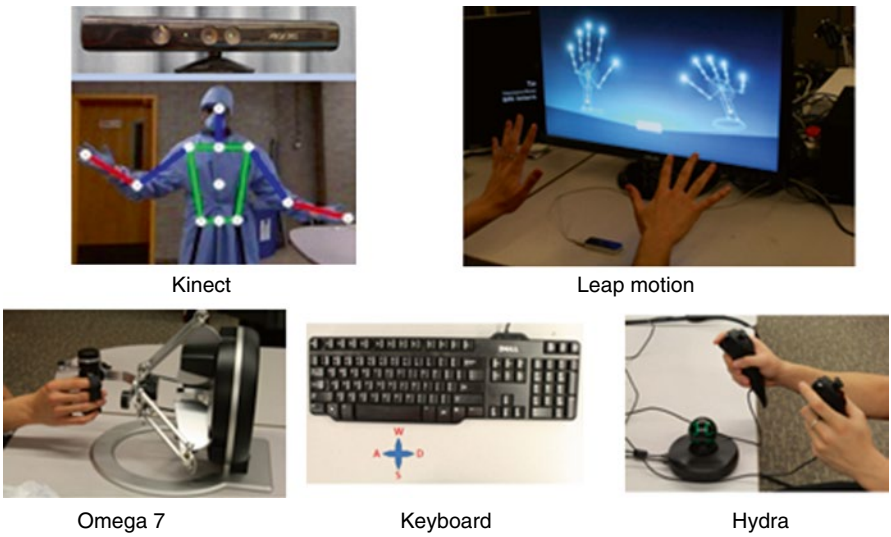

Fig. 17.5 Five different interfaces to control Taurus: touch-based and touch-less among them

low-pass filter to cancel the noise variation caused by the control input modalities. The following subsections give further details about the key modules included.

Registration

The registration process is a prerequisite of interface operation to retrieve parameters once the interface is selected. It consists on mapping the reference frame in which the user works with the frame associated with the task space. In the beginning of teleoperation, the first 10 control input coordinates are recorded and an origin of the user space is generated from the running average of them. This origin of the user space is then mapped to the origin of the robot space. During teleoperation, the operator's movement relative to this origin is then interpreted as practical control instructions. This process applies to all the interfaces other than the keyboard, since the latter does not use 3D coordinates to evoke control motions, and rather keystrokes are used instead. The registration process takes place whenever the foot pedal is reactivated by the user, since each time the user starts the teleoperation from different positions and thus the origin of the user space should be updated every time before the practical teleoperation.

Safety Operation and Region Determination

Virtual bounding boxes are implemented around both the user and task space in order to ensure safe motion during robot teleoperating. In the user space, a virtual rectangular region is created around the user hands to maintain the input coordinates within a permissible operational range. Working within this region also assures that the hands are within the optical sensors' field of view. Analogously, a similar region is established around the robot at the task space. This region limits the outer reach of the robot and assures that the robot's movements are maintained within the operational range. The robot's working space is cut in half, as shown in Fig. 17.6, allowing each arm to move only in its half with some overlapping in the middle. This assures that the robot forearms do not collide with the camera. When the limits of the bounding box are reached, a sound beep goes off to alert the user about this situation.

Visual and Auditory Feedback

As mentioned in previous sections, the biggest drawback of working with hand gestures using touchless interfaces for RAS is the lack of force feedback. This problem is addressed using sensory substitution techniques based on vision and audio cues. The operator receives physical contact information about the force exhorted at the tooltip through two bar graphs; each bar indicates the force of one tooltip, as shown in Fig. 17.7. The size and color of each bar changes proportionally with the amount of force applied to the end effector. At the same time, a beep sound is generated with its pitch modulated according to the force's magnitude. Both acoustic and visual channels are meant to increase the user's awareness while

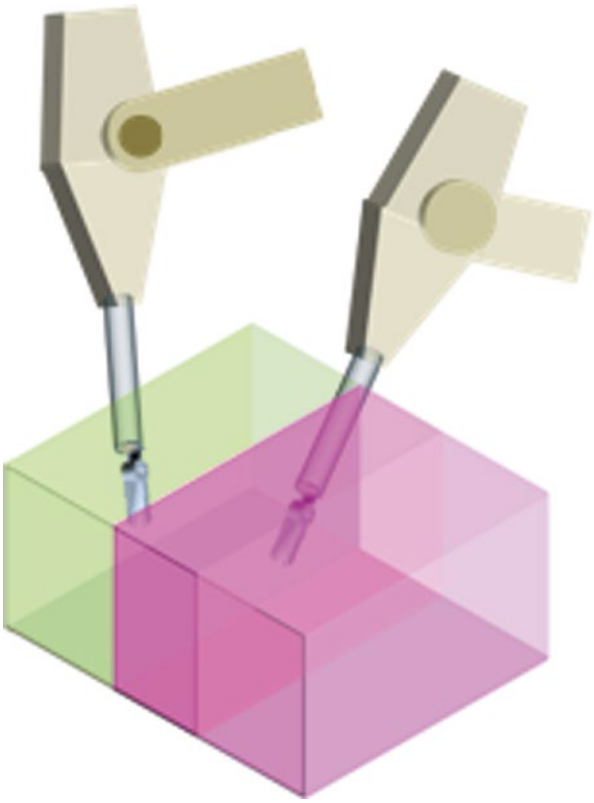

Fig. 17.6 Taurus' operation space. The left gripper is allowed to work only in the *pink region* and right gripper in the *green region*. Both grippers can reach the overlapping area in the middle

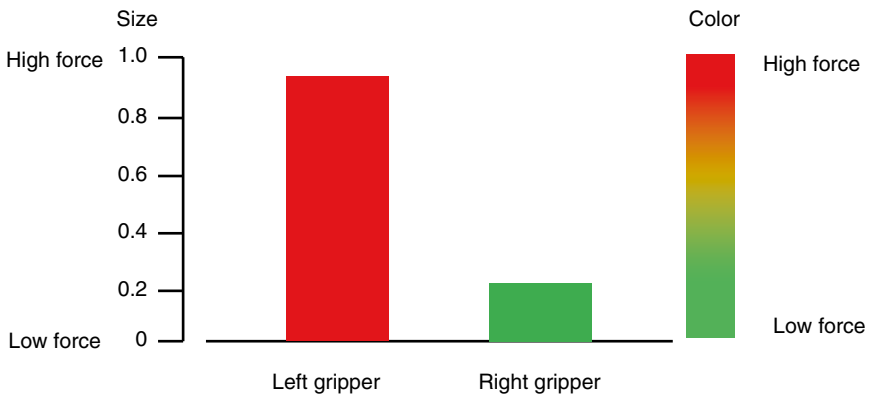

Fig. 17.7 Example of the bar graph. The *left bar* indicates the force of the left gripper and right bar of the right gripper. The size and the color of two bars change according to the amount of force exhorted to each gripper

performing the surgical task. Algorithm 17.2 describes the procedure of generating force based on report tooltip position and the operator's hand position. Due to limited network communication bandwidth, a delay is generated between the time a target position is sent to the robot and the actual robot response is received, creating

a constant lag between the user's hand position and the reported robot's position. The constant dragging force generated by this effect is compensated by factoring the robot's arm speed by a damping factor, when calculating the force feedback. Since the damping factor was selected empirically, this haptic compensation could generate false alarms when fast hand movement occurs. Therefore, a threshold was selected to consider a warning signal as valid.

```
Algorithm 17.2: Position-Position Based Haptic Generation
1: Input: Hand position w, Robot's tooltip position ŵ,
last tooltip position ŵ_old, damping factor k, threshold τ
2: w̃ = Map_hand__position_to_robot_space(w)
2: error=w̃ - ŵ velocity=ŵ-ŵ_old
3: haptic=error+k*velocity
4: If |haptic|>τ
5:    Beep(|α*haptic|), Update_Bar_Graph(|β*haptic|)
6:    ŵ_old=ŵ, go to step 1
7: End
```

Dynamic Use of the User Space

The Kinect control teleoperation modality is based on tracking the user's body movements Tracking is accomplished using an algorithm included in the MS-Kinect SDK which fits a skeleton model to the user 3D view. This results in a continuous stream of body joints and hands' position. These positions are used for controlling Taurus. Once the operator engages the pedal to begin the task, the initial position becomes the origin of the user space; and all the subsequent movements are obtained relative to that initial position. These movements in turn, are tracked and converted to discrete control signals. When the hand motion magnitude is above a predefined threshold τ, a motion instruction is sent to the robot. The direction which exhibits the largest movement is chosen as the user's intentional moving direction. Then, how far away the hand is from the user space origin determines the speed of movement in this direction. The farther the hand is away from the origin, the faster the robot arm moves. This process is described in Algorithm 17.3.

```
Algorithm 17.3: Discrete Control Protocol for Kinect
1: Input: Skeleton S, safety region box B,
pre-defined threshold τ, previous positions buf
2: w=extract_hand_position (S)
3: ŵ=smooth (w, buf)
4: update buf to incorporate new point ŵ
5: If (hand-not-registered)
6:     w_o=ŵ, go to step 2 // w_o is the registered user
space origin
7: Else
8:     dir=identify_movement_direction (w_o,ŵ,τ)
```

```
9:     spd=identify_movement_speed (w_o,ŵ,τ)
10: If (check_safety_region (dir, spd, B))
11:     command=construct_control_packet (dir, spd)
12:     send command to Taurus, go to 2
13: Else send_alarm, go to 2
```

Leap Motion is a desktop infrared sensor which allows hand tracking and hand gesture recognition in real-time. Leap Motion SDK was used to obtain the roll, pitch and yaw angles' magnitudes based on the position and the direction of the hands. The center of the palm was mapped to correspond to the position of Taurus' end-effector. To control the open/close action of the gripper, the angle between the thumb and the palm with the rest of the fingers was measured. A wide angle indicates the "open" command, and a narrow angle is for "close" command.

Omega 7 is a haptic interface with 7-DOF which delivers force feedback reflecting contact forces at a rate of 4 KHz. In order to establish a fair comparison among all five interfaces, the force feedback feature was eliminated from this control interface, and sensorial substitution was applied instead (as with the other interfaces). Omega 7 working space maps the exact position and orientation of both end-effectors; the opening and closing of the robot's tooltip was controlled through a pinching motion between the thumb and index fingers.

Hydra is a control interface often used for gaming. The 3D controls can generate user's hands exact location and orientation. It relies on magnetic motion sensing with a precision down to 1 mm and 1° in position and angle, respectively.

When the keyboard was used as the main input modality, specific key-strokes were assigned to motion control commands. One set of keys were allocated for moving the end effector in one particular direction, and a different set controlled the roll, pitch and yaw angles of the end-effector. While this type of interface was not as intuitive as others, it allowed precise control.

Experiments: Settings and Results

Subjects from Purdue's engineering program were recruited to measure performance of five different interfaces in teleoperation throughout two mock surgical tasks. Task completion time and the robot's tooltip trajectory were recorded, and further analyses were conducted regarding task error, structured variability and learning rate. The setup for each experiment is shown en Fig. 17.8 and the following subsections discuss both experiments in detail.

Incision Task

For this task, subjects were required to perform a curved incision by teleoperating the robot. Each subject performed the task using a different interface for five repetitions. In every case the operator was asked to follow a reference line (see

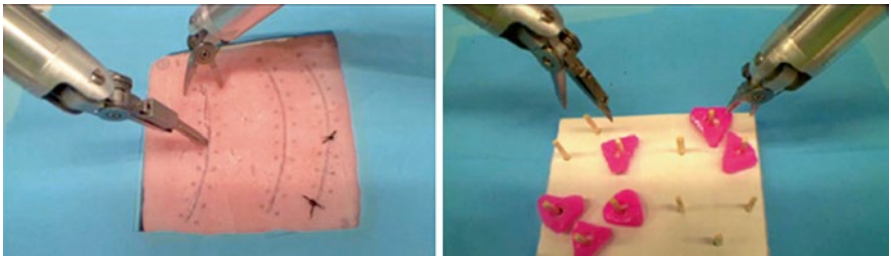

Fig. 17.8 (*left*) Incision task: the right gripper holds the surgical pad while the mounted scalpel on the left makes the incision following a target annotation. (*right*) Peg Transfer Task: the left gripper picks up rubber pegs from each pole and the right gripper transfers and places the pegs on the poles on the opposite side

Fig. 17.5, left) as close as possible while maintaining a fixed incision depth. The operator received haptic feedback in two forms: bar graphs and sound alerts. This feedback was mostly used to adjust the incision depth on the epidermis layer while performing the cut. Task performance was measured using two metrics: distance-from-target annotation and control variance.

The scalpel's tip trajectory for five trials of one subject is shown in Fig. 17.9 along with the reference trajectory in each axis. The tooltip's trajectory obtained on five trials in colored lines, along with a black line reference on each axis. The upper left, upper right and lower left graphs show the 3D trajectories projected onto X, Y and Z axes respectively, while the lower right graph shows the projection onto the XY plane. Visual feedback was the main source of information provided to the user on the x-y plane; incision depth (on the z plane) was presented using acoustic feedback. As seen in the figure, trial-to-trial variability is smaller in the x and y axis as opposed to the z axis. The reason for this is that it is easier to judge deviation from the reference in the x y axes since the camera view and main arm movement are perpendicular to those axes. Motion in the z direction was controlled based on stereoscopic visual feedback which is associated with higher difficulties with distance assessment.

To analyze how close the actual trajectories are to the reference trajectory given in the x-y plane, 10 landmarks were selected along the reference equally spaced; each landmark was used to obtain the normal direction to the reference annotation. The intersection between the normal to the landmark and the actual trajectory [34] was used to measure the point wise error. A zoom-in segment of both trajectories is shown in Fig. 17.10 showing the aforementioned error metric.

The error for each landmark for all five different interfaces is shown in Fig. 17.11. Each error is an average of five trials at the same landmark. In both the beginning and the end of the incision, the error is relatively large compared with the middle section. The reason for this is that approaching the incision point (as well as leaving the incision point) is the most difficult sub-tasks within the tasks; it involves manipulating the tool-tip accurately in x, y and z directions till contact is made with the skin right at the beginning of the trajectory, and then properly determining the incision depth. Once the correct incision depth was reached, the users were required to follow the incision trajectory on the x and y axes, while maintaining the incision

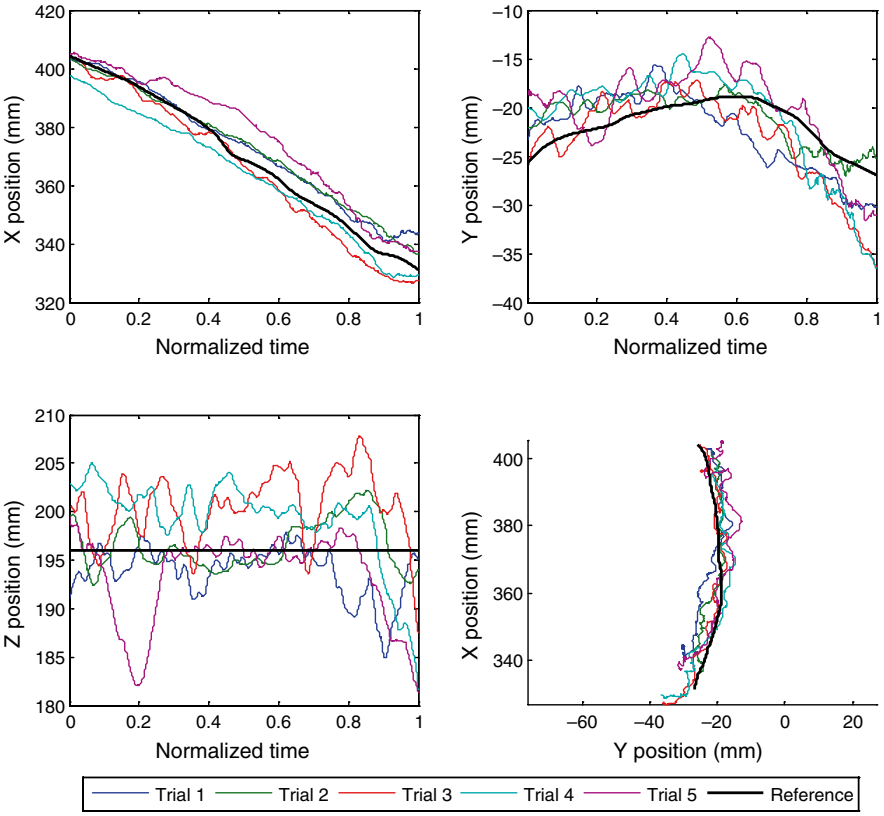

Fig. 17.9 Experimental trajectories from one participant. Both upper figures and the lower left show trajectories across five trials along *x*, *y*, *z* directions versus normalized time. The lower right shows the trials projected onto the *x*-*y* plane. The *black lines* indicate the reference trajectory

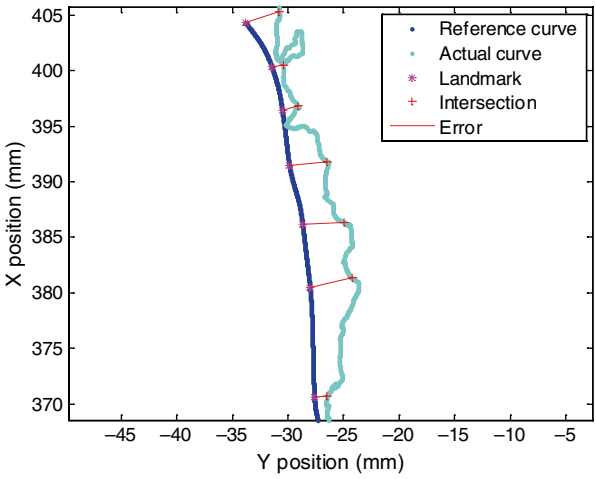

Fig. 17.10 A zoomed-in inspection of the reference trajectory (*blue*) and an experimental trajectory (*cyan*) on the *x*-*y* plane. The *red line* is perpendicular to the reference's tangent at the landmark point and intersects the actual trajectory and the length of the *red line* indicates the discrepancy between experimental trajectory and reference at this landmark

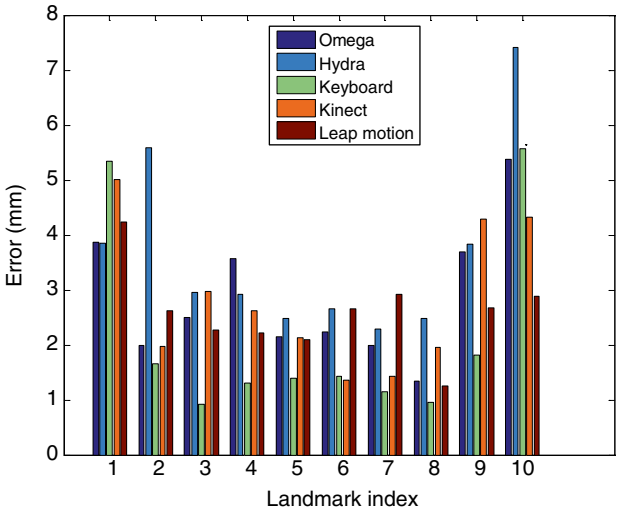

Fig. 17.11 The average error for 10 landmarks across five interfaces

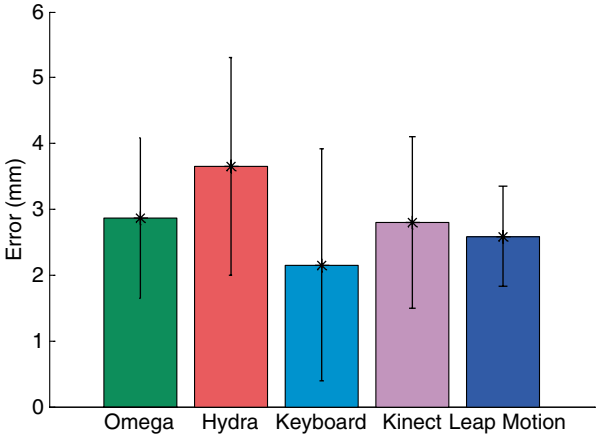

Fig. 17.12 Deviation error from the established incision path in mm

depth constant, which is fairly easy (this resulted in a low error during this segment). An analogy can be established between surgical incision and flying an airplane; taking off and landing is more difficult than just flying following a trajectory at a fixed height.

The average of the error over the 10 landmarks shows the overall deviation from the target trajectory for each interface. The results are shown in Fig. 17.12. While the keyboard control shows the least mean error, no statistical significance was found among the different interfaces.

To evaluate how well the operator was able to keep a constant depth while performing the horizontal incision, the variance of depth position across five interfaces was calculated and shown in Fig. 17.13. Kinect and keyboard, which use a discrete control scheme, show the least variance of all the interfaces; unlike continuous control protocols used by Hydra, Omega and Leap Motion, which use the absolute

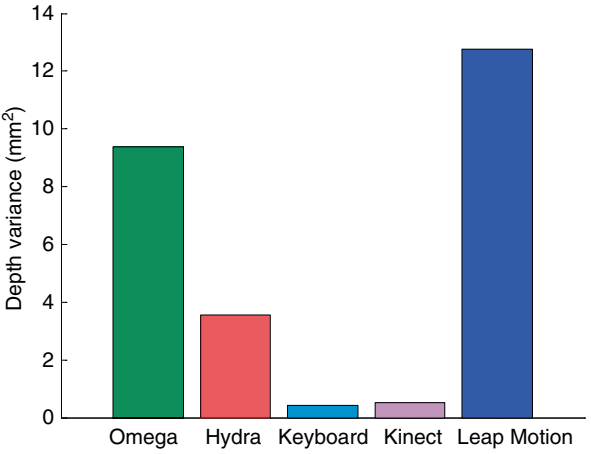

Fig. 17.13 Variance of depth position across different interfaces

position of the hand to drive Taurus' movement. However, no statistical significance was found regarding the difference between these two control schemes.

While the subjects were required to conduct exactly the same task five times, no trajectory was identical to another. The number of joints and degrees of freedom in the human arm, shoulder and torso allow the operator to adopt multiple body configurations for reaching one x, y and z position. This redundancy is both beneficial and problematic. On one hand, it brings flexibility for the subjects in face of obstacles, but it also creates an ill-posed control problem to be resolved by the human motor system [35].

To understand the role of human motor control redundancy and the role that it played across the five implemented interfaces, structured variability in computed using Eq. (17.4) [35].

$$V[t] = \sum_{i=1}^{N} \left(w[t] - \bar{w}[t] \right)^2 d^{-1} N^{-1} \tag{17.4}$$

Where w is the task space vector, $\hat{w}$ is the average of this vector, d is the number of DOFs in task space corresponding to the number of elements in x, and N is the number of trials that are averaged over. This structured variability measures the stability of a variable around a time-varying reference trajectory under perturbation. The result of this analysis applied to the experimental data is shown in Fig. 17.14.

The higher the variance per DOF is, the more control freedom the operator has through the teleoperation task. Results of one-way ANOVA (Analysis of variance) indicate that there are statistical differences between means of variance per DOF over time across five interfaces ($F(4, 49{,}995) = 7885$, $p < 0.01$). Post-hoc test was further conducted and results revealed that all five interfaces are distinct from each other. The boxplot for the variance per DOF is shown in Fig. 17.15. Touch-less interfaces (Kinect and Leap motion) exhibit the highest variance, then follows Omega, Hydra and finally keyboard. Even when both Kinect and keyboard allow

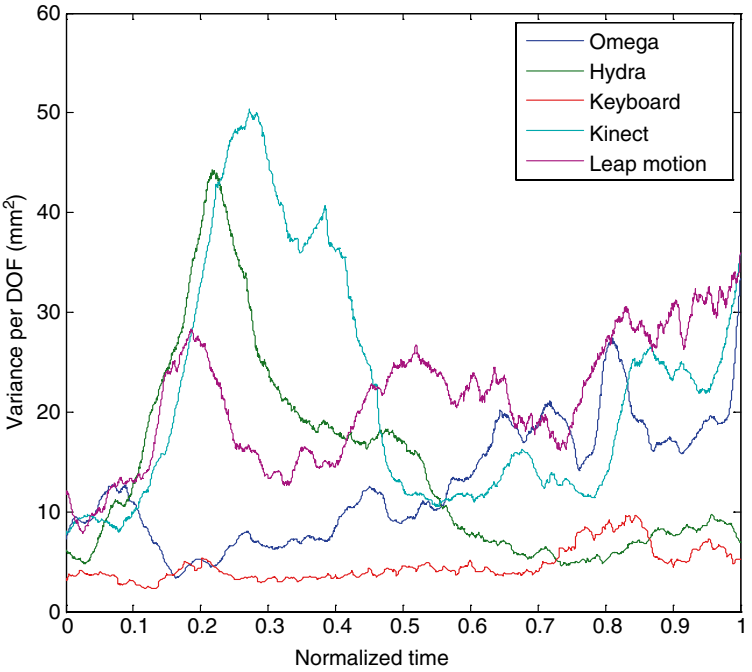

Fig. 17.14 Trial-to-trial variability analysis as a function of normalized time averaged among different trials. The variance per DOF is shown for all five interfaces

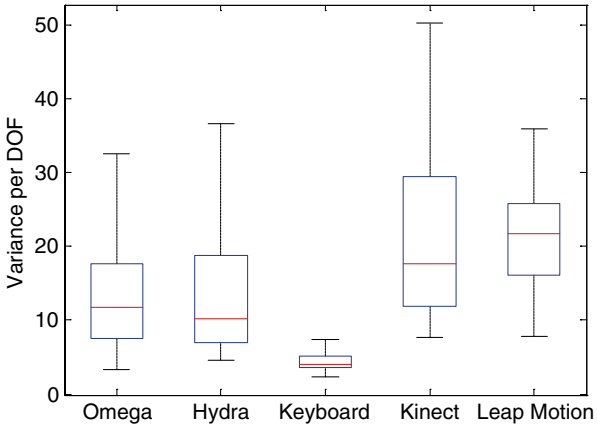

Fig. 17.15 Boxplot of the variance per DOF across five interfaces

discrete control (refer to Algorithm 17.3 for the Kinect discrete control algorithm), they showed opposing results. When using the Kinect to control the robot, large hand movements are required, and thus a potential for a large variability on those movements. Conversely, using the keyboard requires constrained movements (the location of the keys are fixed) and therefore the structured variability is low.

Table 17.1 Average performance for the peg transfer task

Interface	Time ± SD (sec)	Peg drops ± SD	Learning rate (%)
Omega	224.8 ± 59.6	0.4 ± 0.5	76.16
Hydra	441.0 ± 102.2	1.4 ± 2.2	87.51
Keyboard	351.0 ± 65.2	0.8 ± 0.8	83.76
Kinect	912.0 ± 301.2	1.4 ± 0.9	74.61
Leap motion	720.0 ± 310.1	3.6 ± 0.9	59.59

Peg Transfer

The second task involves completing the Fundamentals of Laparoscopic Surgery's (FLS) Peg Transfer task [36]. The operator is required to use the robot to pick up a soft ring from one side of the pegboard using the left arm, pass the ring to the right arm, and move it to one of the poles on the other side of the pegboard. This process is repeated for all six rings, in sequential order (see an example in Fig. 17.8). If the ring is dropped, this is counted as an error. The user is allowed to pick it up and continue the task. Best performance is achieved when minimum number of mistakes is made and shortest learning in completion task time is obtained.

Five engineering students completed the task; each one used a different interface to teleoperate Taurus. The task completion time was recorded for each of the trials in the experiment as well as the number of errors in each attempt. The average task completion time, number of peg drops and the learning rate were obtained and are shown in Table 17.1.

Users' task completion times were used to draw learning curves. These curves reflect the relative improvement over trial number (refer to Fig. 17.16). These results show that using the Leap motion interface to complete the task resulted in the highest learning rate. Another observation is that overall the touchless interfaces have shown a faster learning rate than the touch-based ones.

Conclusion and Future Work

A comparative study among touch-based and touch-less interfaces applied for teleoperating in a mock surgical environment is presented throughout this work. Among the touch-based interfaces, the Omega 7 haptic device, Hydra game controller and a standard keyboard were tested. For the touchless interfaces, the Kinect and Leap Motion controller were selected. Two experiments were conducted to measure the performance of each interface. Both experiments are based on surgical tasks: one involved conducting a horizontal incision on a surgical pad, the other to complete a peg transfer task.

For the first task, the tooltip's trajectory was recorded to measure the task performance using two metrics: distance-to-target annotation and control variance. The experiment revealed that the set of touchless interfaces presented comparable

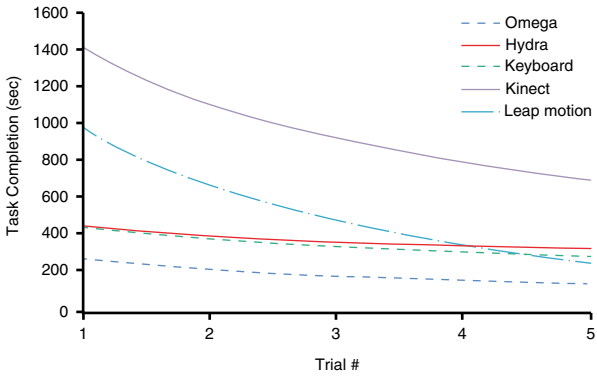

Fig. 17.16 Fitted learning curve for task completion times across all interfaces

deviation error against the touch-based ones when following a target trajectory; however, no statistically significance was found. Nevertheless, it was found that when using the Kinect interface, the variance was minimum (which is a desirable feature when conducting surgical incisions). This can be explained partially by the discrete control policy adopted; however keyboard control is intrinsically discrete as well and it did not show as a good performance when compared to the Kinect. The structured variability study reveals that the touch-less interfaces (Kinect and Leap motion) provide the largest amount of control freedom to the operator, while the keyboard reveals the most constrained among all interfaces. When using free hand gestures to navigate the robot, the operator faces fewer constraints compared with touch-based devices. Such unrestricted hand movements allows a large freedom of maneuver which is associated with skilled in-situ surgery. Conversely, using the keyboard requires constrained movements and therefore the structured variability is low.

The peg transfer experiment revealed that the Omega haptic controller required shorter times for task completion than the Kinect and the Leap Motion interfaces with a significant difference ($p < 0.01$). Results also indicate that overall the touchless interfaces have shown a faster learning rate than the touch-based ones ($r = 59$ % for the Leap Motion). Future work includes increasing the number of subjects tested and enhancing the sensory substitution method.

Acknowledgment This publication was made possible by the NPRP award (NPRP 6-449-2-181) from the Qatar National Research Fund (a member of The Qatar Foundation). The statements made herein are solely the responsibility of the authors.

References

1. da Vinci Surgery – minimally invasive robotic surgery with the da Vinci Surgical System. da Vinci Surgery. [Online]. http://www.davincisurgery.com/. Accessed 19 Apr 2014.
2. Rosen J, Hannaford B, Satava RM. Surgical robotics: systems applications and visions. Springer Science and Business Media; 2011.

3. Rautaray SS, Agrawal A. Vision based hand gesture recognition for human computer interaction: a survey. Artif Intell Rev. 2012;43(1):1–54.
4. von Hardenberg C, Bérard F. Bare-hand human-computer interaction. In Proceedings of the 2001 workshop on perceptive user interfaces. New York; 2001. p. 1–8.
5. Schultz M, Gill J, Zubairi S, Huber R, Gordin F. Bacterial contamination of computer keyboards in a teaching hospital. Infect Control Hosp Epidemiol Off J Soc Hosp Epidemiol Am. 2003;24(4):302–3.
6. Hartmann B, Benson M, Junger A, Quinzio L, Röhrig R, Fengler B, Färber UW, Wille B, Hempelmann G. Computer keyboard and mouse as a reservoir of pathogens in an intensive care unit. J Clin Monit Comput. 2004;18(1):7–12.
7. Kinect. [Online]. http://www.microsoft.com/education/ww/products/Pages/kinect.aspx. Accessed 28 Apr 2014.
8. Weichert F, Bachmann D, Rudak B, Fisseler D. Analysis of the accuracy and robustness of the leap motion controller. Sensors. 2013;13(5):6380–93.
9. Gaur AM, Karanveer, Kumar A, Rana DS. Design and development of touch based switching of myo electric arm. In 2010 IEEE International Conference on Communication Control and Computing Technologies (ICCCCT). Nagercoil, India; 2010. p. 247–9.
10. Hoshi T, Takahashi M, Nakatsuma K, Shinoda H. Touchable holography. In ACM SIGGRAPH 2009 Emerging Technologies. New York; 2009. p. 23:1–23:1.
11. Sodhi R, Poupyrev I, Glisson M, Israr A. AIREAL: interactive tactile experiences in free air. ACM Trans Graph. 2013;32(4):134:1–134:10.
12. Howe RD, Peine WJ, Kantarinis DA, Son JS. Remote palpation technology. IEEE Eng Med Biol Mag. 1995;14(3):318–23.
13. Okamura, AM, Verner, LN, Yamamoto, T, Gwilliam, JC, Griffiths, PG (2011). Force feedback and sensory substitution for robot-assisted surgery. In Surgical Robotics Springer US, pp. 419–448.
14. Prentice R. Drilling surgeons the social lessons of embodied surgical learning. Sci Technol Hum Values. 2007;32(5):534–53.
15. Lingard L, Reznick R, Espin S, Regehr G, DeVito I. Team communications in the operating room: talk patterns, sites of tension, and implications for novices. Acad Med. 2002;77(3):232–7.
16. Leap motion | Mac & PC motion controller for games, design, & more. [Online]. https://www.leapmotion.com/. Accessed 28 Apr 2014.
17. Enter the Hydra | Razer™ | for gamers. By Gamers.™. [Online]. http://www.razerzone.com/minisite/hydra. Accessed 28 Apr 2014.
18. Force dimension – products – omega.7. [Online]. http://www.forcedimension.com/omega7-overview. Accessed 28 Apr 2014.
19. Talamini M, Campbell K, Stanfield C. Robotic gastrointestinal surgery: early experience and system description. J Laparoendosc Adv Surg Tech. 2002;12(4):225–32.
20. Sengül A, van Elk M, Rognini G, Aspell JE, Bleuler H, Blanke O. Extending the body to virtual tools using a robotic surgical interface: evidence from the crossmodal congruency task. PLoS ONE. 2012;7(12), e49473.
21. Jacob MG, Li Y-T, Wachs JP. A gesture driven robotic scrub nurse. In 2011 IEEE International Conference on Systems, Man, and Cybernetics (SMC). Anchorage, USA; 2011, p. 2039–44.
22. Bach-y-Rita P, Kercel SW. Sensory substitution and the human–machine interface. Trends Cogn Sci. 2003;7(12):541–6.
23. Carter T, Seah SA, Long B, Drinkwater B, Subramanian S. UltraHaptics: multi-point mid-air haptic feedback for touch surfaces. In Proceedings of the 26th annual ACM symposium on user Interface software and technology. New York; 2013. p. 505–14.
24. Wachs JP, Stern HI, Edan Y, Gillam M, Handler J, Feied C, Smith M. A gesture-based tool for sterile browsing of radiology images. J Am Med Inform Assoc. 2008;15(3):321–3.
25. Oikonomidis I, Kyriazis N, Argyros AA. Efficient model-based 3D tracking of hand articulations using Kinect. In: BMVC. 2011. p. 1–11.

26. Ren Z, Yuan J, Zhang Z. Robust hand gesture recognition based on finger-earth mover's distance with a commodity depth camera. In Proceedings of the 19th ACM international conference on Multimedia. Scottsdale, USA; 2011. p. 1093–6.
27. Kim Y, Leonard S, Shademan A, Krieger A, Kim PC. Kinect technology for hand tracking control of surgical robots: technical and surgical skill comparison to current robotic masters. Surg Endosc. 2014;28(6):1993–2000.
28. Padoy N. Research homepage of Nicolas Padoy. [Online]. http://www.cs.jhu.edu/~padoy/doku.php/videos. Accessed 28 Apr 2014.
29. Ryden F. Tech to the future: making a 'Kinection' with haptic interaction. IEEE Potentials. 2012;31(3):34–6.
30. Hartmann F, Schlaefer A. Feasibility of touch-less control of operating room lights. Int J Comput Assist Radiol Surg. 2013;8(2):259–68.
31. Johnson R, O'Hara K, Sellen A, Cousins C, Criminisi,A. Exploring the potential for touchless interaction in image-guided interventional radiology. In Proceedings of the SIGCHI conference on human factors in computing systems. New York; 2011. p. 3323–32.
32. Gomez J-B, Ceballos A, Prieto F, Redarce T. Mouth gesture and voice command based robot command interface. In IEEE International Conference on Robotics and Automation, 2009. ICRA'09. Kobe, Japan; 2009. p. 333–8.
33. John JC. Introduction to robotics: mechanics and control. Reading: Addison-Wesley; 1989.
34. Sonka M, Hlavac V, Boyle R. Image processing, analysis, and machine vision. 4th ed. Mason: Cengage Learning; 2014.
35. Nisky I, Hsieh MH, Okamura AM. A framework for analysis of surgeon arm posture variability in robot-assisted surgery. In 2013 IEEE International Conference on Robotics and Automation (ICRA). Madison, USA; 2013. p. 245–51.
36. Ritter EM, Scott DJ. Design of a proficiency-based skills training curriculum for the fundamentals of laparoscopic surgery. Surg Innov. 2007;14(2):107–12.

Part V
Validation in Computer-Assisted Surgical Workflows

Chapter 18
Accuracy and Precision in Computer-Assisted Methods for Orthopaedic Surgery

Federico E. Milano and Olivier Cartiaux

Abstract This chapter reviews the major approaches to the definition of bone cutting accuracy in the field of computer-assisted orthopaedic surgery. The first part of the chapter reviews the different concepts of accuracy found in literature, from localization in image-guided systems to osteotomy accuracy evaluation both using navigation systems and in patient-specific instruments. The second part of the chapter focuses in the efforts toward the standardization of different computer-assisted accuracy measurements in orthopaedic surgery.

Keywords Metrology • Accuracy • Precision • Osteotomy • Bone cutting • Standard

Introduction

The systematic evaluation of accuracy and precision in orthopaedic surgery has been an open research line since the pioneering work by Simon et al. [1] at Carnegie Mellon Robotics Institute. Almost 20 years have passed and there is still no shared definition or common understanding of accuracy in computer-assisted orthopaedic surgery. This is reflected by the words of Abraham [2]: "the definition of accuracy in current navigation reports is inconsistent and can at times be misleading". Literature presents many different definitions of accuracy and precision, and several different technical ways to acquire the data used to estimate those parameters. This situation begs at least for a brief but general review of the existing approaches to this problem and the efforts to generate a common consent.

F.E. Milano (✉)
Department of Bioengineering, Instituto Tecnologico de Buenos Aires,
Avenida Eduardo Madero 399, Buenos Aires C1106AD, Argentina
e-mail: fmilano@itba.edu.ar

O. Cartiaux, Ir, PhD
Computer Assisted and Robotic Surgery, Institut de Recherche Expérimentale et Clinique,
Université Catholique de Louvain,
Avenue Mounier 53, box B1.53.07, Brussels B-1200, Belgium
e-mail: olivier.cartiaux@uclouvain.be

L.E. Ritacco et al. (eds.), *Computer-Assisted Musculoskeletal Surgery: Thinking and Executing in 3D*, DOI 10.1007/978-3-319-12943-3_18

This chapter is divided into two parts: the first part discusses the different definitions commonly found in the literature and their associated measuring methods; the second part examines the ongoing standardization efforts.

Accuracy Is Said in Many Ways

Localization Accuracy in Image-Guided Navigation

Image-guided surgical navigation systems are designed to help the surgeon in the task of correlating what it is seen in the preoperative medical images and the real anatomy of the patient. The principle behind these systems is that there exists a rigid transformation between the preoperative images and the anatomy of the patient. The process to find this transformation is called "registration" and it consists of selecting at least three corresponding pairs of fiducial points in the preoperative images and in the patient anatomy. In the best case, those fiducials are well known anatomical landmarks, but many times, especially in minimally invasive approaches on complex anatomy, those landmarks are very hard to find. Moreover, there are even more fundamental caveats in the registration process, as those described in the work by Fitzpatrick et al. [3]. In that work the authors mention that point-based registration error can be divided into three different errors:

1. Fiducial localization error (FLE): error in locating the fiducial points.
2. Fiducial registration error (FRE): statistic about the distances between corresponding fiducial points after registration (usually reported as registration accuracy by image-guided systems).
3. Target registration error (TRE): distance after registration between points of interest other than the fiducial points.

The main result of Fitzpatrick's work is the derivation of the statistical distribution for TRE, but the most significant contribution from the application viewpoint is the insight about what is a good registration: a low FRE value is good, but it does not guarantee high accuracy unless other things have been taken into account, like using more than three fiducial points, placing those points far apart and surrounding the target of interest. Another important conclusion is that when "FRE falls below a certain threshold, it gives no further information regarding accuracy".

A recent study by Stoll et al. [4] in the orthopaedic oncology domain adds a refinement step to the point-based registration. This refinement step generally depends on proprietary surface digitizing devices (surface probing, laser scanning) and computer algorithms that usually perform a small adjustment to the previous fiducial registration step. In their work, Stoll et al. found that even after the surface refinement algorithm provided by a commercial navigation system, the differences between target points and their corresponding points in the navigated images are in a 95 % CI 6.11–16.96 mm.

Evaluation of Osteotomies

Multiple forms of evaluating osteotomies have been published, depending both on the intended area of application and on the technology applied to acquire the data used to perform the evaluation. Barrera et al. [5] propose a method to assess the 'quality' of bone preparation for knee arthroplasty bone insertion. One of the steps in this assessment process is the estimation of each single planar cut. The method represents the accuracy using five indices for each cut. There is one translational error index (in mm) and three rotational error indices; these last three, combined, result in an overall rotational index (in degrees). The experiments are executed on synthetic knees and the 'achieved' surface is digitized after the cut. The article proposes several methods for capturing the surface but it also warns about the different accuracy and precision parameters of those methods.

In a classic article, Cartiaux et al. [6] propose a method based in the ISO 1101:2004 standard for geometrical tolerancing to evaluate differences between a cutting plane and a target plane. Their work shows that it is possible to express the most significant translational and rotational errors using only the location parameter (L) defined in the mentioned ISO standard. This parameter is the maximum euclidean distance from the executed cutting surface to the target plane in a perpendicular trajectory to the last one. For experimental data gathering a test bed with a block simulating bone tissue is used and errors are estimated with a coordinate measuring machine set in the same frame of reference. The method is also used in [7] for evaluating different bone cutting technologies. In this work the error (L) was 0.92 ± 0.37 mm with a robot-assisted process compared with 1.26 ± 0.88 mm with the freehand process ($p < 0.0001$) and 1.87 ± 2.09 mm with the navigated freehand process ($p < 0.0001$).

So et al. [8] introduce a new registration procedure using fluoro-CT matching and evaluate its accuracy using the postoperative gross measurement of surgical margin. The accuracy in this case is related to the planned margin, and it is not an absolute value.

Dobbe et al. [9] propose a method to measure and estimate the normal of an executed plane. This normal is used to compute the dihedral angle with the target plane, that is decomposed in sagittal and coronal plane angles. Then a distance error between the target and executed plane is computed taking the Euler distance between the centroids of the cross sections defined by target and executed planes. This method is validated using a cadaveric limb, with pre and postoperative computed tomography (CT) scans positioned in a common frame of reference using a registration algorithm. The methodological accuracy and precision is also evaluated, showing that the method introduces an error that it is well below 0.5 mm in mean.

Stiehl et al. suggest [10] using tools borrowed from the field of statistical process control in the domain of accuracy and precision evaluation in computer-assisted orthopaedic surgery. Milano et al. [11] follow that path introducing a definition of accuracy and precision that could be used with the industry proved process performance index as a clinical score and using CT scans to digitize the surgical

specimen resected from the patient. The introduction of an index helps to avoid the problem of measuring the accuracy against a fixed frame of reference. This work also evaluates the methodological error. This error is below 1 mm in all the test cases. A first application of this methodology in the evaluation of surgical accuracy in 61 osteotomies performed on 28 patients is found in the article by Ritacco et al. [12]; this work shows that the accuracy parameter is 2.52 ± 2.32 mm.

In a recent article, Sternheim et al. [13] use a custom navigation system with synthetic and cadaveric pelvic bones to generate a large number of cuts. The cuts are evaluated by CT scanning the bones after the osteotomies and measuring the entry and exit cut distances and deriving the pitch and roll angle differences. In navigated cuts, using synthetic bones, the entry error is 1.6 ± 1.1 mm and the exit error is 2.3 ± 1.1 mm, while in non-navigated cuts the entry error is 2.8 ± 4.9 mm and the exit error is 3.5 ± 4.6 mm.

Patient-Specific Instrumentation

Patient-specific instrumentation (PSI) technology is an alternative to intraoperative navigation. The accuracy of PSI technology adapted for bone tumor surgery has been studied by Cartiaux et al. in [14]. In that article experiments are conducted using synthetic right hemipelvic bone models that are fixed to a test bed, setting a global reference frame for measurement. The test bed is digitized using a CT-scanner and a simulated tumor is introduced in the bone. A mixed seniority group of 24 orthopaedic surgeons performs the bone cuts with a pneumatic oscillating saw. The experiments show that the location accuracy of the cut planes varies significantly in terms of mean and 95 % confidence interval (CI) among the four target planes. The average location accuracy in the anterior and posterior ilium is 1.0 mm (CI 0.8–1.3 mm) and 1.2 mm (CI 0.9–1.6 mm) respectively and it is significantly different from the average in the pubis and ischium, 2.0 mm (CI 1.5–2.7 mm) and 3.7 mm (CI 2.8–4.9 mm) respectively. The surgical margins achieved in the pubis, with an average of 11.8 mm (CI 11.3–12.3 mm), were significantly higher than those achieved in the ischium and anterior and posterior ilium, with an average of 9.2 mm (CI 8.6–9.7 mm), 10.0 mm (CI 9.5–10.6 mm) and 9.7 mm (CI 9.2–10.3 mm) respectively.

Standardization Efforts

Proposal for New ISO Standardization Activities

So far, there is no standardization work within ISO and IEC directly related to accuracy measurement in CAOS.

In 2004, the International Society for Computer Assisted Orthopaedic Surgery (CAOS-International), in conjunction with the American Society for Testing of Materials (ASTM), undertook the creation of a new ASTM standard for assessing

and comparing the performances of CAOS systems [10]. This standard was published in 2010 as ASTM F2554-10 [15] and used the definition of accuracy and precision parameters provided by ASTM standard E177-08 [16]. The standard F2554-10 is used to define the technical specifications (accuracy and precision) of navigation systems and positioning robots for CAOS [17, 18]. In consequence, it cannot be used directly for measuring the accuracy of bone-preparation tasks, but the standard claims that the logical continuation will be to work on additional standards that will address task-specific procedures and surgical applications (joint arthroplasty, osteotomy, tumour biopsy and/or resection, laparoscopy, pedicle screw insertion, brain surgery, and so forth).

Since October 2013, subcommittee ASTM F04.38 has launched a new work item entitled "WK41641 New test method for mechanical influence on computer assisted surgical system accuracy", aiming to measure the effects of the operating room environment on the accuracy of computer aided surgical systems in relation to the equipment utilized for bone preparation. This work item recently resulted in a new standard published in 2014 as ASTM F3107-14 "Standard Test Method for Measuring Accuracy after Mechanical Disturbances on Reference Frames of Computer Assisted Surgery Systems" [19]. Even if this new standard is clinically relevant for CAOS surgeries, the resulting standard will not be able to be used directly to measure the accuracy of the bone-preparation tasks.

The Standard ISO 5725–1:1994 "Accuracy (trueness and precision) of measurement methods and results – Part 1: General principles and definitions" outlines the general principles to be understood when assessing accuracy (trueness and precision) of measurement methods and results [20]. This standard is significant for the standardization activities proposed here because it forms a relevant basis for defining the terminology of accuracy and accuracy measurement in CAOS.

The Standard ISO1101:2012 "Geometrical product specifications (GPS), Geometrical tolerancing, Tolerances of form, orientation, location and run-out" has been used since the 80s in mechanical engineering to define the geometrical tolerances of mechanical parts, regardless of the fabrication process [21]. This standard is significant for the standardization activities proposed here because it has already been in use for bone tumour surgery since 2009 [6, 7, 14, 22–24], considering bone as a material with specific mechanical properties, to define geometrical tolerances and to assess the accuracy of planar bone-cutting, regardless of the assisting technologies used to execute the bone cuts.

By focusing on systematic and global methodologies and approaches for accuracy measurement of bone-preparation tasks in CAOS, the standardization activities that we propose now for ISO are the logical continuation of the previous and current standardization works made by ASTM and CAOS-International concerning the intrinsic performances of surgical assistance systems.

We aim to produce a new consensus-based international standard on accuracy measurement in computerassisted orthopaedic surgery (CAOS), including the terms and definitions concerning accuracy and accuracy measurement in CAOS, and the methods for measuring accuracy of bone-preparation tasks inCAOS (bone-cutting, bone-drilling and bone-assembly). In addition, we aim to produce an informative technical document to provide the users with practical guidance to the clinical use

of the new standard within the workflow of orthopaedic interventions such as joint arthroplasty, spine instrumentation, corrective osteotomy, fracture reduction, bone tumour resection, and so forth.

Proposed Programme of Work

First, we will draw up the terminological basics, including the terms and the definitions concerning accuracy and accuracy measurement in CAOS. These basics will provide the necessary elements for a common language for all the activities of accuracy measurement in CAOS, and especially for consistently understanding and applying the accuracy measurement methods that will be developed for bone-cutting, bone-drilling and bone-assembly. Practically, the basics will include: the elements to define the geometrical specifications of desired bone cutting, drilling and assembly; the elements to define the geometrical accuracy of performed bone cutting, drilling and assembly; the metrology elements to quantify the geometrical accuracy of performed bone cutting, drilling and assembly; and finally the statistical elements to compare the geometrical accuracy of performed bone cutting, drilling and assembly with respect to the desired geometrical specifications.

Second, we will draw up methods for measuring accuracy of bone-cutting, bone-drilling and bone-assembly. Each accuracy measurement method will take the form of a systematic step-by-step approach starting with defining the desired geometrical specifications and then enabling to measure and evaluate the accuracy of performed bone cutting, drilling and assembly. These accuracy measurement methods will be regardless of the CAOS assisting technologies and the systems that could be used during the surgery to assist for the execution of bone cutting, drilling and assembly, such as surgical navigation systems, surgical robots, patient-specific instruments, and so forth.

In consequence, the standardization activities proposed here will result in a new standard document consisting of four parts: the first part for the terminology and the second, third and fourth parts for the three systematic methods for measuring accuracy of bone-cutting, bone-drilling and bone-assembly respectively. This resulting standard will be technical and probably not be able to be used directly in clinical routine. So we propose a second phase in our work program as the following.

In conjunction with the new International Standard, we will draw up a Technical Report as an informative guidance document. The purpose of this Technical Report is to provide the users with practical guidance to the use of the new International Standard for designing and implementing new quality evaluation protocols within the surgical workflow of orthopaedic interventions involving bone-cutting, bone-drilling and/or bone-assembly. Practically, involved orthopaedic interventions are the following:

- Bone tumor surgery: to measure the accuracy of the bone cutting and assembly that are necessary to resect the bone tumor in safe margin and reconstruct the bone defect with a massive bone graft or a prosthesis.
- Spine surgery: to measure the accuracy of the bone drilling necessary to insert screws safely within the pedicles of the vertebrae.

- Knee surgery: to measure the accuracy of the bone cutting and drilling that are necessary to prepare the placement of the femoral and tibial prosthesis components.
- Hip surgery: to measure the accuracy of the bone drilling that are necessary to insert internal screws or nails to reduce and stabilize a femoral neck fracture.
- Corrective surgery: to measure the accuracy of the bone cutting and assembly that are necessary to reposition bone fragments and correct a malunited bone fracture.

The standardization activities proposed here will also consider the variety of technologies and systems that could be used during the intervention, not to execute desired bone cutting, drilling and assembly, but to measure the accuracy of performed bone cutting, drilling and assembly. Such technologies and systems can be intraoperative CT or fluoroscopic images to perform image registration and bone segmentation, navigation systems and robots to perform real-time tracking and tool localization, and so forth. Commonly accepted recommendation is to minimize the measuring errors by using measurement procedures and systems with an accuracy of an order of magnitude much greater than the errors expected during the execution of the bone-preparation tasks. The minimization of measuring errors is complex because it accounts for system calibration process, construction of reference frames, transformation and registration process, and so forth.

Protocols for measuring positional accuracy of surgical tracking systems will not be covered because they are already covered by ASTM standard F2554-10, however they will be of significant importance for the standardization works proposed here.

Expected Contributions

The relevant affected stakeholders can be listed as the following:

- Orthopaedic surgeons and hospitals with orthopaedic surgery departments
- University laboratories active in CAOS research
- Industrials active in the field of medical and surgical devices in orthopaedics (implants, instruments, computer-assisted systems, etc.)
- Regulatory Agencies

The benefits for stakeholders can be listed as the following:

- Surgeons: practical step-by-step guidance to peroperatively measure the accuracy of bone cutting, drilling and assembly in CAOS with respect to a preoperative desired planning.
- Researchers: standardization can contribute to the validation and integration of new CAOS technologies that are still in prototyping in the research laboratories.
- Industrials: these activities can contribute to the assessment of new technologies that are ready for the marketplace.

Overall, standardization can improve the work of, and the communication between, surgeons, researchers and the regulatory agencies. This can push forward

a common language to define and quantify the quality of the bone-preparation tasks before we can correlate the improved accuracy with clinical outcomes.

The contributions of the proposed standard can then be listed as the following:

- Societal benefit: to better know the added value of CAOS technologies and secure acceptance of the notion of quality evaluation of bone-preparation tasks executed with the aid of CAOS technologies;
- Scientific benefit: to propose a common language for clinicians and researchers to assess the accuracy of CAOS interventions, before we can correlate improved accuracy with functional outcomes during future international long-term follow-up studies;
- Technological benefit: to facilitate and improve the clinical integration of CAOS technologies and their use in clinical routine;
- Economic benefit: to increase the use of assistance technologies for orthopaedic surgery.

Toward a First International Workshop

As a result, a work group composed of engineers, surgeons and industry representatives at the international scale has to be formed. We are planning to submit the proposal in 2015 to the ISO Central Secretariat (Geneva) for the development of the new consensus-based standard on accuracy measurement in CAOS. We also believe this is the appropriate time for the CAOS community to initiate a discussion on accuracy standardization. With this in mind, and as a first step, we would like to propose a first international workshop to communicate on this area and solicit the participation and gauge the level of interest of the CAOS community towards the proposed standardization activities.

Conclusion

The objective evaluation of accuracy and precision in computer-assisted orthopaedic surgery is crucial, on the one hand, to assess the performance of different tools and processes applied nowadays during everyday practice. On the other hand, a proper evaluation of future developments in orthopaedic surgery depends to a great extent on the possibility of objectively measuring the performance of new tools and methods during surgical procedures. This review chapter briefly describes the different approaches and achievements of the research line working toward those aims. There is still much work to be done, since computer-assisted surgery is being adopted by and adapted for new orthopaedic applications. The international standardization effort is a well-focused but recent project that, in our opinion, will start producing concrete results in 3–5 years. These are exciting times to work in

this field, when exact definitions and formalization of previous intuitive knowledge open the gate for new developments.

References

1. Simon D, O'Toole, R, Blackwell, M. Accuracy validation in image-guided orthopaedic surgery. In: Medical robotics and computer assisted surgery. New York: Wiley. p 185–92.
2. Abraham JA. Recent advances in navigation-assisted musculoskeletal tumor resection. Curr Orthop Pract. 2011;22(4):297–302.
3. Fitzpatrick JM, West JB. The distribution of target registration error in rigid-body point-based registration. IEEE Trans Med Imag. 2001;20(9):917–27.
4. Stoll KE, Miles JD, White JK, et al. Assessment of registration accuracy during computer-aided oncologic limb-salvage surgery. Int J Comput Ass Rad. 2015. doi:10.1007/s11548-014-1146-1.
5. Barrera OA, Haider H, Garvin KL. Towards a standard in assessment of bone cutting for total knee replacement. Proc Inst Mech Eng H. 2008;222(1):63–74.
6. Cartiaux O, Paul L, Docquier P, et al. Accuracy in planar cutting of bones: an ISO-based evaluation. Int J Med Robot. 2009;5(1):77–84.
7. Cartiaux O, Paul L, Docquier P, et al. Computer-assisted and robot-assisted technologies to improve bone-cutting accuracy when integrated with a freehand process using an oscillating saw. J Bone Joint Surg Am. 2010;92(11):2076–82.
8. So TYC, Lam YL, Mak KL. Computer-assisted navigation in bone tumor surgery: seamless workflow model and evolution of technique. Clin Orthop Relat Res. 2010;468(11):2985–91.
9. Dobbe JGG, Kievit AJ, Schafroth MU, et al. Evaluation of a CT-based technique to measure the transfer accuracy of a virtually planned osteotomy. Med Eng Phys. 2014;36(8): 1081–7.
10. Stiehl J, Bach J, Heck D. Validation and metrology in CAOS. In: Stiehl J, Konermann WH, Haaker RG, et al., editors. Navigation and MIS in orthopedic surgery. Berlin/Heidelberg: Springer; 2007. p. 68–78.
11. Milano FE, Ritacco LE, Farfalli GL, et al. Transfer accuracy and precision scoring in planar bone cutting validated with ex vivo data. J Orthop Res. 2015. doi:10.1002/jor.22813.
12. Ritacco LE, Milano FE, Farfalli GL, et al. Accuracy of 3-D planning and navigation in bone tumor resection. Orthopedics. 2013;36(7):e942–50.
13. Sternheim A, Daly M, Qiu J, et al. Navigated pelvic osteotomy and tumor resection: a study assessing the accuracy and reproducibility of resection planes in Sawbones and cadavers. J Bone Joint Surg Am. 2015;97(1):40–6.
14. Cartiaux O, Paul L, Francq BG, et al. Improved accuracy with 3D planning and patient-specific instruments during simulated pelvic bone tumor surgery. Ann Biomed Eng. 2014;42(1): 205–13.
15. ASTM Standard F2554-10 standard practice for measurement of positional accuracy of computer assisted surgical systems. ASTM International, West Conshohocken; 2010.
16. ASTM Standard E177-08 standard practice for use of the terms precision and bias in ASTM test methods. ASTM International, West Conshohocken; 2008.
17. Clarke JV, Deakin AH, Nicol AC, et al. Measuring the positional accuracy of computer assisted surgical tracking systems. Comput Aided Surg. 2010;15:13–8.
18. Haidegger T, Kazanzides P, Rudas I, et al. The importance of accuracy measurement standards for computer-integrated interventional systems. In: EURON GEM sig workshop on the role of experiments in robotics research at Anchorage, Alaska, USA.
19. ASTM Standard F3107-14 standard test method for measuring accuracy after mechanical disturbances on reference frames of computer assisted surgery systems. ASTM International, West Conshohocken; 2014.

20. ISO Standard 5725–1:1994 accuracy (trueness and precision) of measurement methods and results – Part 1: General principles and definitions. International Organization for Standarization, Geneva; 1994.
21. ISO Standard 1101:2004 Geometrical Product Specifications (GPS) – geometrical tolerancing – tolerances of form, orientation, location and run-out. International Organization for Standarization, Geneva; 2004.
22. Cartiaux O, Banse X, Paul L, et al. Computer-assisted planning and navigation improves cutting accuracy during simulated bone tumor surgery of the pelvis. Comput Aided Surg. 2013;18:19–26.
23. Khan FA, Lipman JD, Pearle AD, Boland PJ, Healey JH. Surgical technique: computer-generated custom jigs improve accuracy of wide resection of bone tumors. Clin Orthop Relat Res. 2013;471:2007–16.
24. Khan FA, Pearle AD, Lightcap C, et al. Haptic robot-assisted surgery improves accuracy of wide resection of bone tumors: a pilot study. Clin Orthop Relat Res. 2013;471:851–9.

Part VI
Emerging Trends

Chapter 19
Computer Simulation Surgery for Deformity Correction of the Upper Extremity

Tsuyoshi Murase

Abstract Three-dimensional (3D) anatomical correction is desirable for treatment of long bone deformity of the extremity. A system including a 3D computer simulation program and a patient matched osteotomy guide (PMI: Patient Matched Instrument) designed on the basis of simulation has recently been introduced to achieve accurate results. This system can benefit deformity correction of the upper extremity where anatomically accurate correction is mostly important. Computer bone models are constructed from the CT data and used for simulation of deformity correction. The most appropriate method of correction is simulated on the computer using those 3D bone models on the basis of deformity evaluation after comparing the affected side with the mirror image of the contralateral healthy side. PMI, which has a shape that exactly fits the specific bone surface, a slit or slits for osteotomy and guiding holes for K-wire insertion, is then designed and manufactured through a rapid prototyping machine. Operation is conducted with use of PMI that is placed in the correct position of the bone and helps a surgeon to cut and correct the deformed bone according to the preoperative simulation.

Malunion of the forearm bones, cubitus varus deformity, and malunited distal radius are well managed with this technique with favorable radiographic and clinical outcomes.

Keywords deformity correction • upper extremity • three-dimensional • computer simulation • patient matched instrument

Introduction

Treatment of symptomatic bone deformity of the extremity resulting from malunited fractures has always been challenging. Anatomically accurate correction is the key to obtaining good functional outcomes after corrective osteotomy, especially for

T. Murase, MD, PhD
Department of Orthopaedic Surgery, Osaka University, Graduate School of Medicine, 2-2, Yamada-oka, Suita 565-0871, Osaka, Japan
e-mail: tmurase-osk@umin.ac.jp

L.E. Ritacco et al. (eds.), *Computer-Assisted Musculoskeletal Surgery: Thinking and Executing in 3D*, DOI 10.1007/978-3-319-12943-3_19

the upper extremity, where the elaborate musculoskeletal mechanism ensures wide, stable, and delicate joint motion [1, 2]. However, conventional preoperative planning with two-dimensional (2D) plain radiographs has not always provided sufficient information to understand the complex three-dimensional (3D) deformity [3–5]. On the other hand, advances in computer technology such as the development of a multidetector computed tomography (CT) scanner, and rapid prototyping technology have made an accurate 3D preoperative simulation possible [6–8]. To establish an accurate surgical treatment for malunited fractures of the extremity, a simulation system consisting of a 3D computer program and a patient matched osteotomy guide (PMI: Patient Matched Instrument) that allows the reproduction of preoperative simulation during actual surgery has been developed [9–15]. This system, despite shortcomings like radiation exposure during CT scanning and time and expense necessary for simulation and manufacturing of a PMI, has been proved to facilitate accurate anatomical correction with a simple osteotomy.

Malunion of the forearm bones, cubitus varus deformity, and malunited distal radius are the representative types of malunited fracture of the upper extremity. Symptoms and functional impairments related to these deformities may cause serious disabilities [16–19]. Although corrective osteotomy has been performed to improve the function and appearance of the extremity, it is not easy to correct three-dimensionally complex bone deformities accurately [20]. Previous studies have suggested the usefulness of frontal and sagittal radiographs in the preoperative planning of corrective osteotomy, although the estimate of 3D deformity with 2D images has limitations [21, 22]. Failure to make an accurate correction may lead to inferior clinical results, especially in the upper extremity, where anatomical bone configuration is of considerable importance to function [19, 23]. The computer program can indicate the optimum pattern and plane of corrective osteotomy by calculating the axis and amount of 3D deformity. The PMI navigates the surgical procedure to realize the preoperative simulation.

Malunited Forearm Fracture

Corrective osteotomy for malunited diaphyseal forearm fractures remains a challenging procedure [24–28]. Anatomical correction of angular deformity, achievement of axial alignment, and restoration of normal length of both bones are considered to be prerequisites for a good clinical outcome [29]. However, malunion with complex 3D deformities of both forearm bones is difficult to assess accurately by plain radiography or cross-sectional imaging [25]. Although simple angular deformity can be assessed by plain radiography, rotational malalignment is difficult to detect on plain radiographs. Furthermore, several studies have revealed that two-dimensional evaluation does not always provide accurate information of complex 3D deformities [20, 30].

Recently, advances in computer technology allow us to accurately evaluate deformity with 3D computer bone models created from computed tomography (CT) data [4, 21, 31]. The newly developed system incorporating a 3D computer simulation program using computer bone models and a patient matched instrument (PMI) have successfully achieved 3D anatomical correction [11, 13, 14, 32].

Construction of 3D Bone Models, Deformity Evaluation and Simulation of Deformity Correction

In planning corrective osteotomy, 3D correction of the deformity is simulated using a computer model of the bones. The affected and contralateral forearms of a patient are scanned with CT with a low-radiation dose technique (scan time 0.5 s, scan pitch 0.562:1, tube current 10–30 mA, tube voltage 120 kV) [33]. Scans were performed in the prone position with the shoulder at full elevation, elbow at full extension, and both limbs overhead. CT data are saved in a standard format (DICOM: Digital Imaging and Communications in Medicine) and sent to a workstation. 3D bone surface models of the entire bilateral radius and ulna are created from 1.25-mm slice digital data (Fig. 19.1) and a 3D correction of the deformity is simulated using commercially available software (Bone Simulater; Orthree Co., Ltd., Osaka, Japan). The degree of deformity is three-dimensionally evaluated by the screw displacement axis technique, which expresses every bone deformity with rotation around and translation along a unique axis in space (Fig. 19.2) [34, 35]. The axis and the rotational and translational amounts were calculated from the distance between the mirror image of the normal bone, which is considered the goal model, and the image of the affected bone superimposed proximally to distally (Fig. 19.3). On the basis of this evaluation, 3D corrective osteotomy of 3 different types (closing wedge, opening wedge, and rotational osteotomy with/without shortening or lengthening) is simulated on the computer (Figs. 19.4 and 19.5) [13]. Shortening or lengthening of the bones is simultaneously simulated on the computer to correct radioulnar discrepancy.

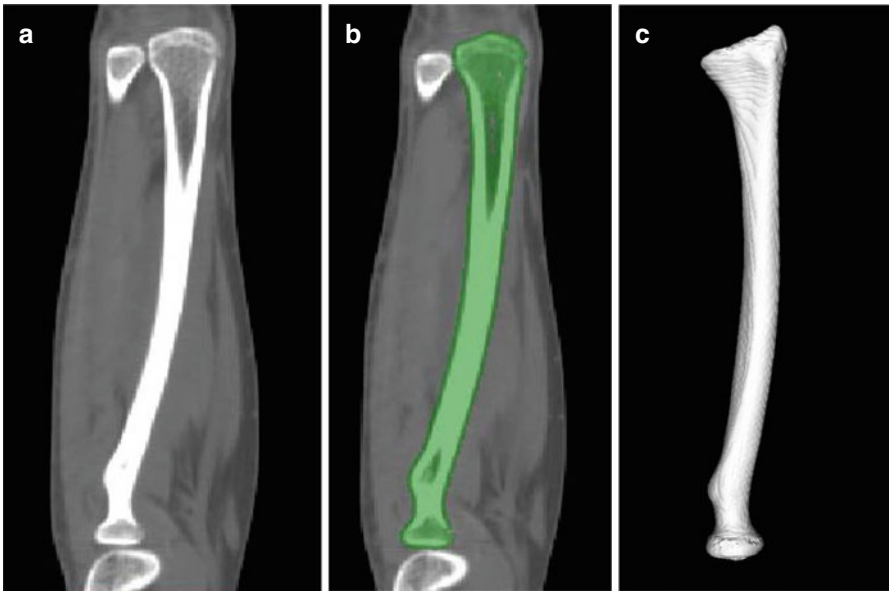

Fig. 19.1 3D bone surface models of the entire bilateral radius and ulna are created from 1.25-mm CT data. CT slice (**a**), segmentation of the radius (**b**) and 3D bone surface model of the radius (**c**)

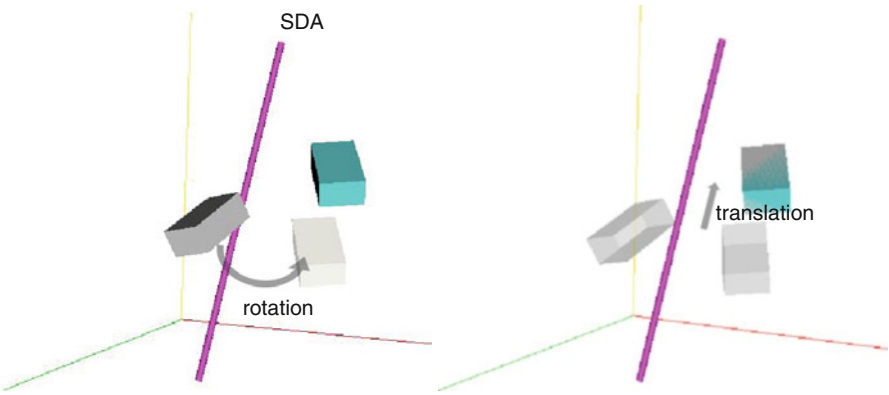

Fig 19.2 In a 3-D space, motion of every body can be expressed in terms of rotation around and translation along one unique axis or the screw displacement axis (SDA)

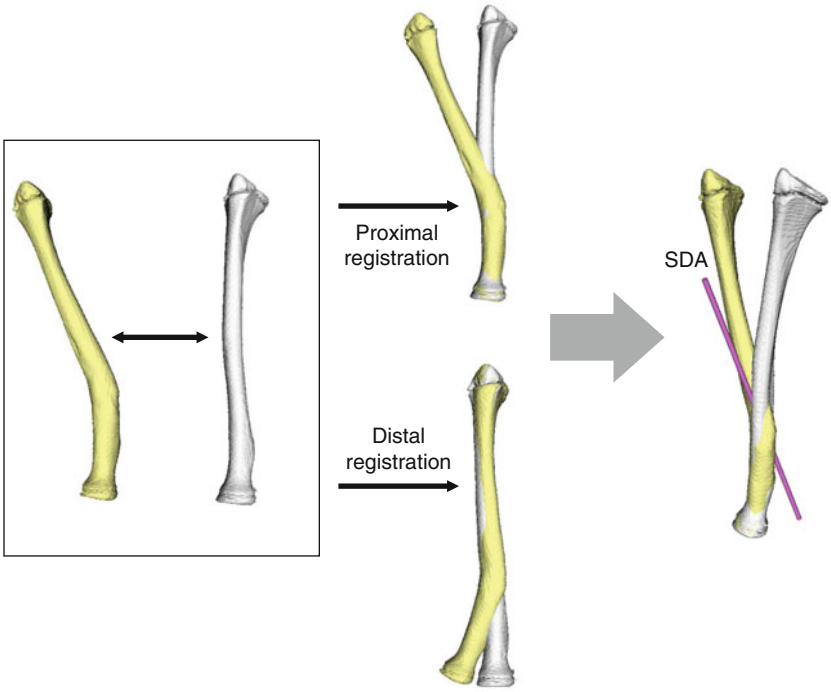

Fig. 19.3 The proximal part of the malunited bone (*yellow*) was superimposed with the corresponding part of the mirror image of the contralateral normal bone (*white*). The same procedure was then used for the distal part. By calculating the difference between the positions of the proximal and the distal parts, we acquired a matrix for the displacement, i.e., deformity of the distal part relative to the proximal part. This displacement can be further defined in terms of rotation around and translation along and a certain axis using the screw displacement axis (SDA) technique, respectively. Thus, bone deformity can be determined as the rotation around and translation along a single unique axis. When the translation is small, the SDA can be simply regarded as the deformity axis

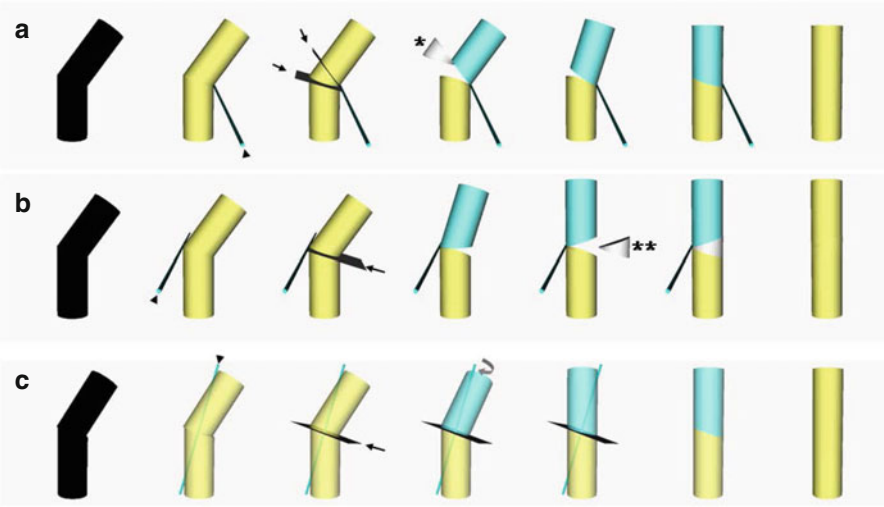

Fig. 19.4 The bended cylinders stand for the deformed bones. Different deformities would show similar silhouette (the left figures of **a**, **b** and **c**). Three-dimensional relation between the bone and deformity axis (*arrow head* of each figures) suggests the most appropriate method of correction. When the axis runs along the concave side of the deformity, a closing osteotomy after removal of a wedge (*asterisk*) brings about the rotation of the bone segment around the deformity axis thereby completes the correction (**a**). When the deformity axis is along the convex side, an opening wedge osteotomy followed by wedge-shaped bone grafting (*double asterisks*) is considered appropriate (**b**). When the axis is nearly parallel to the longitudinal bone axis, a rotational osteotomy (*curved arrow*) can be conducted along on the osteotomy plane, which is perpendicular to the deformity axis (**c**). If the deformity axis is displaced from the bone, closing/opening wedge osteotomy with shortening/lengthening is appropriate. Osteotomy planes are indicated by *arrows*

Design and Manufacturing of Patient Matched Instrument (PMI)

To reproduce the preoperative simulation in the actual surgery, a PMI with guiding holes for Kirschner wires and an osteotomy slit is designed on the basis of a 3D computer simulation using commercially available software (Magics RP; Materialise, Leuven, Belgium or Space-E; NTT Data Engineering Systems Corp., Tokyo, Japan) (Fig. 19.6) [13, 32]. PMI is shaped to closely fit the bone surface while the slit guides accurate osteotomy, and 2 sets of Kirschner wires, inserted through the drill-holes at an angle to the deformity, indicate that reduction is complete when they align parallel to each other. The PMI is then embodied as a plastic model through rapid prototyping machine (Eden250; Objet Geometries, Rehovot, Israel or Formiga P100; Electro Optical Systems GmbH, Munich, Germany) with medical grade plastic material. A reduction guide is prepared preoperatively to maintain the parallel position of the Kirschner wires in the same manner as for the PMI (Fig. 19.7).

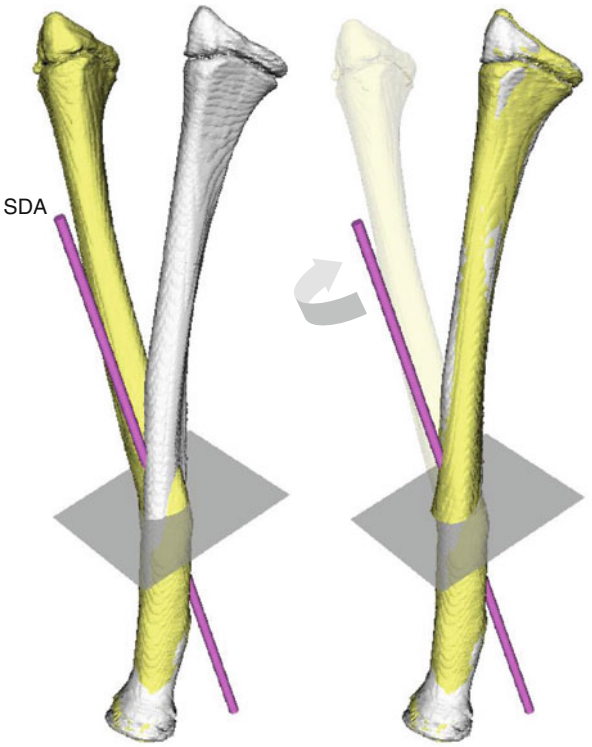

Fig. 19.5 Correction in this case is to be completed by performing a rotational osteotomy of 45° around the axis (SDA) on the plane perpendicular to it (*curved arrow*) because SDA is nearly parallel to the longitudinal bone axis

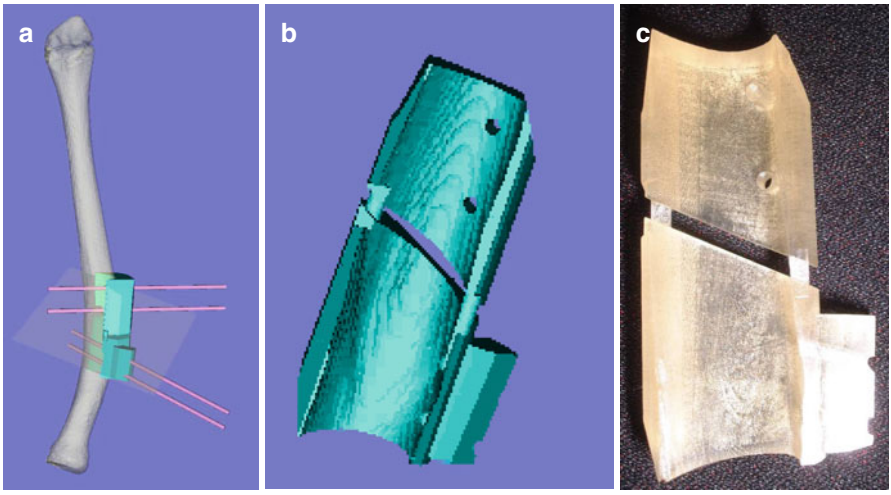

Fig. 19.6 A PMI, which has a shape to exactly fit the bone surface, an osteotomy slit and guide holes for K-wires, is designed (**a**, **b**) and embodied as a plastic model through rapid prototyping machine (**c**)

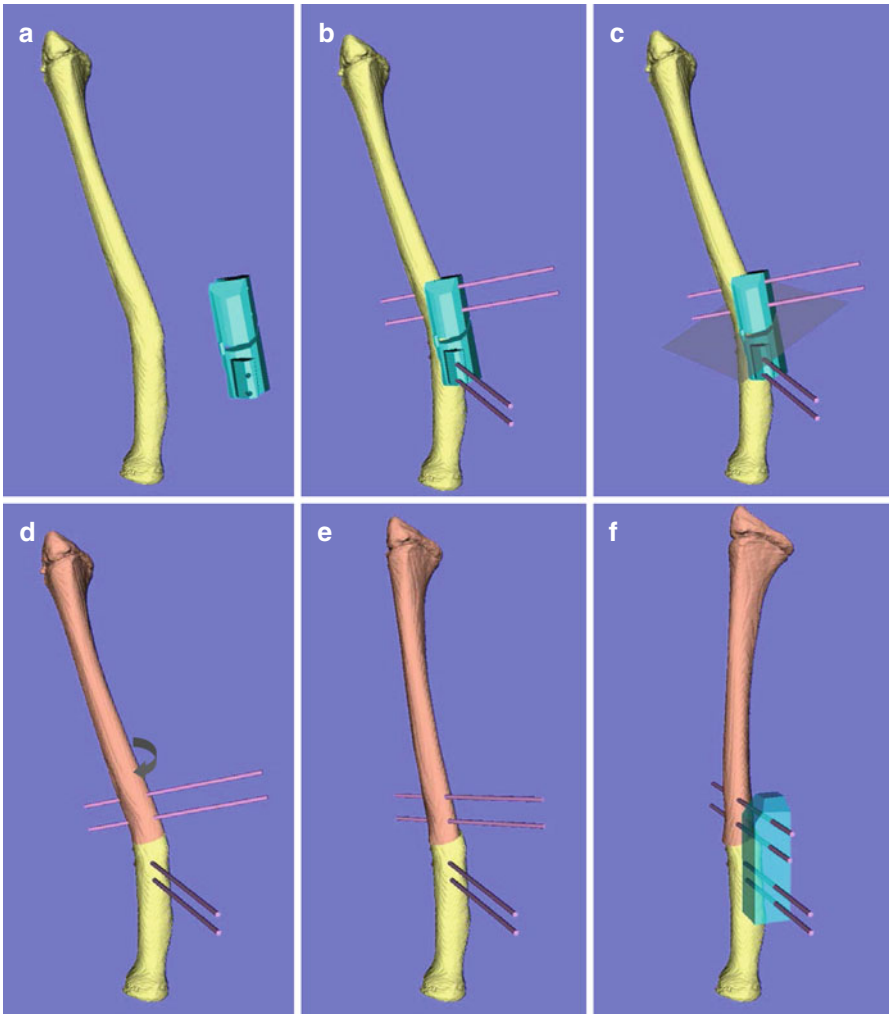

Fig. 19.7 After putting the PMI on the bone surface, it is fixed with Kirschner wires through the drill holes (**a**, **b**) and the bone is divided through the cutting slit (**c**). The PMI is removed (**d**) and the two sets of the Kirschner wires are brought into a parallel status to each other by rotating the distal segment (*curved arrow*, **e**). A reduction guide is used to maintain the reduced position (**f**)

Surgical Technique

The radial and ulnar diaphyses are each exposed through separate incisions as appropriate. PMI is then fitted closely onto the surface of the bone and fixed with Kirschner wires inserted through the guiding holes in PMI (Fig. 19.8). After

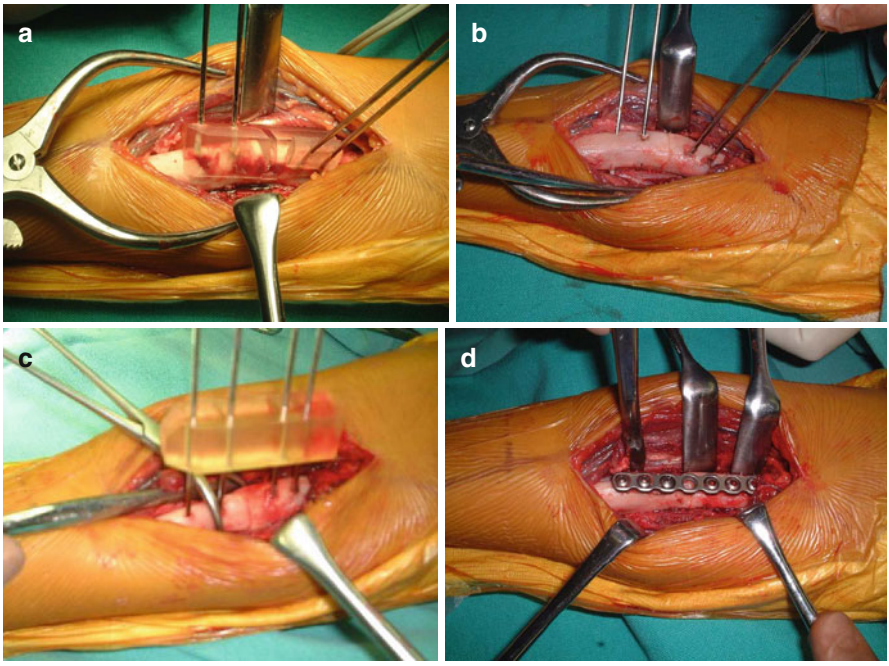

Fig. 19.8 The malunited radius is exposed through the anterior approach. PMI was fitted to the osteotomy site and is fixed it with Kirschner wires (**a**). The bone is divided through the cutting slit on the PMI, which was then removed (**b**). A reduction guide is used to maintain the Kirschner wires to be parallel (**c**). Internal fixation is accomplished with a plate and screws (**d**)

completion of osteotomy with a bone saw applied through the cutting slit, a reduction guide is used to maintain the Kirschner wires in a parallel position for each bone. Internal fixation is then accomplished with a plate and screws (Fig. 19.9).

Clinical Outcomes

The results of previous clinical study with 20 patients operated with this technique showed that the average radiographic deformity angle preoperatively is 21° (range, 12–35°) compared with the normal arm; this is improved to 1° (range, 0–4°) postoperatively [11]. The mean arc of forearm motion significantly improved from 76° preoperatively to 152° postoperatively. However, forearm supination was still restricted by ≥70° in 3 patients whose age at initial injury was <10 years and who had longstanding malunion of ≥96 months. Painful recurrent dislocation of the ulna and radial head resolved or decreased in 4 patients. Average grip strength improved from 82 to 94 % of that of the normal side. Preoperative pain disappeared or decreased substantially after surgery.

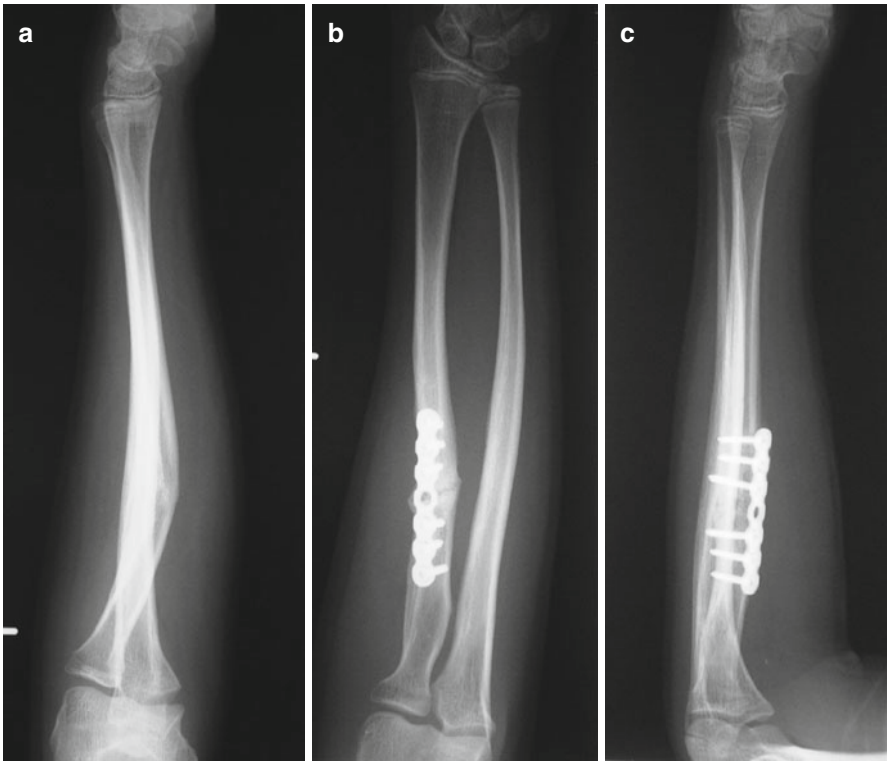

Fig. 19.9 A preoperative radiograph of a 13-year-old boy with malunited diaphyseal fracture of the radius who complained restricted forearm supination. The radius showed a 25° angular deformity at the middle third (**a**). The postoperative AP (**b**) and lateral (**c**) radiographs show good anatomical correction

Cubitus Varus Deformity

Cubitus varus deformity is a malunion of the distal end of the humerus that generally includes varus, internal rotation, and hyperextension deformities [5, 36, 37]. In the past, it was considered a cosmetic problem, and correction of varus deformity alone is an accepted practice [18, 38]. Recently, because joint laxity [17, 39] and tardy ulnar nerve palsy [40] have been reported to be late complications, several investigators have advocated that correction of angular deformity is not enough and that rotational deformity should also be corrected [5, 36]. The previously reported 3D correction, however, was based on preoperative planning using data from plain radiographs and changes in the range of shoulder motion [5, 36, 37]. This procedure was also criticized for its technical difficulty and poor bone contact at the osteotomy site [18]. In contrast, the computer simulation system provides a simple and accurate correction based on 3D data. The contact area at the osteotomy site can be easily visualized using 3D images, which allows practical planning.

Deformity Evaluation of Cubitus Varus Deformity

The bone models of a patient's upper arms and forearms are obtained from the CT data acquired in the same manner that was described in the forearm section.

The proximal part of the mirror image of the normal humerus, which is considered the target model, is superimposed manually on the corresponding part of the affected humerus followed by semiautomatic registration [15, 41, 42]. The same procedure is applied to the distal part. In manual registration, the greater tuberosity, humeral head, and shaft are set as the references for the proximal part and the medial and lateral epicondyles and distal articular surface for the distal part. When morphological change is present at the distal humerus, the proximal parts of the forearm bones were also used as references. Next, the 3D amount of deformity is quantified by subtracting the distance value of the distal humerus from that of the proximal humerus. Then the 3D amount of correction, which is the inverse of the deformity amount, is calculated and used for simulation of deformity correction. The correction amount is 3D data that includes varus–valgus, flexion–extension, rotational, and translational elements (Fig. 19.10).

Simulation for Deformity Correction of Cubitus Varus Deformity

To plan the operation, the following simulation is made (Fig. 19.11) [15]. The distal osteotomy plane (DOP), roughly parallel to the distal articular surface, is set just proximal to the olecranon fossa of the bone model of the affected humerus. DOP is then moved by the correction amount described in the previous section and defined as the proximal osteotomy plane. The wedge-shaped segment cut out by DOP and POP is removed from the affected humerus. Then the simulation of 3D correction is completed by moving the distal segment of the humerus together with the forearm bones by the correction amount. In cubitus varus deformity after supracondylar fracture, the affected humerus is usually overgrown. This type of closing wedge osteotomy accompanied by derotation can accordingly bring about correction of both length discrepancy and angular- rotational deformity. For cases with gross internal rotation deformity, complete rotational correction may decrease the contact area at the osteotomy site to an extent where bony union would be of concern. In that case, the rotational correction is decreased, leaving a residual rotational deformity less than 15° for those cases.

PMI is manufactured to help reproduce the simulation in the actual surgery (Fig. 19.12). PMI has a shape that closely fits the characteristic surface of the posterolateral distal humerus including the lateral epicondyle and lateral half of the olecranon fossa. It also has 2 osteotomy slits and 4 drill holes. The slits guide the precise osteotomy cut; and 2 sets of 2 Kirschner wires, inserted through the drill holes at an angle

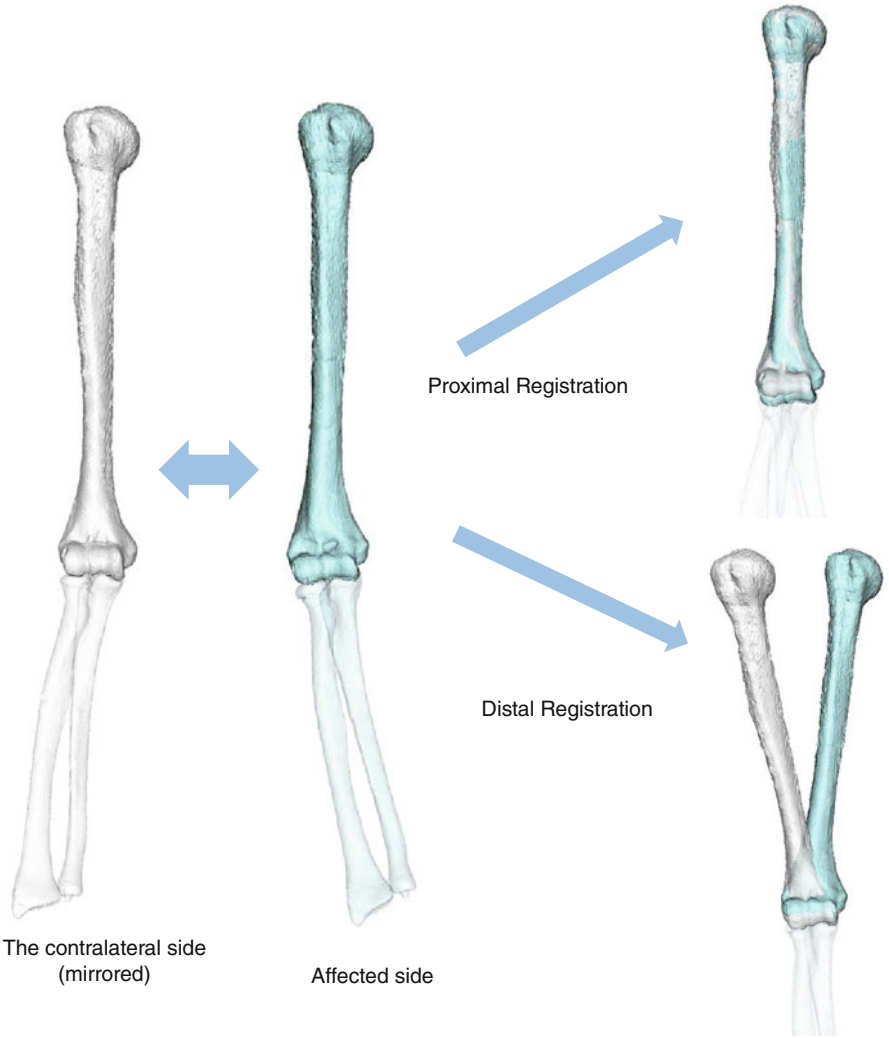

Fig. 19.10 Evaluation of the deformity in 3-D by comparing the affected humerus to the mirror image of the contralateral normal humerus. The proximal part of the mirror image of the normal humerus, which is considered the target model, is superimposed on the corresponding part of the affected humerus (proximal registration). The same procedure is applied to the distal part of the humerus (distal registration). Then the computer software automatically calculates the 3-D amounts of deformity and correction using the transformation data required for the distal and proximal registration

to the deformity, indicate that the reduction is completed when they become parallel to each other. A reduction guide to maintain the parallel position of the Kirschner wires is prepared preoperatively in the same manner as the PMI (Fig. 19.4a–h).

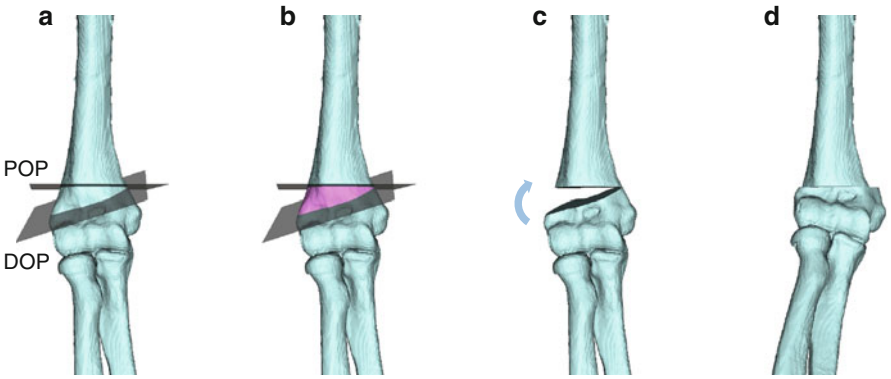

Fig. 19.11 The distal osteotomy plane (DOP), roughly parallel to the distal articular surface, is set just proximal to the olecranon fossa of the bone model of the affected humerus (**a**). DOP is then moved by the correction amount described in Fig. 19.10 and defined as the proximal osteotomy plane (POP, **b**). The wedge-shaped segment cut out by DOP and POP is removed from the affected humerus (**c**). Then the simulation of 3D correction is completed by moving the distal segment of the humerus together with the forearm bones by the correction amount (**d**)

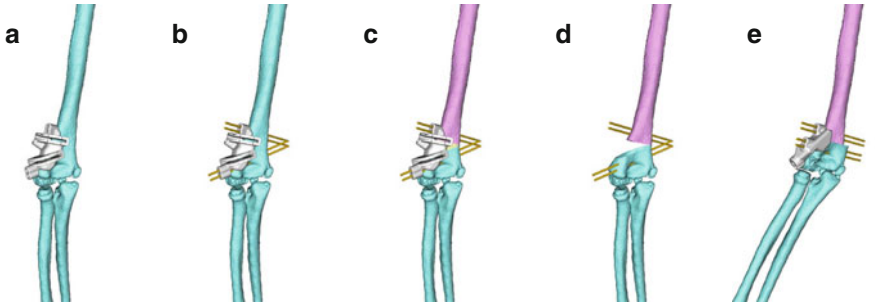

Fig. 19.12 PMI is placed onto the posterolateral surface of the distal radius (**a**) and fixed with K-wires (**b**). Osteotomy is performed through the slits (**c**) and PMI is removed leaving the Kirschner wires in place followed by resection of a wedge-shaped bone created by the osteotomy (**d**). The planned correction is achieved by bringing the Kirschner wires into parallel status, which is then held with a reduction guide (**e**)

Surgical Technique

A posterior approach with the patient in lateral decubitus position is employed. The PMI is placed onto the posterolateral surface of the distal humerus (Fig. 19.13). After placement is carefully assured by checking that all edge of the guide exactly contacted the bone surface, it is fixed with Kirschner wires of diameter 1.5–2.0 mm inserted through metal sleeves mounted on the PMI and osteotomy is performed with a bone saw through the slits. The PMI is then removed leaving the Kirschner wires in place followed by resection of a wedge-shaped bone created by the osteotomy. The planned correction is achieved by bringing the Kirschner wires into parallel status, which is then held with a reduction guide. While the correction

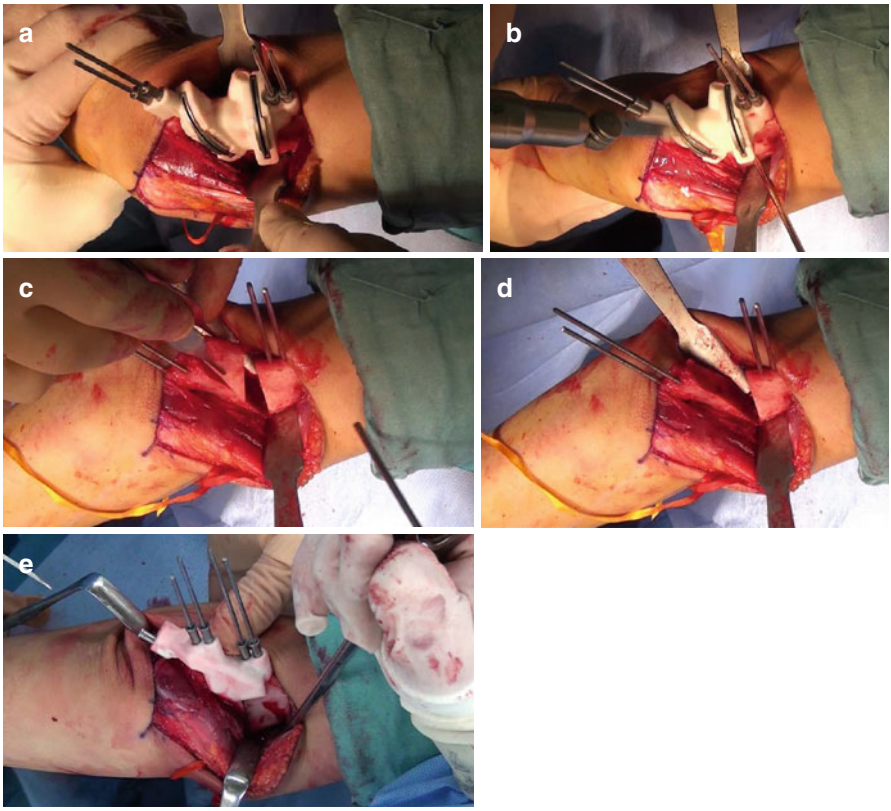

Fig. 19.13 A posterior approach with the patient in lateral decubitus position is employed. PMI is placed onto the posterolateral surface of the distal humerus and fixed with Kirschner (**a**). Osteotomy is performed with a bone saw through the slits (**b**). The PMI is then removed leaving the Kirschner wires in place followed by resection of a wedge-shaped bone created by the osteotomy (**c**, **d**). The planned correction is achieved by bringing the Kirschner wires into parallel status, which is then held with a reduction guide (**e**)

is being maintained, Kirschner wires or tension-band wiring are used for internal fixation for the cases with open physes, bilateral plate fixation is applied for the cases with closed physes (Fig. 19.14). After the operation, a removable long arm splint is applied for 1–2 weeks for the plate fixation group and 3–4 weeks for the K-wire fixation group with 90° elbow flexion, and active and passive ROM exercise is started (Fig. 19.15).

Clinical Outcomes

The results of the previous clinical study with 30 patients operated with this technique showed that bone union was achieved at 4 months after surgery on average [15]. The mean humero-elbow-wrist angle and tilting angle of the affected side were

Fig. 19.14 Preoperative (**a**) and Postoperative (**b**, **c**) radiographs of a 10-year-old boy with left cubitus varus deformity

18° (varus) and 25°, respectively, before surgery, significantly improving to 6° (valgus) and 38°, respectively, after surgery. Hyperextension of the elbow and internal rotation of the shoulder were normalized in all patients. Early plate breakage was observed in one case. After revision surgery, bone union was achieved without loss of correction. Recurrence of mild varus deformity in another case was observed. According to Hahn's rating, 27 cases were rated as excellent, 3 cases as good, and none as poor [43]. 3D corrective osteotomy using a PMI designed and manufactured based on computer simulation is a feasible and useful treatment option for cubitus varus deformity.

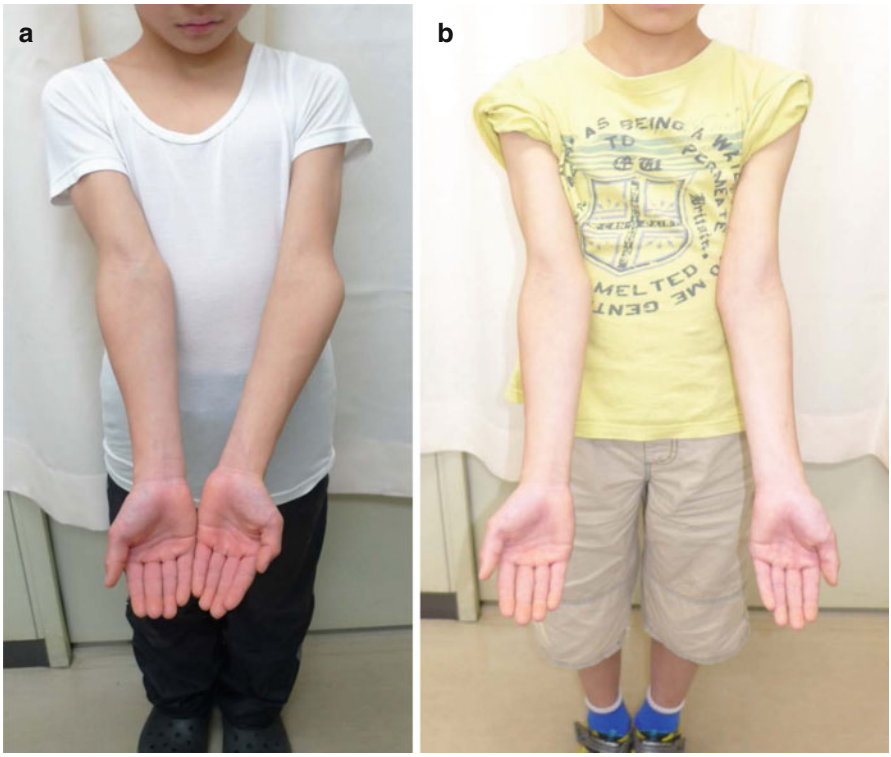

Fig. 19.15 Deformity correction for cubitus varus deformity. Preoperative (**a**) and postoperative (**b**) appearances

Malunited Distal Radial Fracture

Malunited distal radial fracture is one of the most common deformities of the upper extremity. Dorsal tilt, radial shortening, and a decrease in radial inclination have been cited by several investigators, who were trying to plan 3D correction using plain radiographs [1, 44, 45]. Athwal et al. [21] introduced a CT-based computer-assisted 3D surgical planner that calculates corrective position of the distal radius including an evaluation of rotational deformity using the contralateral normal wrist as the template. They applied an intraoperative guidance system, which linked the preoperative plan to the optical tracking device. However, an optical tracking system requires bulky equipment and computers, monitors, and a system operator in the operation room for this surgery, which usually requires minimal settings.

Since 2004, reports have been published on a corrective osteotomy technique using a volar locking plate, a major innovation in malunited distal radius fracture treatment [46–49]. This technique uses a locking system with a rigid fixation ability

that eliminates the necessity for precisely formed bone grafts. Problems involving the extensor, which occur when the dorsal approach is used, can also be avoided through the use of this method. Around the same time, PMI approach was developed as a practical surgical method enabled by three-dimensional computer simulations for correcting upper-limb deformities [10, 13, 50]. In the case of malunited distal radius fracture, the use of preoperative simulations with computer bone models has made it possible to gain precise information on screw positions and directions prior to osteotomy. When screw holes can be created using PMI prior to osteotomy, correction and plate fixation can be done simultaneously, which simplifies the surgical procedure and allows more accurate reproduction of the simulated surgery.

Simulation Technique for Deformity Correction of Malunited Distal Radius Fracture Using a Volar Locking Plate [51]

The bone models of the patient's both forearms are created from the CT data. First, the post-corrective osteotomy position of the plate on the volar surface of the radius is determined using mirror image of the affected side as a reference and the optimal screw positions and angles are determined (Fig. 19.16). Next, the screw positions and directions prior to the correction are calculated and the PMI is designed that will guide drilling of the appropriate screw holes and the osteotomy. In the actual operation, the distal and proximal screw holes are created with use of the PMI before osteotomy. After osteotomy through the slit on the PMI, which is then removed, the distal part of the plate is fixed to the distal segment of the radius with screws through the predrilled holes. Then, by pushing the proximal end of the plate

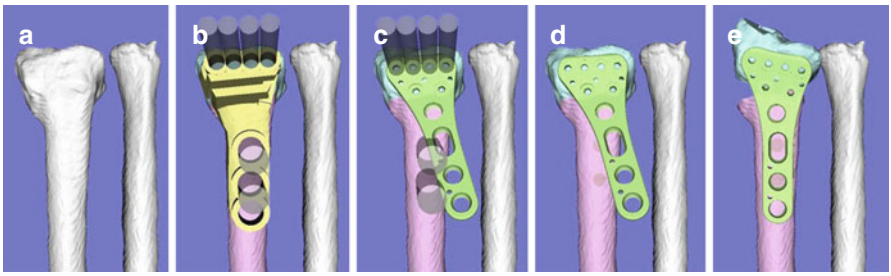

Fig. 19.16 Volar view of 3-D surface models of the distal part of the malunited distal radius and the ulna (**a**). First, the post-corrective osteotomy position of the plate on the volar surface of the radius is determined and the optimal screw positions and directions are determined (**e**). Next, the screw positions and directions prior to the correction are calculated and the PMI is designed that will guide drilling of the appropriate screw holes and the osteotomy (**b**). In the actual operation, the distal and proximal screw holes are created with use of the PMI before osteotomy. After osteotomy through the slit on the PMI, which is then removed, the distal part of the plate is fixed to the distal segment of the radius with screws through the predrilled holes (**c**, **d**). Then, by pushing the proximal end of the plate against the radial diaphysis and fixing it with screws through the predrilled proximal holes, the planned correction can be realized (**e**)

against the radial diaphysis and fixing it with screws through the predrilled proximal holes, the planned correction can be realized. PMI is designed according to the simulation and manufactured through a rapid prototyping machine (Fig. 19.17).

Surgical Technique

The anterior approach to the distal volar radius is employed. The dissection is carefully performed to the bone cortex so that no soft tissue remains. The PMI is placed so that it is aligned with the morphology of the bone cortex on the volar side of the distal radius and the edges are in close contact with the bone. The PMI is then preliminarily fixed in place with at least 2–3 drill bits inserted into the bone and the remainder of the drilling is performed (Fig. 19.18). The use of intraoperative fluoroscopy is recommended to confirm that the distal drilling is performed in the generally planned locations. The metal osteotomy slit is set into the PMI and the osteotomy is performed. Once the osteotomy on the volar side is complete, the PMI is removed and drilling is performed in a series of perforations toward the dorsal bone cortex through the osteotomized surface using a 1.2-mm-diameter K-wire. After this step, the osteotomy is completed using a bone chisel. Once the soft tissue has been sufficiently dissected and the target correction is possible, the plate can be fixed. First, the distal part of the volar locking plate is placed in contact with the distal radius fragment and held so that the plate is in line with the screw holes in the bone. The plate is fixed with locking screws of the appropriate length. This procedure results in the bone and plate being joined by the locking screw system. Finally, the screws are tightened on the proximal side to create semiautomatic correction. After the plate is fixed, it is possible to confirm from the radial side a bone defect in

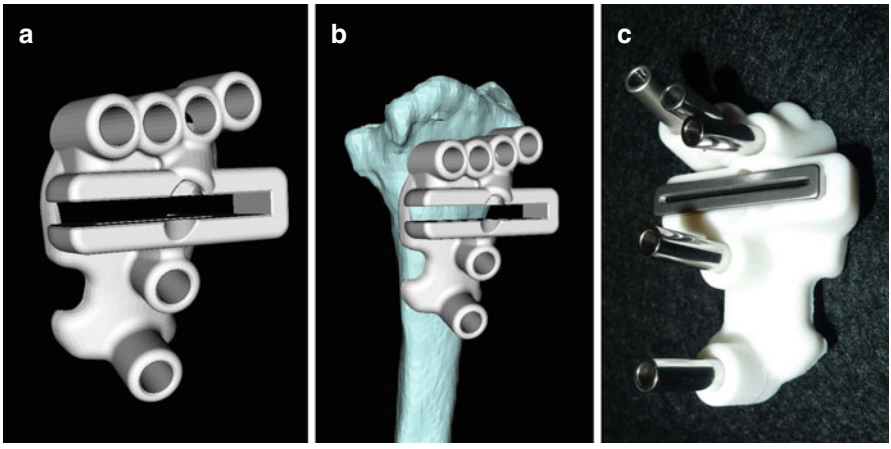

Fig. 19.17 Patient-matched instrument (PMI) design (**a**) with the radius model (**b**) and actual PMI showing the metal sleeve and slit installation (**c**)

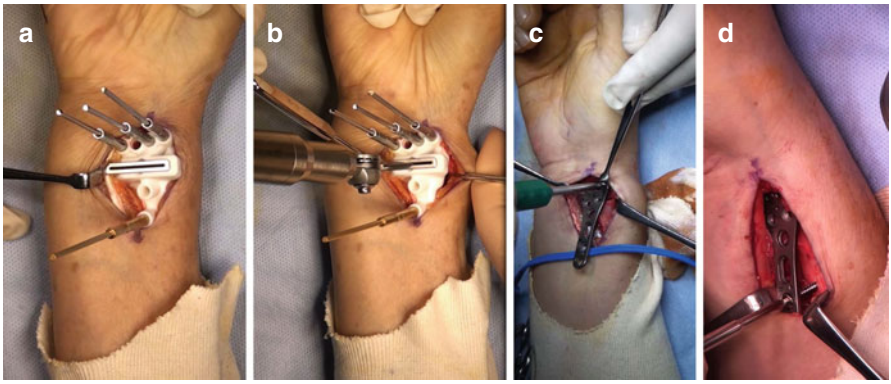

Fig. 19.18 Intraoperative photographs. (**a**) Drilling for screw holes using the PMI. (**b**) Osteotomy of the volar cortical bone using a bone saw through the metal slit installed in the PMI. (**c**) Fixation of the distal side of the plate. (**d**) Fixation of the proximal side of the plate

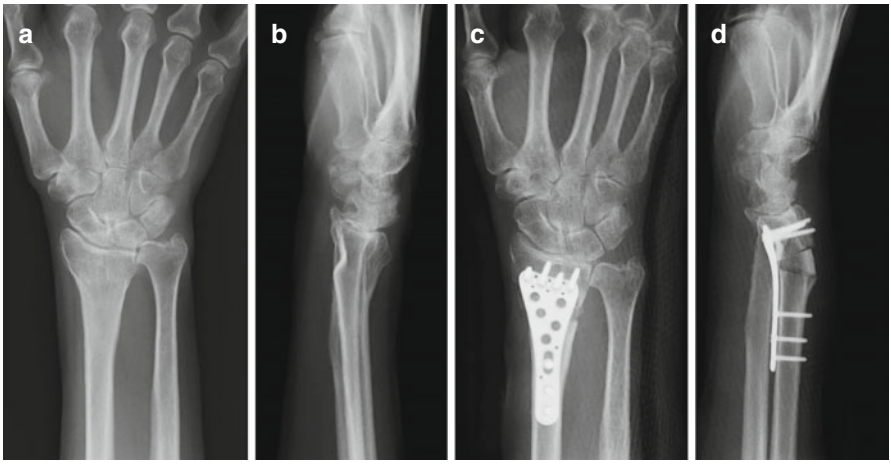

Fig. 19.19 Preoperative AP view (**a**) and lateral view (**b**) as well as postoperative AP view (**c**) and lateral view (**d**) on a plain radiograph. In this case a block bone graft harvested from the ilium was inserted into the bone defect

the osteotomized section. The defect is filled with either corticocancellous or cancellous iliac bone or artificial bone substitute as graft material (Fig. 19.19). Short arm case is applied for approximately 3 weeks after surgery. After cast removal, range of motion exercise with periodic radiographic checks of bone fusion is started.

Surgical Outcome

In the 19 cases performed by this author (three men, 16 women; age range, 26–75; average follow-up period, 19.4 months), volar tilt, radial inclination, and ulnar variance as seen on plain X-rays indicated that corrections were made almost exactly as

planned (Fig. 19.4a–d). Postoperative wrist flexion-extension range of motion was 132°, forearm rotation range of motion was 162°, and grip strength compared to the healthy side was 83 % on average, indicating satisfactory results. Bony union period took 14 weeks. There were two cases in which complications required implant removal; in both cases, osteoporosis caused fractures near the implant as well as screw loosening.

References

1. Fernandez DL. Malunion of the distal radius: current approach to management. Instr Course Lect. 1993;42:99–113.
2. Sarmiento A, Ebramzadeh E, Brys D, Tarr R. Angular deformities and forearm function. J Orthop Res. 1992;10(1):121–33. doi:10.1002/jor.1100100115.
3. Bilic R, Zdravkovic V, Boljevic Z. Osteotomy for deformity of the radius. Computer-assisted three-dimensional modelling. J Bone Joint Surg Br. 1994;76(1):150–4.
4. Jupiter JB, Ruder J, Roth DA. Computer-generated bone models in the planning of osteotomy of multidirectional distal radius malunions. J Hand Surg Am. 1992;17(3):406–15.
5. Uchida Y, Ogata K, Sugioka Y. A new three-dimensional osteotomy for cubitus varus deformity after supracondylar fracture of the humerus in children. J Pediatr Orthop. 1991;11(3):327–31.
6. Brown GA, Firoozbakhsh K, DeCoster TA, Reyna Jr JR, Moneim M. Rapid prototyping: the future of trauma surgery? J Bone Joint Surg Am. 2003;85-A Suppl 4:49–55.
7. Ellis RE, Tso CY, Rudan JF, Harrison MM. A surgical planning and guidance system for high tibial osteotomy. Comput Aided Surg. 1999;4(5):264–74. doi:10.1002/(sici)1097-0150(1999)4:5<264::aid-igs4>3.0.co;2-e.
8. Shimizu T, Fujioka F, Gomyo H, Isobe K, Takaoka K. Three-dimensional starch model for simulation of corrective osteotomy for a complex bone deformity: a case report. Foot Ankle Int. 2003;24(4):364–7.
9. Imai Y, Miyake J, Okada K, Murase T, Yoshikawa H, Moritomo H. Cylindrical corrective osteotomy for Madelung deformity using a computer simulation: case report. J Hand Surg Am. 2013;38(10):1925–32. doi:10.1016/j.jhsa.2013.07.006.
10. Miyake J, Murase T, Moritomo H, Sugamoto K, Yoshikawa H. Distal radius osteotomy with volar locking plates based on computer simulation. Clin Orthop Relat Res. 2011;469(6):1766–73. doi:10.1007/s11999-010-1748-z.
11. Miyake J, Murase T, Oka K, Moritomo H, Sugamoto K, Yoshikawa H. Computer-assisted corrective osteotomy for malunited diaphyseal forearm fractures. J Bone Joint Surg Am. 2012;94(20), e150. doi:10.2106/jbjs.k.00829.
12. Miyake J, Oka K, Moritomo H, Sugamoto K, Yoshikawa H, Murase T. Open reduction and 3-dimensional ulnar osteotomy for chronic radial head dislocation using a computer-generated template: case report. J Hand Surg Am. 2012;37(3):517–22. doi:10.1016/j.jhsa.2011.10.047.
13. Murase T, Oka K, Moritomo H, Goto A, Yoshikawa H, Sugamoto K. Three-dimensional corrective osteotomy of malunited fractures of the upper extremity with use of a computer simulation system. J Bone Joint Surg Am. 2008;90(11):2375–89. doi:10.2106/jbjs.g.01299.
14. Oka K, Murase T, Moritomo H, Yoshikawa H. Corrective osteotomy for malunited both bones fractures of the forearm with radial head dislocations using a custom-made surgical guide: two case reports. J Shoulder Elbow Surg. 2012;21(10):e1–8. doi:10.1016/j.jse.2012.05.035.
15. Takeyasu Y, Oka K, Miyake J, Kataoka T, Moritomo H, Murase T. Preoperative, computer simulation-based, three-dimensional corrective osteotomy for cubitus varus deformity with use of a custom-designed surgical device. J Bone Joint Surg Am. 2013;95(22), e173. doi:10.2106/jbjs.l.01622.
16. Gartland Jr JJ, Werley CW. Evaluation of healed Colles' fractures. J Bone Joint Surg Am. 1951;33-A(4):895–907.

17. O'Driscoll SW, Spinner RJ, McKee MD, Kibler WB, Hastings 2nd H, Morrey BF, et al. Tardy posterolateral rotatory instability of the elbow due to cubitus varus. J Bone Joint Surg Am. 2001;83-A(9):1358–69.
18. Oppenheim WL, Clader TJ, Smith C, Bayer M. Supracondylar humeral osteotomy for traumatic childhood cubitus varus deformity. Clin Orthop Relat Res. 1984;188:34–9.
19. Tarr RR, Garfinkel AI, Sarmiento A. The effects of angular and rotational deformities of both bones of the forearm. An in vitro study. J Bone Joint Surg Am. 1984;66(1):65–70.
20. von Campe A, Nagy L, Arbab D, Dumont CE. Corrective osteotomies in malunions of the distal radius: do we get what we planned? Clin Orthop Relat Res. 2006;450:179–85. doi:10.1097/01.blo.0000223994.79894.17.
21. Athwal GS, Ellis RE, Small CF, Pichora DR. Computer-assisted distal radius osteotomy. J Hand Surg Am. 2003;28(6):951–8.
22. Dumont CE, Thalmann R, Macy JC. The effect of rotational malunion of the radius and the ulna on supination and pronation. J Bone Joint Surg Br. 2002;84(7):1070–4.
23. Schemitsch EH, Richards RR. The effect of malunion on functional outcome after plate fixation of fractures of both bones of the forearm in adults. J Bone Joint Surg Am. 1992;74(7):1068–78.
24. Blackburn N, Ziv I, Rang M. Correction of the malunited forearm fracture. Clin Orthop Relat Res. 1984;188:54–7.
25. Nagy L, Jankauskas L, Dumont CE. Correction of forearm malunion guided by the preoperative complaint. Clin Orthop Relat Res. 2008;466(6):1419–28. doi:10.1007/s11999-008-0234-3.
26. Price CT, Knapp DR. Osteotomy for malunited forearm shaft fractures in children. J Pediatr Orthop. 2006;26(2):193–6. doi:10.1097/01.bpo.0000194699.29269.76 [doi] 01241398-200603000-00008 [pii].
27. Trousdale RT, Linscheid RL. Operative treatment of malunited fractures of the forearm. J Bone Joint Surg Am. 1995;77(6):894–902.
28. van Geenen RC, Besselaar PP. Outcome after corrective osteotomy for malunited fractures of the forearm sustained in childhood. J Bone Joint Surg Br. 2007;89(2):236–9. doi:89-B/2/236 [pii] 10.1302/0301-620X.89B2.18208[doi].
29. Chapman MW, Gordon JE, Zissimos AG. Compression-plate fixation of acute fractures of the diaphyses of the radius and ulna. J Bone Joint Surg Am. 1989;71(2):159–69.
30. Creasman C, Zaleske DJ, Ehrlich MG. Analyzing forearm fractures in children. The more subtle signs of impending problems. Clin Orthop Relat Res. 1984;188:40–53.
31. Zhang YZ, Lu S, Chen B, Zhao JM, Liu R, Pei GX. Application of computer-aided design osteotomy template for treatment of cubitus varus deformity in teenagers: a pilot study. J Shoulder Elbow Surg. 2011;20(1):51–6. doi:S1058-2746(10)00386-1 [pii] 10.1016/j.jse.2010.08.029 [doi].
32. Oka K, Murase T, Moritomo H, Goto A, Nakao R, Sugamoto K, et al. Accuracy of corrective osteotomy using a custom-designed device based on a novel computer simulation system. J Orthop Sci. 2011;16(1):85–92. doi:10.1007/s00776-010-0020-4.
33. Oka K, Murase T, Moritomo H, Goto A, Sugamoto K, Yoshikawa H. Accuracy analysis of three-dimensional bone surface models of the forearm constructed from multidetector computed tomography data. Int J Med Robot. 2009;5(4):452–7. doi:10.1002/rcs.277.
34. Kinzel GL, Hillberry BM, Hall Jr AS, Van Sickle DC, Harvey WM. Measurement of the total motion between two body segments. II. Description of application. J Biomech. 1972;5(3):283–93.
35. Spoor CW, Veldpaus FE. Rigid body motion calculated from spatial co-ordinates of markers. J Biomech. 1980;13(4):391–3.
36. Chung MS, Baek GH. Three-dimensional corrective osteotomy for cubitus varus in adults. J Shoulder Elbow Surg. 2003;12(5):472–5. doi:10.1016/s1058274603000909.
37. Yamamoto I, Ishii S, Usui M, Ogino T, Kaneda K. Cubitus varus deformity following supracondylar fracture of the humerus. A method for measuring rotational deformity. Clin Orthop Relat Res. 1985;201:179–85.

38. Bellemore MC, Barrett IR, Middleton RW, Scougall JS, Whiteway DW. Supracondylar osteotomy of the humerus for correction of cubitus varus. J Bone Joint Surg Br. 1984;66(4):566–72.
39. Abe M, Ishizu T, Nagaoka T, Onomura T. Recurrent posterior dislocation of the head of the radius in post-traumatic cubitus varus. J Bone Joint Surg Br. 1995;77(4):582–5.
40. Abe M, Ishizu T, Shirai H, Okamoto M, Onomura T. Tardy ulnar nerve palsy caused by cubitus varus deformity. J Hand Surg Am. 1995;20(1):5–9. doi:10.1016/s0363-5023(05)80047-4.
41. Besl PJ, MacKay ND. Method for registration of 3-D shapes. IEEE Trans Pattern Anal Mach Intelll. 1992;14(2):239–56.
42. Takeyasu Y, Murase T, Miyake J, Oka K, Arimitsu S, Moritomo H, et al. Three-dimensional analysis of cubitus varus deformity after supracondylar fractures of the humerus. J Shoulder Elbow Surg. 2011;20(3):440–8. doi:10.1016/j.jse.2010.11.020.
43. Hahn SB, Choi YR, Kang HJ. Corrective dome osteotomy for cubitus varus and valgus in adults. J Shoulder Elbow Surg. 2009;18(1):38–43. doi:10.1016/j.jse.2008.07.013.
44. Fernandez DL. Correction of post-traumatic wrist deformity in adults by osteotomy, bone-grafting, and internal fixation. J Bone Joint Surg Am. 1982;64(8):1164–78.
45. Zdravkovic V, Bilic R. Computer-assisted preoperative planning (CAPP) in orthopaedic surgery. Comput Methods Programs Biomed. 1990;32(2):141–6.
46. Henry M. Immediate mobilisation following corrective osteotomy of distal radius malunions with cancellous graft and volar fixed angle plates. J Hand Surg Eur Vol. 2007;32(1):88–92. doi:10.1016/j.jhsb.2006.09.002.
47. Malone KJ, Magnell TD, Freeman DC, Boyer MI, Placzek JD. Surgical correction of dorsally angulated distal radius malunions with fixed angle volar plating: a case series. J Hand Surg Am. 2006;31(3):366–72. doi:10.1016/j.jhsa.2005.10.017.
48. Osada D, Kamei S, Takai M, Tomizawa K, Tamai K. Malunited fractures of the distal radius treated with corrective osteotomy using volar locking plate and a corticocancellous bone graft following immediate mobilisation. Hand Surg. 2007;12(3):183–90. doi:10.1142/s0218810407003560.
49. Prommersberger KJ, Lanz UB. Corrective osteotomy of the distal radius through volar approach. Tech Hand Up Extrem Surg. 2004;8(2):70–7. doi:10.1097/01.bth.0000126572.28568.88.
50. Oka K, Moritomo H, Goto A, Sugamoto K, Yoshikawa H, Murase T. Corrective osteotomy for malunited intra-articular fracture of the distal radius using a custom-made surgical guide based on three-dimensional computer simulation: case report. J Hand Surg Am. 2008;33(6):835–40. doi:10.1016/j.jhsa.2008.02.008.
51. Murase T. Treatment of malunited distal radius fracture. Monthly Book Orthopaedics. 2014;27(4):66–72.

Chapter 20
Spinal Loading System: A Novel Technique for Assessing Spinal Flexibility in Adolescent Idiopathic Scoliosis

Marcelo Elias de Oliveira, Daniel Brandenberger, Daniel Studer, Jacques Schneider, Carol-Claudius Hasler, and Philippe Büchler

Abstract The assessment of curve flexibility and its geometric patterns are important parameters in the surgical decision-making process for patients with adolescent idiopathic scoliosis (AIS). Despite numerous publications in recent years evaluating and comparing different preoperative clinical techniques, there is still no consensus among surgeons as to the most appropriate technique for assessing spinal flexibility. The preoperative tests currently used in clinical practice are subjected to numerous uncertainties and are difficult, depending on the experience of the observers and on the patient's emotional and physical conditions. In order to overcome these limitations, a mechatronic system capable of applying a controlled pure quasi-static axial load to the patient's cervical spine has been developed and clinically evaluated. Our preliminary results suggest that the proposed SLS may be a useful tool for assessing curve flexibility.

Keywords Spinal flexibility • Adolescent idiopathic scoliosis • Spinal loading system

M. Elias de Oliveira, BSc, MSc, PhD (✉)
Institute of Microengineering, Robotic Systems Laboratory,
Swiss Federal Institute of Technology Lausanne, EPFL STI IMT LSRO,
Lausanne, Switzerland

Graduate School for Cellular and Biomedical Sciences, University of Bern, Bern, Switzerland
e-mail: marcelo.eliasdeoliveira@epfl.ch; marcelo.ijk@gmail.com

D. Brandenberger • D. Studer • C.-C. Hasler
Department of Orthopaedics, University Children's Hospital Basel, Basel, Switzerland

J. Schneider
Department of Orthopaedics, University Children's Hospital Basel, Basel, Switzerland

Department of Paediatric Radiology, Children's Hospital Basel, Basel, Switzerland

P. Büchler
Computational Bioengineering Group, Institute for Surgical Technology and Biomechanics,
University of Bern, Bern, Switzerland

L.E. Ritacco et al. (eds.), *Computer-Assisted Musculoskeletal Surgery: Thinking and Executing in 3D*, DOI 10.1007/978-3-319-12943-3_20

Introduction

The adolescent idiopathic scoliosis (AIS) is a musculoskeletal disorder usually characterized by deviations of the spine in the coronal, sagittal, and transverse planes. In severe cases, these deviations may results in rib cage deformities, which can lead to respiratory complications. Its prevalence in the general population is about 2–3 %, appearing most frequently during the puberty (10–16 years of age), out of which about 10 % of the patients require surgical intervention. The prevalence ratio for non-severe spine deformities (curves around 10°) is similar of girls to boys. However, in patients with curves greater than 20° the prevalence ratio for girls to boys increases to more than 5:1. Although it is possible to observe that the overall prevalence of this condition is reduced to 0.1 % for Cobb angles greater than 40° [1].

The assessment of curve flexibility and the geometric patterns of the patient's spine are important parameters in the surgical decision-making process, aiding the surgeon in planning fusion of spinal motion segments and sequence of surgical maneuvers. Clinically, the Adam's forward-bending test is the most commonly used screening test for AIS, however, a definitive diagnosis can be established only based on posteroanterior and lateral radiographs. Geometric patterns of the patient's spine are assessed using the Lenke and King classification systems [2, 3], and by quantifying the spine deformity in the coronal plane based on a measure of the curvature of the spine called Cobb angle. These techniques are combined with preoperative clinical tests to evaluate the severity of the spinal deformity and its flexibility. During preoperative clinical tests, mechanical loads are applied indirectly to the patient's spine and the amount of geometric correction achieved by the application of these forces are clinically interpreted as spinal flexibility.

In the last two decades, several clinical tests for assessing the curve flexibility have been introduced, including push prone radiographs [4], erect or supine side bending radiographs, traction radiographs performed in the normal awake state and under general anesthesia [5–7], and fulcrum bending radiographs [8, 9]. Among them, the side bending radiographs seems to be the most commonly used technique in routine clinical practice [10]. However, all these methods suffer from a major drawback in which forces and moments of unknown magnitudes and directions are indirectly applied to the patient's spinal column by complex transfer mechanisms. These uncertainties are likely to influence the accuracy and reliability of flexibility estimates, which can partially explain the lack of consensus among surgeons [2, 11–14]. In order to overcome these limitations, a low-cost mechatronic system called Spinal Loading System (SLS) capable of generating and applying a pure axial quasi-static tractive force directly to the patient's cervical spine has been developed and clinically evaluated. Our preliminary results suggest that the proposed SLS may be a useful tool for assessing curve flexibility.

Methods

Study Design

A total of five patients (15.4 ± 1.81 years old) presenting with moderate to severe thoracic deformities and scheduled to undergo elective spine surgery at the University Children's Hospital Basel (UKBB), Basel, Switzerland were recruited in this study. The common used and clinically accepted side bending technique and the proposed preoperative SLS were evaluated. Finally, the flexibility of the structural curves were assessed using the Cobb angle. The present study was carried out in accordance with the ethical standards laid down in the 1964 Declaration of Helsinki for research involving human subjects, and it was approved by the local ethics committee of the UKBB and both oral and written informed consent to participate in this study were obtained from patients and their relatives after a full explanation of the study.

Spinal Loading System

The developed SLS consists of a modular assembly system composed of aluminium structural frame elements. It is characterized essentially by three degrees of freedom in the upper transverse plane frame, and by a frictionless rotating mechanism in the low transverse plane, as shown in Fig. 20.1. The designed three degrees of freedom mechanism ensures the application of a pure axial load to the patient's cervical spine, as shown in Fig. 20.2.

The SLS is equipped with a motion controller driver (MCLM 3006, Faulhaber Minimotor SA, Switzerland); a DC-servomotor (2642W012CR, Faulhaber Minimotor SA, Germany) with integrated precision gearbox 26/1(S) 66:1 and encoder; and a load platform Nintendo Wii balance board (Nintendo, Kyoto, Japan). The considered load platform is a low-cost bluetooth-operated device composed of four calibrated strain-gauges, and it has been proven to be accurate and suitable for clinical research [16].

Control logic provides the SLS with closed-loop position control dependent of the patient's body weight (BW) percentage reduced by applying a quasi-static tractive force to the patient's cervical spine, which is computer-controlled via an RS232 serial port. A software with a friendly graphical user interface (GUI) was developed as shown in Fig. 20.3. The software was written in ANSI/ISO C++ and developed on ×86 GNU/Linux systems with GNU C Compiler (GCC) 4.3.3, libcwiid, Qt and VTK. Patient's information and experimental data such as time stamp in milliseconds, force distribution in the four individual strain-gauge sensors type, center of the resulting force, and strains rates are stored in ASCII format for further offline data analysis. The SLS has the advantage of being easily combined

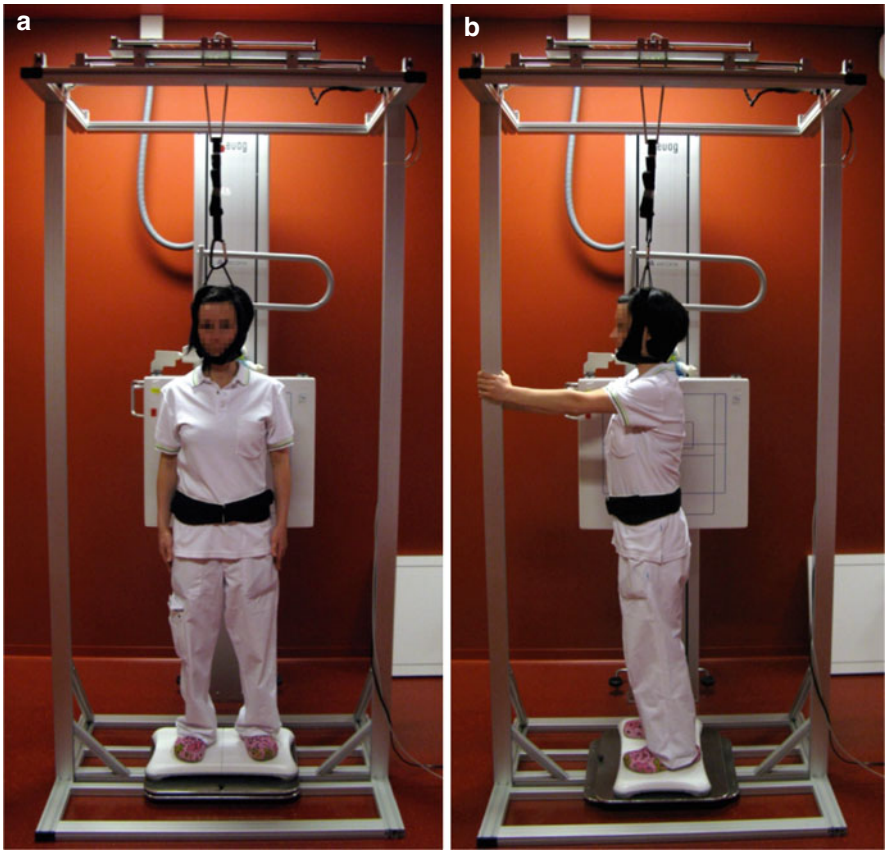

Fig. 20.1 Spinal Loading System. (**a**) Patient in upright normal position on the load platform for a routine anteroposterior radiograph. (**b**) The frictionless rotating mechanism rotated clockwise by degrees. The direction of the rotation is determined according to the deformity patterns of the patient's spine (Reproduced from Elias de Oliveira [15] with permission)

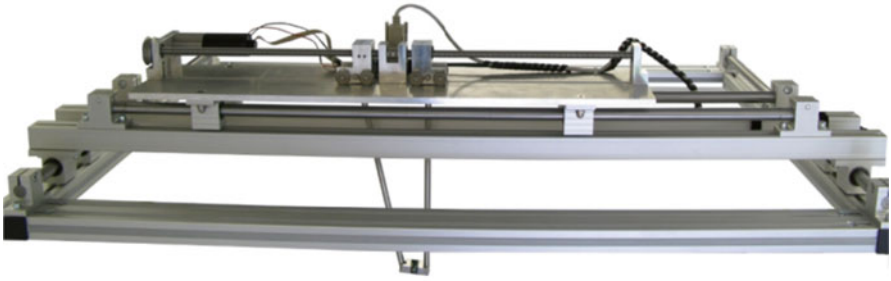

Fig. 20.2 Three degrees-of-freedom mechanism capable of applying a pure axial mechanical load to the patient's cervical spine (Reproduced from Elias de Oliveira [15] with permission)

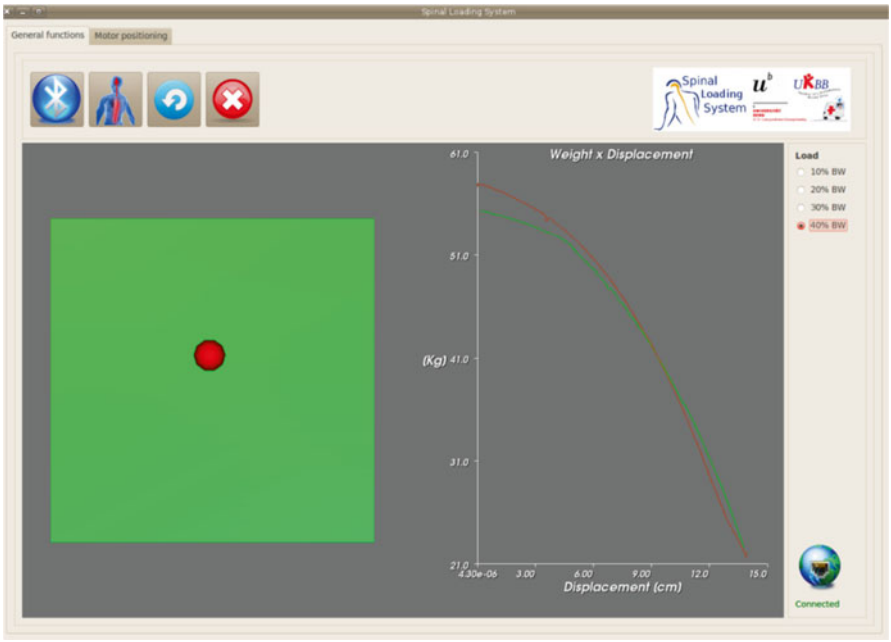

Fig. 20.3 Spinal Loading System intuitive control interface. Calibration procedure assuming the human spine as a spring-like structure. *Left*: Phantom's center of mass. *Right*: Displacement-released weight curve. The *red* and *green* curves represent the loading and unloading conditions, respectively. The load shift between these curves is explained by the initial positioning of the designed mechanism for application of pure axial loads (Reproduced from Elias de Oliveira [15] with permission)

with conventional X-ray devices, since its a portable modular assembly system, adjustable, and lightweight, as shown in Figs. 20.1 and 20.4.

Data Acquisition

Before the evaluation of the proposed preoperative method for assessing the curve flexibility in AIS was started, a preoperative radiologic evaluation using the widely accepted side bending technique has been performed.

Consequently, a standard commercial cervical traction head halter commonly used in physiotherapy treatment (Basler Orthopädie Renè Ruepp AG, Basel, Switzerland) has been used to ensure the application of the forces directly to the patient's spinal column. The head halter components were gently placed on the posterior portion of the head (occiput) and on the lowermost part of the face (chin), as shown in Fig. 20.1.

The patients were asked to stand in upright normal position in the SLS working space and were instructed to relax the group of abdominal, back, and neck muscles

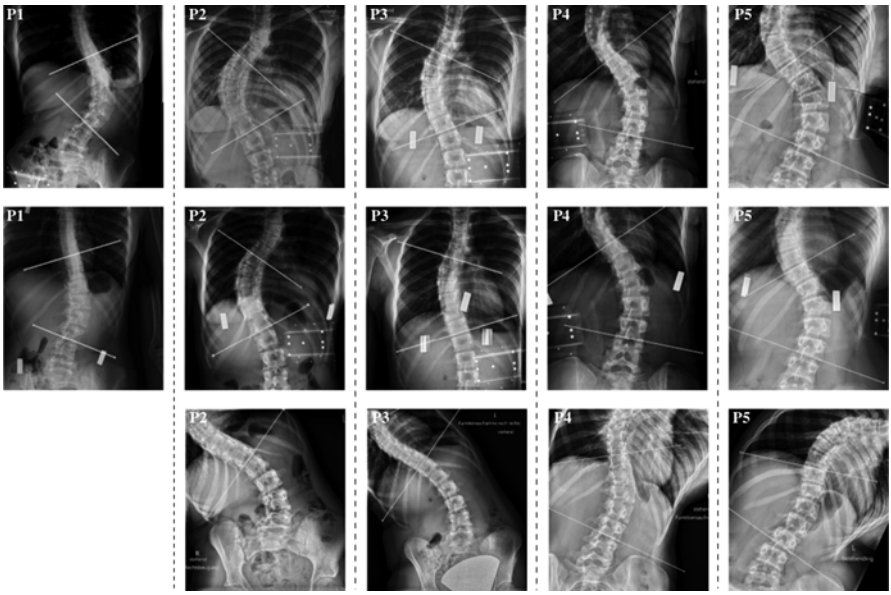

Fig. 20.4 Cobb angle measurements. *First row*: anteroposterior radiographs in normal upright position. *Second row*: Pure axial quasi-statistic tractive load corresponding to 30 % of the patient's body weight generated by the proposed SLS. *Third row*: Lateral bending posteroanterior radiographs. It is important to note that the patient P1 did not perform the lateral bending test and, therefore, could not be included in this study (Reproduced from Elias de Oliveira [15] with permission)

and not to move between consecutive anteroposterior and lateral radiographs. A preload tractive force corresponding to 5 % of the patient's body weight was applied to positioning the three degrees of freedom slider component in the patient's location. Anteroposterior and lateral radiographs of the lumbar and thoracic spines were acquired in the unloaded condition. Lateral radiographs were acquired by rotating the patient around its own axis on the frictionless platform by 90° according to the deformity pattern of the patient's spine.

The SLS software was initialized, and the actual patient's body weight was registered for determination of the stop-criterion. Loads acting vertically upward with magnitudes determined from the previously measured patient's body weight (BW) were applied. The quasi-static tractive forces were applied stepwise from 10 % BW to 30 % BW in 10 % BW step. After the stop-criterion was reached, additional coronal and sagittal radiographs of the patient's spine were acquired under loaded conditions. The patients were monitored by the medical staff members during the application of the quasi-static tractive forces and were continuously instructed to relax all group of muscles associated with posture and balance.

The resulting loads, forces distribution on the four individual strain-gauge sensors, patient's center of mass, and strain-rates were continuously acquired at a sampling frequency of 15 Hz and stored in ASCII format for post-processing.

Finally, the software tool developed by [17] has been used to assess the Cobb angles of the structural curves in all considered conditions, i.e., normal upright

position, side bending, and under the application of a pure axial quasi-static load, and their respective curve flexibilities have been computed.

Results

To assess the amount of correction of the structural curves achieved by the lateral bending technique and by the proposed SLS, the Cobb angles measured from lateral bending and SLS radiographs were subtracted from their respective Cobb angles measured on radiographs acquired on normal upright positions. The mean Cobb angle in normal upright position measured 58.85° (range, 45.88–71.21°). Average curve flexibility was 29.87° (range, 16.86–45.40°) on lateral bending, and 12.60° (range, 4.54–27.66°) on the application of a pure axial quasi-static tractive load corresponding to 30 % of the patient's body weight. The average final applied load was 16.45 Kg, ranging from 14.43 to 17.79 Kg. The Table 20.1 summarizes the spinal deformities characteristics, patients' information, curves reduction for both techniques, and determined magnitude of the quasi-static tractive load as a function of the patient's body weight.

Pearson's correlation coefficient was used to assess the relationship between patient-specific spinal flexibility computed with the proposed preoperative technique (SLS) and with the lateral bending. A low correlation coefficient $\rho_{x,y} = 0.25$ has been observed (Fig. 20.5), substantiating that different clinical tests may possibly lead to different interpretation of the curve flexibility and, consequently, to different decision making during preoperative surgical planning.

Discussion

Clinically, the understanding of curve flexibility is strictly related to the curve correction achieved by the application of mechanical forces resulting from single or combined preoperative tests. Current methods being used to assess patient-specific

Table 20.1 Spinal deformities characteristics and patient's general information

Case	Age	Apex	BMI	Load	Cobb angle [degrees]		
				[Kg]	NUP	SLS	LB
P1	15	L1	20.05	17.79	66.6	38.94	–
P2	16	T9	19.94	16.88	71.21	62.94	25.81
P3	13	T8	20.69	16.09	45.88	34.05	25.69
P4	18	T8	17.88	14.43	50.19	45.65	33.33
P5	15	L1	19.77	17.10	60.38	49.67	23.33

Reproduced from Elias de Oliveira [15] with permission

NUP normal upright position, *SLS* spinal loading system, *LB* lateral bending, *BMI* body mass index. Load: Pure axial quasi-static tractive load corresponding to 30 % of the patient's body weight generated by the SLS

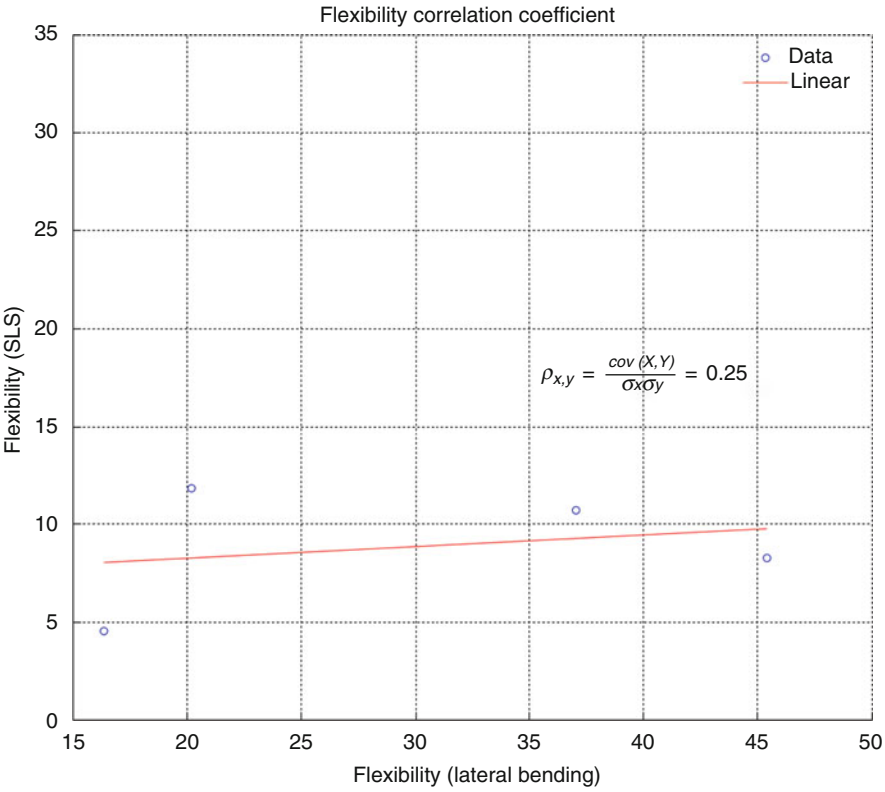

Fig. 20.5 Correlation coefficient between the curve flexibility using both lateral bending and the proposed SLS. The amount of correction of the structural curve induced by the application of forces during preoperative tests is clinically referred to as patient-specific curve flexibility (Reproduced from Elias de Oliveira [15] with permission)

curve flexibility include push prone radiographs; erect or supine lateral bending radiographs; fulcrum bending radiographs; and traction radiographs. These methods play an important role in the surgical decision-making process, aiding the surgeon in determining the structural nature of the curve. However, the magnitudes, directions, and application points of the resultant forces are unknown. Moreover, these forces are transmitted indirectly to the patient's spinal column and are generated by complex mechanisms of transmission involving passive and active muscular forces, as well as by external forces that may be applied to the patient's spinal column by a medical fellow, depending on the performed preoperative test. These clinical tests are subjected to numerous uncertainties and are difficult, depending on the experience of the observers and on the patient's preoperative emotional and physical conditions. All these aspects may explain partially the lack of consensus among surgeons and the large variability of spinal instrumentation configuration in AIS [13, 14]. To date, no study has been conducted to evaluate the intra-and inter-observer variability and reliability of these preoperative tests in

determining curve flexibility, which for ethical reasons cannot be conducted due to the high ionizing radiation exposure to patients and medical personnel. However, the ethical viability of such study may be reconsidered if the X-ray detection method proposed by [18] would be used.

Several studies comparing different preoperative clinical tests have been conducted to investigate the statistical variability of measured curve flexibilities [4, 5, 7, 19]. Despite these results, the quantitative correlations between different preoperative clinical tests were not reported. A possible explanation for this observation may be a low correlation coefficient, indicating that the measured spinal flexibility is a sensitive measure, depending on the selected preoperative clinical test and subject to uncertainties. Our results have shown a low Pearson's correlation coefficient. It is important to note that only quasi-static tractive forces of low magnitudes were considered in our study, and the increase of the magnitude of this mechanical load may possibly result in no statistically significant differences between the measured curve flexibilities, which can give a misleading indication of the patient's spinal flexibility and of the equivalences between different preoperative clinical tests.

All these previously mentioned shortcomings were considered during the development of the proposed preoperative clinical test. Although further studies are required to confirm our evidences, the developed SLS may present a higher reliability than the currently used clinical tests, since it ensures the automatic application of a pure quasi-static tractive axial force with a pre-established magnitude to the patient's cervical spine. The designed three degrees of freedom mechanism locate in the upper transverse plane frame ensures the application of a pure axial load, which do not depend on the position of the patient with respect to the SLS working space and, therefore, the effects of shear forces and moments can be neglected or are nonexistent. It is a portable and lightweight modular assembly system, which can be easily adapted to conventional X-ray devices. Thanks to its frictionless rotating mechanism in the low transverse plane, the SLS allows multiple views radiographs of the patient's anatomy without having to move the radiation source. The proposed preoperative technique may also be more appropriate for patients presenting spine deformities in the lumbar region, as well as in the initial levels of the thoracic spine. Our results suggest that the SLS may be recommended for patients suffering from neuromuscular scoliosis and with cognitive deficits, since their mobility may be impaired. Finally, the proposed technique significantly reduces the amount of radiation exposure to medical staff, since the patients do not need any external help during the image acquisition procedure, and only minor discomfort has been reported by the patients during the clinical tests.

In this work, we emphasized that our understanding of curve flexibility is intimately associated with the performed clinical test. To eliminate the uncertainties related to the currently used preoperative techniques in AIS, a low-cost and relatively simple mechatronic system called Spinal Loading System has been designed to increase the reliability and accuracy of measurements of flexibility in structural curves, preserving the commonly used radiology protocols in AIS preoperative tests. To the best of our knowledge, this is the first attempt to automatically and systemati-

cally generate and apply a pure axial quasi-static tractive force directly to the patient's cervical spine. We hope that this work will prove to be useful for surgeons, and specially for patients suffering from congenital and neuromuscular scoliosis.

References

1. Asher MA, Burton DC. Adolescent idiopathic scoliosis: natural history and long term treatment effects. Scoliosis. 2006;1(1):2.
2. Lenke LG, Betz RR, Bridwell KH, Clements DH, Harms J, Lowe TG, Shufflebarger HL. Intraobserver and interobserver reliability of the classification of thoracic adolescent idiopathic scoliosis. J Bone Joint Surg. 1998;80(8):1097.
3. King HA, Moe JH, Bradford DS, Winter RB. The selection of fusion levels in thoracic idiopathic scoliosis. J Bone Joint Surg Am. 1983;65(9):1302–13.
4. Vedantam R, Lenke LG, Bridwell KH, Linville DL. Comparison of push-prone and lateral-bending radiographs for predicting postoperative coronal alignment in thoracolumbar and lumbar scoliotic curves. Spine. 2000;25(1):76.
5. Polly DW, Sturm PF. Traction versus supine side bending. Which technique best determines curve flexibility? Spine. 1998;23(7):804.
6. Vaughan JJ, Winter RB, Lonstein JE. Comparison of the use of supine bending and traction radiographs in the selection of the fusion area in adolescent idiopathic scoliosis. Spine. 1996;21(21):2469.
7. Davis BJ, Gadgil A, Trivedi J, Ahmed ENB. Traction radiography performed under general anesthetic: a new technique for assessing idiopathic scoliosis curves. Spine. 2004;29(21):2466.
8. Luk KD, Cheung KM, Lu DS, Leong JC. Assessment of scoliosis correction in relation to flexibility using the fulcrum bending correction index. Spine. 1998;23(21):2303.
9. Cheung KMC, Luk KDK. Prediction of correction of scoliosis with use of the fulcrum bending radiograph. J Bone Joint Surg Am. 1997;79(8):1144–50.
10. Knapp DR, Price CT, Jones ET, Coonrad RW, Flynn JC. Choosing fusion levels in progressive thoracic idiopathic scoliosis. Spine. 1992;17(10):1159.
11. Krismer M, Bauer R, Sterzinger W. Scoliosis correction by Cotrel-Dubousset instrumentation. The effect of derotation and three dimensional correction. Spine. 1992;17(8 Suppl):S263.
12. Puno RM, An KC, Puno RL, Jacob A, Chung SS. Treatment recommendations for idiopathic scoliosis: an assessment of the Lenke classification. Spine. 2003;28(18):2102.
13. Robitaille M, Aubin CE, Labelle H. European spine journal official publication of the European Spine Society the European Spinal Deformity Society and the European Section of the Cervical Spine Research Society. Struct Multidisc Optim. 2007;16(10):1604.
14. Aubin CE, Labelle H, Cheriet F, Villemure I, Mathieu PA, et Jean Dansereau. Évaluation tridimensionnelle et optimisation du traitement orthopédique de la scoliose idiopathique adolescente. Med Sci (Paris) 2007;23:904–9. http://dx.doi.org/10.1051/medsci/20072311904.
15. de Oliveira ME. A non-invasive technique for assessing the spinal flexibility in adolescent idiopathic scoliosis. Ph.D. thesis, University of Bern; 2013.
16. Clark RA, Bryant AL, Pua Y, McCrory P, Bennell K, Hunt M. Validity and reliability of the Nintendo Wii Balance. Board for assessment of standing balance. Gait Posture. 2010;31(3):307. doi:10.1016/j.gaitpost.2009.11.012.
17. de Oliveira ME, Hasler C, Studer D, Schneider J, Büchler P. In Proceedings of the XXIII Congress of the International Society of Biomechanics. Brussels, Belgium; 2011.
18. Charpak G. Prospects for the use in medicine of new detectors of ionizing radiation. Bull Acad Natl Med. 1996;180(1):161–8; discussion 168–9. http://www.ncbi.nlm.nih.gov/pubmed/8696873.
19. Hamzaoglu A, Talu U, Tezer M, Mirzanli C, Domanic U, Goksan SB. Assessment of curve flexibility in adolescent idiopathic scoliosis. Spine (Phila Pa 1976). 2005;30(14):1637–42.

Chapter 21
3D Projection-Based Navigation

Kate A. Gavaghan and Matteo Fusaglia

Abstract Preoperative computer assisted planning and intraoperative image guidance aid surgeons in the conduction of safe procedures, improve their spatial understanding and highlight anatomical structures of interest. In the 1970's, for the first time, basic image guidance data was displayed on a monochrome computer display. Today, the majority of image guided surgical systems display a range of computer generated data intraoperatively on high definition monitors.

Recently, augmented reality technologies have allowed virtual image guidance data to be merged with the patient in a single view, removing the need for sight diversion to a nearby monitor. 3D projection systems allow augmented reality visualisation to be achieved with minimal setup time and without the need for obtrusive equipment or intraoperative device calibration. Whilst navigated projection devices can be used to visualise a range of virtual data directly on the patient in a geometrically correct position, error introduced by viewing angle renders the device most useful for the projection of superficial anatomical structures, surface maps or decomposed 3D position data. Despite the described benefits of augmented reality visualisation for image guidance, few clinical reports exist and further validation of the advantages to the patient and surgeon are required to advance the general acceptance of this technology which remains in its infancy.

Keywords Augmented reality • Intraoperative guidance • Preoperative planning

Introduction

Image guided surgical systems guide surgeons to targets, aid in the conduction of safe preoperatively planned surgical tasks and implantations, improve the surgeon's spatial understanding and highlight anatomical structures of interest. Early stereotactic image guided procedures predated computers and thus, medical images were simply overlaid with transparent patterned templates, aligned with fiducial

K.A. Gavaghan, PhD, BSc, Beng (✉) • M. Fusaglia, MSc, BEng
Image Guided Therapy, ARTORG Center for Biomedical Engineering Research, University of Bern, Murtenstrasse 50, Bern 3010, Switzerland
e-mail: Kate.gavaghan@artorg.unibe.ch; matteo.fusaglia@artorg.unibe.ch

L.E. Ritacco et al. (eds.), *Computer-Assisted Musculoskeletal Surgery: Thinking and Executing in 3D*, DOI 10.1007/978-3-319-12943-3_21

markings [1] (Fig. 21.1). Guidance feedback was limited to sets of coordinates that were read directly off the display. In the 1970s, basic guidance data was, for the first time, displayed and updated on a monochrome computer display [2]. Today, preoperatively planned tasks and actions performed intraoperatively on the patient are generally reflected on high definition computer monitors that are positioned adjacent to the patient.

The displayed intraoperative view typically contains an augmented virtual representation of the surgical scene consisting of compilations of image data, 3D anatomical models of underlying anatomy of interest, locations of instruments, surgical plan data and measurement data such alignment angles and position, distances, volumes or functional information.

Whilst offering vast improvements over earlier display techniques and technologies, modern day computer monitors, like the earliest displays, continue to display data away from the situs. The separation and removal of data from the patient requires the diversion of sight and attention away from the patient reducing safety and inducing errors resulting from the mental alignment of the two scenes and from the hand eye coordination required to execute surgical tasks while following presented data. Augmented reality (AR), defined as the augmentation or supplementation of a real world view with real time computer generated information that is registered to the real world scene, allows feedback information to be alternatively displayed in the direct view of the patient.

Within this chapter, the principles and history of augmented reality displays are described. More specifically, a novel augmented reality approach employing overlay projection is presented. The design of the 3D overlay system and reports of its preliminary use in surgical applications is provided. Finally, challenges pertaining to the realization of 3D projection solutions a presented, along with a discussion of current research topics and a vision of the role that 3D projection, and augmented reality in general, are likely to play in orthopaedic surgery in the future.

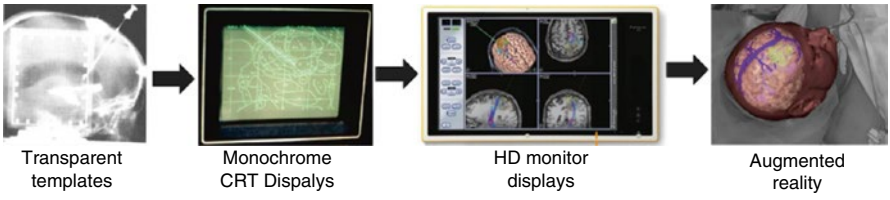

Fig. 21.1 Chronological representation of image guidance displays. Transparent templates of stereotactic grid coordinates were used in the pre-computer age. Early monochrome computer displays were used to for the presentation of stereotactic grid locations for a planned insertion trajectory in the 1970s [2]. Today, complex 3D representations of data are presented on high definition monitors and in the future, augmented reality will allow data to be displayed directly in the view of the patient without the need for a secondary display [3]

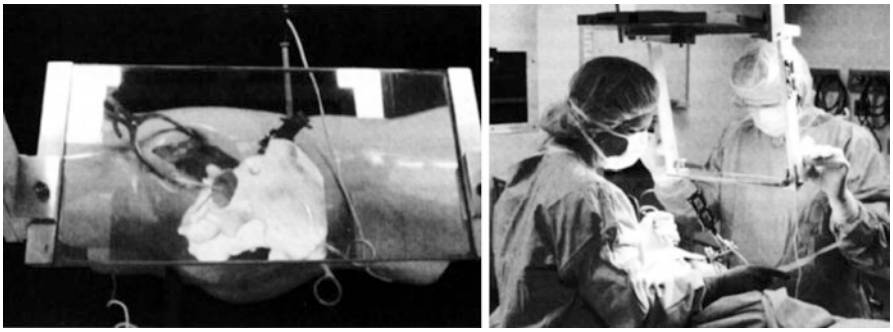

Fig. 21.2 The semitransparent augmented reality display as described by Nikou et al. employed in image guided orthopedic surgery

History of Augmented Reality in Orthopedic Surgery

In the early 2000s, AR technologies for the display of image guidance data were first developed by a number of research groups. Primarily, systems developed by DiGioia [4], Blackwell [5], Masamune [6] and Stetten [7] and later Fichtinger [8] utilised semi-transparent monitors combined with half silvered mirrors to display 3D data directly in the view of the patient (Fig. 21.2). Masamune et al. and Stetten et al. presented overlay systems capable of displaying medical images above the patient, thus avoiding the need for sight diversion traditionally required to consult the medical images. Similarly, Blackwell et al. [5], Nikou et al. [9] and DiGioia et al. [10]a, described the benefits of applying semi-transparent AR displays to a range of navigated orthopaedic surgeries including arthroscopy, pelvic screw fixation and the positioning of the acetabular and femoral prosthetic implant components for total hip replacement surgery. The system allowed surgeons for the first time to view patient and computer generated anatomical models and guidance data in a single view by giving the illusion of 3D models floating immediately above the patient. The approach was initially promising but the need for obtrusive equipment around the surgical scene and the associated limited workspace, long setup times and complex calibrations prevented the widespread use of the approach in navigated orthopaedic or any other form of surgery.

Additionally, the significant distance between the display and the patient, rendered the technologies highly effected by parallax error. To correct the perspective of the 3D data for viewing angle, head tracking glasses were proposed, however, tracking of the user's eye, which was computed from the location of tracked glasses, continued to be reported as a primary source or error.

More recently, 3D overlay projection techniques have been investigated as a means of achieving AR visualization in surgical applications. The projection of light directly onto the patient provides an immersive fused scene whilst overcoming deficiencies in limited workspace, obtrusive equipment requirements, elaborate set up times and reduced surgical vision experienced by previous systems.

The use of standard data projectors for image guidance data visualisation was first explored by Sugimoto et al. in 2010 for the display of underlying organs and planned port locations for laparoscopic visceral surgery [11]. The projector was statically positioned above the patient and projected images of volume rendered patient anatomy were coarsely registered to the patient via manual alignment of the projected navel. Despite deficiencies in accuracy, integration and set up complexity, Sugimoto et al. highlighted the potential of 3D projection technology concluding that the image overlay assisted in the three dimensional understanding of anatomical structures leading to improved surgical outcomes resulting from reductions in operation time, intra-operative injuries and bleeding [11]. Augmented reality was found to aid in the determination of correct dissection planes and the localisation of tumours, adjacent organs and blood vessels. It has been predicted that such technology could be used to avoid injury to invisible structures and to minimize the dissection and resection of neighbouring tissues [12].

Projection Based Navigation

Building on the preliminary work of Sugimoto et al., a hand held and portable projection device which can display registered updated image guidance data, including the real time locations of tracked instruments, was developed in 2011 at the University of Bern, Switzerland [13]. The device, designed specifically for the augmented reality display of surgical image guidance data, took advantage of the recent miniaturisation of projection technologies and the introduction of commercially available laser projection devices. The device, which is connected to a surgical image guidance system in the same way as a standard monitor (VGA/DVI), is depicted in Fig. 21.3.

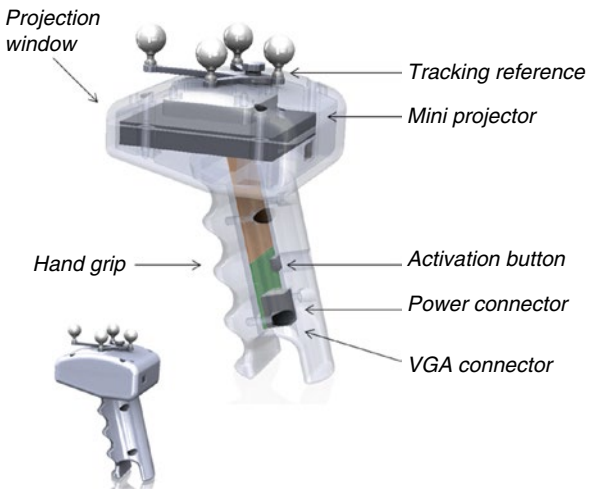

Fig. 21.3 Design of a portable 3D projection device for use with surgical image guidance systems

Miniaturisation of the projection technology has rendered this modern day device portable and handheld. By attaching a reference marker that can be tracked by a surgical navigation system's tracking sensor, the projection content can be updated in real-time for the current projection volume, allowing it to be moved freely in the tracking working volume.

Unlike conventional projectors, the absence of optical projection lenses and the matching of laser spot size growth rate to the image growth rate, results in a projected image that is always in focus. The use of laser projection technology allows the handheld device to be used from any distance from a projection surface (providing that sufficient image size and intensity can be maintained) without the need to manually or automatically focus the image. The incorporated RGB laser projector technology, contains a video processor and a micro-electro-mechanical system (MEMS) actuated mirror which reflects the combined RGB laser output, producing an active scan cone of $43.7° \times 24.6°$. The projected images have a resolution of 848×480 pixels, a frame rate of 60 Hz and light intensity of 10 lm, bright enough to be visible in ambient light.

Accurate alignment of the virtual scene with the patient is the primary challenge pertaining to the creation of a projected augmented reality view during surgery. As the real view changes, or as objects of interest within the real scene change their position, the virtual scene must be updated, realigned, and displayed faster than the eye can detect. To facilitate the geometrically correct alignment of projected data with the patient, augmentation data such as virtual models of real anatomy, labels, or interactive measurements created from medical imaging data must be rendered in a virtual scene at the same view as the projected image.

This alignment firstly requires registration of the images to the patient as is performed in standard image guided procedures and additionally, calibration of the projection device in order to determine its view relative to its tracked position. A model of the transformations required for the projection devices functionality is graphically displayed in Fig. 21.4.

Images for projection are rendered in a virtual image guidance scene at the view of the projection using a virtual camera model whose pose in the 3D virtual scene is defined by the relative pose of the projection and the patient. The patient-to-image registration process results in the transformation relating the patient to the position sensor $T_{patient}^{sensor}$ and the 3D pose of the projection device reference marker within the surgical scene is tracked by the navigation system in the coordinate system of the position sensor (T_{marker}^{sensor}). The transformation defining the relationship between the origin of projection and the tracked reference marker ($T_{projector}^{marker}$) is determined during a calibration process. The view of the virtual camera relative to the image data is defined by the projector's field of view and image aspect ratio and its pose ($T_{projector}^{sensor}$) defined by Eq. (21.1).

$$T_{projector}^{sensor} = T_{marker}^{sensor} \cdot T_{projector}^{marker} \tag{21.1}$$

Once rendered at a geometrically correct view, the aligned virtual data can be projected directly on the patient, providing a single merged scene.

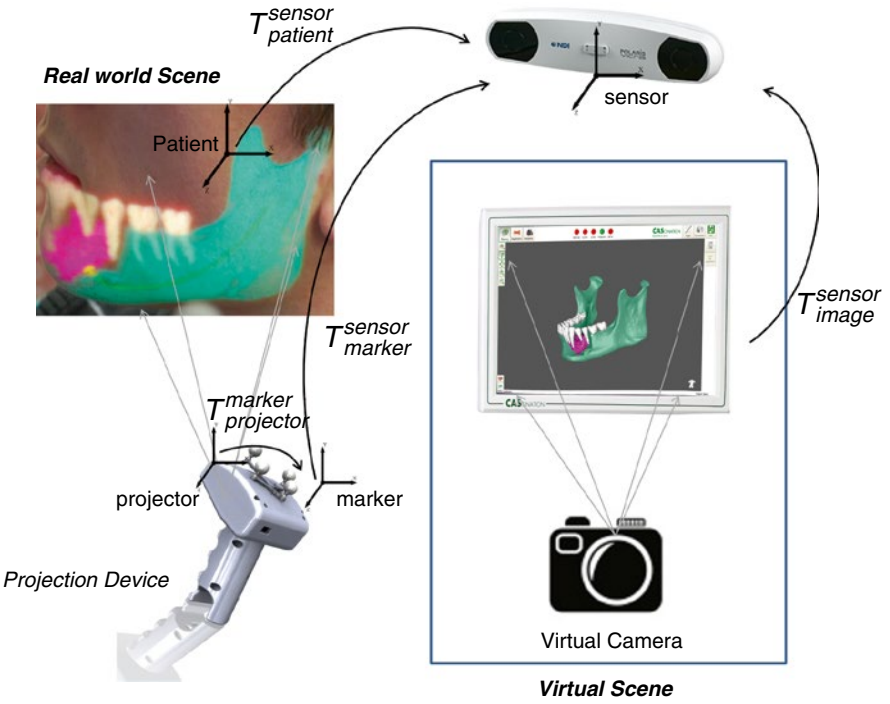

Fig. 21.4 Projection system functional model

Geometric Projection Calibration

For geometric calibration, a projection device can be modelled as a reverse pin-hole camera model in which the relationship between a point in space ($\tilde{\mathrm{M}} = [X, Y, Z, 1]$) and its representation as an image pixel value ($\tilde{\mathrm{m}} = [u, v, 1]$) is given by:

$$\mathrm{s}\,\tilde{\mathrm{m}} = A[R, T]\tilde{\mathrm{M}} \tag{21.2}$$

where extrinsic parameters R and T are the rotation and translation which relate the world coordinate system to the camera coordinate system, s is an arbitrary scale factor and A is the intrinsic parameter matrix of the projector:

$$A = \begin{pmatrix} \alpha & \gamma & u_0 \\ 0 & \beta & v_0 \\ 0 & 0 & 1 \end{pmatrix} \tag{21.3}$$

The calibration process involves the digitisation of 3D real world corner positions, M_i, of projected checkerboard corner positions from a number of projections

conducted at different projection angles. Corresponding 2D image pixel coordinates of the checkerboard corners, $m_{i,}$ are extracted directly from the image being projected. With the collected point pairs $(M, m)_i$, and the intrinsic parameters (scale factors α, β principal point (u_0, v_0) and the pixel skew, γ, set to that of the virtual camera model, equation (2) can be solved for extrinsic parameters $[R, T]$ $(T_{plane}^{projector})$.

For each projection, p, the pose of the tracked projection plane $(T_{plane}^{sensor})_p$ and the projector's tracking marker $(T_{marker}^{sensor})_p$ are recorded by the position sensor and the calibration transformation relating the calibrated origins of projection to the projector's tracking marker, $(T_{projector}^{marker})_p$, is given by:

$$\left(T_{projector}^{marker}\right)_p = \left(T_{marker}^{sensor}\right)_p^{-1} \cdot \left(T_{plane}^{sensor}\right)_p \cdot \left(T_{plane}^{projector}\right)_p^{-1} \tag{21.4}$$

The application of a tracking marker in a reproducible location on the device housing means that calibration of the projection device need only be performed once during development, eliminating the need for time consuming calibration processes intraoperatively.

Integrated into a standard surgical image guidance system, the calibrated device projects with a mean accuracy of 1.3 mm inclusive of patient to image registration error [13].

Clinical Application

Prior to application of the projection device within a clinical procedure, the usual tasks required by an image guided application must be completed. For example, imaging, surgical planning, instrument calibration and patient to image registration must be performed. The image overlay projection device described herein can be integrated into existing surgical image guidance systems and can thus rely on the available tracking, instrument calibration and patient to image registration capabilities. Based on tracking and projector calibration data, images for projection can thereafter be rendered at the geometrically correct view for overlay directly onto the patient anatomy.

All data presented by an image guidance system (for example 3D anatomical models, surgical planning data such as resection planes, safety margins, guidance targets, reconstruction angles, implant positions, tool positions and even written text) can be displayed directly onto the surgical site using a projection device. Some modalities, however, are more suited to the approach. In Fig. 21.5, use of the device for the augmented reality display of a tumour location and preoperatively planned optimal bone resection margins onto patient specific tibia models for the application described in [14] is depicted.

The projection enables the underlying hidden location of the tumour to be immediately visualised and translates the preoperatively planned margins directly onto the bone surface. In these images, however, it is evident that the display of underlying anatomy models displayed on the patient or organ surface are effected by

Fig. 21.5 Projection of a segmented tumor and resection margins onto a patient specific model of a tibia

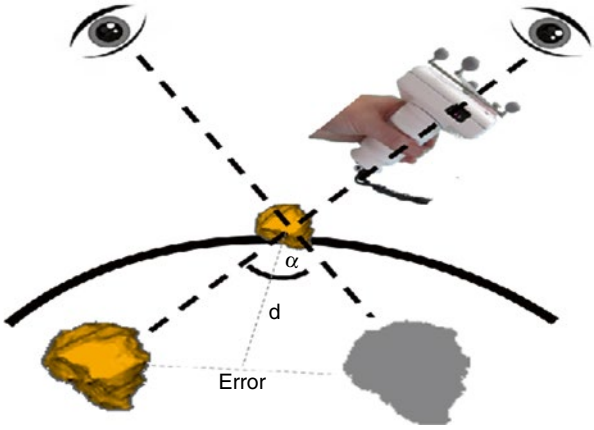

Fig. 21.6 Error in an objects perceived location due to viewing angle as experienced during the projection of underlying anatomy onto the patient skin or organ/structure surface (refer to Eq. (21.5)

parallax error (refer to Fig. 21.6). Direct projection onto the patient suffers from the related issue of parallax error which, due to the projection of 3D virtual data onto a 2D viewing plane, causes the perception of the location of projected underlying anatomy to change with viewing angle. The amount of error introduced depends on the viewing angle of the user and the depth at which the anatomy lies, as defined by Eq. (21.5). When employing the projection of 3D models for surgical guidance, the possible influence of parallax should be calculated and considered in relation to the accuracy requirements of the clinical application.

$$error = 2d \cdot \tan\frac{\alpha}{2} \tag{21.5}$$

Whilst it is possible for the projected image to be corrected in order to compensate for the users viewing angle, doing so would require the use of cumbersome and poorly accepted eye tracking technology and the view would be limited to a single user. Alternatively, the projected image guidance data can be designed to be minimally affected by, or independent of, the user's viewing angle.

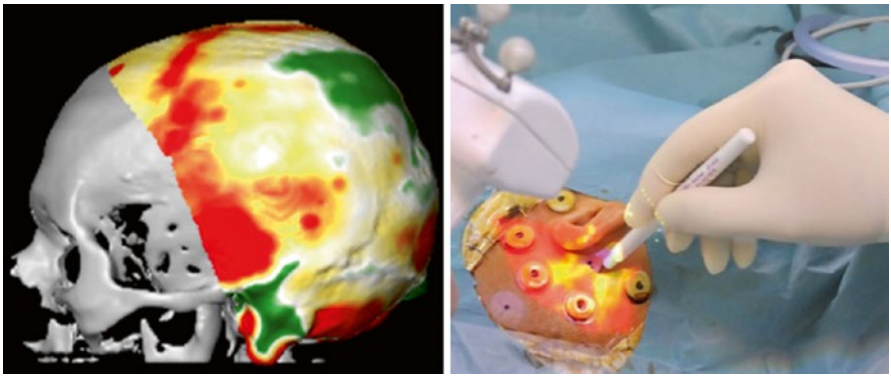

Fig. 21.7 Projection of a bone thickness map for determining the optimal location for an implantation site

The display of 3D models of anatomy lying close to the projection surface, such as superficial vessels, will be minimally affected by parallax error. Additionally, guidance data designed on the projection surface such as surface maps representing the distribution of an anatomical property will be completely unaffected by viewing angle. An example of a clinical case in which such type of guidance data was used to determine an optimal area of bone thickness for the placement of an implant is depicted in Fig. 21.7.

To enable the use of overlay projection for the targeting of deep lying structures, without the introduction of parallax error, guidance data can be decomposed into two dimensional information that can be rendered on the patient (or projection) surface. In the case depicted in Fig. 21.8, an application designed to represent tool orientation and depth to a planned location in the form of a shooting target and scaled depth bar, allowed targets to be located without the need to visualise guidance on a separate monitor and without inaccuracies introduced by viewing angle [15].

Challenges and Future Outlook

By removing the need for sight diversion and by reducing the required hand eye coordination, image overlay projection can be used during surgical procedures, such as the resection of tumours, to more intuitively visualise the underlying anatomy, preoperative planned data or intraoperative measurements. The projection of 3D image data poses a number of advantages over previously employed augmented reality systems for surgical navigation including reduced setup time and complexity, reduced size and obtrusiveness, and the elimination of intraoperative calibration. Usable with existing image guidance systems, projection devices additionally reduce the required investment and remove the need for additional required intraoperative tasks.

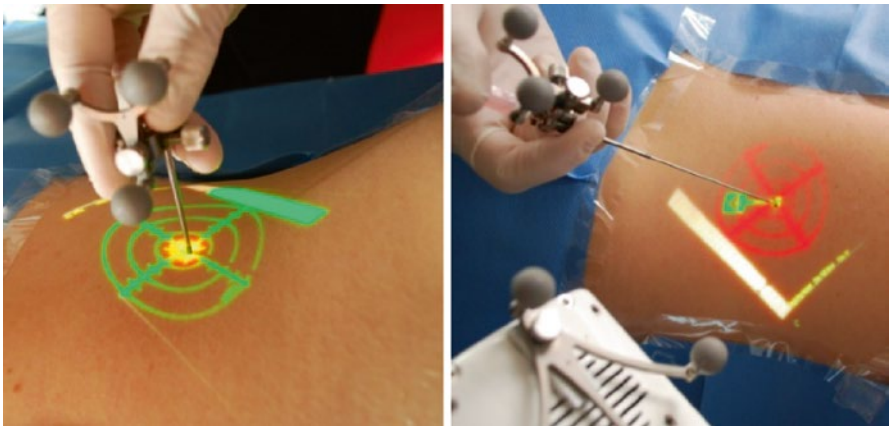

Fig. 21.8 Projection of instrument orientation and depth relative to a planned target, represented in 2D surface rendered data for the elimination of parallax error

Whilst the benefits of projection guidance for surgery applications are evident, quantitative clinical evaluations of their effectiveness are yet to be performed. To date, validation of AR systems for surgery have consisted primarily of feasibility studies conducted in laboratory environments or within small numbers of clinical cases. Presented results are typically reported as subjective evaluations of usefulness, with little or no significant or quantitative data. Evaluation of projection technologies in wide-spread and larger clinical trials would more clearly highlight benefits and disadvantages of the technology, and aid in the future evolution of systems. Projection devices for image guided surgery remain in their infancy and the future success of projected surgical guidance within orthopaedics and other surgical domains perhaps depends on the identification of applications for which projection can be most effective and for which targeted software applications are developed.

Another fundamental challenge facing the development and use of augmented reality systems relates to data visualization. While AR eliminates the need for sight diversion, the display of additional information can potentially be misleading or disturbing during the performance of surgical procedures. Virtual data promises to provide additional information to the operating surgeon however, it also has the potential to interfere with the surgeon's primary view. Virtual data must possess sufficient contrast and clarity to be easily visible while not masking structures in the real patient view. Typically, virtual data is displayed in strong primary colours, in order to enhance contrast, while transparency is applied to ensure information under the projection can be seen. Additionally, functionality via a user interface that allows data models to be displayed or turned off would ensure that augmentation will only be used when needed.

References

1. Bennett AMH. A stereotaxic apparatus for use in cerebral surgery. Br J Radiol. 1960;33(390):343–51.
2. Bertrand G, Olivier A, Thompson CJ. Computer display of stereotaxic brain maps and probe tracts. Acta Neurochir (Wien). 1974;21:235–43.
3. Intraoperative Imaging and Image-Guided Therapy. In: Jolesz F, editor. Springer Science and Business Media, 2014.
4. DiGioia A, Colgan B, Koerbel N. Computer-aided surgery. In: Satava R, editor. Cybersurgery: advanced technologies for surgical practice. New York: Wiley; 1998. p. 121–39.
5. Blackwell M, Nikou C, DiGioia AM, Kanade T. An image overlay system for medical data visualization. Med Image Anal. 2000;4(1):67–72.
6. Masamune K, Masutani Y, Nakajima S, Sakuma I, Dohi T, Iseki H, Takakura K."Three-dimensional slice image overlay system with accurate depth perception for surgery. In Lecture Notes in Computer Science Volume 1935, Medical Image Computing and Computer-Assisted Intervention – MICCAI. 2000. p. 395–402.
7. Stetten GD, Chib VS, Tamburo RJ. Tomographic reflection to merge ultrasound images with direct vision. Proceedings 29th applied imagery pattern recognition workshop. 2000. p. 200–5.
8. Fichtinger G, Deguet A, Masamune K, Balogh E, Fischer G, Mathieu H, Taylor RH, Fayad LM, Zinreich SJ. Needle insertion in CT scanner with image overlay - cadaver studies. Proceedings of the 7th International Conference on Medical Image Computing and Computer-Assisted Intervention (MICCAI), Springer-Verlag, 2004. p. 795–803.
9. Nikou C, Digioiai A, Blackwell M, Jaramaz B, Kanade T, Digioia A. Augmented reality imaging technology for orthopaedic surgery. Oper Tech Orthop. 2000;10(1):82–6.
10. Blackwell M, Morgan F, DiGioia AM. Augmented reality and its future in orthopaedics. Clin Orthop Relat Res. 1998;354:111–22.
11. Sugimoto M, Yasuda H, Koda K, Suzuki M, Yamazaki M, Tezuka T, Kosugi C, Higuchi R, Watayo Y, Yagawa Y, Uemura S, Tsuchiya H, Azuma T. Image overlay navigation by markerless surface registration in gastrointestinal, hepatobiliary and pancreatic surgery. J Hepatobiliary Pancreat Sci. 2010;17(5):629–36.
12. Marescaux J, Rubino F, Arenas M, Mutter D, Soler L. Augmented-reality-assisted laparoscopic adrenalectomy. JAMA. 2004;292(18):2214–5.
13. Gavaghan KA, Peterhans M, Oliveira-Santos T, Weber S. A portable image overlay projection device for computer-aided open liver surgery. IEEE Trans Biomed Eng. 2011;58(6):1855–64.
14. Bou Sleiman H, Ritacco LE, Aponte-Tinao L, Muscolo DL, Nolte L-P, Reyes M. Allograft selection for transepiphyseal tumor resection around the knee using three-dimensional surface registration. Ann Biomed Eng. 2011;39(6):1720–7.
15. Oliveira-Santos T, Klaeser B, Weitzel T, Krause T, Nolte L, Peterhans M, Weber S. A navigation system for percutaneous needle interventions based on PET/CT images: design, workflow and error analysis of soft tissue and bone punctures. Comput Aided Surg. 2011;16(5):203–19.

Afterword

D. Luis Muscolo and Miguel A. Ayerza

Accuracy of surgical procedures has been traditionally associated mainly with manual natural abilities and experience of surgeons. Some surgeons may feel comfortable with this surgical precision, after passing through a painful period of time called learning curve, and with potentially even more painful consequences for patients. However, many others performing surgical procedures demanding high accuracy, would be left with the uncomfortable sensation of an inadequate precision obtained, and should rely anxiously in a postoperative x-ray, or the pathology report of acquired margins.

In the past, and also at many of most prestigious centers at present time, surgeon would visually incorporate 2D images from the patients, and after a mentally poorly understood process, would elaborate a 3D plan and perform surgery. All this implies a process with high potential for significant errors, and is not in correspondence with present technical advances for imaging processing and computerized techniques.

Doctors, and surgeons in particular, are generally eager for advances, but at the same time somehow reluctant to change what they had learn through their manual learning curves.

Advances in the practice of surgery implies a combination of basic sciences, technology and an increase in surgeons manual dexterity. However, although leading surgeons may be familiar and may participate in the incorporation of new science in their practice, few would be prepared to incorporate advanced computerized techniques. This gap between basic science, technology and medical practice is not new, and generally is filled by young surgeons with that expertise, but they are in few number, and they need an appropriate reception among their surgical team.

At the time, in which surgeons still need to rely in postoperative x-rays in order to confirm that what they preoperatively planed was executed accordingly, is hard to think of any orthopaedic surgical procedure in which new technologies as computerized techniques would not have a place. Probably one of our main priority for surgical procedures today, is to increase accuracy, precision.

L.E. Ritacco et al. (eds.), *Computer-Assisted Musculoskeletal Surgery: Thinking and Executing in 3D*, DOI 10.1007/978-3-319-12943-3

In recent years the potential use of computerized techniques in orthopaedic surgery had been explored by groups at different parts of the world with variable acceptance.

For joint replacement the validity of the use of these techniques had been controversial. There is no clear evidence that for a regular hip or knee replacement, small variations in what was planned and what was obtained in surgery would reflect on short or medium follow ups. However, most of those trials had been randomized with surgeons with strong experience and expertise with traditional surgery. In grossly deformed malaligned joints, or patients with previous failed surgeries, some results suggest the beneficial effect of computerized techniques. In addition, incorporation of these techniques in orthopaedic training programs, may sharply reduce that damaging learning curve, at present time necessary for joint replacement surgeons.

Some surgeries may greatly improve results with incorporation of those techniques. The possibility to preoperatively virtually plan correction of spine deformities, determine with precision the type of instrumentation to be used, and perform risky surgical maneuvers of save screw placement, may improve surgeons confidence and results.

Trauma patients and several pediatric diseases causing severe limb malaligments may also benefit. Preoperative virtual planning reduction of complex limb or pelvic fractures, and correcting osteotomies, may help not only to perform the procedure with accuracy, but also determine the precise osteosinthesis to be used, with significant reduce of osteosinthesis materials inventories, and therefore cost.

There have been preliminary reports of the use of computerized surgery in addition with arthroscopy, in order to help the surgeon to detect with precision lesions of acetabular labrum in the hip or osteocondral lesions of the knee.

Also in complex surgical reconstructive mandibular procedures and lesions including costal or sternum pathologies, computerized techniques are progressively being incorporated to increase precision in those procedures.

Probably one of the main areas in which these techniques are having the greatest impact is in orthopaedic oncology. Surgeons must determine with the highest precision where the bone should be cut to preserve as much unaffected tissue without invading tumor margins. Most preoperative plans are made using 2D images of the lesion. Incorporation of 3D planning and execution with potential increased accuracy, most likely will influence prognosis of those tumor patients. Extensive masses growing in complex anatomical areas, and even small tumor located purely intramedular in a long bone, makes it difficult for the surgeon to determine the exact position of osteotomies intraoperatively, and are strong indications for navigation technologies.

These are new technologies with present limitations. It is a continuously evolving technique with apparent influence for higher surgical precision. There is a need for more precise and simpler navigated instrument, and to clearly define sources of potential errors in the whole workflow.

Questions arise related to clinical application of these techniques. Equipment is costly, but is it cost effective? The surgical team must have training in computerized

techniques that requires additional time and expenses. Surgical time, at the beginning, may be prolonged. Some experienced surgeons may not consider these techniques necessary. However, similar arguments are usually raised when new technologies, that would change surgeons habits, are introduced. The whole surgical team needs to transit a period of time in which progressively they realize the potential value to increase accuracy and gain confidence.

These implies a collaborative effort among bioengineers, doctors and supporting medical personal at the operating room, and even more important during the preoperative planning. Possibly, those medical institutions willing to incorporate computerized-assisted surgeries on a regular basis, will need to stablish units dedicated to coordinate the whole process.

Probably present, and improved computerized techniques, are going to have a great impact in accuracy in many of our surgical procedures in the future. They have the potential to be incorporated as a valuable, and possibly indispensable tool, in most surgical environments.

Index

A
Ablation. *See* Local tumor ablation
Additive manufacturing (AM), 170, 184, 193–195
Adolescent idiopathic scoliosis (AIS)
  Adam's forward-bending test, 294
  curve flexibility, 299–301
  data acquisition, 296–299
  Lenke and King classification systems, 294
  prevalence, 294
  SLS (*see* Spinal loading system (SLS))
  study design, 295
Allograft selection
  bone augmentation and reconstruction, 15
  cadaveric implants, 10
  centralised bone banks, 10
  computerised manual selection, 10–11
  image-to-image volume registration approach, 11
  manual selection, 10
  shape and surface prediction methods, 15
  surface-based registration method
    contralateral limb symmetry, 11–12
    intercalary implants, 11
    iterative closest point (ICP) based registration, 13
    processing pipeline, 12–13
    results, 14
    system testing and validation, 12
    three-dimensional template matching process, 12
    transepiphyseal tumor resection, 11
  template-based method, 11
American Society for Testing of Materials (ASTM), 262–263
Ankle arthroplasty, 171
Anterior cruciate ligament (ACL) reconstruction, 66–67
Anterior pelvic plane (APP), 20
Anterior transpedicular screw (ATPS) technique, 204
Arthroscopic hip surgery. *See* Hip arthroscopy, FAI
ASTM. *See* American Society for Testing of Materials (ASTM)
Augmented reality (AR)
  definition, 304
  image guidance displays, 304
  orthopedic surgery, history, 305–306
  projection device
    benefits of, 312
    clinical application, 309–312
    data visualization, 312
    design of, 306
    functional model, 307, 308
    geometric calibration, 308–309
    miniaturisation, 307
    patient-to-image registration process, 307
    RGB laser projector, 307

B
Biological reconstruction, 10
Blueprint® solution, 171
Bone grafting, 14
Bone motion monitors (BMM), 223
Bone tumor navigation
  CATS technique, 67
  in pelvis (*see* Pelvic tumor surgery)
  planar conformation for, 7

L.E. Ritacco et al. (eds.), *Computer-Assisted Musculoskeletal Surgery: Thinking and Executing in 3D*, DOI 10.1007/978-3-319-12943-3

Bone tumor navigation (*cont.*)
PSI, 171–173
sacral tumors, 72, 73
Brainlab Hip CT, 21–22

C
Cadaveric implants, 10
CAOS. *See* Computer aided orthopaedic surgery (CAOS)
Caspar, 102
Centralised bone banks, 10
Cervical spine, 203–204
Charged coupled device (CCD) cameras, 60
Chondrosarcoma
in pelvis, 72, 74, 75
in sacrum, 73
3D preoperative planning, 92
Chordomas, 72, 73
CMF surgery. *See* Cranio-maxillofacial (CMF) surgery
Cobb angle, 294, 298, 299
Computer aided orthopaedic surgery (CAOS)
accuracy and precision
ASTM standard, 262–263
bone-cutting, 264
bone-drilling and assembly, 264
bone-preparation tasks, 263
bone tumor surgery, 264
CAOS-International, 262, 263
corrective surgery, 265
definition, 259
economic benefit, 266
hip surgery, 265
ISO Central Secretariat, 266
knee surgery, 265
osteotomies, 261–262
PSI technology, 262
scientific benefit, 266
societal benefit, 266
spine surgery, 264
stakeholders benefits, 265–266
Standard ISO1101:2012, 263
Standard ISO 5725–1:1994, 263
technological benefit, 266
bone defect, reconstruction of, 93, 94
bone tumor navigation, 93, 95
bone tumor resection, 93, 94
GPS, 90
image-guided surgical navigation systems, 260
intraoperative setup, 92
local recurrence, 96
median registration error, 95
multiplanar osteotomy, pointer marking, 93, 94
pelvic tumors, 90
point to point registration, 93
preoperative preparation
image acquisition, 91
image segmentation, 91–92
3D preoperative planning, 92
tomography and resonance fusion, 91
prosthesis, placement of, 89, 90
software technical crash, 95
surface refinement registration, 93, 94
surgical precision, 90
survival, rate of, 96
time for, 95
TKA (*see* Total knee arthroplasty (TKA))
Computer assisted tumor surgery (CATS), 67
Computer Numeric Controlled (CNC) techniques, 191
Coned hemipelvic replacement, 82
Coordinate measurement machine (CMM), 192
Cranio-maxillofacial (CMF) surgery
computer-assisted facial soft-tissue simulation, 41
components for, 45
direct and inverse surgical planning, 48, 50, 51
fast patient-specific models, 48, 49
GPU-based simulation models, 46
inverse soft tissue modeling, 50–52
MSM-based approach, 45
MTM, 46
post-operative scenario, functional aspects of, 46–48
segmentation of, 45
spatially-varying Gaussian Process Modeling, 48, 49
head and neck cancer, 29–30
image-guided techniques, 44
inborn/acquired facial disfigurements, 43
malocclusion, 44
orthognathic surgeries, 44
plate and implants, in-house production of, 30
stereo visualization and haptic feedback
bone segmentation, 34–35
components, virtual surgery planning, 31
DOF and DOFF, 32
force-feedback, 33
implant design, 38–39
input/output interface, 32
mandibular reconstruction, 35–36, 39–40

motion parallax, 32
planning system hardware, 33–34
semi-automatic orbit segmentation method, 37–38
surgery training simulators, 32
3D visualization, 31–32
traffic accidents, 30
two-dimensional (2D) graphical interface, 30
Cryoablation, 153
Cubitus varus deformity
clinical outcomes, 283–284
cosmetic problem, 279
deformity evaluation, 280, 281
distal osteotomy plane, 280, 282
joint laxity, 279
PMI, 280–282, 284
surgical technique, 282–285
tardy ulnar nerve palsy, 279
Custom implants
accuracy, 196–197
additive manufacturing, 193–195
cost of, 194–195
finite element analysis, 191
fixation modelling, 189–190
history of
additive manufacturing, 184
CAD-CAM femoral hip stems, 183
distal femoral replacement, 182
hemi-pelvic replacement, 182
ISTA, 183
joint and bone reconstruction, 182
limb salvage implants, 182, 184–185
rapid prototyping, 184
3D designs, 182–183
3D printing, 183–184
image processing
CT artefacts and scatter, 186, 188
segmentation, 187
3D models, 187, 188
thresholding, 186, 187
implant body, modelling of, 188, 189
manufacturing techniques
ALM technology, 191–192
CMM technology, 192
CNC milling, 191
patient specific cutting jigs, 192–193
navigation/robotic systems, 193
vs. off-the-shelf implants, 182
planned post-operative outcome, 187, 189
pre-operative planning, 187, 189
process workflow, 186
3D imaging techniques, 182, 186
time, 195–196
Custom jigs, 101
Cutting jigs, 192–193

D
Degrees-of-force-feedback (DOFF), 32
Degrees-of-freedom (DOF), 31, 32, 250, 251, 296
Digital Imaging and Communications in Medicine (DICOM), 60, 273
Distal radius fracture
surgical outcome, 284, 288–289
surgical technique, 287–288
volar locking plate, 286–287
Dynamic reference frame (DRF), 60

E
Equidistant method, 23–25
Ewing's sarcoma
in pelvis, 72
in sacrum, 73

F
Femoroacetabular impingement (FAI)
anatomical lesions, 18
computer navigation and pre-operative planning
advantages, 19
A2 Surgical, 25–26
Brainlab Hip CT, 21–22
challenges, 26
consistent reproducibility and accuracy, 18
encoder linkages, position tracking, 23
equidistant method, 23–25
HipMotion, 20–21
long-term clinical outcomes, 18
preoperative CT/MRI imaging, 19
Fiducial localization error (FLE), 260
Fiducial registration error (FRE), 260
Finite element analysis (FEA), 191
Forearm fractures. *See* Malunited forearm fracture

G
Gaming technology. *See* Touch-based and touch-less interfaces
Gap balancing technique. *See* Total knee arthroplasty (TKA)
GNU C Compiler (GCC), 295
Gradient Vector Flow (GVF) snake based approach, 45

H
Hip arthroscopy, FAI
anatomical lesions, 18
computer navigation and pre-operative planning
advantages, 19
A2 Surgical, 25–26
Brainlab Hip CT, 21–22
challenges, 26
encoder linkages, position tracking, 23
equidistant method, 23–25
HipMotion, 20–21
preoperative CT/MRI imaging, 19
HipMotion, 20–21
Hydra game controller
control Taurus, 242
depth variance, 249, 250
deviation error, 249
DOF, 250, 251
magnetic motion sensing, 246
peg transfer task, 250

I
Imascap, 171
International Society for Computer Assisted Orthopaedic Surgery (CAOS-International), 262, 263
International Society for Technology in Arthroplasty (ISTA), 183
International Society for the Study of Custom Prostheses (ISSCP), 183

J
Japanese Orthopedic Association (JOA), 228
Joule-Thompson effect, 153

K
Kinect control
control Taurus, 242
depth variance, 249, 250
deviation error, 249
discrete control protocol, 245–246
DOF, 250, 251
peg transfer task, 250

L
Leap Motion controller
control Taurus, 242
depth variance, 249, 250
desktop infrared sensor, 246
deviation error, 249
DOF, 250, 251
peg transfer task, 250
Limb salvage implants
bone condition/indication, 185
failed standard joint replacements, revision of, 184
functional expectations, 185
life expectancy, 185
for malignant bone tumours, 184
minimising musculoskeletal resection, 185
patient age, 184–185
skeletal locations, 185
unusual bony anatomy, 185
Local tumor ablation
complications, 158
cryoablation, 153
CT-guided positioning, 155
indications, 153
metastasis surgery, 155
microwave ablation, 153
osteoid osteoma, 152, 153
per-operative workflow, 155, 156
pitfalls of, 158
post-operative MRI scan, 155, 157
preoperative preparations, 154–155
radiofrequency ablation, 152–153
results, 158

M
Malocclusion, 44
Malunited distal radius fracture
surgical outcome, 284, 288–289
surgical technique, 287–288
volar locking plate, 286–287
Malunited forearm fracture
clinical outcomes, 278, 279
PMI
internal fixation, 278, 279
Kirschner wires, 275, 277, 278
rapid prototyping machine, 275
3D computer simulation, 275, 276
3D bone models, 273
bended cylinders stand, 273, 275
bilateral radius and ulna, 273
proximal part, 273, 274
screw displacement axis technique, 273, 274, 276
Mass-spring modeling (MSM), 45
Mass Tensor Modeling (MTM), 46
Measured resection technique. *See* Total knee arthroplasty (TKA)
Mega implants. *See* Limb salvage implants

Metastasis
local ablation, 155
in pelvis, 73
Microwave ablation (MWA), 153
Milling technique, 165
Mimics®, 186
Mobelife, 176
MWA. *See* Microwave ablation (MWA)

N
Navigated freehand cutting (NFC) technology
cadaveric leg specimens, 109–110
distal femur
average cutting time, 107–108
early elementary prototype, 107
errors, frequency and magnitude of, 108–109
instruments, 103
navigated power tools, 105, 106
smart views, 105–107
surgical planning
alignment techniques, 104, 105
CT studies, 104
2D guidance component, 105, 106

O
Off-the-shelf implants, 182, 183
Omega 7 haptic device
control Taurus, 242
depth variance, 249, 250
deviation error, 249
DOF, 250, 251
mapping, 246
peg transfer task, 250
On-Tool Tracking (OTT), 111
Ortholock, 133
Osteoid osteoma, 152, 153
Osteosarcoma
metallic mega implant, 184
in paediatric patients, 72
in pelvis, 72
in sacrum, 73
OtisMed prosthesis, 168–169

P
Patient matched instrument (PMI)
malunited distal radial fracture, 286–288
malunited forearm fracture
internal fixation, 278, 279
Kirschner wires, 275, 277, 278
rapid prototyping machine, 275
3D computer simulation, 275, 276
Patient specific implants. *See* Custom implants
Patient-specific instruments (PSI), 176–177, 262
current applications
ankle arthroplasty, 171
bone tumor surgery, 171–173
corrective osteotomies, 173–174
hip prosthesis, 171
ilio-sacral screws, 176
Paprovsky pathology, 175–176
shoulder arthroplasty, 171
spine instrumentation, 170–171
synostosis, 175
history of, 164–166
for TKA
cost analysis, 167
feasibility, 167
implant positioning, accuracy of, 169
instrument design, 170
manufacturing process, 167
MRI and CTscan models, 168
navigation systems, 166
OtisMed prosthesis, 168–169
preoperative planning, 167
segmentation method, 168
3D printing technology, 166–167
Patient's specific templates, spine surgery
advantages, 200, 202, 204, 212
articular processes, 201, 202, 206, 207, 211
bone surface, 202, 204, 206–209, 211–213
cervical spine, 203–204
cost for, 211, 212
fabrication process, 201
fluoroscopic guidance, 200
free-hand technique, 200, 210
guide screws placement, 211, 213
image-guided approach, 200, 210
pedicle screws placement, 200
software and 3D printer, 212
template and vertebral bone, 201–202
thoraco-lumbar spine (*see* Thoraco-lumbar spine)
vertebral laminae, 202, 206–208, 211
Peg transfer task, 247, 252, 253
Pelvic tumor surgery
challenges
anatomy, 74
complications, 77
consitencies, 75
functions, preservation of, 77
marginal and intralesional resections, 75–76
reconstruction, 76–77
size, 74

Pelvic tumor surgery (*cont.*)
chondrosarcoma, 72, 74
chordomas, 72
computer-assisted navigation
automatic segmentation, 80
benefits, 85–86
CT-fluoro matching, 79
custom made implants, design of, 81–82
instruments, 83
Kirschner wires, preoperative implantation of, 79
manual segmentation, 80
MRI and CT scans, image correlation, 79–80
non custom implants, 82
osteotomy, order of, 84
reduced soft tissue exposure, 83
registration points, 77–78, 81
resection plane planning, 80–81
sources of error, 84–85
tracker and camera positioning, 82–83
conventional techniques, 78
Ewing's sarcoma, 72
metastases, 73
osteosarcomas, 72
preoperative virtual planning, 3, 4
Personalized medicine, 163, 181
PMI. *See* Patient matched instrument (PMI)
PSI. *See* Patient-specific instruments (PSI)

R
Radiofrequency ablation (RFA), 152–153
Rapid prototyping (RP), 166, 184
ROBODOC, 102
blood loss in, 221
BMM, 223
clinical trial, 220
digitizer, 223–224
multicenter US trial, 221
orthopaedic procedures, 220
preoperative planning workstation, 221
Sutter General Hospital in Sacramento, 220
THA (*see* Total hip arthroplasty (THA))
TKA (*see* Total knee arthroplasty (TKA))
Robotic minimally invasive surgery (RMIS), 238

S
Sacral tumors, 72, 73
ScanIP®, 186
Shoulder arthroplasty, 171
Simplified Orthopaedic Surgery (SOS) system. *See* Navigated freehand cutting (NFC) technology
SLS. *See* Spinal loading system (SLS)
Spinal loading system (SLS)
advantage, 295, 298
Cobb angle measurements, 298, 299
correlation coefficient, 299, 300
DC-servomotor, 295
graphical user interface (GUI), 295, 297
low-cost mechatronic system, 294
motion controller drive, 295
Pearson's correlation coefficient, 299
spinal deformities characteristics, 299
three degrees of freedom mechanism, 295, 296
Spine surgery, 264
intra-operative navigation
anterior and posterior spinal instrumentation, 117–118
complications, 123, 125–126
drill, 120, 121
giant cell tumor, 117–118
intra-operative CT image, 118, 119
intraoperative fluoroscopy, 116
navigation probes, 118–121
percutaneous screw placement, 121, 124–126
posterior lateral incision, 118
post-operative CT image, 120, 123
preoperative planning, 116–117
small incision, 118–119
3D navigation, benefit of, 127
tubular retractor system, placement of, 118, 120
patient's specific templates (*see* Patient's specific templates, spine surgery)
Standard keyboard
control Taurus, 242
depth variance, 249, 250
deviation error, 249
DOF, 250, 251
peg transfer task, 250
Surgical navigation
ACL reconstruction, 66–67
bone tumor surgery, 67
computer-assisted systems, 60
data acquisition, 60
2D-3D registration, 61, 63
fracture fixation, 65–66
image-to-patient registration, 61
intraoperative setup of, 60, 61
joint arthroplasty, 64–65
potential errors, 67, 68
spine surgery, 64

surface-matching technique, 61, 62
tracking, 62, 63
Synostosis, 175

T
Target registration error (TRE), 260
Taurus robot
controlled manipulators, 239, 240
dexterous and compact arms, 239
features, 237
high fidelity telemanipulation robot, 239
implementation of, 237
Kinect control teleoperation, 245–246
kinematic configuration, 240–241
mapping interfaces, actions, 242–243
region determination, 243
registration process, 243
Robot Control Scheme module, 239
safety operation, 243, 244
3D Vision 2, 240
trajectory generation, 241–242
visual and auditory feedback, 243–245
visual and sound cues, 239
Telerobotic surgery. *See* Touch-based and touch-less interfaces
Thoraco-lumbar spine
full contact template design, 208
low contact design template
clinical trial, 205
CT evaluation, 206, 207, 209
four point contact points design, 205
multiple low contact points, 206
porcine spine, 206, 209
stereolithography, 205
V-shaped knife edges, 205
Three dimensional allografts, 10
3D printing technology, 166–167, 183–184
TKA. *See* Total knee arthroplasty (TKA)
Total hip arthroplasty (THA)
ROBODOC
bone preparation procedure, 224–225
bone, rotary cutting tool, 224
Brooker type 3 heterotopic ossification, 228
clinical outcomes, 220
clinical reports, 225, 226
complications, 226
dual energy X-ray absorptiometry, 227
European law, 225
femoral canal preparation, 227
German group, 226
Harris hip scores, 226–227
JOA hip scores, 228
ORTHODOC, 221–222
osseointegration, 220
periprosthetic bone remodeling, 227
pin-based system, 228
surgical navigation, role of, 65
Total hip replacements (THR), 100
Total knee arthroplasty (TKA)
CAS technique
anteroposterior axis, 130–131
clinical examination of deformity, 131–132
clinical transepicondylar axis, 130
complications, 145–147
vs. conventional technique, 146–147
CT-based navigation, 65
femur anatomical survey, 134–135
final knee kinematics, 143–144
initial setting, 133
intra-operative planning, 137–138
jigs navigation, 138–142
posterior condylar angle, 130
posterior condylar axis, 130
pre-operative X-ray analysis, 132
resections, verification of, 139, 143
soft tissue balancing, 141, 143, 144
surgical transepicondylar axis, 130
tibial anatomical survey, 136–137
custom jigs, 101
NavioPFS, 102–103
NFC technology (*see* Navigated freehand cutting (NFC) technology)
passive/active robots, 102
patient-specific instruments
cost analysis, 167
3D printing technology, 166–167
feasibility, 167
implant positioning, accuracy of, 169
instrument design, 170
manufacturing process, 167
MRI and CTscan models, 168
navigation systems, 166
OtisMed prosthesis, 168–169
preoperative planning, 167
segmentation method, 168
ROBODOC
alignment methods, 230
clinical outcomes, 220
clinical reports, 225, 226
fixation, 223
HSS and WOMAC scores, 230
Knee Society scores, 229
postoperative range of motion, 229
prospective randomized study, 229, 231
Zimmer's iAssist, 101, 102
Total knee replacements (TKR), 100
Touch-based and touch-less interfaces

Total knee arthroplasty (TKA) (*cont.*)
disadvantage, 236
haptic controllers, 237
incision task
bar graphs and sound alerts, 247
control variance, 247
depth variance, 249, 250
distance from-target annotation, 247
DOF, 250, 251
error, 247, 249
reference trajectory, 247, 248
scalpel's tip trajectory, 247, 248
tooltip's trajectory, 247, 248
keyboards, 3D joysticks, 237
Leap Motion and pedals, 237
natural gesturing, 236
optical sensors, 237
peg transfer task, 252
RMIS, 238
sensorial substitution methods, 237
systematic evaluation, 238–239
Taurus robot (*see* Taurus robot)
Tumor ablation. *See* Local tumor ablation

U
Upper extremity, deformity correction
cubitus varus deformity (*see* Cubitus varus deformity)
malunited distal radius fracture
surgical outcome, 284, 288–289
surgical technique, 287–288
volar locking plate, 286–287
malunited forearm fracture (*see* Malunited forearm fracture)
three-dimensional (3D) deformity, 272

V
Virtual preoperative planning (VPP)
advantages, 4
allograft selection (*see* Allograft selection)
bone tumor resection, planar conformation for, 7
head and neck cases, 5
image acquisition, 6
image segmentation, 6–7
limitations, 4
meetings, 5–6
pelvis tumor, 3, 4
3D planning, 6, 7
tomography and resonance fusion, 3, 7
tumour injuries, instruction on, 5
2D images and 3D anatomical models, 3
2D planning, 6
virtual navigation, 6
Volar locking plate, 286–287